



**Technische Universität München**

**Fakultät für Chemie**

Professur für Siliciumchemie

**Synthesis, reactivity and catalytic application of NHC-stabilized  
tetryliumylidenes**

Debotra Sarkar

Vollständiger Abdruck der von der Fakultät für Chemie der Technischen Universität München  
zur Erlangung des akademischen Grades eines

Doktors der Naturwissenschaften (Dr. rer. nat.)

genehmigten Dissertation.

Vorsitzende: Prof. Dr. Kathrin Lang

Prüfende der Dissertation:

1. Prof. Dr. Shigeyoshi Inoue

2. Prof. Dr. Angela Casini

Die Dissertation wurde am 06.10.2020 bei der Technischen Universität München eingereicht und  
durch die Fakultät für Chemie am 17.11.2020 angenommen



This thesis "Printed and/or published with the support of the German Academic Exchange Service."

## Abstract

This thesis comprises the isolation and characterization of the NHC-stabilized tetryliumylidene compounds and their fascinating reactivity toward small molecules. This led to the synthesis of novel silicon and germanium carbonyls analogs, namely heavier silaacylium ion, silaaldehyde, and germaacylium ion. Further application of the germyliumylidene and germaacylium ion in catalytic functionalization of CO<sub>2</sub> demonstrates their potential as alternatives to expensive transition metals.

## Kurzfassung

Die vorliegende Doktorarbeit befasst sich mit der Synthese und Charakterisierung von NHC-stabilisierten Tetryliumylidenen sowie deren Reaktivität gegenüber kleinen Molekülen. Es wurden neuartige Silizium- und Germanium-basierte Carbonyl-Analoga synthetisiert: Silaacylium-Ion, Silaaldehyd und Germaacylium-Ion. Untersuchungen zur Funktionalisierung von CO<sub>2</sub> zeigten, dass das Germyliumyliden und das Germaacylium-Ion potenzielle Alternativen für hochpreisige Übergangsmetallkatalysatoren sind.

## Acknowledgement

I would like to express a sincere thanks to my supervisor Prof. Dr. Shigeyoshi Inoue for his excellent guidance, constant encouragement, optimism, and wonderful cooperation during every stage of my doctoral thesis. His expertise on the main group chemistry and very honest and critical review of my work helped me to understand of various aspects of synthetic organometallic chemistry. I am very grateful for getting an opportunity to work in his research group.

I am thankful to DAAD (Deutscher Akademischer Austauschdienst) for my doctoral fellowship.

I am wholeheartedly thankful to Dr. Catherine Weetman for her all-around help and being an amazing colleague and good friend. I am very fortunate to discuss and learn from her.

I would like to thank Dr. Tibor Szilvási, Mr. Sayan Dutta, Prof. Debasis Koley, Prof. Dominik Münz for their help with theoretical calculations.

I would like to thank, Dr. Syed Usman Ahmad, Dr. Prasenjit Bag and Dr. Vitaly Nesterov, for the good scientific discussion.

I am very thankful to Dr. Daniel Franz, Mrs. Paula Nixdorf, Franziska Hanusch, Dr. Philipp J. Altmann, for measuring crystals and for their very kind and helpful nature. I would like to thank Dr. Alexander Pöthig and Dr. Christian Jandl for their help in solving the crystal structures.

I am thankful to my bachelor student Mr. Emeric Schubert for his excellent help and it has been a great experience working with him. I am very thankful to all the past and present members of AK Inoue group.

I appreciate Prof. Silvarajan Nagendran, Prof. Shivajirao L Gholap, Prof. Arindam Indra for their help.

## Acknowledgement

I would like to thank my closest friend Dr. Priyabrata Ghana, Dr. Ravi Yadav, Dr. Sekhar Saha, Dr. Soumya Mukherjee, Dr. Arundhati Roy, Dr. Soumen Sinhababu, Dr. Subrata Kundu for constantly supporting me during my PhD journey.

I would like to thank my best friend Mrs. Sourima Chowdhury, my sister Mrs. Sudeshna Sarkar and brother in law Dr. Samir Kumar Sarkar.

Finally, I wish to pay tribute to my parents Mr. Mahadev Chandra Sarkar and Mrs. Aparna Sarkar, who sacrificed their worldly interests to promote my education. I am luckiest to have you all.

## List of abbreviations

Ab initio = Latin: "from the beginning"

$\text{BAr}^{\text{F}}_4 = \text{BArF} = \text{B}\{3,5\text{-(CF}_3\text{)}_2\text{-C}_6\text{H}_3\}_4$

$\text{BAr}^{\text{Cl}}_4 = \text{B}(3,5\text{-Cl}_2\text{-C}_6\text{H}_3)_4$

Bu = Butyl

$\text{Cp}^* = 1,2,3,4,5\text{-pentamethyl-cyclopentadiene}$

CAAC = Cyclic alkyl-amino carbene

$\text{CH}_3\text{CN} = \text{Acetonitrile}$

DFT = Density-functional theory

DMAP = 4-(dimethylamino)-pyridine

dme = Dimethoxyethane

Eind = 1,1,3,3,5,5,7,7-octaethyl-s-hydrindacen-4-yl

$\text{Et}_2\text{O} = \text{Diethylether}$

FLP = Frustrated Lewis pair

e.g. = Latin (exempli gratia): "for example"

et al. = Latin (et alii): "and others"

Et = Ethyl

HOMO = Highest occupied molecular orbital

HBpin = Pinacolborane

IDipp = 1,3-bis(2,6-diisopropyl-phenyl)-imidazol-2-ylidene

i.e. = Latin (id est): "that is"

$\text{IMe}_4 = 1,3,4,5\text{-tetramethyl-imidazol-2-ylidene}$

$i\text{Pr}_2\text{Me}_2 = 1,3\text{-diisopropyl-4,5-dimethyl-imidazol-2-ylidene}$

## List of abbreviation

LUMO = Lowest occupied molecular orbital

Mes = 2,4,6-trimethylphenyl; mesityl

m-Ter = <sup>Mes</sup>Ter = 2,6-bis(2,4,6-trimethyl-phenyl)phenyl

NBO = Natural bond orbital

<sup>n</sup>Bu = n-butyl

NMR = Nuclear magnetic resonance

NHC = N-heterocyclic carbene

OTf = Triflate

ppm = Parts per million

PCy<sub>3</sub> = Tricyclohexyl phosphine

PPh<sub>3</sub> = Triphenyl phosphine

R = Organic group

rt = Room temperature

SC-XRD = Single crystal X-ray diffraction

SIDipp = saturated IDipp; 1,3-bis(2,6-diisopropyl-phenyl)-imidazolidin-2-ylidene

<sup>t</sup>Bu = Tertiarybutyl

Tipp = 2,4,6-triisopropylphenyl

thf = Tetrahydrofuran

TMS = Trimethylsilyl

TMSCN = Trimethylsilyl cyanide

WCA = Weakly coordinating anion

XRD = X-ray diffraction

$\delta$  = chemical shift



## Publication List

- **Chalcogen-atom transfer and exchange reactions of NHC-stabilized heavier silaacylium ions**  
D. Sarkar, D. Wendel, S.U. Ahmad, T. Szilvási, A. Pöthig, S. Inoue\*  
Dalton Transaction, 46 (46), 16014-16018
- **The quest for stable silaaldehydes: synthesis and reactivity of a masked silacarbonyl**  
D. Sarkar, V. Nesterov, T. Szilvási, P.J. Altmann, S. Inoue\*  
Chemistry-A European Journal, 25 (5), 1198-1202
- **N-heterocyclic carbene-stabilized germa-acylium ion: reactivity and utility in catalytic CO<sub>2</sub> functionalizations**  
D. Sarkar, C. Weetman, S. Dutta, E. Schubert, C. Jandl, D. Koley\*, S. Inoue\*  
Journal of the American Chemical Society, 142 (36), 15403-15411
- **Germylumylidene: a versatile low valent group 14 catalyst**  
D. Sarkar, C. Weetman, S. Dutta, E. Schubert, C. Jandl, D. Koley, S Inoue\*

## Publications beyond the scope of this thesis

- **From Si (II) to Si (IV) and back: reversible intramolecular carbon – carbon bond activation by an acyclic iminosilylene**  
D. Wendel, A. Porzelt, F.A.D. Herz, D. Sarkar, C. Jandl, S. Inoue\*, B. Rieger\*  
Journal of the American Chemical Society 139 (24), 8134-8137
- **Reactivity studies on aminotroponiminatogermylene stabilized ruthenium (II) complexes**  
D. Yadav, D. Singh, D. Sarkar, S. Sinhababu, M.K. Sharma, S. Nagendran\*  
Journal of Organometallic Chemistry 888, 37-43

## Poster List

- **The quest for stable silaaldehydes: synthesis and reactivity of a masked silacarbonyl**

D. Sarkar, S. Inoue

9<sup>th</sup> European Silicon Days, Saarbrücken, September 09<sup>th</sup> – 12<sup>th</sup> **2018**

- **Silaphosphinidenyl tetrylenes: new catalyst for CO<sub>2</sub> conversion**

D. Sarkar, S. Inoue

ICCOC-GTL16, Saitama University, Saitama, Japan, 1<sup>st</sup>-6<sup>th</sup> Sep **2019**

# Contents

<b>1. Introduction .....</b>	<b>1</b>
<b>2. Tetrylenes [R<sub>2</sub>E:] .....</b>	<b>4</b>
2.1. Isolation of tetrylenes .....	4
2.2. Tetrylenes in small molecule activation .....	5
2.3. Catalytic application of tetrylenes .....	8
<b>3. Tetrylium ions [R<sub>3</sub>E]<sup>+</sup> .....</b>	<b>11</b>
3.1. Classification of tetrylium ions .....	11
3.2. Preparation of tetrylium ions .....	13
3.3. Catalytic application of tetrylium ions .....	14
<b>4. Tetryliumylidene ions [RE:]<sup>+</sup> .....</b>	<b>16</b>
4.1. Silyliumylidene ions [RSi:] <sup>+</sup> .....	17
4.2. Reactivity of silyliumylidene ions .....	20
4.3. Small molecule activation by silyliumylidenes .....	23
4.4. Silyliumylidenes in catalysis .....	24
4.5. Germyliumylidenes and stannylumylidenes .....	25
4.6. Small molecule activation by germyliumylidenes and stannylumylidenes .....	30
4.7. Catalytic application of germyliumylidenes and stannylumylidenes .....	33
4.8. Plumbyliumylidenes .....	34
<b>5. Scope of this work .....</b>	<b>36</b>
<b>6. Chalcogen-atom transfer and exchange reactions of NHC-stabilized heavier silaacylium ions .....</b>	<b>42</b>
<b>7. The quest for stable silaaldehydes: synthesis and reactivity of a masked silacarbonyl.....</b>	<b>49</b>
<b>8. N-heterocyclic carbene-stabilized germa-acylium ion: reactivity and utility in catalytic CO<sub>2</sub> functionalizations .....</b>	<b>57</b>
<b>9. Germyliumylidene: a versatile low valent group 14 catalyst .....</b>	<b>68</b>
<b>10. Summary and outlook .....</b>	<b>73</b>
<b>11. Bibliographic details for complete references .....</b>	<b>81</b>
<b>11.1. References.....</b>	<b>112</b>

## Contents

# 1. Introduction

Carbon, silicon, germanium, tin, and lead make up the group 14 elements of the periodic table. Despite belonging to the same group, the chemistry of carbon differs markedly from that of its heavier congeners (E = Si-Pb).<sup>1-9</sup> For example, CO<sub>2</sub> exists as a gaseous monomer and possesses two C=O double bonds. In contrast, SiO<sub>2</sub> is solid and consists of a polymeric  $\sigma$ -bonded Si-O network (e.g., quartz). In the same vein, CH<sub>4</sub> is stable in air, but, SiH<sub>4</sub> is flammable under the same conditions; furthermore, PbH<sub>4</sub> is only stable below 10K in solid H<sub>2</sub> or D<sub>2</sub> matrices.<sup>6, 10</sup> The differences between the properties of the group 14 elements can be mainly attributed to two significant factors, i) less effective s/p hybridization as the effective nuclear charge increase down the group, ii) distinct electronegativity differences between carbon and heavier elements (Figure 1).<sup>2-7</sup>

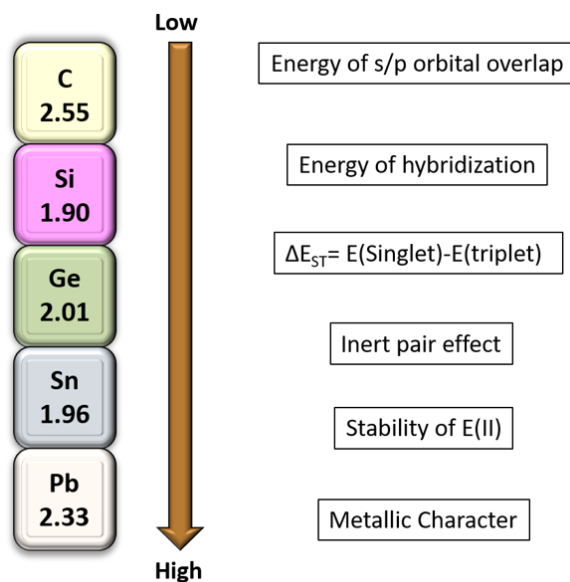


**Figure 1:** Electronegativity scale of the group 14 elements and general electronic features.

The fundamental diversity between lighter and heavier elements has fascinated chemists to analyze the bonding and electronic properties of the heavier carbon homologs. The last few decades have witnessed a spectacular progress in low-valent heavier group 14 chemistry, (i. e.

## Introduction

compounds in low oxidation state and/ or sub-coordination numbers), including the isolation of elusive zero-valent, divalent, and trivalent analogs of carbon (Figure 2).<sup>2-7</sup>

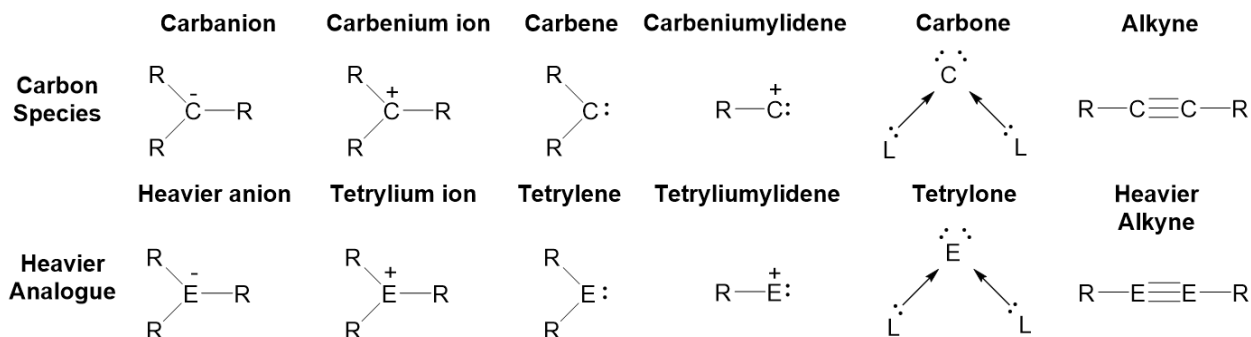


**Figure 2:** Selected example of low valent carbon species and heavier analogs (E = Si-Pb).

Interestingly, some of these molecules have now shown small molecule activation, which was previously considered the domain of transition metal complexes.<sup>9, 11-13</sup> For example, in a seminal study, Power et al. demonstrated activation of H<sub>2</sub> with a digermene R-Ge≡Ge-R, (R = Tipp<sub>2</sub>-C<sub>6</sub>H<sub>3</sub>, Tipp = 2,4,6-*i*-Pr<sub>3</sub>C<sub>6</sub>H<sub>2</sub>).<sup>14</sup> Analogously, tetrylenes [R<sub>2</sub>E:] and tetryliumylidenes [R-E:]<sup>+</sup> are capable of activating a range of small molecules, including the activation of strong σ-bond containing species (e.g., H-H, N-H)<sup>12, 15, 16</sup> Notably, activation of the N-H bond in NH<sub>3</sub> is challenging for transition metal complexes, with only a handful of examples reported.<sup>17-19</sup> This is an important transformation as it is industrially relevant for catalytic hydroamination or C-N bond formation.<sup>17</sup> Thus, the question rises can heavier low valent group 14 compounds provide a catalytic alternative of expensive and rare transition metal complexes?

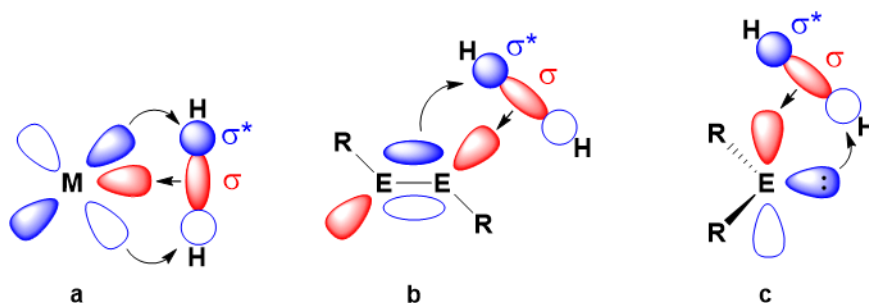


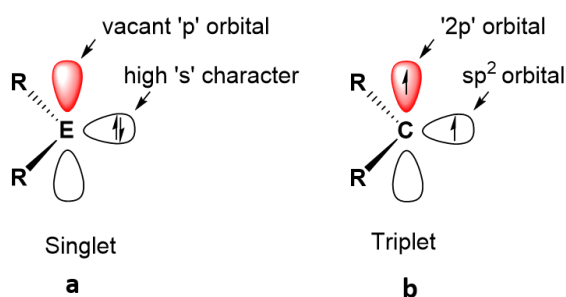
**Figure 3:** Frontier orbitals involved in the activation of H<sub>2</sub>, a) transition metals, b) multiple bonds c) singlet main group compounds (e.g., tetrylenes).

## Introduction

Theoretical studies have revealed heavier low valent group 14 compounds with their vacant coordination sites, and a relatively modest HOMO-LUMO gap possesses transition metal like frontier molecular orbitals.<sup>9, 11-13</sup> These energetically available orbitals are enabled oxidative addition reactions at low valent group 14 center (Figure 3).<sup>9, 11-13</sup> However, reductive elimination from the resultant high-oxidation state compound is challenging, and is currently the limiting factor in their catalytic applications.<sup>4, 20-28</sup> Thus, developing economy efficient low valent group 14 compounds, which can be utilized in diverse catalysis, is one of the thriving areas of research in modern organometallic chemistry.

## 2. Tetrylenes [R<sub>2</sub>E:]

Tetrylenes [R<sub>2</sub>E:] (E = Si-Pb) are heavier analogs of carbenes [R<sub>2</sub>C:].<sup>2, 29-31</sup> Like carbenes, tetrylenes are neutral, possessing four valence electrons with two bonding and two non-bonding electrons. They can exist in either singlet ground state (a lone pair and one vacant 'p'-orbital) or triplet ground state (two unpaired electrons). However, on descending the group, the singlet-triplet energy gap ( $\Delta E_{ST} = E_{\text{Singlet}} - E_{\text{Triplet}}$ ) increases due to high energy separation between the valence 's'- and 'p'-orbitals (Figure 4).<sup>2, 32, 33</sup> Thus, heavier tetrylenes prefer a singlet ground state (Figure 4a) and contain both Lewis acid (vacant orbital) and -base (lone pair) character. In contrast, having a low  $\Delta E_{ST}$  value, carbenes are known to exist as both singlet and triplet ground states, depending on the substituent attached to the carbonic carbon.<sup>29, 33</sup>



H <sub>2</sub> E:	H <sub>2</sub> C:	H <sub>2</sub> Si:	H <sub>2</sub> Ge:	H <sub>2</sub> Sn:	H <sub>2</sub> Pb:
$\Delta E_{ST}$ (kcal mol <sup>-1</sup> )	-14.0	16.7	21.8	24.8	34.8

**Figure 4:** Electronic features of tetrylenes and carbenes.

### 2.1. Isolation of tetrylenes

Tetrylenes are electron-deficient species, and they have an affinity to dimerize and oligomerize. Suitable thermodynamic and/or kinetic protection is required to isolate compounds of the type, [R<sub>2</sub>E:] (Figure 5).<sup>2, 31</sup> The thermodynamic stabilization strategy generally utilizes intra- or intermolecular electron donors, which partially fill electron deficiency of the empty 'p'-orbital either by coordination or with mesomeric effect (Figure 5a).<sup>2, 31</sup> The kinetic stabilization employs sterically demanding groups to shield the empty 'p'-orbital from self-oligomerization or attack from external nucleophiles (Figure 5b).<sup>2, 31</sup> A plethora of cyclic and acyclic tetrylenes have been



## Tetrylene

isolated supported by the widely used Cp\* ligand {Cp\* = ( $\eta^5$ -C<sub>5</sub>Me<sub>5</sub>)} or by inclusion of heteroatoms (e.g. S, O, N etc.) adjacent to E center together with suitable bulky ligands.<sup>2, 31</sup> Interestingly, use of intermolecular donor (e.g. NHC) or donor-acceptor combinations further allow taming of the highly reactive tetrylene, such as silicon dihalide [X<sub>2</sub>Si:],<sup>34, 35</sup> tetrylene hydrides [R(E)H]<sup>25</sup> and parent tetrylenes [H<sub>2</sub>E:] (Figure 5c-d).<sup>6, 36</sup>

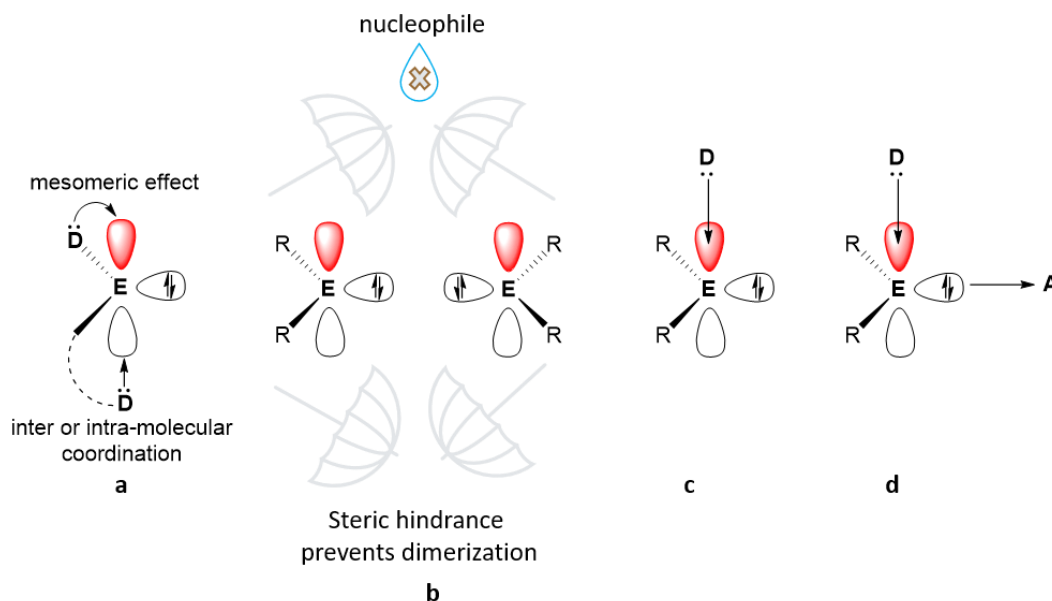


**Figure 5:** Strategies to isolate tetrylenes *via*, a) inter or intra molecular, b) kinetic c) electron rich bulky donor and d) donor-acceptor based stabilization [D = donor, A = acceptor, R = substituent].

## 2.2. Tetrylenes in small molecule activation

The chemistry of tetrylenes has gained significant attention in the last decades due to their application in small molecule activation,<sup>11, 12, 20, 37</sup> catalysis,<sup>9, 25</sup> and as ligands in transition metal chemistry.<sup>38</sup> Unlike carbenes, heavier tetrylenes (R<sub>2</sub>E:, E = Si-Pb) are weak donors, due to increasing 's'-character on descending the group (so-called "inert pair effect") and also arouses less basicity than carbenes.<sup>2, 39</sup> However, despite the less basic character [R<sub>2</sub>E:] compounds show novel reactivities due to their ambiphilic nature.<sup>11, 12, 20</sup>

Owing to a lower HOMO-LUMO gap and transition metal like frontier molecular orbitals several tetrylenes shows single site small molecule activation.<sup>11, 12, 20</sup> Typically for [R<sub>2</sub>E:], the HOMO

## Tetrylene

corresponds to the E-centered lone pair, whereas the LUMO is associated with a formally vacant orthogonal orbital of  $\pi$ - symmetry.<sup>2, 40</sup> Lower HOMO-LUMO gaps lead to increased triplet character in the ground state and, therefore, yield higher reactivity. The factors which influence HOMO-LUMO gaps have been studied intensely and have revealed its dependency on  $\angle$ R-E-R bond angles and the electronic nature of the substituent R (Figure 6).<sup>20, 40-42</sup>

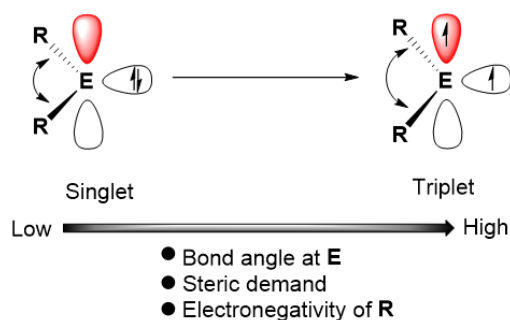


**Figure 6:** Steric and electronic effect on the ground state of tetrylene.

Sterically demanding groups (**R**) result in a wider  $\angle$ R-E-R bond angle. Obtuse  $\angle$ R-E-R angles cause higher 'p'-orbital character of the HOMO, which subsequently raises the HOMO energy level and thus decreases the HOMO-LUMO gap.<sup>40, 43</sup> Thereby, an acyclic tetrylene could show higher reactivity towards a small-molecule compared to cyclic ones.<sup>43</sup> In 2008, Power and coworkers reported the facile activation of H<sub>2</sub> and NH<sub>3</sub> with a sterically encumbered diaryl stannylene (Ar\*-Sn-Ar\* **J1**, Ar\* = 2,6-Dipp<sub>2</sub>-C<sub>6</sub>H<sub>3</sub>, Dipp = 2,6-*i*Pr<sub>2</sub>-C<sub>6</sub>H<sub>3</sub>,  $\angle$ C-Sn-C = 117.6°).<sup>44</sup> Later, they reported facile cleavage of CO, H<sub>2</sub>, and NH<sub>3</sub> with a bulky diaryl germylene (Ar\*-Ge-Ar\* **J2**,  $\angle$ C-Ge-C = 112.8°).<sup>45, 46</sup> In a seminal study, Matsuo and Tamao reported the first example of a germanium analog of a ketone, namely germanone [Eind<sub>2</sub>GeO] **J4** (Eind = 1,1,3,3,5,5,7,7-octaethyl-*s*-hydrindacen-4-yl), *via* activation of N<sub>2</sub>O with a bulky germylene Eind<sub>2</sub>Ge **J3**.<sup>47</sup> Few cyclic tetrylenes are also capable of activating small molecules. Activation of NH<sub>3</sub> or H<sub>2</sub>S with a  $\beta$ -diketiminato silylene [CH{(C=CH<sub>2</sub>)(CMe)Dipp<sub>2</sub>}Si] **J5**<sup>48</sup> and NH<sub>3</sub> by  $\beta$ -diketiminato germylene **J6** have also been reported.<sup>49</sup>

Another strategy to minimize HOMO-LUMO gaps is *via* the inclusion of bulky  $\sigma$ -donor ligands (e.g. silyl and boryl based ligand systems) to the E center, which destabilizes the HOMO and increases the triplet character.<sup>50, 51</sup> In 2012, Aldridge and Jones reported the ability of a boryl(amido)

## Tetrylene

silylene  $[\{\text{DippN}(\text{SiMe}_3)\}\{\text{NDippCH}_2\text{B}\}\text{Si}]$  **J7** to activate the H-H bond.<sup>51</sup> Further, density functional theory (DFT) calculations revealed a smaller singlet-triplet gap for the boryl(amido)silylene ( $103.9 \text{ kJ mol}^{-1}$ ) compared to diamido silylene  $[(\text{Me}_2\text{N})_2\text{Si}, 209.3 \text{ kJ mol}^{-1}]$ .<sup>51</sup> Thus, it clearly indicates the substituent effect on the Si(II) center and its consequence in reactivity. Later, they have thoroughly studied the ligand effect on the HOMO-LUMO gap of germynes **J8-11** (Figure 7).<sup>50</sup> The boryl substituted germylene **J11** was found to be the most reactive and unstable, as it readily undergoes intramolecular C-H bond activation.<sup>50</sup>

$m\text{-TerGeR}$	R	$\angle \text{C}^{m\text{-Ter-Ge-R}}$ ( $^\circ$ )	E (HOMO)	E (LUMO)	$\Delta E$ ( $\text{kJ mol}^{-1}$ )
<b>J8</b>	NHDipp	96.01	-528	-253	275
<b>J9</b>	$\text{CH}(\text{SiMe}_3)_2$	105.4	-471	-294	177
<b>J10</b>	$\text{Si}(\text{SiMe}_3)_3$	112.6	-446	-312	134
<b>J11</b>	$\text{B}(\text{NDippCH}_2)_2$	110.4	-424	-305	119

**Figure 7:** Electronic effect on the ground state of germylene.

Markedly,  $[(m\text{-Ter})\text{Ge}\{\text{Si}(\text{SiMe}_3)_3\}]$  **J10** ( $m\text{-Ter} = 2,6\text{-Mes}_2(\text{C}_6\text{H}_3)$ ,  $\text{Mes} = 2,4,6\text{-Me}_3\text{C}_6\text{H}_2$ ) is stable at room temperature with a moderate HOMO-LUMO gap ( $134 \text{ kJ mol}^{-1}$ ). Nevertheless, it is reactive enough that it can activate  $\text{H}_2$  and  $\text{NH}_3$ .<sup>50</sup> However, due to a large HOMO-LUMO gap  $m\text{-TerGe}(\text{NHDipp})$  **J8** was found to be inert towards  $\text{H}_2$  and  $\text{NH}_3$ .<sup>50</sup> Recently, our group demonstrated isolation of acyclic NHI-silylsilylene **J12** [NHI = N-heterocyclic imine,  $\{\text{DippNCH}_2\text{N}\}$ ], which inserted into the C=C bond of the aromatic ring of the NHI ligand leading to silepin formation **J13** at room temperature (Figure 8).<sup>52, 53</sup> Surprisingly, **J13** reverts back to the **J12** at low temperatures

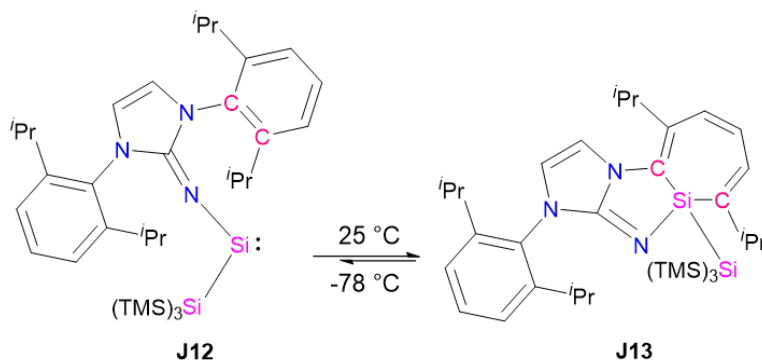


**Figure 8:** Steric and electronic effect on the ground state of silylene.

## Tetrylene

(-78 °C).<sup>52</sup> This reversible bond activation further allows the use of silepin **J13** as a synthetic equivalent of silylene **J12** in the activation of a range of small molecules (H<sub>2</sub>, NH<sub>3</sub> and CO<sub>2</sub>).<sup>52</sup> Strikingly, oxidation of bulky silyl substituted NHI-silylene [(<sup>t</sup>Bu<sub>3</sub>Si){(DippNCH)<sub>2</sub>N}Si] **J14** with N<sub>2</sub>O, led to the long desired neutral three coordinate silanone [(<sup>t</sup>Bu<sub>3</sub>Si){(DippNCH)<sub>2</sub>N}Si=O] **J15**.<sup>54</sup> Intriguingly, tin and lead homologs of carbon monoxide [{(RECH<sub>2</sub>)<sub>2</sub>C<sub>5</sub>H<sub>5</sub>N}E=O] (R = (C<sub>6</sub>H<sub>4</sub>)<sup>t</sup>BuCH<sub>2</sub>N<sub>2</sub>, E = Sn **J18**, Pb **J19**), was isolated from the reaction of corresponding bis-tetrylene {(RECH<sub>2</sub>)<sub>2</sub>C<sub>5</sub>H<sub>5</sub>N} (R = (C<sub>6</sub>H<sub>4</sub>)<sup>t</sup>BuCH<sub>2</sub>N<sub>2</sub>, E = Sn **J16**, Pb **J17**), and water.<sup>55</sup> Reversible activation of C=C (alkene),<sup>56-58</sup> P-P,<sup>59</sup> Si-H<sup>60</sup> and P-H<sup>60</sup> bonds with tetrylenes has also been achieved in the last few years (Figure 9).

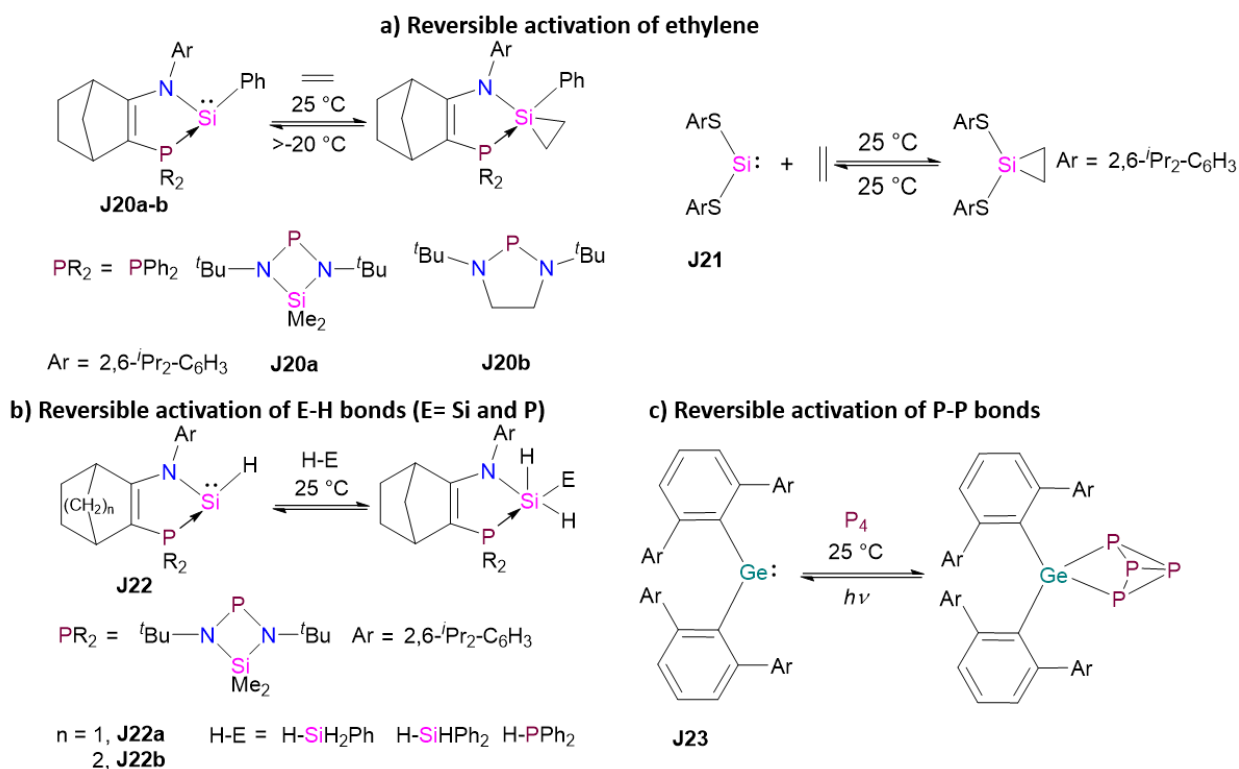


**Figure 9:** Selected examples of reversible small molecule activation with tetrylenes.

## 2.3. Catalytic application of tetrylenes

Beyond the activation of the small molecules, few tetrylenes have shown catalytic activities.<sup>9, 25</sup> In 2014, Jones and co-workers demonstrated the catalytic hydroboration of aldehydes and ketones with an acyclic amido-hydrido germylene **J24** and stannylene **J25** compound (Figure 10).<sup>21</sup> Interestingly, **J25** shows remarkable turn over frequency for this catalytic transformation,

## Tetrylene

and higher than known transition metal catalysts. The initial step involves *in situ* generation of E(II) [E = Ge or Sn] hydride complexes from the corresponding alkoxy E(II) complex (E = Ge or Sn) and HBpin, followed by hydrometallation of the carbonyl and release of the product (Figure 10). Later, the same group demonstrated the catalytic hydroboration of CO<sub>2</sub> to a methanol equivalent employing the same catalysts (**J24-25**).<sup>23</sup>

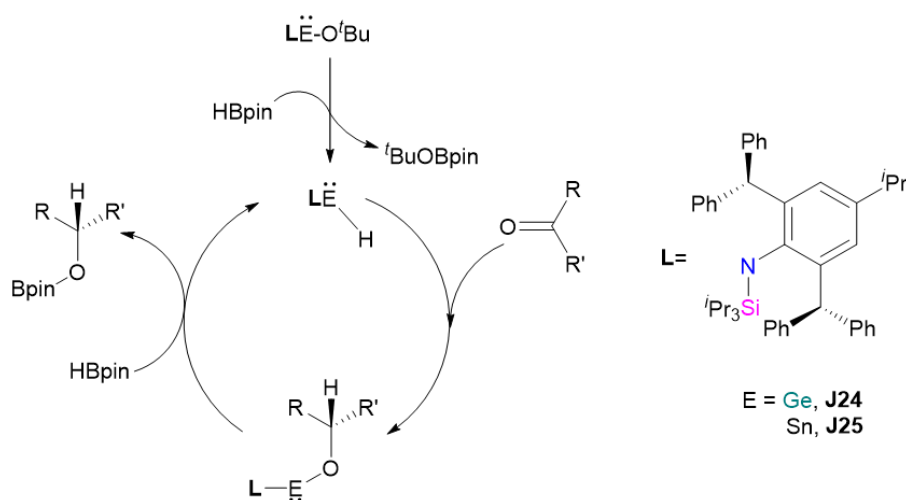


**Figure 10:** Catalytic hydroboration of ketones and aldehydes.

Catalytic hydroboration of aldehydes has also been demonstrated by tetrylene-phosphorus FLP **J26-28** and NHC-phosphinidanyl tetrylenes **J29-30**.<sup>61, 62</sup> Khan et al. reported N-heterocyclic germylene **J31** and stannylene **J32** catalyzed hydroboration and cyanosilylation of aldehydes.<sup>27</sup>

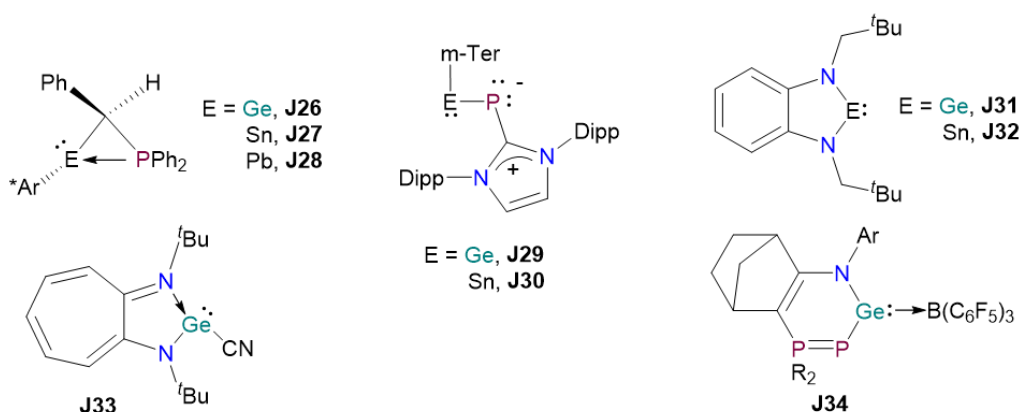


**Figure 11:** Tetrylene catalysts [ $\text{Ar}^* = 2, 6\text{-Tipp}_2\text{-C}_6\text{H}_3$ ,  $\text{Ar} = 2,6\text{-}i\text{Pr}_2\text{-C}_6\text{H}_3$  and  $\text{PR}_2 = \text{P}(i\text{BuN})_2\text{SiMe}_2$ ].

## Tetrylene

Nagendran et al. reported the utility of cyanogermylene **J33** toward cyanosilylation of aldehyde.<sup>22</sup> Very recently, Kato and co-workers have demonstrated the catalytic hydrosilylation of CO<sub>2</sub> with a N,P-heterocyclic germylene/BCF Lewis pair **J34**.<sup>24</sup>

### 3. Tetrylium ions $[\text{R}_3\text{E}]^+$

As a class of reactive intermediates, the chemistry of carbocations has been well established for more than a century.<sup>63</sup> Based on their valency, carbocations are classified as carbenium ions  $[\text{R}_3\text{C}]^+$  and carbonium ions  $[\text{R}_5\text{C}]^+$ .<sup>63, 64</sup> Carbenium ions are three coordinate, trigonal planar, and possess three valence electrons with one vacant 'p'-orbital and a cationic charge (Figure 12).<sup>63</sup> They generally appear as intermediates in  $\text{S}_{\text{N}}1$  reactions, and are often used as hydride abstraction reagents [e.g., trityl cation  $\{(\text{Ph}_3\text{C})^+(\text{BF}_4)^-\}$ ].<sup>63</sup>

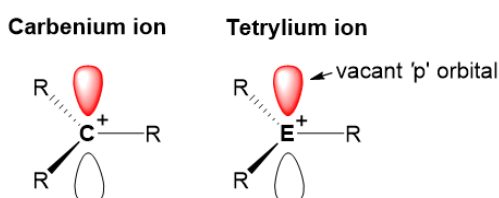


**Figure 12:** Carbenium and tetrylium ions (E = Si-Pb).

In contrast to carbenium ions, its heavier analogs "tetrylium ions"  $[\text{R}_3\text{E}]^+$ , [E = Si-Pb] are highly reactive species (Figure 12).<sup>4, 7, 8</sup> They are prone to react with any available nucleophiles, including inert solvents (e.g., arene) and even, counter anions. Thus, isolation of donor free  $[\text{R}_3\text{E}]^+$  complexes in the condensed phase is a challenging task. The "bonafide" silylium  $\{[\text{Mes}_3\text{Si}]^+\{\text{CB}_{11}\text{Me}_5\text{Br}\}^-\}$  **K1**,<sup>65</sup> germylium  $\{[\text{tBu}_2\text{MeSi}]_3\text{Ge}\}^+\{\text{B}(\text{C}_6\text{F}_5)_4\}^-$  **K2**,<sup>66</sup> and stannylum  $\{[\text{Tipp}]_3\text{Sn}\}^+\{\text{B}(\text{C}_6\text{F}_5)_4\}^-$  **K3**, Tipp = 2,4,3-*i*-Pr<sub>3</sub>-C<sub>6</sub>H<sub>2</sub>) ions were isolated almost a century after the first discovery of carbenium ions.<sup>67</sup> Isolation of tetrylium ions requires suitable kinetic protection together with a non-coordinating counter anion and non-coordinating solvent.<sup>4, 8, 68</sup>

#### 3.1. Classification of tetrylium ions

Tetrylium ions can be broadly categorized depending on the number of the organic substituent (R) attached to the E center, i.e., i) primary  $[\text{H}_2\text{RE}]^+$ , ii) secondary  $[\text{HR}_2\text{E}]^+$ , iii) tertiary  $[\text{R}_3\text{E}]^+$ , with the parent tetrylium ion  $[\text{H}_3\text{E}]^+$  only bearing hydrogen atoms.<sup>4, 8</sup> Tetrylium ions are highly electron-deficient species, and very often, they interact with donor and solvent. Thus, based on electronic stabilization they are further classified into the following groups (Figure 13).

## Tetrylium ions

- i) **Donor free:** These are known as a "true tetrylium ions," the electropositive **E** center is protected by a bulky aryl or silyl group to prevent the interaction with solvent and counter anion (Figure 13, compound **K1-3**).<sup>65-67</sup>
- ii)  **$\sigma$ -donor stabilized:** This is the standard type and generated *via* the interaction of electron-deficient **E** center with the donor atom of a solvent molecule<sup>69, 70</sup> **K4-6** or halogen atom from weakly coordinated counter anion (WCA) **K7**.<sup>68, 71</sup> Poor donors, such as the Si-H bond of hydro silane are also known to stabilize the electropositive **E** center by the end on Si-H-Si interaction, (Figure 13, compound **K8**).<sup>72</sup>
- iii)  **$\pi$ -donor stabilized:** These kinds of tetrylium ions are rare, and are supported by intermolecular interaction with aromatic  $\pi$ -bond (Figure 13, e.g., compound **K9**).<sup>71, 73</sup>
- iv) **Transition metal-stabilized:** Ferrocene stabilized tetrylium ions **K10** are a unique example of this particular class and possess distinct electronic features. DFT calculations reveal a pair of three centered- two-electron bonds between two Cp ring, Fe and Si center, which is a crucial factor in the remarkable stability of this complex.<sup>74</sup>

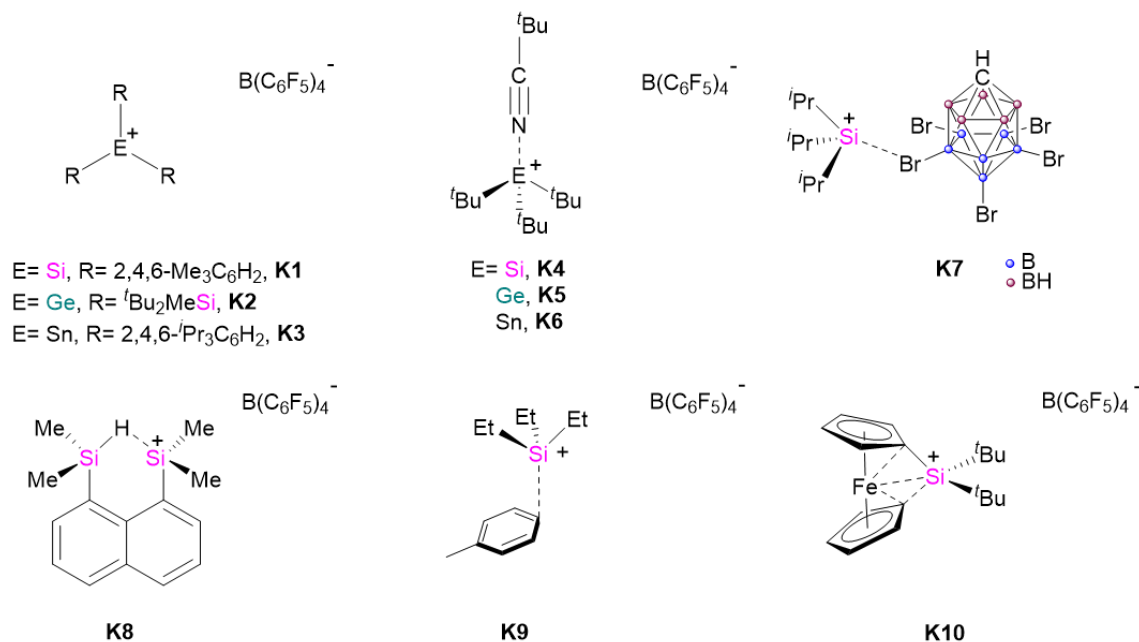


**Figure 13:** Classification of tetrylium ions.



### 3.2. Preparation of tetrylium ions

Tetrylium ions generally are prepared by electrophilic substrate abstraction from a tetra-coordinate E center.<sup>4, 8</sup> Abstraction of the hydride from R<sub>3</sub>EH by a trityl cation [Ph<sub>3</sub>C<sup>+</sup>] furnishes the corresponding [R<sub>3</sub>E]<sup>+</sup> ion (Figure 14a).<sup>4, 8, 75</sup> A plethora of tetrylium ions have been synthesized utilizing this methodology.<sup>4, 8, 75</sup> Other approaches that lead to tetrylium ions are dehydrogenative (Figure 14b) or dearylate proteolysis (Figure 14c).<sup>4, 8</sup> Recently, Oestreich et al. reported the donor stabilized parent-silylium ion **K13** in the condensed phase from the reaction of PhSiH<sub>3</sub> and [C<sub>6</sub>H<sub>6</sub>H]<sup>+</sup>[Br<sub>6</sub>CB<sub>11</sub>H<sub>6</sub>]<sup>-</sup> (Figure 14c).<sup>76</sup>

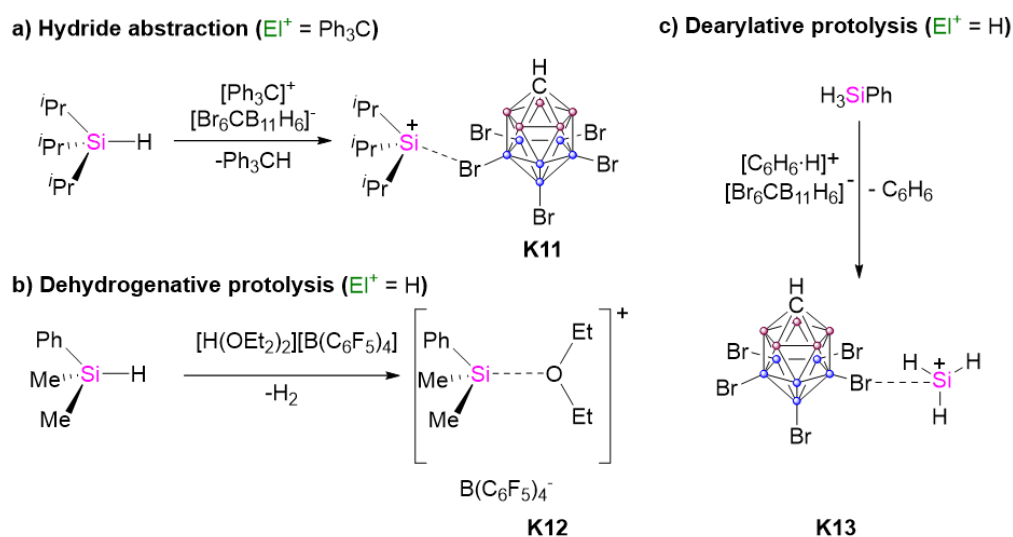


**Figure 14:** Diverse approaches to preparation of tetrylium ions ( $E^+$  = Electrophile).

The aforementioned procedures are limited to the synthesis of less sterically demanding tetrylium ions and often provide donor-stabilized cations. To overcome this obstacle, an allyl group abstraction trick was found as a fruitful approach (Figure 15a).<sup>65, 67</sup> Utilizing this strategy, Lambert and Reed reported bonafide silylium cation **K1**.<sup>65</sup> Similarly, Müller et al. reported the first example of donor free stannylum cation **K3**.<sup>67</sup> Another modern approach to access the donor-free tetrylium cation was proposed by Sekiguchi et al., who have synthesized bonafide germylium  $[(^tBu_2MeSi)_3Ge]^+ [B(C_6F_5)_4]^-$  **K2** and stannylum cation  $[(^tBu_2MeSi)_3Sn]^+ [B(C_6F_5)_4]^-$  **K14** via oxidation of corresponding tetryl radical  $[(^tBu_2MeSi)_3E]$ , E = Ge, Sn (Figure 15b).<sup>66</sup>

## Tetrylium ions

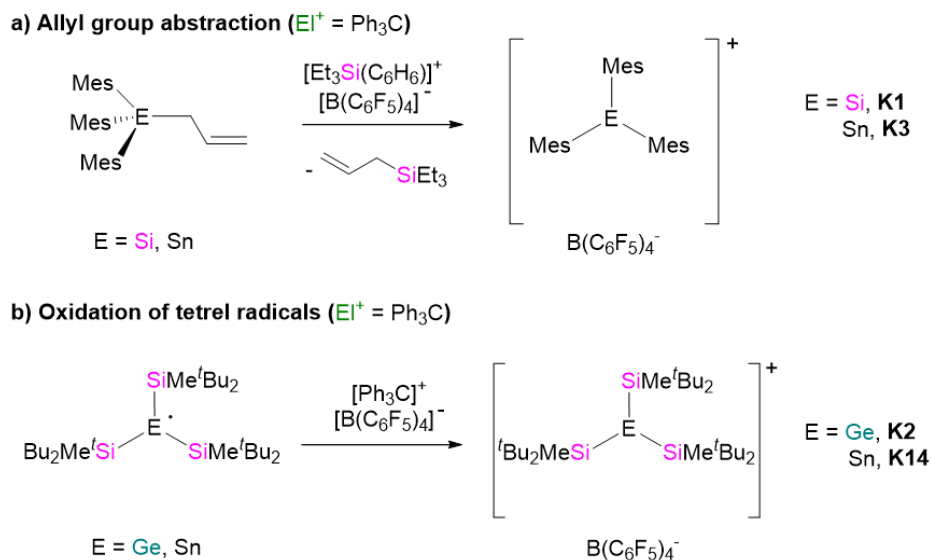


**Figure 15:** Unique approach to preparation of tetrylium ion ( $EI^+$  = electrophile).

### 3.3. Catalytic application of tetrylium ions

Among the tetrylium ions, silylium ions are a well-known catalyst for versatile application.<sup>4, 8</sup> Strong Lewis acidity of the silylium ions facilitate catalytic hydrodefluorination reactions, C-C cross-couplings and Diels-Alder reactions.<sup>4, 8, 77</sup>

**Catalytic hydrodefluorination of  $C(sp^3)$ -F bond:** In 2005, Ozerov and co-workers demonstrated the first silylium ion catalyzed hydrodefluorination of  $C(sp^3)$ -F bond.<sup>78</sup> The proposed mechanism follows two consecutive pathways (Figure 16). The initial step involves the silylium ion mediated fluoride abstraction of the C-F bond and generation of a carbocation. At the final step, the

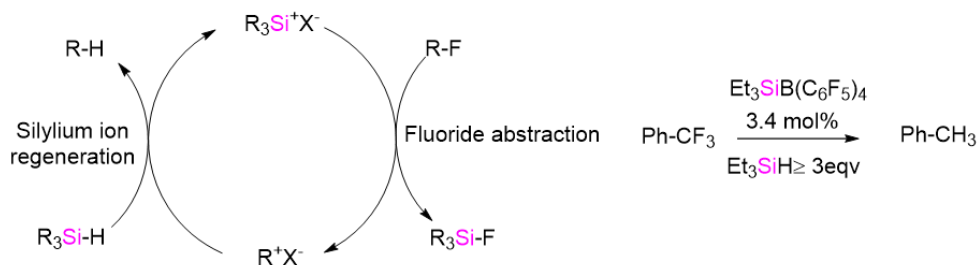


**Figure 16:** Schematic diagram of silylium ion catalyzed hydrodefluorination of  $C(sp^3)$ -F bond.

carbocation abstracts the hydride from silane and forms a C-H bond with the regeneration of silylium ion. The overall process is thermodynamically driven, as Si-F bonds ( $\approx 159 \text{ kcal mol}^{-1}$ ) are

## Tetrylium ions

more robust than C-F bonds ( $\approx 108 \text{ kcal mol}^{-1}$ ), and C-H bonds ( $\approx 100 \text{ kcal mol}^{-1}$ ) are more durable than Si-H bonds ( $\approx 90 \text{ kcal mol}^{-1}$ ).<sup>4</sup>

**Catalytic C-H arylation:** Silylium ion catalyzed C-C cross-coupling of aryl fluorides with arenes and alkanes have been reported.<sup>77, 79</sup> Siegel et al. reported the silylium ion catalyzed intramolecular C-C coupling of fluoroarenes.<sup>77</sup> Recently, Nelson et al. demonstrated the intermolecular silylium ion catalyzed C-C coupling reaction (Figure 17).<sup>79</sup> This C-H arylation is initiated *via* fluoride abstraction by  $[\text{Me}_3\text{Si}]^+$ , followed by C-H insertion reactions of the resulting phenyl cation. The  $\beta$ -silyl group in the fluoroarene substrate is key to this selective intermolecular transformation. On the one hand, the silyl group stabilizes the aryl cation intermediate and, on the other hand, serves as an internal silylium ion  $[\text{Me}_3\text{Si}]^+$  precursor.

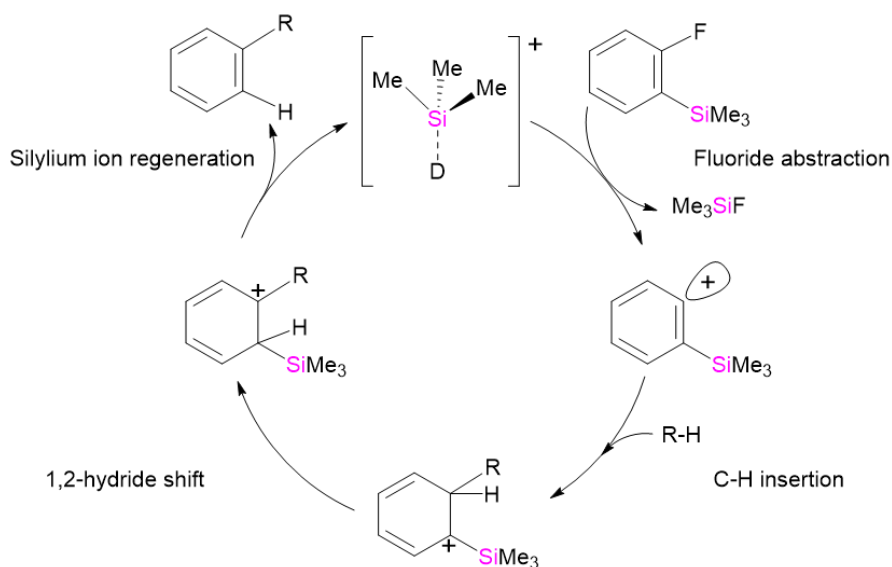


**Figure 17:** Schematic diagram of silylium ion catalyzed C-H arylation.

Recently catalytic hydrodefluorination of alkanes with a germylium ion  $[\{\text{Et}_3\text{Ge}\}^+\{\text{B}(\text{C}_6\text{F}_5)_4\}^-]$ <sup>80</sup> **K15** and versatile catalytic hydrogenation (imine, ketones and aldehyde) by stannylum ion  $[\{\text{Pr}_3\text{Sn}\}^+\text{OTf}^-]$  **K16** have been reported.<sup>81</sup>

## 4. Tetryliumylidene ions $[RE:]^+$

Tetryliumylidenes  $[R-E:]^+$  are mono coordinated E(II) cations, that possess a stereo chemically active lone pair and two vacant 'p'-orbitals.<sup>7</sup> Thereby, it combines the characteristics of highly electrophilic tetrylium cations (one empty 'p' orbital and cationic charge) and the Lewis ambiphilicity of tetrylenes (one empty 'p'-orbital and one lone pair) (Figure 18), which can be used in a wide range of synthetic and catalytic applications.

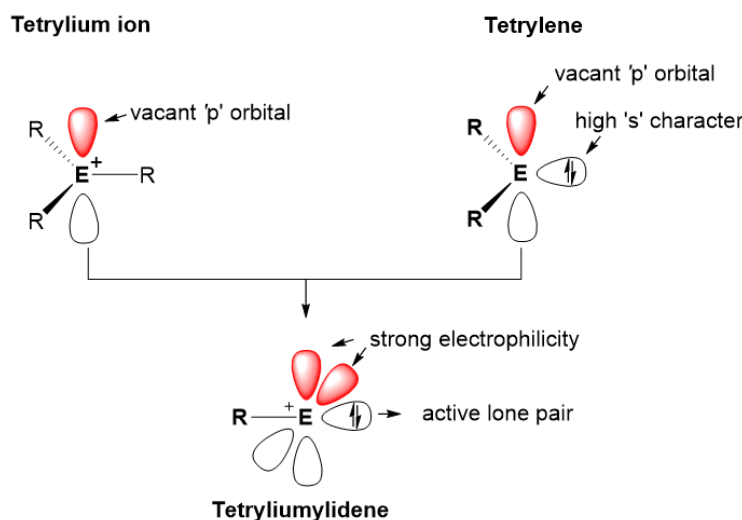


**Figure 18:** Electronic features of tetryliumylidenes.

The unique electronic features enhance the reactivity of tetryliumylidenes in comparison to both tetrylium ions and tetrylenes. Thus, isolation of tetryliumylidenes in the condensed phase is a challenging task that requires precise ligand design (kinetic and thermodynamic stabilization), a non-coordinating counter anion, and a non-coordinating solvent.<sup>68</sup> One-coordinate tetryliumylidene  $[R-E:]^+$  could have only been observed as short lived intermediates in the gas phase as well as in the solar spectrum,<sup>82, 83</sup> neither kinetic stabilization nor electronic stabilization is found to be adequate to stabilize them in the condensed phase.<sup>84</sup> To enable their isolation, donor stabilization from a Lewis base is mandatory to minimize the electrophilicity of E center *via* partially occupying the 'p'-orbitals (Figure 19).<sup>7</sup> Depending on the coordination, tetryliumylidenes are classified into three subclasses, i) two, ii) three and iii) poly coordinate or nido cluster types.

## Tetryliumylidene ions

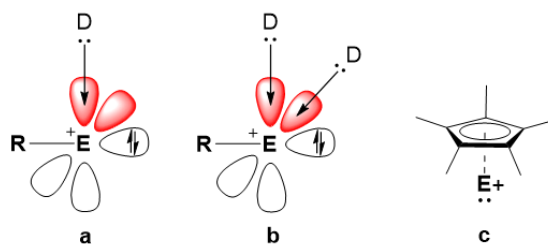


Figure 19: Two, three and poly coordinate tetryliumylidenes.

### 4.1. Silyliumylidene ions $[\text{RSi}]^+$

The first example of silyliumylidene was introduced by the group of Jutzi, who succeeded the isolation of a nido cluster type silyliumylidene **L1**  $\{[\eta^5\text{-C}_5\text{Me}_5\text{Si}]^+\{\text{B}(\text{C}_6\text{F}_5)_4\}^-\}$ , *via* protonation of decamethylsilicocene  $\{(\eta^5\text{-C}_5\text{Me}_5)_2\text{Si}\}$  with  $[(\text{Me}_5\text{C}_5\text{H}_2)^+\{\text{B}(\text{C}_6\text{F}_5)_4\}^-]$ .<sup>85</sup> The stability of **L1** was

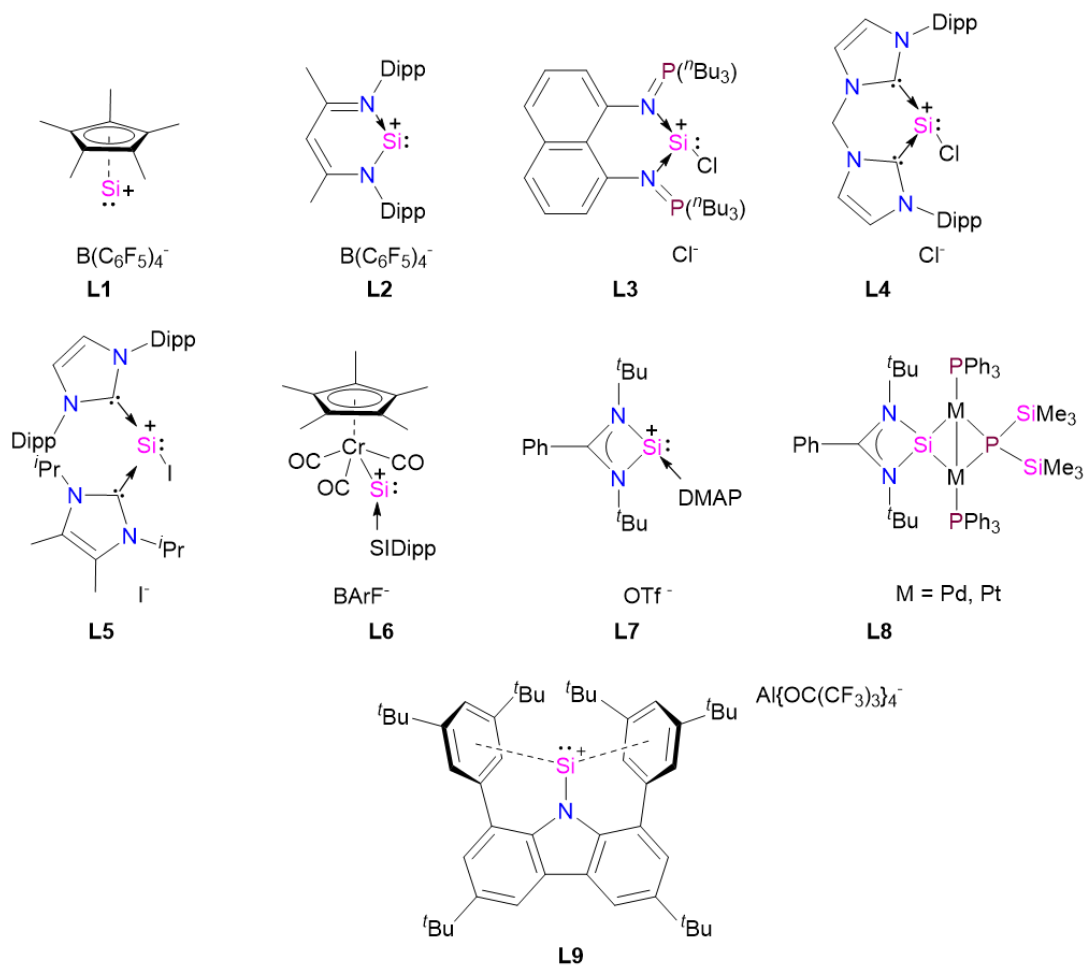


Figure 20: Selected examples of silyliumylidene ions.

associated with the strong  $\pi$ -complexation with ( $\eta^5$ -C<sub>5</sub>Me<sub>5</sub>) ligand, which was markedly reflected by the upfield shift of the Si(II) atom ( $\delta = -400.2$  ppm) in the <sup>29</sup>Si NMR spectrum. In 2006, Driess and co-workers demonstrated the first example of two coordinate N-heterocyclic silyliumylidene **L2**,<sup>86</sup> synthesized through protonation of the ligand backbone of  $\beta$ -diketiminato silylene. Compound **L2** is stabilized by  $6\pi$  electron delocalization and intramolecular donation from the N-atom of the sterically encumbered  $\beta$ -diketiminato ligand.<sup>86</sup> Notably, in the <sup>29</sup>Si NMR spectrum, compound **L2** ( $\delta = 40.5$  ppm) exhibits a strong downfield shift in contrast to compound **L1** ( $\delta = -400.2$  ppm), indicating the deshielded Si(II) nuclei and more Lewis acidic character compared to **L1**.

The application of NHCs in the stabilization of low valent main group centers has contributed to the renaissance era of main group chemistry.<sup>36</sup> In this regard, the year 2009 is highly significant. This year Roesky et al. achieved the isolation of IDipp·SiCl<sub>2</sub> from the simple reaction of two equivalents of the NHC·IDipp with HSiCl<sub>3</sub>.<sup>34</sup> Later, IDipp·SiCl<sub>2</sub> was widely utilized as a raw Si(II) precursor in the synthesis of a range of low valent silicon compounds.<sup>34</sup> For example, *via* a ligand exchange method, reaction with a chelating ligand and IDipp·SiCl<sub>2</sub>, yielded a bis(iminophosphorane) and a bis-NHC ligand substituted chloro silyliumylidene complex, **L3** and **L4** respectively.<sup>87, 88</sup> Subsequently, Filippou et al., found that the treatment of <sup>i</sup>Pr<sub>2</sub>Me<sub>2</sub> with IDipp·SiI<sub>2</sub> resulted in the displacement of one iodide providing a different NHC substituted acyclic silyliumylidene **L5** [(IDipp)(<sup>i</sup>Pr<sub>2</sub>Me<sub>2</sub>)SiI]<sup>+I<sup>-</sup></sup>.<sup>35</sup> Later, the same group reported the electron rich transition metal substituted Si(II) cation **L6**, which showed a remarkable downfield NMR shift ( $\delta = 828.6$ ) in the <sup>29</sup>Si NMR spectrum.<sup>89</sup> Besides these examples, other silyliumylidene complexes such as DMAP-stabilized amidinate silyliumylidene **L7** and transition metal anchored [PhC(N<sup>t</sup>Bu)<sub>2</sub>Si{M-(PPh<sub>3</sub>)<sub>2</sub>P(SiMe<sub>3</sub>)<sub>2</sub>}] (**M** = Pd and Pt) **L8** and quasi-mono-coordinate silyliumylidene compound **L9** have been reported (Figure 20).<sup>90-92</sup>

Monoanionic bulky aryl ligands are sterically tunable by varying the wingtip substituents. Thereby, aryl ligands are widely used to stabilize the low valent group 14 molecules.<sup>3, 15, 93</sup> In 2014, with the combination of sterically encumbered aryl substituent and NHCs, the group of Tokitoh, Sasamori, Matsuo, as well as the Inoue group independently demonstrated access to

## Tetryliumylidene ions

various tricoordinate NHC-stabilized aryl-silyliumylidene complexes (Figure 21).<sup>94, 95</sup> Tokitoh et al., succeeded in the isolation of **L10-12** via the treatment of corresponding bromo disilene with four equivalents of IMe<sub>4</sub> (1,3,4,5-tetramethylimidazol-2-ylidene) (Figure 21a).<sup>94</sup> At a similar time, Inoue and co-workers contribution reported the facile access of **L13** and **L14**, through the reaction of corresponding aryl silane (m-TerSiHCl<sub>2</sub> and TippSiHCl<sub>2</sub>) with three equivalent of IMe<sub>4</sub> as the dehydrochlorination reagent.<sup>95</sup> Strikingly, this is the first example where silyliumylidene

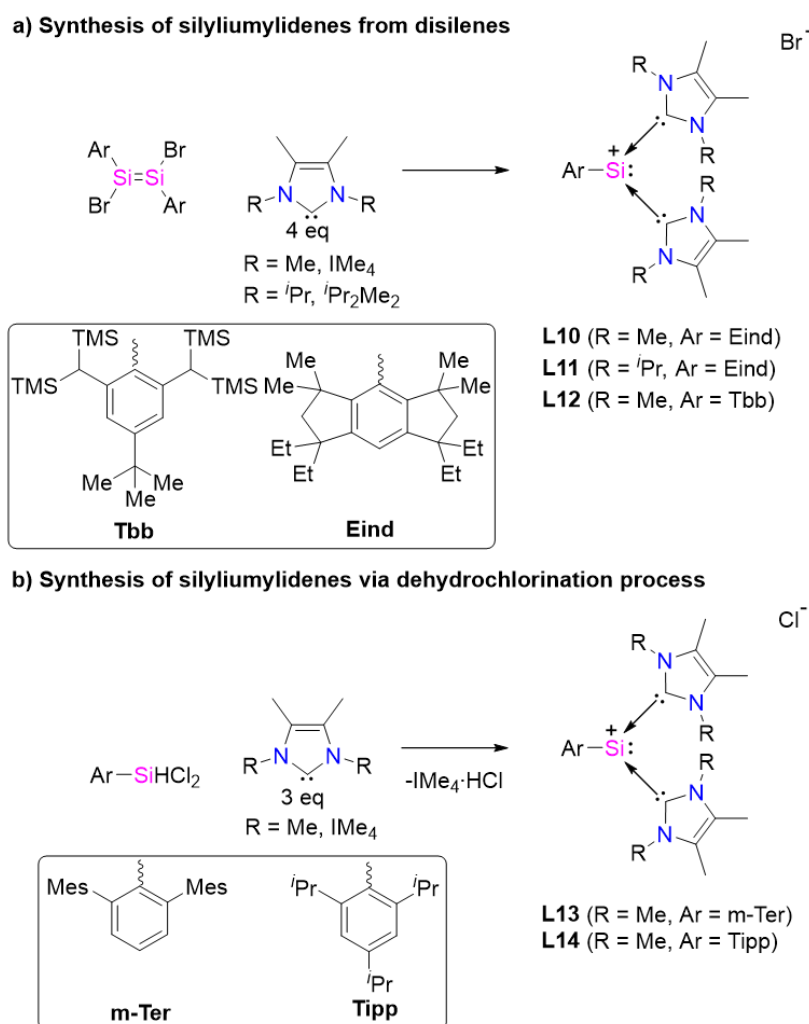


**Figure 21:** Synthesis of NHC stabilized aryl substituted silyliumylidenes.

was directly prepared from a Si(IV) precursor. Following an analogous strategy, bulky silyl-substituted silyliumylidene complexes [{{<sup>t</sup>Bu<sub>3</sub>Si}Si(IMe<sub>4</sub>)<sub>2</sub>}<sup>+</sup>Cl<sup>-</sup>], [{{<sup>t</sup>Bu<sub>2</sub>MeSi}Si(IMe<sub>4</sub>)<sub>2</sub>}<sup>+</sup>Cl<sup>-</sup>] and [{{<sup>t</sup>Bu<sub>2</sub>MeSi}Si(*i*Pr<sub>2</sub>Me<sub>2</sub>)<sub>2</sub>}<sup>+</sup>Cl<sup>-</sup>] have been reported.<sup>96</sup> Very recently, an important milestone was

achieved by So et al., where the  $\text{IMe}_4$  stabilized parent silyliumylidene  $[\{\text{H-Si}(\text{IMe}_4)_2\}^+\text{I}^-]$  was obtained from the reaction of  $[\text{IDippSiI}]_2$  and  $\text{IMe}_4$ .<sup>97</sup> Also, DFT calculations revealed that the initial step involved the generation of a highly reactive bis-  $\text{IMe}_4$  stabilized Si(I) radical cation intermediate, which subsequently abstracts the proton from solvent (toluene) to yield  $[\{\text{H-Si}(\text{IMe}_4)_2\}^+\text{I}^-]$ .<sup>97</sup>

## 4.2. Reactivity of silyliumylidene ions

Silyliumylidene undergoes salt-metathesis reactions with metal salts, due to the weakly coordinating counter anion. In this regard, **L1** has revealed to be a very useful precursor to prepare functionalized low valent silicon compounds (Figure 22-23).<sup>98</sup> Jutzi and co-workers achieved an asymmetric disilene  $\text{E}-[\{\eta^1\text{-Me}_5\text{C}_5\}\{\text{N}(\text{TMS})_2\}\text{Si}]_2$  **L16** *via* the direct treatment of  $\text{LiN}(\text{TMS})_2$  with **L1**.<sup>85</sup> Later they discovered that compound **L16** was in dynamic equilibrium with the silylene  $(\text{Me}_5\text{C}_5)\text{SiN}(\text{TMS})_2$  **L15** in solution, due to the low energy barrier between **L15** and **L16**.<sup>99</sup> The first aryl-substituted monomeric Si(II) species **L17**, was also prepared from **L1**.<sup>100</sup>

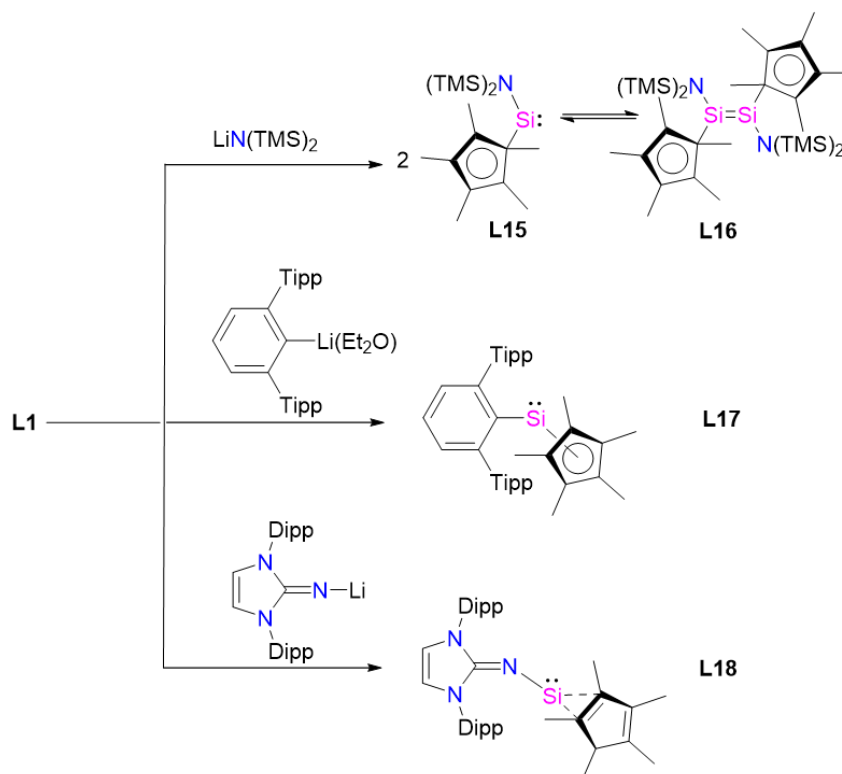


**Figure 22:** Silyliumylidene **L1** as a precursor to low valent silicon compounds (TMS =  $\text{SiMe}_3$ ).



## Tetryliumylidene ions

Our group reported the bulky imino-substituted acyclic silylene **L18** from the reaction of  $\text{Li}[\text{NC}\{\text{N}(\text{Dipp})\text{CH}_2\}_2]$  and **L1**.<sup>101</sup>

However, the reactivity with  $\text{Li}[\text{HC}(\text{CMeNDipp})_2]$  and **L1** did not afford the desired N-substituted silylene  $[(\text{C}_5\text{Me}_5)\{\text{HC}(\text{CMeNDipp})_2\}_2\text{Si}]_2$ , instead it undergoes further reaction to form a tricyclic Si(IV) constitutional isomer **L19**.<sup>102</sup> The substitution reaction with the lithium disilenide  $[\text{Tipp}_2\text{Si}=\text{Si}(\text{Tipp})(\text{Li}\{\text{dme}\}_2)]$  led to the first carbon-based substituent cyclotrisilene **L20**.<sup>103</sup> The same group later utilized **L1** as a stoichiometric source for the synthesis of the neutral silicon cluster **L21**.<sup>104</sup> Compound **L1** was also utilized for the synthesis of a metal-substituted silylene.<sup>105</sup> Interestingly, the reaction of **L1** with  $\text{Na}[\text{Fe}(\eta^5\text{-C}_5\text{Me}_5)(\text{CO})_2]$  gave rise to a ferrio-substituted silylene  $[\text{Fe}(\eta^5\text{-C}_5\text{Me}_5)(\text{CO})_2\{\text{Si}(\eta^3\text{-C}_5\text{Me}_5)\}]$  **L22**, which was stable at low temperatures ( $-30\text{ }^\circ\text{C}$ ).<sup>105</sup> However, under ambient conditions, **L22** converted to product **L23** via C-H bond activation of one of the Cp\* methyl groups.<sup>105</sup>

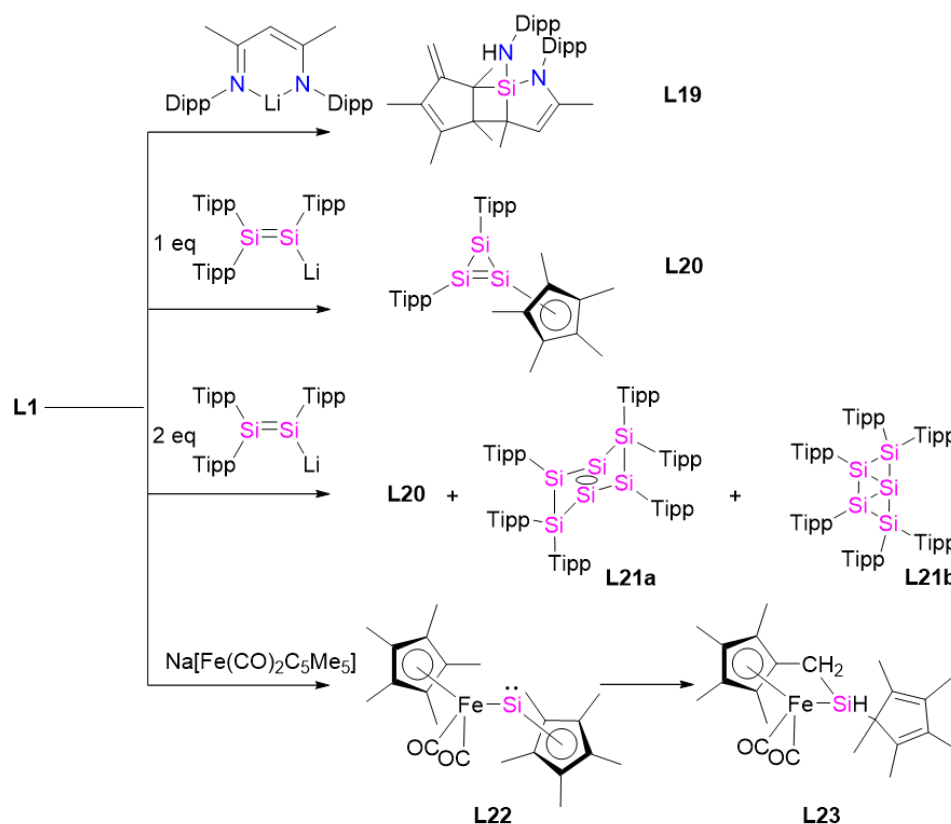


**Figure 23:** Salt metathesis reactivity of silyliumylidene **L1**.

## Tetryliumylidene ions

Driess et al. demonstrated the easy access to a Si(0) complex (silylone) from silyliumylidene **L4** (Figure 24).<sup>88</sup> The reduction of compound **L4** in the presence of two equivalents of sodium naphthalenide ( $\text{NaC}_{10}\text{H}_8$ ) yields the bis-NHC stabilized cyclic silylone **L24**.<sup>88</sup>

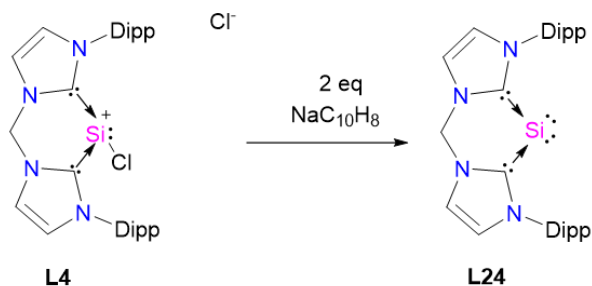


**Figure 24:** Synthesis of silylone from silyliumylidene.

So et al. demonstrated unique reactivities of a DMAP stabilized silyliumylidene complex **L7** (Figure 25): addition of **L7** to a bis-silylene resulted in the formation of the first example of bis-silylene substituted silylium cation **L25**.<sup>90</sup> Further, reduction of **L7** using K-selectride yielded the silyl- silylene complex **L26**.

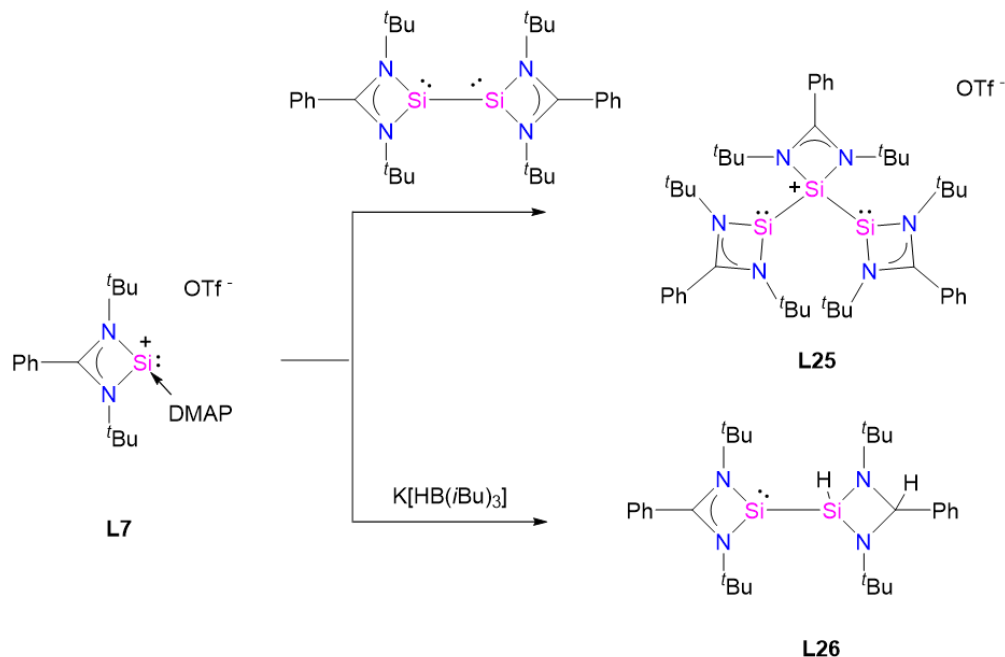


**Figure 25:** Reactivity of silyliumylidene **L7**.

### 4.3. Small molecule activation by silyliumylidenes

The nucleophilicity of silyliumylidene was applied to activate various small molecules. The activation of elemental sulfur with **L3** and **L7** leads to the base stabilized silathionium complex  $[(C_5H_3)P^nBu_3]_2SiS]^+Cl^-$  **L27** and  $[CHPh(NC^tBu)_2]SiS]^+OTf^-$  **L28**, respectively.<sup>87, 90</sup> While, Filippou's metal-substituted silyliumylidene  $[(\eta^5-C_5Me_5)(CO)_3CrSi(SiDipp)]^+[BAR^F_4]^-$  **L6** reacts with  $N_2O$  to give the first example of three coordinate silanone  $[(\eta^5-C_5Me_5)(CO)_3CrSiO]^+[BAR^F_4]^-$  **L29**.<sup>89</sup>

Inoue et al., have employed their silyliumylidenes **L13-14** in a variety of small-molecule activation reactions, ranging from C–H bonds in terminal alkynes, chalcogens, to small gaseous molecules such as  $CO_2$  and  $H_2S$  (Figure 26).<sup>106</sup> In 2014, Inoue and co-workers demonstrated terminal C-H bond activation of phenyl acetylene to yield **L30** as the Z-isomer.<sup>95</sup> Further fascinating reactivity of **L13-14** with  $CO_2$  led to the silicon analog of the acylium ion  $[R-C=O]^+$  **L31-32** and elimination of  $CO$ .<sup>107</sup>

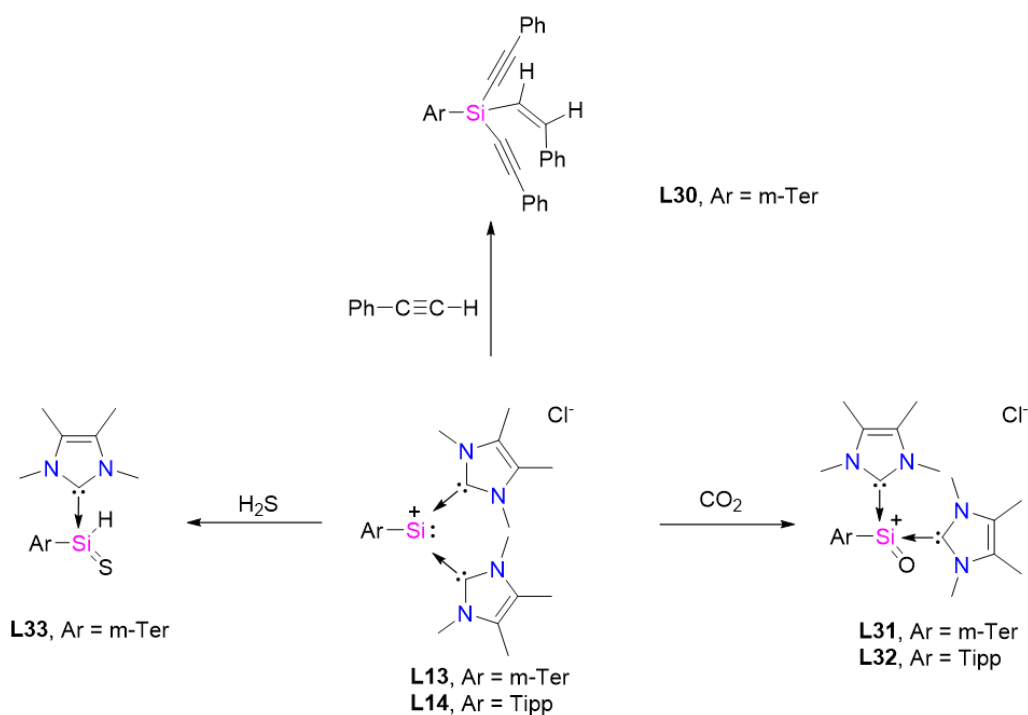


**Figure 26:** Reactivity of silyliumylidene **L13** and **L14** with small molecules.

Notably, **L32** was only stable up to  $-30\text{ }^{\circ}\text{C}$ , as, under ambient conditions, decomposition occurs due to decreased kinetic stabilization (*m*-Ter vs. Tipp).<sup>107</sup> Interestingly, the reactivity of **L13** with  $\text{H}_2\text{S}$  led to the donor stabilized heavier sulfur analog of silaaldehyde  $[\{m\text{-TerSi(S)H}\}(\text{IME}_4)]$  **L33**.<sup>108</sup>

#### 4.4. Silyliumylidenes in catalysis

In 2011, Jutzi et al. manifested the usability of silyliumylidene **L1** as a catalyst for the degradation of oligoethers into dioxane and mono ethers (Figure 27).<sup>109</sup> DFT calculations revealed that the  $\text{O}\rightarrow\text{Si}$  dative bond in the  $\text{DME}\cdot\text{L1}$  complex is electrostatic. The subsequent enhancement of positive charge induces a rearrangement of the  $\sigma$ -bond and lone-pair electrons in the framework of the two DME molecules, which leads to the formation of dimethyl ether and diglyme. Then, the diglyme molecule degraded similarly to 1,4-dioxane and dimethyl ether, and the catalyst **L1** is regenerated. Compound **L1** has also been utilized in the catalytic hydrosilylation of terminal alkenes and alkynes (Figure 28).<sup>110</sup> The proposed mechanism proceeds through initial

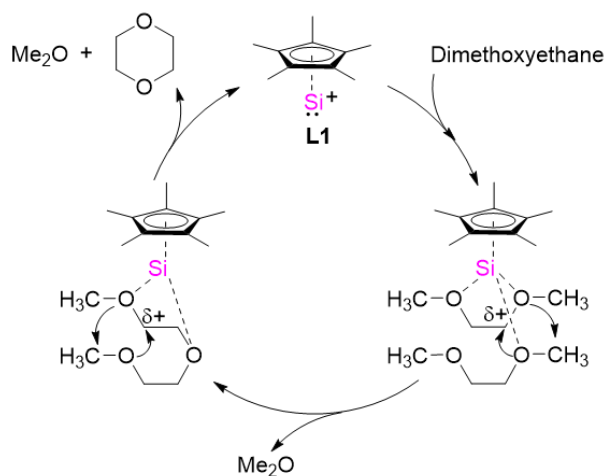


**Figure 27:** Silyliumylidene **L1** catalyzed degradation of oligoethers into dioxane.

coordination of the Si-H bond to the Lewis acidic Si center, followed by the insertion of alkene/alkyne and release of the product. This catalytic process was found to be useful for a range of alkene/alkynes, leading to the selective *anti*-Markovnikov product under ambient conditions with low catalyst loadings (0.1-0.001 mol %). In the same article, the authors described the **L1** catalyzed Si/O coupling between hydrosilane and silyl ether (Piers-Rubinsztajn reaction),

## Tetryliumylidene ions

which was hitherto only possible with  $B(C_6F_5)_3$ . Notably, this reaction is significant for the production of industrially valuable metal-free elastomer and branched silicones.<sup>110</sup>

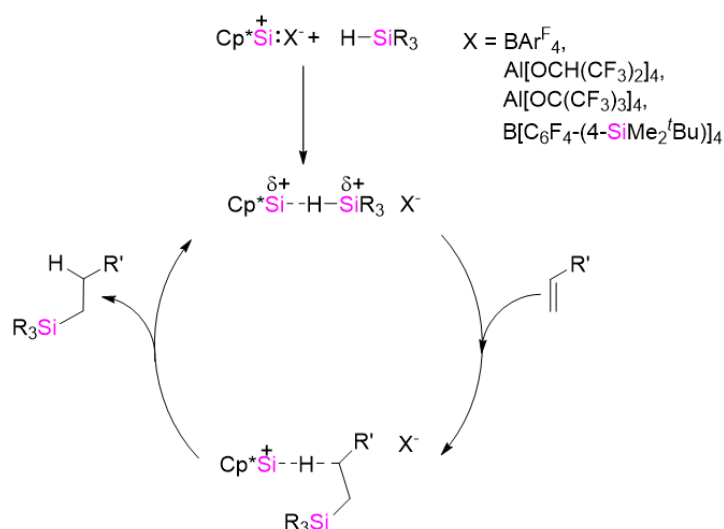


**Figure 28:** Silyliumylidene **L1** catalyzed hydrosilylation of the alkene.

Recently, So and co-workers introduced  $[H-Si(IME_4)_2]^+I^-$  as a catalyst for hydroboration of  $CO_2$ , aldehydes, ketones, and pyridines.<sup>28</sup> *Ab initio* calculations suggested that the hydroboration of  $CO_2$  proceeds *via* a Lewis base-catalyzed pathway, where the coordination of the silicon lone pair to  $CO_2$  facilitates the catalytic turnover. However, with the exception of aldehydes, reduction of ketones and pyridines require high catalyst loadings and temperatures to ensure complete conversion.

## 4.5. Germyliumylidenes and stannylumylidenes

In contrast to silicon, germanium and tin are considerably stable at the +II oxidation state due to the larger energy gap between 's'- and 'p'- orbitals. Therefore, isolation of germyliumylidenes and stannylumylidenes is somewhat easier in the condensed phase. Typical synthetic routes involve dehalogenation of the germynes and stannynes, rendering the corresponding germyliumylidene and stannylumylidene. It is of note that the chemistry of **E(II)** cations (**E** = Ge and Sn) were developed in parallel and often utilizing a similar ligand framework.

The first example of a germyliumylidene  $[(\eta^5-C_5Me_5)Ge]^+BF_4^-$  **L34** and stannylumylidene  $[(\eta^5-C_5Me_5)Sn]^+BF_4^-$  **L35** was reported in the 1980s, almost two decades before the isolation of the

## Tetryliumylidene ions

silyliumylidene **L1** (Figure 29).<sup>111</sup> Compound **L34** and **L35**, were isolated *via* reacting the corresponding tetrylene [ $\text{Cp}_2^*\text{E}$ ,  $\text{E} = \text{Ge}$  and  $\text{Sn}$ ] with  $\text{HBF}_4$ .<sup>111</sup> Later,  $\text{Ge(II)}$  **L36** and  $\text{Sn(II)}$  cation of [2.2.2] paracyclophane **L37** were reported.<sup>112</sup> Notably, these compounds were embedded with threefold internal  $\eta^6$ -coordination.<sup>112</sup> However, in **L34-37** the Lewis acidity of the **E** center was partially quenched by the coordination from halogen substituent of the WCA.

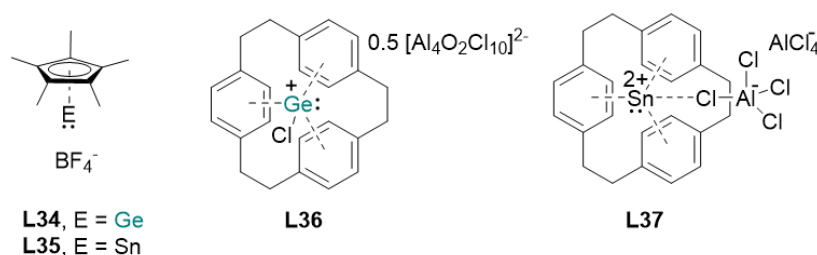


**Figure 29:**  $\text{Ge(II)}$  and  $\text{Sn(II)}$  cations embedded within aromatic ring systems.

In 1996, Reger reported a poly(pyrazole)borate substituted  $\text{Ge(II)}$  cation **L38** with an iodide counter anion.<sup>113</sup> The shortest  $\text{Ge}\cdots\text{I}$  distance in this complex was found to be longer than the sum of the covalent radii, further supporting the lack of a covalent interaction between  $\text{Ge}$  and  $\text{I}$ . This investigation kick-started the use of monoanionic N-donor ligands in the field of tetryliumylidene chemistry.<sup>7</sup> Later, several groups have stabilized low valent  $\text{Ge(II)}$  and  $\text{Sn(II)}$  centered cations by employing various monoanionic bulky N-donor ligands, such as aminotroponiminato **L39-41**,<sup>114, 115</sup>  $\beta$ -diketiminato **L42-43**,<sup>116-119</sup> chiral (1,1-bis[(4S)-4-phenyl-1,3-oxazolin-2-yl]ethane) **L44**, **L45** and **L46-47**.<sup>120-122</sup> In 2012, Jones and Krossing synthesized quasi-mono coordinate  $\text{Ge(II)}$  and  $\text{Sn(II)}$  cations using a bulky amido ligand **L48-L49**.<sup>123</sup> Dehalogenation of the monomeric amido germanium and tin chloride by  $\text{LiAl}[\text{OC}(\text{CF}_3)_3]_4$  or  $\text{AgAl}[\text{OC}(\text{CF}_3)_3]_4$  led to the formation of the desired complex.<sup>123</sup> Further, SC-XRD revealed a  $\eta^2$ -interaction between the metal center and flanking arene moiety, which is diminished by the addition of a Lewis base (DMAP) **L50-51**.<sup>123</sup> Very recently, pseudo-mono coordinated  $\text{Ge(II)}$  and  $\text{Sn(II)}$  cation **L52-53** were stabilized by a bulky carbazolyl moiety.<sup>124</sup> Besides these examples, mono and dicationic  $\text{Ge(II)}$  and  $\text{Sn(II)}$  cations stabilized by crown ether or cryptand ligand were reported (Figure 30).<sup>125-128</sup>

## Tetryliumylidene ions

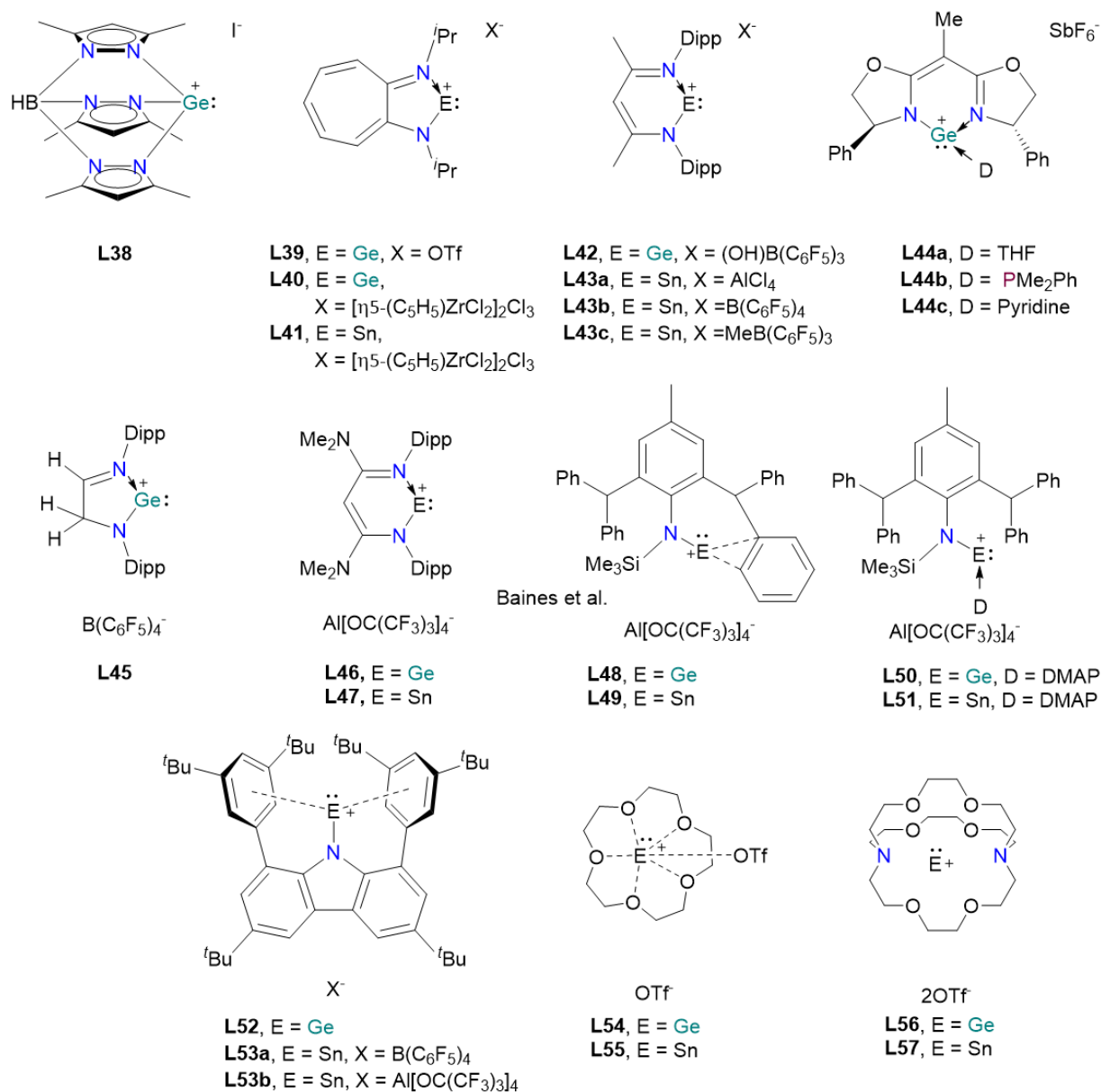


**Figure 30:** Monoanionic N-donor substituted Ge(II) and Sn(II) cations.

The isolation of halogen-substituted germyliumylidenes and stannylumylidenes have received attention.<sup>7</sup> They can be easily functionalized by salt metathesis and also serve as a precursor for the synthesis of other low valent Ge and Sn compounds.<sup>7</sup> This can be accomplished using the ancillary ligands, such as NHC or neutral bidentate N-ligands.<sup>7</sup> Analogous to the synthesis of **L3**

## Tetryliumylidene ions

and **L4**,<sup>87, 88</sup> the reaction of  $\text{GeCl}_2 \cdot \text{dioxane}$  with imidophosphorane and bis-NHC gave rise to compound **L58** and **L59**.<sup>129, 130</sup> Fascinatingly, reduction of **L59** in the presence of sodium naphthalenide led to the first example of a  $\text{Ge}(0)$  complex (germylone).<sup>130</sup> Very recently, the group of Driess reported the parent germyliumylidene **L60**, which is stabilized by a borate

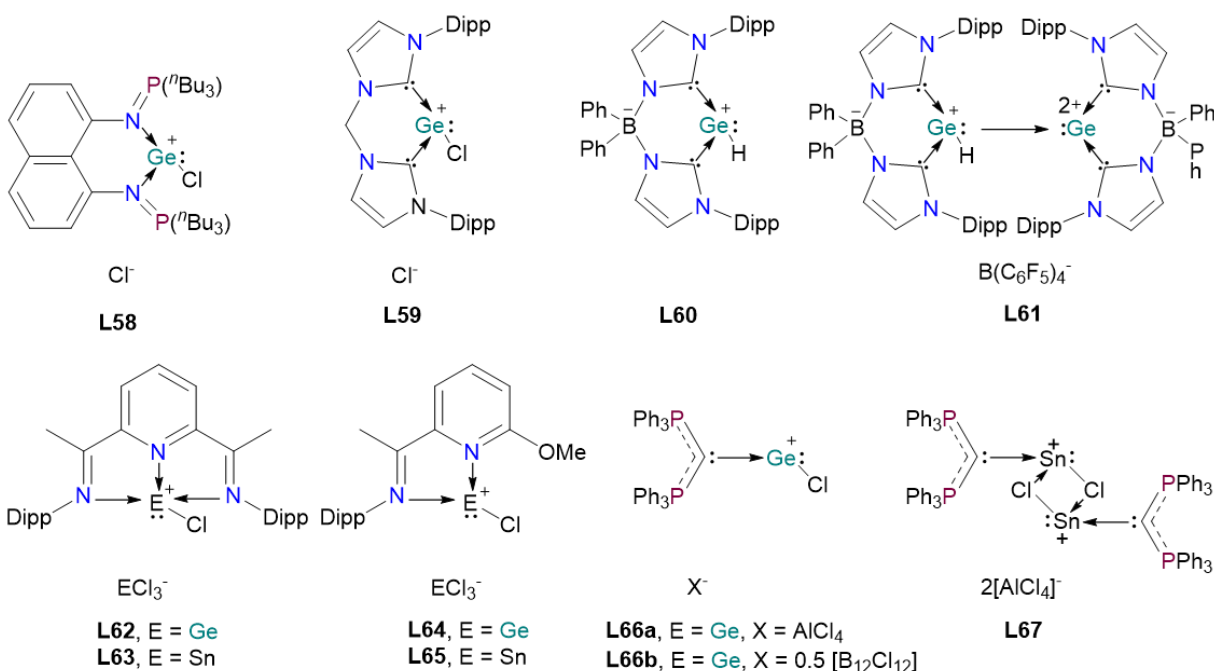


**Figure 31:** Ge(II) and Sn(II) cations stabilized by neutral ligands.

spacer based bis-NHC system.<sup>131</sup> Compound **L60** showed intriguing reactivity with the trityl cation  $[(\text{Ph}_3\text{C})^+\{\text{B}(\text{C}_6\text{F}_5)_4\}^-]$ , *via* deprotonation, it led to the unprecedented  $[\text{HGe}^+ \rightarrow \text{Ge}^{2+}]$  complex **L61**.<sup>131</sup> Roesky, Stalke et al. demonstrated the isolation of **L62** and **L63** through an autoionization method.<sup>132</sup> The direct reaction of the Schiff base 2,6-diacetylpyridinebis-(2,6-diisopropylanil) with the corresponding dihalides ( $\text{GeCl}_2 \cdot \text{dioxane}$  and  $\text{SnCl}_2$ ) led to the desired cationic complexes.<sup>132</sup> Similarly, compounds **L64** and **L65** were reported by the group of Jambor.<sup>133</sup> It has to be noted that complexes **L58-65** are either three or four coordinate. The two coordinate neutral monoanionic  $[\text{L} \rightarrow \text{GeCl}]^+$  species was unknown until the report of the Alcarazo et al., who demonstrated the two-coordinate  $[\text{GeCl}]^+$  cation, which is stabilized by simultaneous  $\sigma$ - and  $\pi$ -donation from a monodentate carbodiphosphorane ligand **L66**.<sup>134</sup> However,  $[\text{L} \rightarrow \text{SnCl}]^+$  are not stable species in the monomeric form and therefore **L67** is isolated as a dimer.<sup>134</sup>



## Tetryliumylidene ions

Another modern approach to stabilize extremely electrophilic Ge(II) and Sn(II) cations involve electronic stabilization. In this approach, instead of a bulkier organic ligand, an electron-rich coordinatively unsaturated transition metal fragment was employed for the synthesis of **L68** and **L69** (Figure 32).<sup>135, 136</sup>

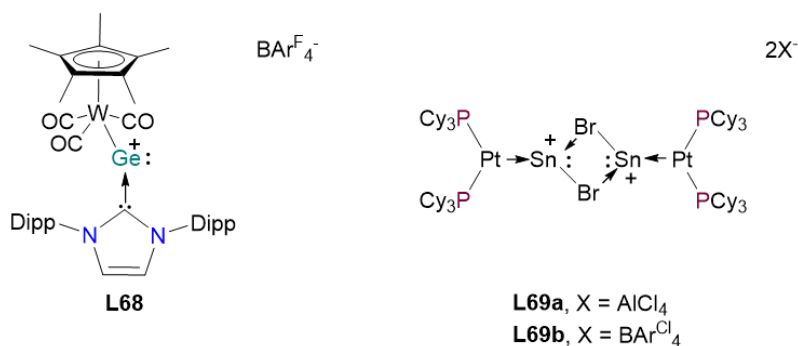


**Figure 32:** Ge(II) and Sn(II) cations stabilized by transition metals [ $\text{BAr}^{\text{Cl}}_4 = \text{B}(3,5\text{-Cl}_2\text{-C}_6\text{H}_3)_4$ ].

Examples of aryl-substituted Sn(II) cations are limited and Ge(II) cations were unknown prior to the example demonstrated by our group (**chapter 8**).<sup>7</sup> Wesemann and co-workers reported mono NHC coordinated Sn(II) cations **L70-71** (Figure 33).<sup>137</sup> Hydride abstraction from  $[\text{Ar-SnH}(\text{NHC})]$  (Ar = *m*-Ter, Tipp<sub>2</sub>-C<sub>6</sub>H<sub>3</sub>), with  $\text{B}(\text{C}_6\text{F}_5)_3$  or  $\{(\text{Ph}_3\text{C})^+(\text{Me}_3\text{NB}_{12}\text{C}_{12})\}$  afforded the desired complexes **L70-71**.

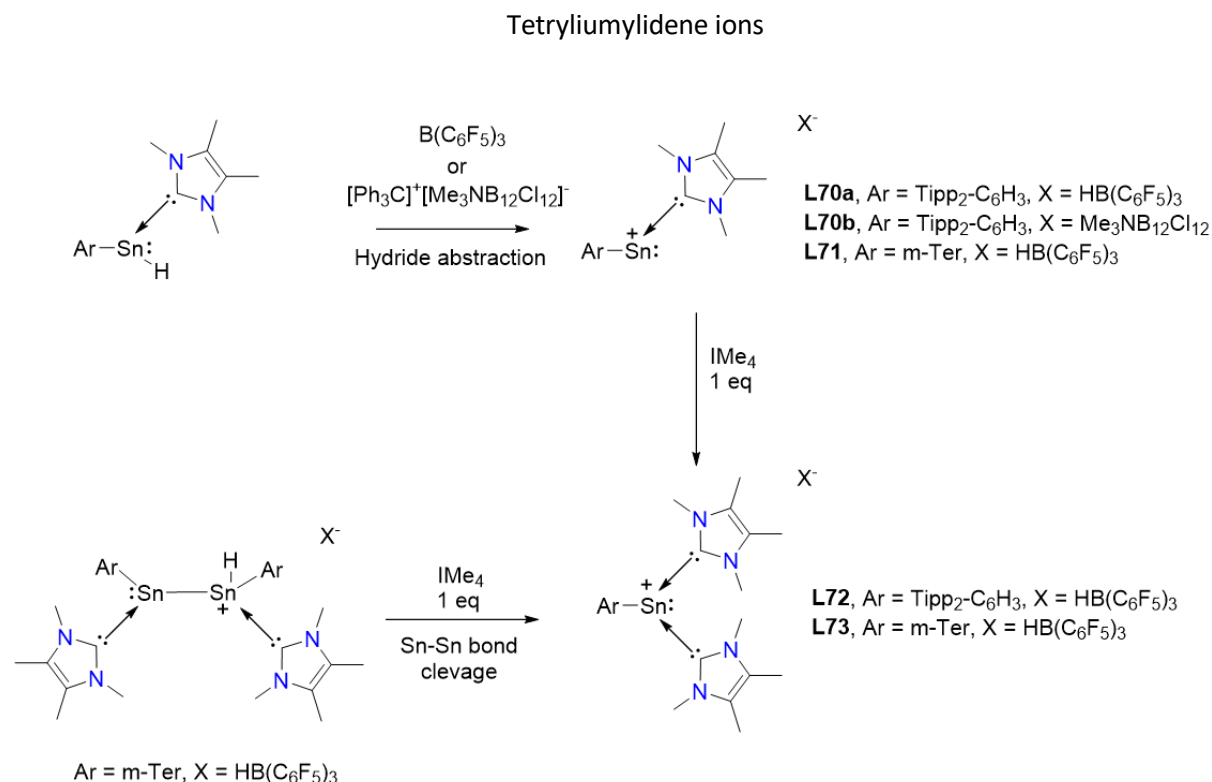


**Figure 33:** Sterically demanding aryl substituted Sn(II) cations.

Interestingly the addition of one equivalent of IMe<sub>4</sub> to **L70a** led to the bis NHC stabilized stannylidene **L72**.<sup>137</sup> Alternatively, bis-NHC stabilized stannylidene **L73** can be achieved through NHC mediated Sn-Sn cleavage.<sup>137</sup> However, compounds **L70-73** are only characterized by NMR spectroscopy, as SC-XRD of the molecular structures of these compounds are yet to be reported. A Lewis base free arene stabilized Sn(II) cation [{Tipp<sub>2</sub>-C<sub>6</sub>H<sub>3</sub>Sn(C<sub>6</sub>H<sub>6</sub>)}<sup>+</sup>{Al{OC(CF<sub>3</sub>)<sub>3</sub>}<sub>4</sub>}<sup>-</sup>] **L74** was reported *via* dehydrogenation of stannylidene cation [(Tipp<sub>2</sub>-C<sub>6</sub>H<sub>3</sub>SnH<sub>2</sub>)<sup>+</sup>{Al{OC(CF<sub>3</sub>)<sub>3</sub>}<sub>4</sub>}<sup>-</sup>].<sup>138</sup>

#### 4.6. Small molecule activation by germyliumylidenes and stannylidene ions

Activation of small molecules with Sn(II) cations are yet to be reported, and there are limited examples of small molecule activation with Ge(II) cations.<sup>129, 136, 139, 140</sup> Driess et al., demonstrated the first germyliumylidene mediated small molecule activation. The reactivity of **L58** with elemental sulfur leads to the germathionium complex **L75** (Figure 34).<sup>129</sup>

### Tetryliumylidene ions

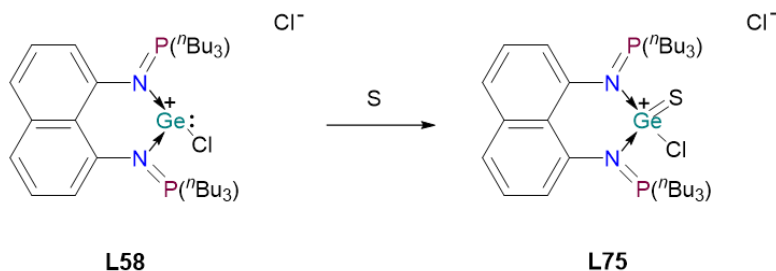


**Figure 34:** Activation of small molecules with **L58**.

Shortly after, the group of Tobita reported activation of homo and heteroatomic  $\sigma$ -bonds.<sup>136</sup> The small HOMO-LUMO gap (2.78 eV) of **L68** enabled the insertion of the germanium center into H-H bond at 60 °C. Compound **L68** also activated Si-H and B-H bonds yielding insertion products **L76** (Figure 35). Intriguingly, the insertion reactions with hydrosilane and hydroborane were found to be reversible at elevated temperatures.<sup>136</sup>

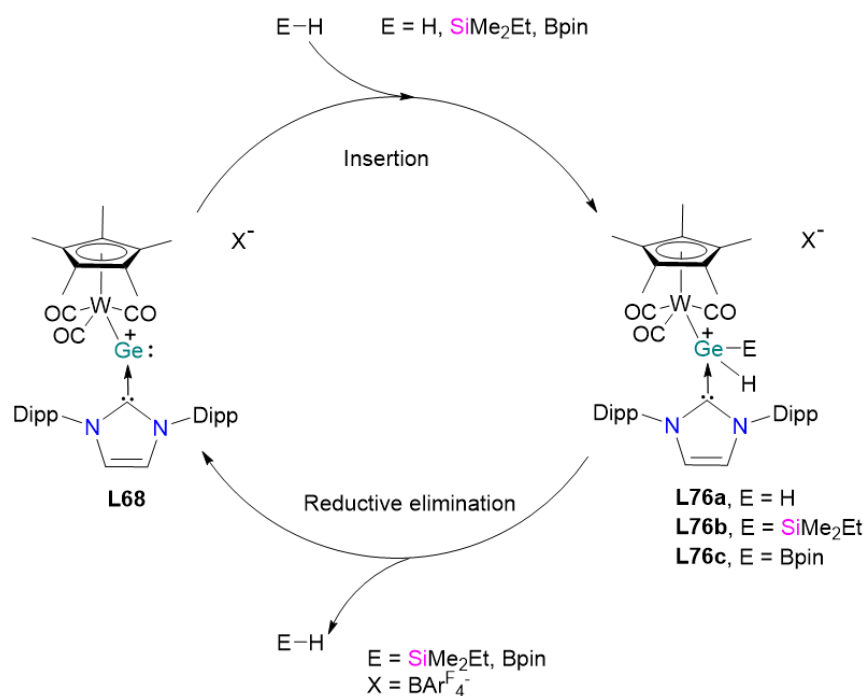


**Figure 35:** Activation of small molecules with **L68**.

In 2015, Aldridge and co-workers reported an alkyl substituted acyclic two coordinate germanium cation **L77**.<sup>139</sup> Lack of  $\pi$ -donor stabilization in this molecule leads to a small HOMO-LUMO gap (1.94 eV) and facilitates versatile oxidative reaction chemistry including C-Cl bond insertion and

## Tetryliumylidene ions

[2+1] cycloaddition with **L78** (Figure 36a).<sup>139</sup> Interestingly, the reaction of **L77** with TMSN<sub>3</sub> and TMSCHN<sub>2</sub> allows for the synthesis of (**L79a** and **L79b**), the first examples of heavier group 14 element cations containing M=E multiple bonds (E=C, N).<sup>139</sup> Recently, the same group have reported cyclic NHC-germyliumylidene **L81-82** mediated N-H bond activation (Figure 36b).<sup>140</sup>

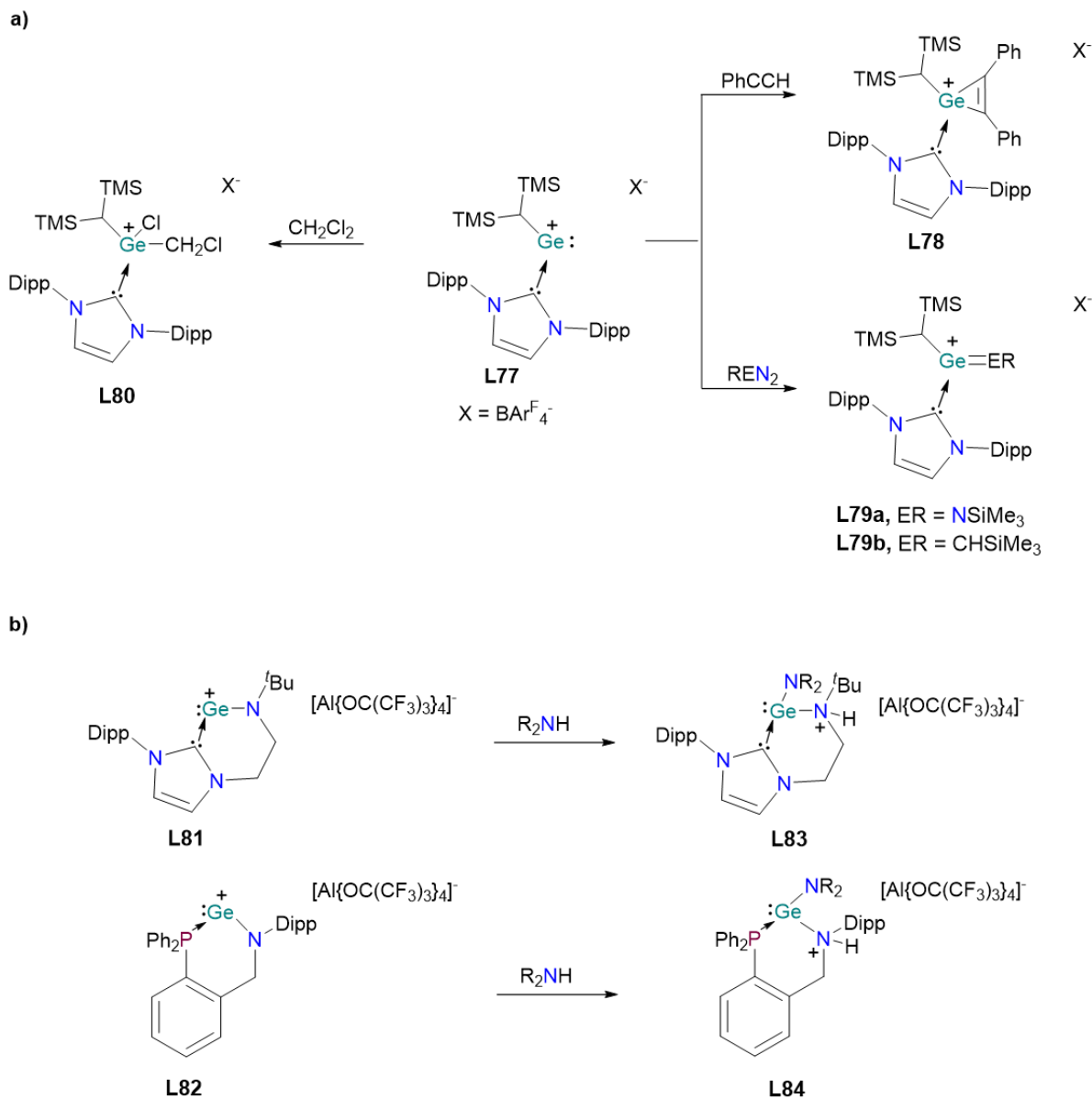


**Figure 36:** Activation of small molecules with **L77**, **L81** and **L82**.

## 4.7. Catalytic application of germyliumylidenes and stannylumylidenes

Despite the unique electronic features and reactivities of germyliumylidenes and stannylumylidenes, their catalytic application is limited.<sup>141, 142</sup> Recently, Rivard and co-workers demonstrated the catalytic reduction of ketones with an NHC stabilized siloxygermyliumylidene complex **L85** (Figure 37).<sup>141</sup> However, this required long reaction times and high catalyst loadings (10 mol%).

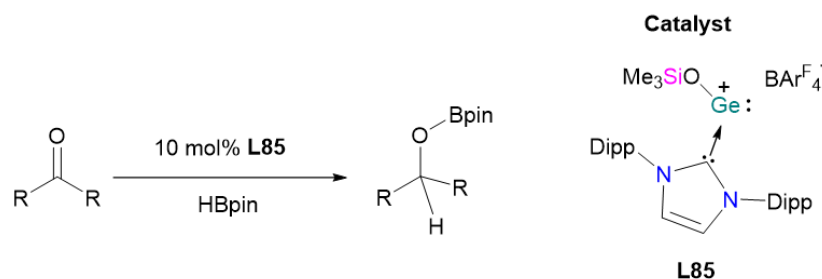


**Figure 37:** Germyliumylidene **L85** catalyzed hydroboration of ketone.

Nagendran et al. reported the N-heterocyclic germyliumylidene **L86** catalyzed hydroboration of aldehydes and ketones with a broad substrate scope and low catalyst loading (Figure 38).<sup>142</sup> It was proposed that the catalysis proceeds through a cascade reaction *via* the formation of a Ge(II)

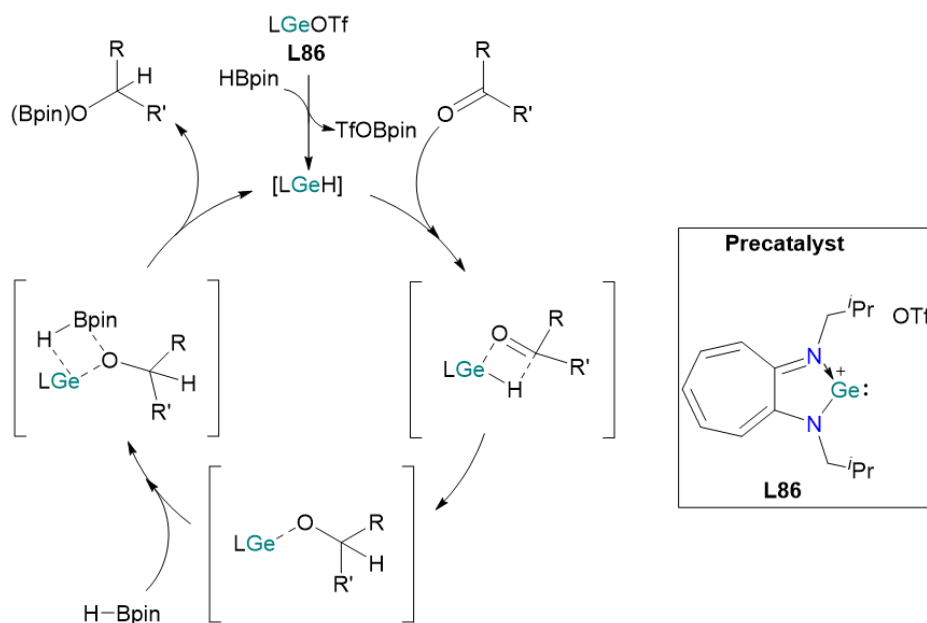


**Figure 38:** Germyliumylidene **L86** catalyzed hydroboration of ketones and aldehydes.

## Tetryliumylidene ions

hydride complex, which is considered to be the active catalyst in this cycle (Figure 38). The germanium center, in this case, acts as a Lewis acidic center, with the initial step involving the coordination of the carbonyl to the Ge(II) center followed by hydrogermylation and regeneration of catalyst *via* hydroboration of the alkoxy-germylium cation intermediate.

Chien and Rausch reported the  $[\{(\eta^5\text{-C}_5\text{Me}_5)\text{Sn}\}^+(\text{BC}_6\text{F}_5)_4]^-$  **L87**, a derivative of stannylumylidene  $[\{(\eta^5\text{-C}_5\text{Me}_5)\text{Sn}\}^+(\text{BF}_4)]^-$ . Compound **L87** was further utilized as an effective co-catalyst in the Ziegler–Natta polymerization of ethylene and propylene.<sup>143</sup>

### 4.8. Plumbyliumylidenes

Low coordinated Pb(II) cations  $[\text{R-Pb}]^+$ , so-called plumbyliumylidenes are rare.<sup>7</sup> The first plumbyliumylidene  $[\{(\text{C}_5\text{H}_5)\text{Pb}\}^+(\text{BF}_4)]^-$  **L88** and  $[\{(\text{Me}_5\text{C}_5)\text{Pb}\}^+(\text{BF}_4)]^-$  **L89** were reported by Jutzi et al., by adopting the similar strategy to the synthesis of **L34-35**.<sup>111, 144</sup> Compounds **L88-89** show an extremely upfield shift in their  $^{207}\text{Pb}$  NMR spectrum **L88** ( $\delta = -5041$  ppm) and **L89** ( $\delta = -4961$  ppm), due to the strong  $\eta^5$ -coordination of the Cp and Cp\* ring to the Pb(II) center. In an elegant study, Power et al. demonstrated bulky terphenyl substituted quasi-mono-coordinate plumbyliumylidene  $[\{\{\text{Tipp}_2(\text{C}_6\text{H}_3)\text{Pb}\}\text{PhMe}\}^+(\text{BC}_6\text{F}_5)_3\text{Me}]^-$  **L90**.<sup>145</sup>

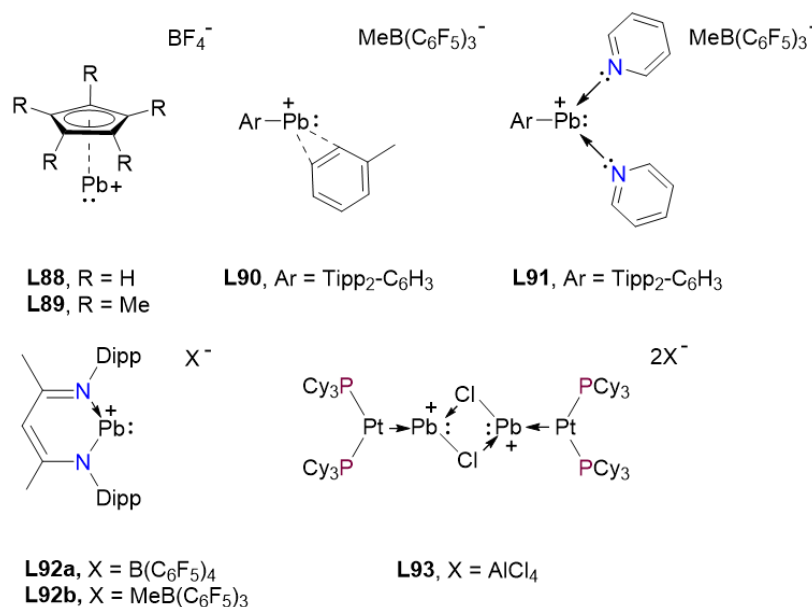


**Figure 39:** Pb(II) cations.

## Tetryliumylidene ions

Compound **L90** was synthesized *via* Lewis acid-mediated  $B(C_6F_5)_3$  methyl abstraction from  $\{Tipp_2-(C_6H_3)PbMe\}$ .<sup>145</sup> Interestingly, the treatment of **L90** with pyridine led to the bis-pyridine stabilized Pb(II) cation **L91**. Later an N-heterocyclic plumblyliumylidene **L92** and  $(Cy_3P)_2Pt$  anchored dimeric plumblyliumylidene complex  $[(Cy_3P)_2Pt(Pb)Cl]^+\{AlCl_4\}^-]_2$  **L93** was isolated.<sup>119, 135</sup> However, the reactivity and application of plumblyliumylidenes are yet to be reported.

## 5. Scope of this work

The last decades have witnessed landmark achievements in heavier low valent group 14 chemistry, including their transition metal mimetic behavior towards small molecules.<sup>2-7</sup> This is a crucial step towards the development of a new transition metal-free sustainable catalysts. Among the heavier low valent group 14 compounds, tetryliumylidenes possess striking electronic features due to an active lone pair and vacant 'p'-orbitals. The chemistry of tetryliumylidene is still in its infancy,<sup>7</sup> particularly their reactivity towards small molecules, which is relatively unexplored.<sup>9, 11, 12, 25, 146</sup> Thus, development of tetryliumylidene complexes and their applications in small molecules activation, with the ultimate goal being catalysis, is highly desirable.

Bis-NHC-stabilized bulky aryl-substituted tetryliumylidenes, of general formula  $[\text{Ar-E}(\text{NHC})_2]^+\text{X}^-$  (Ar = aryl group, X = counter anion), represents the most suitable candidates for fulfilling the desired electronic features to enable versatile small molecule activation (Figure 40).<sup>106</sup> First of all, aryl ligands are sterically tunable by varying the wingtip substituents. Therefore, the stability

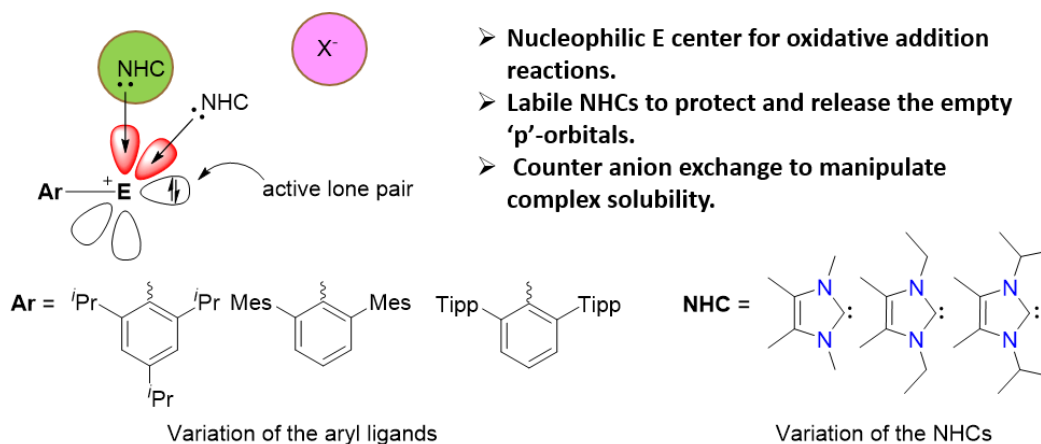


**Figure 40:** Tunable features of bis NHC-stabilized aryl-tetryliumylidenes.

and reactivity of tetryliumylidenes can be easily tuned by changing the substituents on the aryl group. Secondly, owing to the persuasive electron donation from the adjacent NHC(s), E centers are strong  $\sigma$ -donors (highly nucleophilic) and poor  $\pi$ -acceptors. Thus,  $[\text{Ar-E}(\text{NHC})_2]^+\text{X}^-$  compounds are prone to oxidative addition towards small molecules. Additionally, the coordinated NHCs are labile, and depending on reaction conditions, set free the occupied 'p'-



orbital on the E center. This provides an additional reactive site, and in turn increases the reactivity of the compounds. Interestingly, the solubility of these complexes is also adjustable by simple counter anion exchange reactions (e.g., Cl or I with bulky WCAs (e.g.,  $\text{BAr}^{\text{F}_4}$ ).<sup>68</sup>

Considering the chemical abundance of the silicon in the earth's crust, the molecular chemistry of silicon is always a center of attraction for main group research.<sup>147-149</sup> In this context, isolation of new silicon-based multiple bond complexes and their possible application in catalysis or material science has gained tremendous attention.<sup>149</sup> The reactivity of silyliumylidenes towards small molecules has led to unusual silicon-main group multiple bond complexes.<sup>7, 106</sup> At the start of this thesis, there were only two reported reactivities of  $[\{\text{m-TerSi}(\text{IME}_4)_2\}^+\text{Cl}^-]$  **L13** with small molecules ( $\text{PhCCH}$  and  $\text{CO}_2$ ).<sup>95, 107</sup> The reactivity of  $[\{\text{m-TerSi}(\text{IME}_4)_2\}^+\text{Cl}^-]$  **L13** with  $\text{CO}_2$  led to the formation of silaacylium ion  $[\{\text{m-TerSiO}(\text{IME}_4)_2\}^+\text{Cl}^-]$  **L31**. However, heavier silaacylium ions  $[\{\text{m-TerSi}(\text{E})(\text{IME}_4)_2\}^+\text{Cl}^-]$  (E = S, Se and Te), could not be isolated because of the lack of heavier silaacyl halide precursor  $\text{R-Si}(\text{E})\text{X}$  (E = S, Se and Te; X = F, Cl, Br and I). Heavier silaacylium has only been theoretically predicted and isolation of this short lived species in the condensed phase is challenging.<sup>150</sup> Further their inherent reactivity can also be useful to use as a potential chalcogen transfer reagent. Thus, our initial goal subjected the reactivity of  $[\{\text{m-TerSi}(\text{IME}_4)_2\}^+\text{Cl}^-]$  **L13** with

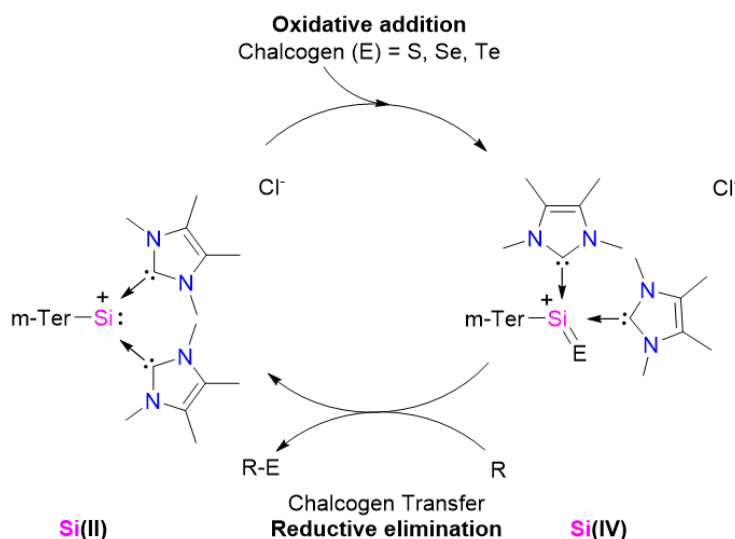


**Figure 41:** Isolation of heavier silaacylium ion and chalcogen transfer reaction (R = organic substrate like alkene or alkyne).

chalcogens to synthesize the heavier silaacylium ions  $[\{m\text{-TerSi}(E)(\text{IMe}_4)_2\}^+\text{Cl}^-]$  ( $E = \text{S}, \text{Se}$  and  $\text{Te}$ , Figure 41). Furthermore, chalcogen transfer from  $[\{m\text{-TerSi}(E)(\text{IMe}_4)_2\}^+\text{Cl}^-]$  to organic compounds or other metal centers will be the ultimate goal of this project, as this should allow for regeneration of  $[\{m\text{-TerSi}(\text{IMe}_4)_2\}^+\text{Cl}^-]$ .

Activation of  $\text{H}_2\text{O}$  with low valent  $\text{Si}(\text{II})$  complexes is highly interesting, as could provide a route to the formation of an elusive silaformyl compound which contains a monomeric  $(\text{H})\text{Si}=\text{O}$  motif.<sup>151, 152</sup> Donor-acceptor stable silaformamide  $\{\text{RNSi}(\text{O})\text{H}\}$  and silaacylhalide  $\{\text{ClSi}(\text{O})\text{H}\}$  was reported *via* reaction of corresponding silylene with  $\text{H}_2\text{O}\cdot\text{B}(\text{C}_6\text{F}_5)_3$  adduct.<sup>151, 152</sup> However, silaaldehyde  $\{\text{R-Si}(\text{O})\text{H}\}$ , one of the most sought after species in silacarbonyl chemistry, was not demonstrated before. This a challenging target as absence of suitable stabilization to the  $\text{Si}=\text{O}$  bond results in head to tail dimerization due to the inherent zwitterionic nature of  $\text{Si}^+-\text{O}^-$ .

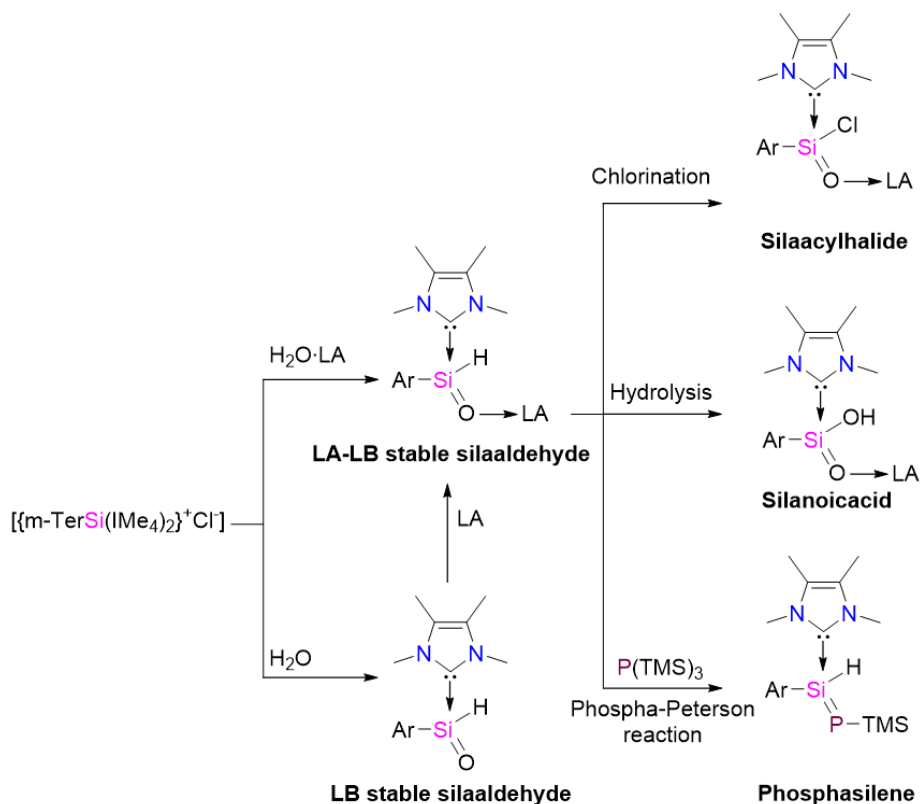


**Figure 42:** Isolation and functionalization of a silaaldehyde.

Typically, isolation of silanone species ( $\text{R}_2\text{Si}=\text{O}$ ) was realized using sterically demanding ligands also with suitable electronic stabilization.<sup>5</sup> Hence, it may not be erroneous to contemplate that isolation of silaaldehyde is more challenging than silanone, due to the lack of steric protection (R

vs H).<sup>5</sup> Additionally, due to low steric bulk and subsequent inherent reactivity of silaaldehydes, they are easily functionalizable, which possibly gives rise to a diverse range of silacarbonyl or silicon-heteroatomic multiple bond species (Figure 42). We presumed reactivity of silyliumylidene [ $\{m\text{-TerSi}(\text{IME}_4)_2\}^+\text{Cl}^-$ ] with  $\text{H}_2\text{O}$  will provide access to the hitherto unknown NHC stabilized silaaldehyde. The reactivity of silyliumylidene with  $\text{H}_2\text{O}$  in absence or presence of Lewis acid (e.g.  $\text{B}(\text{C}_6\text{F}_5)_3$ ,  $\text{GaCl}_3$  and  $\text{ZnCl}_2$ ) will be performed to isolate the donor or donor-acceptor stable silaaldehyde, respectively. Further, functionalization of the silaaldehyde complex to other silacarbonyls (silaacylhalide, silaester and silanoic acid), or phosphasilene will also be targeted.

Silicon compounds with +IV oxidation state are highly stable. Thus, it makes traditional redox-based catalysis very challenging due to the difficulties associated with reductive elimination and, therefore, release of the functionalized substrate. One potential method to overcome this obstacle is to utilize a metal center that is stable in both high and low oxidation states. In this regard, germanium presents itself as a suitable candidate. In recent years, the transition metal like reactivity of germanium has been shown, providing the first examples of low-valent main group dihydrogen activation and multiple bond catalysis.<sup>14, 26</sup> With the latter example possible due to the ability of germanium to switch between its +II and +IV oxidation states.<sup>26</sup> Thereby, we envisaged that NHC-stabilized aryl germyliumylidene [ $\{\text{ArGe}(\text{NHC})_2\}^+\text{Cl}^-$ ] would be a suitable precursor for both activation of small molecules and further catalytic use (Figure 43).

Electrophilic Ge(II) catalyzed hydroboration and cyanosilylation of carbonyls are known.<sup>21-23, 27, 61, 142</sup> However, low valent nucleophilic Ge(II) has never been utilized for the same purposes. In fact, prior to this thesis, only one example of catalytic conversion of  $\text{CO}_2$  with a germylene/ $\text{B}(\text{C}_6\text{F}_5)_3$  FLP compound was reported.<sup>24</sup> The germanium center in [ $\{\text{Ar-Ge}(\text{NHC})_2\}^+\text{X}^-$ ] is nucleophilic and, therefore, exploring the catalytic activity of germyliumylidenes in organic transformations is a main goal of this thesis.

## Scope of this work

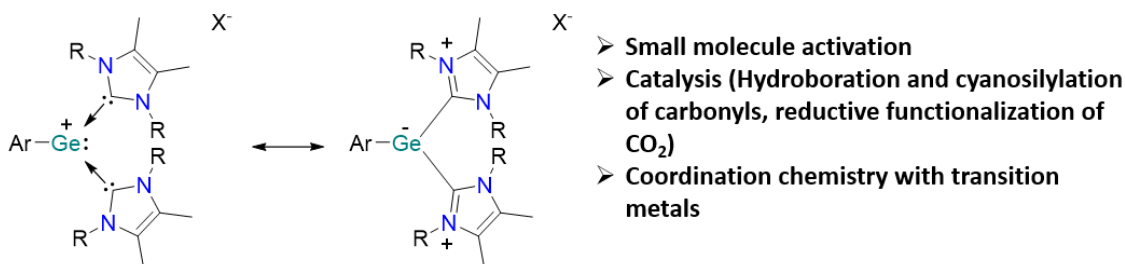


**Figure 43:** NHC-stabilized aryl-germyliumylidene and its possible applications (R = Me, Pr, *i*Pr). Neutral germanones (R<sub>2</sub>Ge=O) are reported.<sup>47, 153-156</sup> However, a cationic germanium oxide, so-called germaacylium ion [R-Ge=O]<sup>+</sup>, is an elusive species only observed in high pressure and Fourier transformation mass spectrometry.<sup>157</sup> One potential approach to obtain a germaacylium ion [{Ar-GeO(NHC)<sub>2</sub>}<sup>+</sup>X<sup>-</sup>] is *via* the oxygenation of the germyliumylidene [{Ar-Ge(NHC)<sub>2</sub>}<sup>+</sup>X<sup>-</sup>] with various oxygen transfer reagents (e.g., N<sub>2</sub>O, pyridine-N-oxide etc.). With the desired compound in hand, reactivity studies will be undertaken to assess its classical acylium ion [R-CO]<sup>+</sup> like behavior (Figure 44). For example, if the germaacylium ion [Ar-GeO]<sup>+</sup> can be used to synthesize the heavier germaacylium analogs [{Ar-GeS(NHC)<sub>2</sub>}<sup>+</sup>X<sup>-</sup>] or [{Ar-GeSe(NHC)<sub>2</sub>}<sup>+</sup>X<sup>-</sup>], respectively, by chalcogenation of the Ge=O bond with Lawesson's reagent (MeOPhPS<sub>2</sub>)<sub>2</sub> or Woollin's reagent (PhPSe<sub>2</sub>)<sub>2</sub>.<sup>158, 159</sup> Furthermore, the transition metal oxide like reactivity of the germaacylium ion will be investigated, such as oxide transfer reactions to an organic substrate (e.g., PPh<sub>3</sub>, R-NC, NHC etc.).<sup>160, 161</sup>

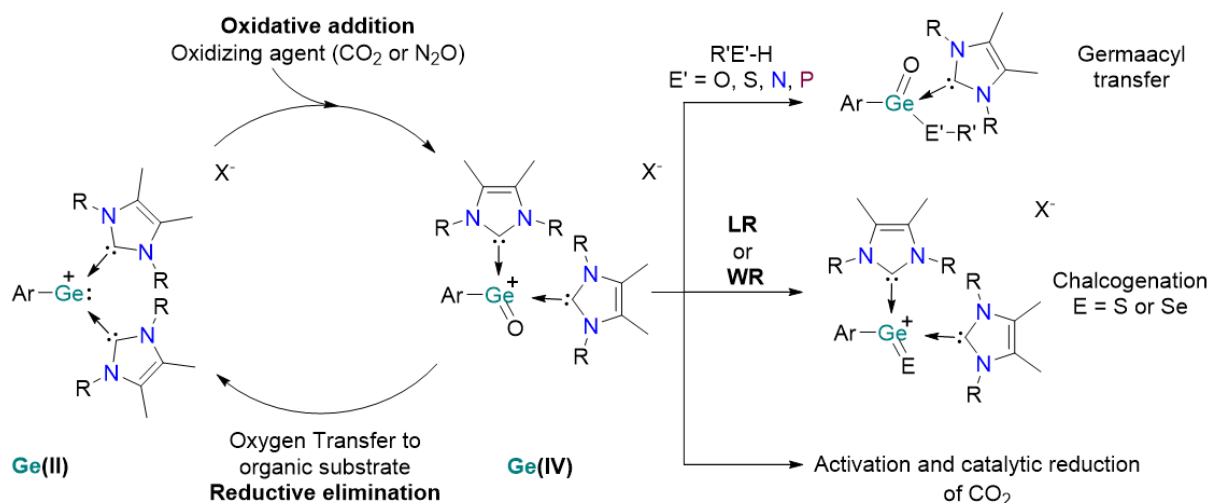


**Figure 44:** NHC-stabilized aryl-germaacylium compound and its possible reactivity (R = Me, Pr, *i*Pr, R = Alkyl or Aryl, LR = Lawesson's reagent, WR = Woollin's reagent).

## Scope of this work

Additionally, transition metal oxide mediated reversible activation of CO<sub>2</sub> is known,<sup>162, 163</sup> this concept has been utilized to enable transition metal oxide catalyzed CO<sub>2</sub> reduction.<sup>164, 165</sup> DFT studies revealed the strong charge density at oxygen is important in this catalysis as it leads to the formation of a hypercoordinate silicate. This is vital in enabling turnover, as reduction of CO<sub>2</sub> occurs at the activated Si-H bond.<sup>164</sup> However, such catalytic reactivity with group 14 metal oxides is currently unknown. Considering the inherent polarized nature of the Ge<sup>+</sup>-O<sup>-</sup> bond and stability of germanium at multiple oxidation states, we envisioned that the cationic germaacylium ion [ $\text{Ar-GeO(NHC)}_2\text{X}^+$ ] might show similar catalytic activity with CO<sub>2</sub> like transition metal oxides. Overall, this thesis focuses on the isolation of the novel tetryliumylidene compounds and their potential application towards small molecule activation and catalysis.

## 6. Chalcogen-atom transfer and exchange reactions of NHC-stabilized heavier silaacylium ions

**Title:** Chalcogen-atom transfer and exchange reactions of NHC-stabilized heavier silaacylium ions

**Status** Communication, published online October 27, 2017

**Journal** Dalton Trans., 2017, 46, 16014–16018

**Publisher** Royal Society of Chemistry

**DOI** 10.1039/c7dt03998k

**Authors** Debotra Sarkar, Daniel Wendel, Syed Usman Ahmad, Tibor Szilvási, Alexander Pöthig and, Shigeyoshi Inoue

*Reprinted with permission. © 2017 The Royal Society of Chemistry*

**Content** Fridel-Craft acylation is one of the essential tools to introduce the acyl group to an organic moiety. This reaction proceeds through the intermediacy of an acylium ion  $[R-CO]^+$ , which is typically generated *in situ* by the treatment of acyl halide  $[R-CO(Cl)]$  with Lewis acids ( $BF_3$ ,  $AlCl_3$ , and  $ZnCl_2$  etc.). The heavier analogs of acylium ion ( $[R-CE]^+$ ,  $E = S, Se$  and  $Te$ ) appear as highly reactive species and are unstable in the condensed phase. Akin to the carbon compounds, its silicon analog, so-called heavier silaacylium ions  $[R-SiE]^+$ , are also highly reactive and is still unprecedented. This could be attributed to the lack of a suitable silaacyl halide precursor  $[R-SiE(Cl)]$ , along with the significant electronegativity difference between Si and E in addition to the poor  $\pi$ -overlap between silicon and heavier chalcogens.

Herein, we report the facile access to a heavier silaacylium ion  $[\{m-Ter(SiE)(NHC)_2\}Cl]$ , **2** ( $E = S$ ), **3** ( $E = Se$ ), **4** ( $E = Te$ ) ] *via* the reaction of silyliumylidene  $\{m-Ter(Si)(NHC)_2\}Cl$  (**1**) with elemental chalcogens. Strikingly, **1** is regenerated through the treatment of **2-4** with AuI. This demonstrates a unique approach to recover the Si(II) precursor from the Si(IV) chalcogenide. Furthermore, chalcogen scrambling reaction  $4 \rightarrow 3 \rightarrow 2$  could also be achieved, which is in line with Si-E bond energies.

### **Author Contributions**

- Debotra Sarkar planned and executed all experiments. Debotra Sarkar and Dr. Daniel Wendel co-wrote the manuscript. Dr. Syed Usman Ahmad contributed with significantly important discussions. Dr. Tibor Szilvási designed and performed the theoretical investigations. Dr. Alexander Pöthig conducted all SC-XRD measurements and processed the resulting data. All work was performed under the supervision of Prof. Shigeyoshi Inoue.

Cite this: *Dalton Trans.*, 2017, **46**, 16014Received 24th October 2017,  
Accepted 27th October 2017

DOI: 10.1039/c7dt03998k

rsc.li/dalton

## Chalcogen-atom transfer and exchange reactions of NHC-stabilized heavier silaacylium ions†

Deotra Sarkar,<sup>a</sup> Daniel Wendel,<sup>a</sup> Syed Usman Ahmad,<sup>b</sup> Tibor Szilvási,<sup>c</sup>  
Alexander Pöthig<sup>id</sup><sup>a</sup> and Shigeyoshi Inoue<sup>id</sup><sup>\*a</sup>

Heavier analogues of silaacylium ions 2–4 (*m*-TerSiE(NHC)<sub>2</sub>Cl; *m*-Ter = 2,6-Mes<sub>2</sub>C<sub>6</sub>H<sub>3</sub>; Mes = 2,4,6-Me<sub>3</sub>C<sub>6</sub>H<sub>2</sub>; 2 (E = S), 3 (E = Se), 4 (E = Te)) were synthesized by the reaction of the NHC-stabilized silyliumylidene cation 1 with elemental chalcogens. Fascinating regeneration of 1 from the reaction of 2–4 with AuI was achieved, as successful recovery of a parent Si(II) species from a silachalcogen Si(IV) compound. Furthermore, unique chalcogen exchange reactions from 4 → 3 → 2 were observed in line with the calculated silicon–chalcogen bond energies.

The Friedel–Crafts reaction has proved to be indispensable in order to introduce the carbonyl functionality in organic backbones.<sup>1</sup> This reaction proceeds through the intermediacy of the electrophilic acylium cation [RCO]<sup>+</sup> (Chart 1a), generated *via in situ* treatment of acyl halides with Lewis acids such as BF<sub>3</sub>, MF<sub>5</sub> (M = P, As, Sb), AlCl<sub>3</sub> or ZnCl<sub>2</sub>.<sup>2</sup> In contrast, examples of respective heavier analogues of acylium cations ([ArCE]<sup>+</sup>; E = S, Se, Te) are still very sparse,<sup>3</sup> probably due to the limited variety of synthetic methods and the lack of suitable precursors. Theoretical calculations have given insight into the highly reactive nature of heavier acyl halides ([XYC = E]; E = Se, Te; X, Y = H, F, Cl, Br and I) by the virtue of a small HOMO–LUMO gap.<sup>4</sup> In this context, it is noteworthy to mention that until now only a few thioaroyl cations, ([PhCS]<sup>+</sup>[SbF<sub>6</sub>]<sup>−</sup>)<sup>3b,c</sup> and ([MesCS]<sup>+</sup>[(C<sub>6</sub>F<sub>5</sub>)<sub>4</sub>B]<sup>−</sup>)<sup>3a</sup> have been synthesized either by reacting thiobenzoyl chloride with AgSbF<sub>6</sub> or by the borinium ion-mediated C–S double bond cleavage of CS<sub>2</sub>. X-ray crystallographic and DFT studies were carried out to shed light on the different resonance structures of thioaroyl cations (Chart 1b). However, to the best of our knowledge, respective selenium

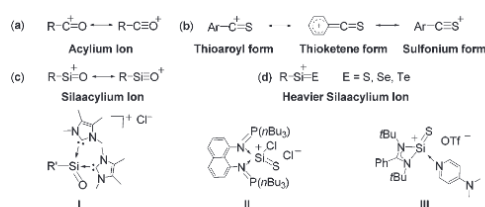


**Chart 1** (a) Acylium ion, (b) thioaroyl ion, (c) silaacylium ion, (d) heavier silaacylium ion and reported examples I, II and III (R = alkyl, aryl; R' = *m*-Ter, Tipp, Ar = aryl, *m*-Ter = 2,6-Mes<sub>2</sub>C<sub>6</sub>H<sub>3</sub>, Mes = 2,4,6-Me<sub>3</sub>C<sub>6</sub>H<sub>2</sub>, Tipp = 2,4,6-*i*Pr<sub>3</sub>-C<sub>6</sub>H<sub>2</sub>).

and tellurium analogues still remain inaccessible. Akin to carbon compounds, silicon analogues of these species ([ArSi = E]<sup>+</sup>; E = S, Se, Te), namely heavier silaacylium ions (Chart 1d), are also considered as reactive species and still unprecedented. This is presumably due to the lack of precursor silaacylhalides (for example, Ar(x)Si = E; X = F, Cl, Br, I; E = S, Se, Te) along with the large electronegativity difference, weak  $\pi$ -bonding nature and a longer bond length between silicon and heavier chalcogens.<sup>5</sup> Consequently, the isolation of such compounds is still challenging.

Recently, we reported the isolation of NHC-stabilized silaacylium ions I (Chart 1c) ([R'Si(O)(NHC)<sub>2</sub>]Cl; R' = *m*-Ter, Tipp; *m*-Ter = 2,6-Mes<sub>2</sub>C<sub>6</sub>H<sub>3</sub>; Mes = 2,4,6-Me<sub>3</sub>C<sub>6</sub>H<sub>2</sub>, Tipp = 2,4,6-*i*Pr<sub>3</sub>C<sub>6</sub>H<sub>2</sub>, NHC = 1,2,3,4-tetramethylimidazol-2-ylidene), by utilizing a bulky terphenyl and Tipp group as a steric protector and two NHCs as external donors.<sup>6</sup> In comparison to neutral compounds,<sup>7</sup> there are only two instances of cationic [RSi = S]<sup>+</sup> compounds (II and III) reported in the literature (Chart 1d).<sup>8</sup> Despite the isolation of oxygen and sulfur analogues of silaacylium ions, cationic [RSi = Se]<sup>+</sup> and [RSi = Te]<sup>+</sup> compounds have not been reported yet, although the electronic states and the spectroscopic properties have been theoretically investigated.<sup>9</sup> Apart from academic and/or experimental interests heavier silicon–chalcogenides showed considerable promise towards

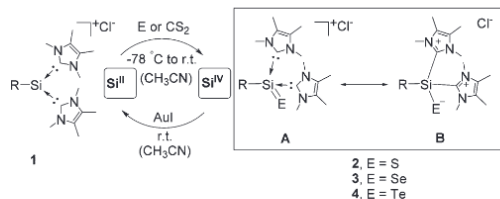
<sup>a</sup>Department of Chemistry, WACKER-Institute of Silicon Chemistry and Catalysis Research Center, Technische Universität München, Lichtenbergstraße 4, 85748 Garching, Germany. E-mail: s.inoue@tum.de

<sup>b</sup>Fielding Environmental, 3575 Mavis Rd, Mississauga, ON L5C 1 T7, Canada

<sup>c</sup>Department of Chemical and Biological Engineering, University of Wisconsin Madison, 1415 Engineering Drive, Madison, Wisconsin 53706-1607, USA

† Electronic supplementary information (ESI) available. CCDC 1547818–1547820. For ESI and crystallographic data in CIF or other electronic format see DOI: 10.1039/c7dt03998k

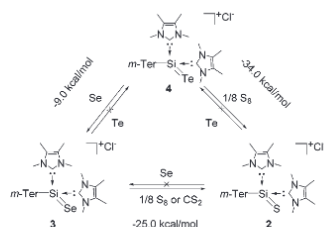




**Scheme 1** Synthesis of compounds 2–4 with their possible representation: (A) Two NHC stabilized heavier silylium ion and (B) zwitterionic form of heavier silylium ion, and regeneration of NHC-stabilized silyliumylidene **1** ( $R = m\text{-Ter}$ ;  $m\text{-Ter} = 2,6\text{-Me}_2\text{C}_6\text{H}_3$ ;  $\text{Mes} = 2,4,6\text{-Me}_3\text{C}_6\text{H}_2$ ).

silicon-based device fabrications: for instance, the use of SiTe in thermoelectric materials,  $\text{SiTe}_2$ ,  $\text{Si}_2\text{Te}_3$  in optoelectronics materials,<sup>10</sup> or  $\text{SiS}_2$  and  $\text{SiSe}_2$  as electrocatalytic materials for counter electrodes (CE) in dye-sensitized solar cells (DSSCs).<sup>11</sup> With this incentive, we report the isolation of NHC-stabilized heavier analogues of silylium ions, containing Si=S (**2**), Si=Se (**3**) and Si=Te (**4**) bonds by the reaction of elemental chalcogen with the NHC-stabilized silyliumylidene **1**<sup>6b</sup> (Scheme 1). All compounds were characterized *via* X-ray crystallography, multinuclear NMR, IR and UV-Vis spectroscopy. Further detailed DFT calculations were carried out to shed light on the electronic and bonding nature of those compounds. Additionally, an alternative pathway to compound **2** is presented by the reaction of carbon disulfide with **1** *via* facile C=S bond cleavage.<sup>13</sup> With respect to reactivity studies, we showed the fascinating regeneration of **1** by treatment of  $[\text{ArSiE}]^+$  (**2**, **3** and **4**) with AuI and further chalcogen exchange reactions between **2**, **3** and **4** (Scheme 2), in good agreement with the bond dissociation energy (BDE) data (Table 1) of the corresponding Si–E bond.

Silyliumylidene ions  $[\text{RSi}]^+$  bear a unique electronic nature; the central silicon atom possesses a lone pair electron pair as well as a vacant p-orbital with a positive charge.<sup>12</sup> Motivated by this electronic feature and our previous report,<sup>6a,12b-d</sup> we thought that silyliumylidene ions would be excellent precursors for the preparation of hitherto unknown silylium ions by the reaction with chalcogen atoms. Therefore, we treated **1**



**Scheme 2** Chalcogen exchange reactions of 2–4 with reaction energies.

**Table 1** Calculated value for **2**, **3**, and **4** (a) Bond Dissociation Energy (BDE) in  $\text{kcal mol}^{-1}$ , (b) Natural Population Analysis (NPA) (b1, Si) (b2, E), (c) Wiberg Bond Index (WBI), (d) Mayer Bond Order (MBO), (e) IR stretching in  $\text{cm}^{-1}$  and (f) calculated GIAO  $^{29}\text{Si}$  NMR shift in ppm of the Si=E bond, E = S, Se, Te

	BDE <sup>[a]</sup>	NPA <sup>[b1]</sup>	NPA <sup>[b2]</sup>	WBI <sup>[c]</sup>	MBO <sup>[d]</sup>	IR <sup>[e]</sup>	GIAO <sup>[f]</sup>
<b>2</b>	90.8	1.41	−0.74	1.40	1.64	643	−35.7
<b>3</b>	62.7	1.32	−0.63	1.41	1.36	525	−43.2
<b>4</b>	47.5	1.17	−0.47	1.39	1.26	474	−70.4

with elemental chalcogen in acetonitrile at  $-78\text{ }^\circ\text{C}$ , which resulted in the formation of compounds **2**, **3** and **4**, with a yield of 85%, 56% and 87%, respectively (Scheme 1). All three compounds are stable under inert atmosphere and show high solubility in polar aprotic solvents such as acetonitrile and dichloromethane, but are poorly soluble in aromatic, aliphatic hydrocarbon and ethereal solvents.

Oxidative addition and reductive elimination under the regeneration of parent molecules are essential steps in effective catalytic cycles. In this context, recovering a Si(*n*) compound from its relatively stable Si(*iv*) complex under mild conditions is considerably challenging.<sup>14</sup> Although there are some reports on the reactivity of compounds containing the Si=E bond toward small molecules or alkenes,<sup>7n-o</sup> no interconversion between a Si(*n*) species and its multiple bonded silachalcogen Si(*iv*) analogue has been found so far.<sup>14</sup> Even the examples of reversible chalcogen-atom transfer to main group as well as transition metal and actinide complexes are limited.<sup>15</sup> With this in mind, we treated 2–4 with the conventional chalcogen scavenger  $\text{PPh}_3$ ,<sup>7n-o</sup> but no chalcogen transfer occurred, probably due to steric reasons. When we treated 2–4 with coinage metal halides, we observed the regeneration of the parent silyliumylidene **1** in the case of AuI (Scheme 1). For AgI, we could only regenerate **1** from **2** and **3**, which is distinctly different from the reactivity of thio- and selenogermanones  $[\text{LPhGe} = \text{E}]$ , E = S, Se, (L =  $(t\text{-Bu})_2\text{ATI}$ ; ATI = amino-triponiminate) towards AgI.<sup>16</sup> Unfortunately, no reactivity was observed with CuI. The reaction is presumably driven by coordination of the chalcogen to the soft Au and Ag centre through precipitation of free metal and metal-chalcogenide; however, the reaction mechanism is still unclear.<sup>17</sup>

X-ray analysis revealed that all three cations have a central silicon atom that is tetra-coordinated by two NHCs and bonded to one *m*-terphenyl group and the corresponding chalcogen atom (Fig. 1). The Si...Cl distances in **2**, **3** and **4** are well above 5 Å, suggesting no direct contact between the silicon and the chlorine atom. In compound **2** (see the  $\text{ESI}^\dagger$ ), the Si=S lengths are 2.013(1) Å and 2.018(1) Å for the two independent molecules, which is shorter than the cationic Si–S single bond (2.160 Å) in  $\{[\text{iPrNC}(\text{NiPr}_2)_2\text{SiSPh}]^+\text{PhS}^-\}$ ,<sup>18</sup> and nearly close to NHC or donor stabilized neutral or cationic Si=S bonds reported before (1.96–2.00 Å).<sup>7b,d,e,k,8</sup> In compound **3** (Fig. 1a) the Si=Se bond lengths are 2.1516(9) Å and 2.1571(8), which are similar to Lewis base stabilized tetra-coordinated Si=Se double bonded compounds (2.13 to

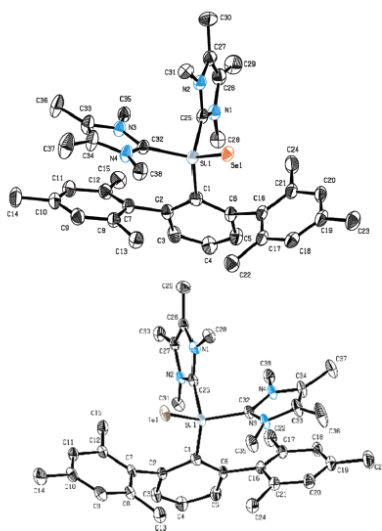


Fig. 1 Molecular structure of **3** (top, only one independent molecule shown) and **4** (bottom). Hydrogen atoms and the chloride counterion are omitted for clarity. Ellipsoids are shown at the 50% probability level. Selected bond lengths [Å] and bond angles [°]: **3** Si1–Se1 2.1516(9)/Si2–Se2 2.1571(8), Si1–C1 1.910(3)/Si2–C39 1.920(2), Si1–C25 1.944(3)/Si2–C70 1.947(3), Si1–C32 1.937(3)/Si2–C63 1.938(3); Se1–Si1–C1 118.29(9)/Se2–Si2–C39 118.23(9), Se1–Si1–C25 107.17(9)/Se2–Si2–C70 106.77(9), Se1–Si1–C32 112.40(9)/Se2–Si2–C63 111.81(9), C1–Si1–C25 107.9(1)/C39–Si2–C70 108.0(1), C1–Si1–C32 111.0(1)/C39–Si2–C63 111.9(1), C25–Si1–C32 97.9(1)/C70–Si2–C63 97.9(1). **4** Si1–Te1 2.3941(6), Si1–C1 1.913(2), Si1–C25 1.943(2), Si1–C32 1.944(2); Te1–Si1–C1 119.88(7), Te1–Si1–C25 106.40(7), Te1–Si1–C32 111.07(7), C1–Si1–C25 107.08(9), C1–Si1–C32 111.14(9), C25–Si1–C32 98.94(9).

2.16 Å),<sup>7a,b,e,k</sup> but significantly shorter than the cationic Si–Se single bond length (2.308 Å) in  $\{[\text{PrNC}(\text{NiPr}_2)_2\text{NiPr}_2\text{SiSePh}]^+\text{PhSe}^-\}$ .<sup>18</sup> Similarly, the Si=Te bond length of **4** (Fig. 1b) is 2.3941(6) Å and falls in the range of other neutral tetra-coordinated Si=Te compounds (2.38 to 2.39 Å).<sup>7a,b,k</sup>

The <sup>29</sup>Si NMR spectra of compound **2**, **3** and **4** exhibit sharp signals at  $\delta = -36.0$  ppm,  $\delta = -41.4$  ppm and  $\delta = -72.2$  ppm, respectively, which are in good agreement with the calculated data (Table 1, **2**  $\delta = -35.7$  ppm, **3**  $\delta = -43.2$  ppm and **4**  $\delta = -70.4$  ppm) and are close to recently reported heavy silaalkaldehydes  $[\text{Ter}^*(\text{HSiE})\text{NHC}^{\text{IMe}_4}]$ ,  $\text{Ter}^* = 2,6\text{-Bis}(2,4,6\text{-triisopropylphenyl})\text{phenyl}$ .<sup>7b</sup> Compound **2** depicts a significantly upfield shift in comparison to tetra-coordinated cationic silathionium compounds **II** ( $\delta = -14.09$  ppm)<sup>8b</sup> and **III** ( $\delta = -26.7$  ppm)<sup>8a</sup> (Chart 1d).

In order to understand the bonding nature of all three compounds, IR spectroscopy has been carried out. In the solid state, the IR spectrum of **2** displayed a strong Si=S absorption band at 645 cm<sup>-1</sup>, whereas for compounds **3** and **4**, strong absorption bands were observed at 524 cm<sup>-1</sup> and 475 cm<sup>-1</sup> assignable to the Si=Se and Si=Te bond, respectively.

The experimental IR data fit quite well with the calculated values [Calculated B97-D/6-31G(d)]Se, Te:cc-pVTZ-PP level of theory,  $\tilde{\nu}_{\text{Si}=\text{S}} = 643$  cm<sup>-1</sup>,  $\tilde{\nu}_{\text{Si}=\text{Se}} = 525$  cm<sup>-1</sup>,  $\tilde{\nu}_{\text{Si}=\text{Te}} = 474$  cm<sup>-1</sup>] and reveal red shifts in comparison to NHC coordinated silachalcogen compounds [ $\tilde{\nu}_{\text{Si}=\text{S}} = 665\text{--}683$  cm<sup>-1</sup>,  $\tilde{\nu}_{\text{Si}=\text{Se}} = 578\text{--}614$  cm<sup>-1</sup>,  $\tilde{\nu}_{\text{Si}=\text{Te}} = 595$  cm<sup>-1</sup>].<sup>7e,k</sup> Still, all three absorption bands are large enough to distinguish them from a silicon–chalcogen single bond [for example, (MeH<sub>2</sub>Si)<sub>2</sub>E,  $\tilde{\nu}_{\text{Si}-\text{S}} = 461$  cm<sup>-1</sup>,  $\tilde{\nu}_{\text{Si}-\text{Se}} = 380$  cm<sup>-1</sup>,  $\tilde{\nu}_{\text{Si}-\text{Te}} = 328$  cm<sup>-1</sup>].<sup>19</sup> To get deeper insight into the electronic structure of silicon–chalcogen bonds, we performed DFT calculations employing the B97-D/6-31G(d)]Se, Te:cc-pVTZ-PP level of theory. The HOMO of these compounds (Fig. S19–21†) shows mainly the lone pair of the chalcogen with some extension to the silicon center which can be considered as an asymmetric  $\pi$ -orbital. The LUMO of the compounds is dispersed over the NHC skeletons and is related to the NHC  $\pi$ -system (Fig. S19–21†). In addition, the calculated Mayer Bond Order (MBO) of these molecules indicates some multiple-bond character of the Si=E bond (MBO, **2** = 1.64, **3** = 1.36, **4** = 1.26). Equally, Wiberg bond indices (WBI) also support partial Si=E multiple bonding nature (WBI, **2** = 1.40, **3** = 1.41, **4** = 1.39), which is larger than the silyl chalcogenide anion  $[\text{H}_3\text{Si}-\text{E}]^-$ , disilyl chalcogenide  $[\text{H}_2\text{Si}-\text{E}-\text{SiH}_3]$  (Tables S4–6†), NHC stabilized heavy aldehydes ( $[(\text{NHC}^{\text{IMe}_4})][\text{H}_2\text{Si}-\text{E}]$ ) and  $[(\text{NHC}^{\text{IMe}_4})][\text{LHSi}-\text{E}]^-$ ,<sup>7b</sup> and similar to bis-NHC stabilized terminal Si(IV) chalcogenides.<sup>7a</sup> Interestingly, the calculated symmetric valence IR vibrational frequency of reference structures  $[\text{H}_3\text{Si}-\text{E}]^-$  and  $[\text{H}_3\text{Si}-\text{E}-\text{SiH}_3]$  show much lower values compared to compounds **2–4**, while the doubly bonded reference structures  $[\text{H}_2\text{Si}=\text{E}]$  possess only slightly larger IR values. This can also indicate that the double bond resonance structure has considerable contribution to the description of the bonding situation of **2–4**. We note that the short bond distance can be partially explained by strong hyperconjugative effects between the lone pairs of the chalcogen atoms and the  $\sigma^*(\text{Si}-\text{C})$  bonds; similar interactions have been found as important factors in other silachalcogenides.<sup>7b</sup> In terms of NBO analysis, the Si atom of these compounds possesses a large positive net charge, while the E atom bears a negative charge (see Table 1). This indicates a polarization of the Si–E bond which is responsible for the betaine representation of **2–4** (Scheme 1). Overall, theoretical results lead us to the conclusion to draw both possible resonance structures **A** and **B**, for compounds **2–4** in Scheme 1, although **B** may be more relevant.

We performed chalcogen exchange reactions, which display the first example of Si=E scrambling (Scheme 2). The reaction of compound **4** with equimolar amounts of elemental sulfur fully led to compound **2** at room temperature within 8 h. However, the conversion from **4** to **3** with equimolar amounts of elemental Se took a prolonged time, 15 days and elevated temperatures to reach an optimized yield of 45%. Similarly, the reaction of **3** with sulfur gave **2** in 35% yield after 22 days.

Interestingly, no reaction was observed upon treating **3** with the same equivalents of tellurium. Likewise, the reaction of compound **2** with Se and Te did not form **3** or **4** even after an

extended reaction time. Here, only unidentified products were observed at elevated temperatures. We calculated the reaction energies of the exchange reactions (Scheme 2, see details in the ESI†) which explain the experimental findings. The exchange reaction energy between **4** and **3** is  $-9.0 \text{ kcal mol}^{-1}$  which indicates why only Se to Te exchange can occur. Similarly, the one-way exchange reaction between **3** and **2** is rationalized with the reaction energy of  $-25.0 \text{ kcal mol}^{-1}$ . The largest calculated exchange reaction energy is between **4** and **2** ( $-34.0 \text{ kcal mol}^{-1}$ ) in line with the observed fast and clean exchange reaction. This overall reactivity pattern also follows the Si=E bond strength (BDE, Table 1). The formation of the strong Si=S bond is the driving force of the reaction with  $S_8$  whereas the relative stability of the Si=Se bond over the Si=Te bond may be responsible for the observed one-way Te–Se exchange reaction.

## Conclusions

In conclusion, we present a simple approach for the synthesis of NHC-stabilized heavier silylium ions **2–4** starting from the corresponding NHC-stabilized silyliumylidene **1**. These complexes are rare examples of cationic silicon compounds with a terminal silicon–chalcogen bond. In addition, we achieved the regeneration of **1**, from **2–4** by the treatment with Aul, which represents a unique regeneration of a Si(II) cation from a Si(IV) sila-chalcogen compound. Moreover, intriguing chalcogen exchange reactions were observed, in good agreement with the calculated Si–E bond dissociation energy. Further reactivities of compounds **2–4** are currently under investigation in our lab.

## Conflicts of interest

There are no conflicts to declare.

## Acknowledgements

We gratefully acknowledge financial support from WACKER Chemie AG, the European Research Council (SILION 637394) and the DAAD (fellowship for D. S.).

## Notes and references

- (a) Z. Wang, in *Comprehensive Organic Name Reactions and Reagents*, John Wiley & Sons, Inc., 2010; (b) J. K. Groves, *Chem. Soc. Rev.*, 1972, **1**, 73–97.
- (a) M. G. Davlieva, S. V. Lindeman, I. S. Neretin and J. K. Kochi, *New J. Chem.*, 2004, **28**, 1568–1574; (b) B. Chevrier, J. M. Le Carpentier and R. Weiss, *J. Am. Chem. Soc.*, 1972, **94**, 5718–5723; (c) E. Lindner, *Angew. Chem., Int. Ed. Engl.*, 1970, **9**, 114–123; (d) P. H. Gore, *Chem. Rev.*, 1955, **55**, 229–281.
- (a) Y. Shoji, N. Tanaka, D. Hashizume and T. Fukushima, *Chem. Commun.*, 2015, **51**, 13342–13345; (b) G. A. Olah, G. K. S. Prakash and T. Nakajima, *Angew. Chem., Int. Ed. Engl.*, 1980, **19**, 812–813; (c) E. Lindner and H. G. Karmann, *Angew. Chem., Int. Ed. Engl.*, 1968, **7**, 548–548.
- (a) N. B. Jaufeerally, H. H. Abdallah, P. Ramasami and H. F. Schaefer III, *Theor. Chem. Acc.*, 2012, **131**, 1127–1137; (b) R. G. Pearson, *J. Chem. Sci.*, 2005, **117**, 369–377; (c) H.-Y. Liao, M.-D. Su and S.-Y. Chu, *Chem. Phys.*, 2000, **261**, 275–287; (d) R. G. Parr and P. K. Chattaraj, *J. Am. Chem. Soc.*, 1991, **113**, 1854–1855.
- R. Okazaki and N. Tokitoh, *Acc. Chem. Res.*, 2000, **33**, 625–630.
- (a) S. U. Ahmad, T. Szilvási, E. Irran and S. Inoue, *J. Am. Chem. Soc.*, 2015, **137**, 5828–5836; (b) S. U. Ahmad, T. Szilvási and S. Inoue, *Chem. Commun.*, 2014, **50**, 12619–12622.
- (a) A. Burchert, R. Müller, S. Yao, C. Schattenberg, Y. Xiong, M. Kaupp and M. Driess, *Angew. Chem., Int. Ed.*, 2017, **56**, 6298–6301; (b) D. Lutters, A. Merk, M. Schmidtmann and T. Müller, *Inorg. Chem.*, 2016, **55**, 9026–9032; (c) Y. C. Chan, Y. Li, R. Ganguly and C. W. So, *Eur. J. Inorg. Chem.*, 2015, 3821–3824; (d) Y. Xiong, S. Yao, R. Müller, M. Kaupp and M. Driess, *Angew. Chem., Int. Ed.*, 2015, **54**, 10254–10257; (e) K. Hansen, T. Szilvási, B. Blom, E. Irran and M. Driess, *Chem. – Eur. J.*, 2015, **21**, 18930–18933; (f) K. Chandra Mondal, S. Roy, B. Dittrich, B. Maity, S. Dutta, D. Koley, S. K. Vasa, R. Linser, S. Dechert and H. W. Roesky, *Chem. Sci.*, 2015, **6**, 5230–5234; (g) F. M. Mück, D. Kloß, J. A. Baus, C. Burschka, R. Bertermann, J. Poater, C. Fonseca Guerra, F. M. Bickelhaupt and R. Tacke, *Chem. – Eur. J.*, 2015, **21**, 14011–14021; (h) R. Tacke, C. Kobelt, J. A. Baus, R. Bertermann and C. Burschka, *Dalton Trans.*, 2015, **44**, 14959–14974; (i) K. Junold, J. A. Baus, C. Burschka, D. Auerhammer and R. Tacke, *Chem. – Eur. J.*, 2012, **18**, 16288–16291; (j) S. H. Zhang, H. X. Yeong and C. W. So, *Chem. – Eur. J.*, 2011, **17**, 3490–3499; (k) S. Yao, Y. Xiong and M. Driess, *Chem. – Eur. J.*, 2010, **16**, 1281–1288; (l) J. D. Epping, S. Yao, M. Karni, Y. Apeloig and M. Driess, *J. Am. Chem. Soc.*, 2010, **132**, 5443–5455; (m) A. Mitra, J. P. Wojcik, D. Lecoanet, T. Müller and R. West, *Angew. Chem., Int. Ed.*, 2009, **48**, 4069–4072; (n) T. Iwamoto, K. Sato, S. Ishida, C. Kabuto and M. Kira, *J. Am. Chem. Soc.*, 2006, **128**, 16914–16920; (o) N. Tokitoh and R. Okazaki, *Adv. Organomet. Chem.*, 2001, **47**, 121–166.
- (a) H. X. Yeong, H. W. Xi, Y. Li, K. H. Lim and C. W. So, *Chem. – Eur. J.*, 2013, **19**, 11786–11790; (b) Y. Xiong, S. Yao, S. Inoue, E. Irran and M. Driess, *Angew. Chem., Int. Ed.*, 2012, **51**, 10074–10077.
- (a) S. Chattopadhyaya, A. Pramanik, A. Banerjee and K. K. Das, *J. Phys. Chem. A*, 2006, **110**, 12303–12311; (b) S. Chattopadhyaya and K. K. Das, *Chem. Phys. Lett.*, 2004, **399**, 140–146.
- (a) X. Shen, Y. S. Puzyrev, C. Combs and S. T. Pantelides, *Appl. Phys. Lett.*, 2016, **109**, 113104; (b) Y. Ma, L. Kou, Y. Dai and T. Heine, *Phys. Rev. B: Condens. Matter*, 2016, **94**,

- 201104; (c) S. Keuleyan, M. Wang, F. R. Chung, J. Commons and K. J. Koski, *Nano Lett.*, 2015, **15**, 2285–2290; (d) E. G. Doni-Caranicola and A. P. Lambros, *J. Opt. Soc. Am.*, 1983, **73**, 383–386.
- 11 C.-T. Li, Y.-L. Tsai and K.-C. Ho, *ACS Appl. Mater. Interfaces*, 2016, **8**, 7037–7046.
- 12 (a) P. Bag, S. U. Ahmad and S. Inoue, *Bull. Chem. Soc. Jpn.*, 2017, **90**, 255–271; (b) V. S. V. S. N. Swamy, S. Pal, S. Khan and S. S. Sen, *Dalton Trans.*, 2015, **44**, 12903–12923; (c) P. Jutzi, *Chem. – Eur. J.*, 2014, **20**, 9192–9207; (d) G. Bertrand, *Science*, 2004, **305**, 783–785.
- 13 F. M. Mück, J. A. Baus, M. Nutz, C. Burschka, J. Poater, F. M. Bickelhaupt and R. Tacke, *Chem. – Eur. J.*, 2015, **21**, 16665–16672.
- 14 (a) D. Wendel, A. Porzelt, F. A. D. Herz, D. Sarkar, C. Jandl, S. Inoue and B. Rieger, *J. Am. Chem. Soc.*, 2017, **139**, 8134–8137; (b) F. Lips, J. C. Fettinger, A. Mansikkamäki, H. M. Tuononen and P. P. Power, *J. Am. Chem. Soc.*, 2014, **136**, 634–637; (c) R. Rodriguez, D. Gau, Y. Contie, T. Kato, N. Saffon-Merceron and A. Bacciredo, *Angew. Chem., Int. Ed.*, 2011, **50**, 11492–11495.
- 15 (a) D. E. Smiles, G. Wu and T. W. Hayton, *Inorg. Chem.*, 2014, **53**, 12683–12685; (b) W. Adam, R. M. Bargon and W. A. Schenk, *J. Am. Chem. Soc.*, 2003, **125**, 3871–3876; (c) W. Adam and R. M. Bargon, *Chem. Commun.*, 2001, 1910–1911; (d) Z. K. Sweeney, J. L. Polse, R. G. Bergman and R. A. Andersen, *Organometallics*, 1999, **18**, 5502–5510; (e) Z. K. Sweeney, J. L. Polse, R. A. Andersen, R. G. Bergman and M. G. Kubinec, *J. Am. Chem. Soc.*, 1997, **119**, 4543–4544; (f) L. M. Berreau and L. K. Woo, *J. Am. Chem. Soc.*, 1995, **117**, 1314–1317.
- 16 D. Yadav, R. K. Siwatch, G. Mukherjee, G. Rajaraman and S. Nagendran, *Inorg. Chem.*, 2014, **53**, 10054–10059.
- 17 (a) L. Prokeš, P. Kubáček, E. M. Peña-Méndez, F. Amato, J. E. Conde, M. Alberti and J. Havel, *Chem. – Eur. J.*, 2016, **22**, 11261–11268; (b) A. Sahu, L. Qi, M. S. Kang, D. Deng and D. J. Norris, *J. Am. Chem. Soc.*, 2011, **133**, 6509–6512; (c) Z. Sun, Z. Yang, J. Zhou, M. H. Yeung, W. Ni, H. Wu and J. Wang, *Angew. Chem., Int. Ed.*, 2009, **48**, 2881–2885; (d) J. Majimel, D. Bacinello, E. Durand, F. Vallée and M. Tréguer-Delapierre, *Langmuir*, 2008, **24**, 4289–4294.
- 18 F. M. Mück, J. A. Baus, C. Burschka and R. Tacke, *Chem. – Eur. J.*, 2016, **22**, 5830–5834.
- 19 J. E. Drake, B. M. Glavinčevski and R. T. Hemmings, *Can. J. Chem.*, 1980, **58**, 2161–2166.

## 7. The quest for stable silaaldehydes: synthesis and reactivity of a masked silacarbonyl

**Title:** The quest for stable silaaldehydes: synthesis and reactivity of a masked silacarbonyl

**Status** Communication, published November 16, 2018

**Journal** Chem. Eur.J.2019, 25,1198 –1202

**Publisher** WILEY-VCH Verlag GmbH & Co. KGaA, Weinheim

**DOI** 10.1002/chem.201805604

**Authors** Debotra Sarkar, Vitaly Nesterov, Tibor Szilvási, Philipp J. Altmann, Shigeyoshi Inoue

*Reprinted with permission. © 2019 Wiley-VCH Verlag GmbH & Co. KGaA, Weinheim*

**Content** Aldehydes [R-(C=O)H] are one of the most important functionalities among the carbonyls. It is commonly utilized as a precursor for the synthesis of other carbonyl compounds, and carbon-carbon or carbon-hetero atomic multiple bond species. Thus, the chemistry of aldehydes is well studied. In contrast, the chemistry of the silicon analogs of aldehydes, so-called silaaldehydes [R-(Si=O)H] is relatively unexplored. This could be attributed to the large difference in electronegativities combined with the poor  $\pi$  overlap between silicon and oxygen, which renders the Si-O bond strongly polarized ( $\text{Si}^{\delta+}\text{-O}^{\delta-}$ ) and weak. Thus, in the absence of suitable steric protection, they undergo “head-to-tail” oligomerization/polymerization. This process is even more facile for silaaldehydes than silanones ( $\text{R}_2(\text{Si}=\text{O})$ ), due to decreased steric protection. Therefore, isolation of silaaldehyde in the condensed phase presents a formidable synthetic challenge. In this study, we report the isolation and reactivity of donor-acceptor stabilized silaaldehyde  $[\{(m\text{-Ter}(\text{H})\text{SiO})(\text{GaCl}_3)\}(\text{NHC})]$  **4**, (NHC =  $\text{IME}_4$ ). Compound **4** was prepared by the hydrolysis of NHC-stabilized silyliumylidene  $[\{m\text{-TerSi}(\text{NHC})_2\}\text{Cl}]$  **1**, in the presence of a Lewis acid ( $\text{GaCl}_3$ ). The subsequent transformation of **4** to the corresponding silacarboxylate

The quest for stable silaaldehydes: synthesis and reactivity of a masked silacarbonyl

[*m*-Ter(SiO)(OGaCl<sub>2</sub>)}(NHC)]<sub>2</sub> **7**, silaacyl chloride [*m*-Ter(Cl)SiO)(GaCl<sub>3</sub>)}(NHC)] **9**, phosphasilene [*m*-Ter(H)SiPTMS)}(NHC)] **10**, unveil its true potential as a synthon in silacarbonyl chemistry.

### Author Contributions

- Debotra Sarkar planned and executed all experiments. Debotra Sarkar and Dr. Vitaly Nesterov co-wrote the manuscript. Dr. Tibor Szilvási designed and performed the theoretical investigations. Dr. Philipp J. Altmann conducted all SC-XRD measurements and processed the resulting data. All the work was performed under the supervision of Prof. Shigeyoshi Inoue.

The quest for stable silaaldehydes: synthesis and reactivity of a masked silacarbonyl

## Carbene Ligands

# The Quest for Stable Silaaldehydes: Synthesis and Reactivity of a Masked Silacarbonyl

 Debotra Sarkar,<sup>[a]</sup> Vitaly Nesterov,<sup>[a]</sup> Tibor Szilvási,<sup>[b]</sup> Philipp J. Altmann,<sup>[a]</sup> and Shigeyoshi Inoue<sup>\*[a]</sup>

Dedicated to Professor Rainer Streubel on the Occasion of his 60th Birthday

**Abstract:** The first donor–acceptor complex of a silaaldehyde, with the general formula (NHC)(Ar)Si(H)OGaCl<sub>3</sub> (NHC = N-heterocyclic carbene), was synthesized using the reaction of silyliumylidene–NHC complex [(NHC)<sub>2</sub>(Ar)Si]Cl with water in the presence of GaCl<sub>3</sub>. Conversion of this complex to the corresponding silacarboxylate dimer [(NHC)(Ar)SiO<sub>2</sub>GaCl<sub>2</sub>]<sub>2</sub>, free silaacetal ArSi(H)(OR)<sub>2</sub>, silaacyl chloride (NHC)(Ar)Si(Cl)OGaCl<sub>3</sub>, and phosphasilene–NHC adduct (NHC)(Ar)Si(H)PTMS unveil its true potential as a synthon in silacarbonyl chemistry.

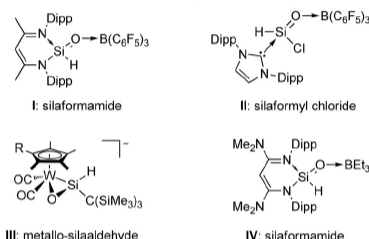
The carbonyl group is an important and ubiquitous functionality in the field of organic chemistry, life sciences, and beyond.<sup>[1]</sup> Although aldehydes, ketones, and carboxylic acid derivatives are generally well-known stable organic compounds, the synthesis and isolation of their stable heavier group 14 analogues is challenging.<sup>[2]</sup> The instability and high tendency of the latter to oligomerize are attributed to the different nature of the heavier E=O bonds (E = Si–Pb), which exhibit higher zwitterionic character E<sup>δ+</sup>–O<sup>δ-</sup> due to the significant decrease in electronegativity of heavier elements and their intrinsic propensity to form weaker π-bonds descending the group. Recent years have witnessed considerable advances in the isolation of monomeric silacarbonyl compounds including silanones (R<sub>2</sub>SiO) and silanoic acid (RSi(O)OH) derivatives.<sup>[3–9]</sup> Rational steric and electronic protection, Lewis base or Lewis base/acid complex formation are the key approaches to achieve the required stabilization.<sup>[3–10]</sup> Nevertheless, despite this success, our knowledge about the reactivity of silicon analogues of carbonyl compounds and their synthetic potential remains limited.

[a] D. Sarkar, Dr. V. Nesterov, P. J. Altmann, Prof. Dr. S. Inoue  
 WACKER-Institute of Silicon Chemistry and  
 Catalysis Research Center, Technische Universität München  
 Lichtenbergstraße 4, 85748 Garching bei München (Germany)  
 E-mail: s.inoue@tum.de

[b] Dr. T. Szilvási  
 Department of Chemical and Biological Engineering  
 University of Wisconsin-Madison, 1415 Engineering Drive  
 Madison, WI 53706-1607 (USA)

Supporting information and the ORCID identification number(s) for the author(s) of this article can be found under:  
<https://doi.org/10.1002/chem.201805604>

a) described compounds with silaformyl group (R = Me, Et):



b) present work:

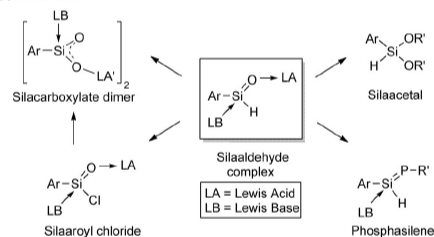


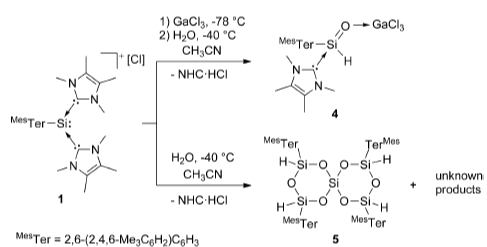
Figure 1. (a) Silaformyl compounds I–IV. (b) Present work.

Among reported silacarbonyls, derivatives containing a silaformyl group (–Si(H)O) are rare (I–IV, Figure 1a),<sup>[6–9]</sup> whereas a stable analogue of an aldehyde (RSi(H)O) with three-coordinate silicon is not known. Driess and co-workers reported a silaformamide–borane complex (I) with essential Si=O double-bond character synthesized by reacting corresponding hydroxysilylene with water–borane adduct H<sub>2</sub>O–B(C<sub>6</sub>F<sub>5</sub>)<sub>3</sub>.<sup>[6]</sup> Several years later, Roesky, Frenking, and co-workers described the isolation of silaformyl chloride complex (II)<sup>[7]</sup> via the reaction of the silylene dichloride–NHC adduct (IDipp)Cl<sub>2</sub>Si: with H<sub>2</sub>O–B(C<sub>6</sub>F<sub>5</sub>)<sub>3</sub> and an additional equivalent of the NHC. Hashimoto, Tobita, and co-workers isolated anionic η<sup>2</sup>-silaaldehyde complex (III) with a Si–O motif within the coordination sphere of tungsten, considered as a three-membered metallacycle rather than a silaaldehyde π-complex.<sup>[8]</sup> More recently, the group of Aldridge in an elegant study demonstrated the synthetic utility of nacnac-supported chlorosilylene to access a number of silacarbonyls, including silaformamide IV.<sup>[9]</sup>



Previously we succeeded in the isolation of stable three-coordinate imino(silyl) silanones [(IDipp)N](R<sub>3</sub>Si)SiO (IDipp = [HC(DippN)]<sub>2</sub>C; R = tBu, SiMe<sub>3</sub>) with prolonged lifetime in solution.<sup>[3a]</sup> Our quest for a stable silaaldehyde started from the investigation of the reactivity of a NHC-stabilized silyliumylidene [(IMe<sub>4</sub>)<sub>2</sub>(<sup>Mes</sup>Ter)Si:]Cl (1, <sup>Mes</sup>Ter = 2,6-(2,4,6-Me<sub>3</sub>C<sub>6</sub>H<sub>2</sub>)<sub>2</sub>C<sub>6</sub>H<sub>3</sub>, IMe<sub>4</sub> = [(Me)C(MeN)]<sub>2</sub>C)<sup>[11]</sup> and hydridosilylene (IMe<sub>4</sub>)(tBu<sub>3</sub>Si)(H)Si: (2).<sup>[12]</sup> These compounds react with carbon dioxide, affording NHC-stabilized silaacylium salt [(IMe<sub>4</sub>)<sub>2</sub>(<sup>Mes</sup>Ter)Si(O)]Cl (3) with comparably high double-bond character of the Si=O bond,<sup>[5c]</sup> and NHC-free cyclotrisiloxane [(tBu<sub>3</sub>Si)(H)SiO]<sub>3</sub> regarded as a trimer of silaaldehyde intermediate.<sup>[13]</sup> Exploration of the reactivity of silyliumylidene (1) towards chalcogens and H<sub>2</sub>S enabled an access to NHC-stabilized heavier chalcogen silaacylium derivatives<sup>[14]</sup> and thiosilaaldehyde.<sup>[15]</sup> Herein, we report our study devoted to the synthesis of a silaaldehyde, isolated as a Si<sub>2</sub>O-donor-acceptor complex, and its unique reactivity showing strong relationship to the chemistry of carbonyl congeners (Figure 1b).

Treatment of silyliumylidene complex 1 with equimolar amounts of gallium chloride and water in acetonitrile at low temperatures led to the formation of complex 4 together with corresponding imidazolium chloride (Scheme 1). Recrystalliza-



Scheme 1. Hydrolysis of silyliumylidene complex 1 in the presence and absence of the Lewis acid (GaCl<sub>3</sub>).

tion of the raw product from acetonitrile/toluene solution (2:1) at -30 °C furnished colorless crystals of 4 in a moderate yield (61 %).

The <sup>1</sup>H NMR spectrum of compound 4 in CD<sub>3</sub>CN shows a distinct signal of silicon-bound hydrogen at 4.98 ppm (<sup>1</sup>J<sub>Si,H</sub> = 234 Hz). It lies within the range of values reported for silaformyl compounds I, II (broad signals at 5.64 and 5.55 ppm, respectively)<sup>[6,7]</sup> and III (4.29 ppm, <sup>1</sup>J<sub>Si,H</sub> = 190.6 Hz),<sup>[8]</sup> and considerably upfield-shifted compared to the formyl proton of the corresponding aldehyde <sup>Mes</sup>TerCHO (9.65 ppm).<sup>[16]</sup> The <sup>29</sup>Si NMR spectrum of 4 exhibits a resonance at -45.0 ppm, which is very close to that of silaformyl chloride II (-49.8 ppm).<sup>[7]</sup>

The molecular structure of complex 4 was unambiguously confirmed by single-crystal X-ray diffraction analysis (Figure 2), which revealed a distorted tetrahedral geometry of the silicon atom.

The Si–O bond distance in 4 is 1.605(3) Å. Surprisingly, it is only marginally shorter than Si–O single bonds in acyclic organodisiloxanes (R<sub>3</sub>Si)<sub>2</sub>O (1.61–1.64 Å) or siloxanes R<sub>3</sub>SiOR' (ca.

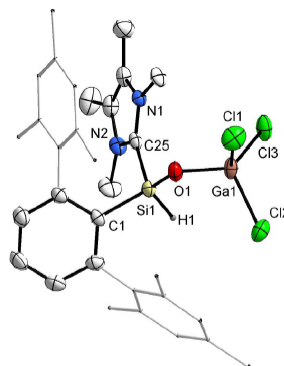


Figure 2. Molecular structure of 4. Hydrogen atoms except H1 are omitted for clarity.

1.64 Å), and even slightly longer than those in halogenodisiloxanes (X<sub>3</sub>Si)<sub>2</sub>O (1.58–1.59 Å, X = F, Cl).<sup>[17]</sup> This bond is also elongated compared to those in I, II, and IV (1.552(2), 1.568(15), and 1.5514(10) Å, respectively)<sup>[6,7,9]</sup> and in three-coordinate silanones (1.52–1.54 Å).<sup>[3]</sup>

In the solid state, the IR spectrum of 4 displayed a strong absorption band at 975 cm<sup>-1</sup>. Although Si=O stretching vibrations of parent silaaldehydes in argon matrix are observed at higher wave numbers (H<sub>2</sub>SiO,  $\tilde{\nu}$  = 1202 cm<sup>-1</sup>, and MeSi(H)O,  $\tilde{\nu}$  = 1207 cm<sup>-1</sup>),<sup>[18a]</sup> this value is large enough to distinguish it from the absorption of Si–O single bonds ( $\tilde{\nu}$  = 800–900 cm<sup>-1</sup>).<sup>[18b]</sup> Thus, the structural and IR data suggest strong dominance of the zwitterionic resonance structure 4B or equivalent Lewis structure 4C into the ground state of the molecule (Figure 3).

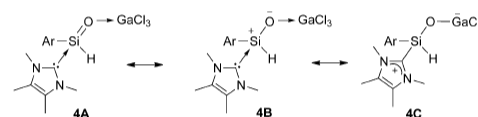


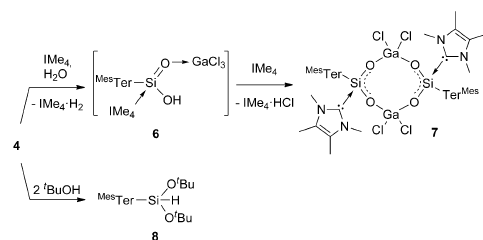
Figure 3. Resonance structures of silaaldehyde 4.

DFT calculations at B97-D/def2-SVP level of theory showed a good agreement between calculated metric parameters, the <sup>29</sup>Si NMR as well as IR data ( $\delta$  = -41.2 ppm,  $\tilde{\nu}$  = 964 cm<sup>-1</sup>) of 4 and the experimentally obtained data. HOMO and LUMO of 4 are mainly located at the aryl ligand/chlorine atom and NHC ligand/Si-C<sub>NHC</sub> σ\* orbital/aryl ligand, respectively (Figure S22). No indication of possible Si–O π-orbital was observed. Natural charges of Si and O atoms (1.67 and -1.22, respectively) indicate strong charge separation. Obtained Wiberg bond index (WBI), and Mayer bond order (MBO) of the Si–O bond (0.74 and 1.21, respectively) indicate a single bond with negligible double-bond character. The computed mechanism of formation of 4 includes barrier-free protonation of 1 involving

$\text{H}_2\text{O}\cdot\text{GaCl}_3$  complex and following transformations toward **4** with low energy barriers (Scheme S1 in the Supporting Information).

Interestingly, the use of other Lewis acid reagents, such as  $\text{AlCl}_3$ ,  $\text{B}(\text{C}_6\text{F}_5)_3$ ,  $\text{BX}_3$  ( $\text{X} = \text{F}, \text{Cl}, \text{Br}$ ), or  $\text{ZnX}_2$  ( $\text{X} = \text{F}, \text{Cl}$ ), instead of gallium chloride in the reaction of **1** with water did not lead to any selective transformation. In an attempt to procure an acceptor-free silaaldehyde  $^{\text{Mes}}\text{Ter}(\text{IMe}_2)\text{Si}(\text{H})\text{O}$ , hydrolysis of **1** was also performed in the absence of any Lewis acid (Scheme 1). However, it resulted in the formation of a mixture of unidentified products, from which only sterically hindered spiro-siloxane **5** was isolated in 9.2% yield. The structure of **5** was confirmed using multinuclear NMR spectroscopy and single-crystal X-ray diffraction analysis (see the Supporting Information). An attempt to remove the NHC from **4** using  $\text{BPh}_3$  at 80 °C led to the isolation of the corresponding borane–NHC adduct and unidentified decomposition products.

In order to access the donor–acceptor complex of a silacarboxylic acid (**6**), silaaldehyde complex **4** was reacted with water in the presence of the NHC as a hydrogen scavenger (Scheme 2). Reaction led to the formation of an unprecedented



Scheme 2. Synthesis of siladicarboxylate **7** and silaacetal **8**.

gallium silacarboxylate complex (**7**) isolated in low yield (8%) if one equivalent of the NHC was employed. The yield of **7** was improved to 22% using two equivalents of the NHC. The corresponding 2,2-dihydroimidazolidine and imidazolium salt were identified as by-products. Additionally, alcoholysis of complex **4** with *tert*-butanol provided silaacetal **8** isolated in 79% yield (Scheme 2).

Molecular structures of **7** and **8** were confirmed using X-ray diffraction analysis. In the solid state, compound **7** exists as a centrosymmetric dimer containing two silacarboxylate ( $^{\text{Mes}}\text{TerSiO}_2$ ) fragments bridged by two  $\text{GaCl}_2$  units in a similar manner found in gallium(III) carboxylate complexes (Figure 4).<sup>[19]</sup> Each silicon center has a distorted tetrahedral geometry. The  $\text{Si1}-\text{O2}$  (1.586(17) Å) and  $\text{Si1}-\text{O1}$  (1.603(17) Å) distances are close to each other and to the  $\text{Si}-\text{O}$  distance found in **4**. These distances are also comparable to those in the donor–acceptor-stabilized silanoic acid  $(\text{EtO})(\text{D}\rightarrow)\text{Si}(\text{O}\rightarrow\text{A})\text{OH}$  (1.588(2)–1.626(2) Å) reported by Baceiredo, Kato, and co-workers.<sup>[56]</sup> Moreover, both  $\text{Si}-\text{O}$  bonds in **7** are sufficiently shorter than  $\text{Si}-\text{O}$  single bonds in gallium–siloxane complexes (1.62–1.70 Å).<sup>[20]</sup>

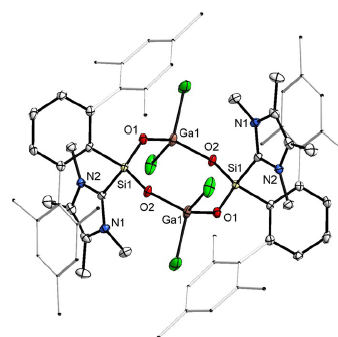
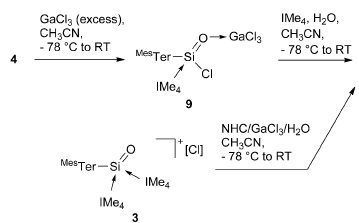


Figure 4. Molecular structure of **7**. Hydrogen atoms are omitted for clarity.

According to our DFT calculation, the  $\text{Si}-\text{O}$  bonds in  $\text{SiO}_2$  moieties in **7** are almost identical (within 0.02 Å). MBOs are the same for all  $\text{Si}-\text{O}$  bonds (1.18) and the same as that found in the starting material. Notably, the HOMO–40 of **7** (Figure S24) shows a cyclic delocalization through the oxygen atoms, thus supporting the heavy silacarboxylate analogy. Conversion of **4** into **7** involves intermediate formation of the acid **6** and starts from the nucleophilic attack of the silicon of **4** by the oxygen of the  $\text{H}_2\text{O}\cdot\text{NHC}$  complex (Scheme S2).

We used the reaction of silaaldehyde complex **4** with an excess of gallium chloride to access novel silaacyl chloride **9** (Scheme 3). An analytically pure sample of **9** was obtained in



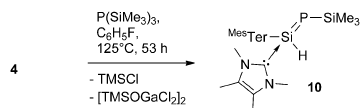
Scheme 3. Synthesis of silaacyl chloride complex **9** and alternative approaches to siladicarboxylate complex **7**.

low yield (9%) as a very moisture-sensitive solid with low solubility in polar organic solvents. All attempts to characterize single crystals of **9**, using X-ray diffraction analysis, led to their contamination with the corresponding acid  $\text{Ar}(\text{IMe}_2)\text{-Si}(\text{O})(\text{GaCl}_2)\text{OH}$  (**6**) due to partial hydrolysis (see the Supporting Information).

In order to examine a relationship to classical acyl transfer reactions, we performed hydrolysis of silaacyl derivatives **9** and **3** with water under various conditions. It was found that reaction of silaacyl chloride **9** with water in the presence of NHC leads to selective formation of siladicarboxylate dimer **7**, whereas the reaction of silaacyl salt **3**<sup>[5c]</sup> with a  $\text{NHC}/\text{GaCl}_3/$

H<sub>2</sub>O mixture (1:1:1) provides the same product in 43% yield (Scheme 3).

Aldehydes and ketones are known as important reagents not only in C–C bond forming reactions, but also for the construction of mono- and heteronuclear C=E double bonds (E = C, N, P).<sup>[1]</sup> We found that reaction of **4** with tris(trimethylsilyl)-phosphine at elevated temperature in fluorobenzene yields selectively thermally stable NHC-supported phosphasilene **10** (Scheme 4). Although the mechanism of this transformation re-



Scheme 4. Synthesis of phosphasilene **10** from silaaldehyde complex **4**.

mains unclear, it may involve nucleophilic attack of the phosphorus reagent on the electropositive silicon, leading to elimination of transient [TMSOGaCl<sub>2</sub>]<sup>-</sup> anion and following formation of TMSOGaCl<sub>2</sub> dimer,<sup>[22]</sup> TMSCl, and phosphasilene **10** (Scheme S3). Notably, the analogous reaction of aldehydes RCHO with bis(trimethylsilyl)phosphines R'PTMS<sub>2</sub> in the presence of AlCl<sub>3</sub> is known to yield corresponding phosphalkenes R(H)C=PR'.<sup>[21]</sup>

The same phosphasilene complex **10** was obtained alternatively using a convenient two-step approach starting from Mes<sub>3</sub>TerSi(H)Cl<sub>2</sub> (see the Supporting Information). Reaction products in both cases were identical and showed the same spectroscopic data. Moreover, **10** was characterized by X-ray diffraction analysis (Figure 5). The obtained spectroscopic and structural data of **10** are in good agreement with those of the previously described similar phosphasilene–NHC complex bearing a more bulky D<sup>ip</sup>Ter aryl substituent at the silicon atom.<sup>[23,24]</sup>

In summary, we have synthesized and characterized the first donor–acceptor complex of an aryl silaaldehyde. Notably, it

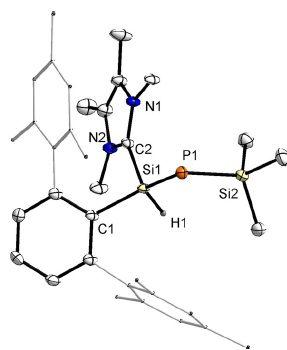


Figure 5. Molecular structure of **10**. Hydrogen atoms except H1 are omitted for clarity.

reacts as a masked silacarbonyl, providing an access to a number of stable derivatives, thus showing a relationship to carbonyl chemistry. Difficulties in the preparation of the corresponding donor and acceptor-free silaaldehyde complexes, as well as the isolation of free spiroloxane, underline the low stability of the corresponding free silaaldehyde. Thus, the quest for stable free silaaldehydes remains challenging.

### Acknowledgements

We gratefully acknowledge financial support from WACKER Chemie AG, the European Research Council (SILION 637394), the DAAD (fellowship for D.S.), Dr. A. Pöthig for crystallographic advice, Mr. J. Sicklinger for IR measurements.

### Conflict of interest

The authors declare no conflict of interest.

**Keywords:** N-heterocyclic carbenes · silaaldehydes · silacarbonyl groups · silanones · silyliumylidenes

- [1] J. Clayden, N. Greeves, S. Warren, *Organic Chemistry*, 2nd ed., Oxford Press, Oxford, 2012.
- [2] a) Y. Xiong, S. Yao, M. Driess, *Angew. Chem. Int. Ed.* **2013**, *52*, 4302; *Angew. Chem.* **2013**, *125*, 4398; b) S. S. Sen, *Angew. Chem. Int. Ed.* **2014**, *53*, 8820; *Angew. Chem.* **2014**, *126*, 8964.
- [3] Ambient temperature stable silanones with three-coordinate silicon: a) D. Wendel, D. Reiter, A. Porzelt, P. J. Altmann, S. Inoue, B. Rieger, *J. Am. Chem. Soc.* **2017**, *139*, 17193; b) A. Rosas-Sánchez, I. Alvarado-Beltrán, A. Baceiredo, N. Saffon-Merceron, S. Massou, D. Hashizume, V. Branchadell, T. Kato, *Angew. Chem. Int. Ed.* **2017**, *56*, 15916; *Angew. Chem.* **2017**, *129*, 16132; c) I. Alvarado-Beltrán, A. Rosas-Sánchez, A. Baceiredo, N. Saffon-Merceron, V. Branchadell, T. Kato, *Angew. Chem. Int. Ed.* **2017**, *56*, 10481; *Angew. Chem.* **2017**, *129*, 10617; d) A. C. Filippou, B. Baars, O. Chernov, Y. N. Lebedev, G. Schnakenburg, *Angew. Chem. Int. Ed.* **2014**, *53*, 565; *Angew. Chem.* **2014**, *126*, 576.
- [4] Silanones with four-coordinate silicon: a) R. Rodríguez, T. Troadec, D. Gau, N. Saffon-Merceron, D. Hashizume, K. Miqueu, J. M. Sotiropoulos, A. Baceiredo, T. Kato, *Angew. Chem. Int. Ed.* **2013**, *52*, 4426; *Angew. Chem.* **2013**, *125*, 4522; b) Y. Xiong, S. Yao, R. Müller, M. Kaupp, M. Driess, *Nat. Chem.* **2010**, *2*, 577; c) S. Yao, Y. Xiong, M. Driess, *Chem. Eur. J.* **2010**, *16*, 1281; d) Y. Xiong, S. Yao, R. Müller, M. Kaupp, M. Driess, *J. Am. Chem. Soc.* **2010**, *132*, 6912; e) Y. Xiong, S. Yao, M. Driess, *J. Am. Chem. Soc.* **2009**, *131*, 7562.
- [5] a) R. Rodríguez, I. Alvarado-Beltrán, J. Saouli, N. Saffon-Merceron, A. Baceiredo, V. Branchadell, T. Kato, *Angew. Chem. Int. Ed.* **2018**, *57*, 2635; *Angew. Chem.* **2018**, *130*, 2665; b) R. Rodríguez, D. Gau, J. Saouli, A. Baceiredo, N. Saffon-Merceron, V. Branchadell, T. Kato, *Angew. Chem. Int. Ed.* **2017**, *56*, 3935; *Angew. Chem.* **2017**, *129*, 3993; c) S. U. Ahmad, T. Szilvási, E. Irran, S. Inoue, *J. Am. Chem. Soc.* **2015**, *137*, 5828; d) Y. Wang, M. Chen, Y. Xie, P. Wie, H. F. Schaefer III, P. v. R. Schleyer, G. H. Robinson, *Nat. Chem.* **2015**, *7*, 509; e) R. Rodríguez, D. Gau, T. Troadec, N. Saffon-Merceron, V. Branchadell, A. Kato, T. Baceiredo, *Angew. Chem. Int. Ed.* **2013**, *52*, 8980; *Angew. Chem.* **2013**, *125*, 9150; f) R. S. Ghadwal, R. Azhakar, H. W. Roesky, K. Pröpper, B. Dittrich, S. Klein, G. Frenking, *J. Am. Chem. Soc.* **2011**, *133*, 17552–17555; g) Y. Xiong, S. Yao, M. Driess, *Angew. Chem. Int. Ed.* **2010**, *49*, 6642; *Angew. Chem.* **2010**, *122*, 6792; h) Y. Xiong, S. Yao, M. Driess, *Dalton Trans.* **2010**, *39*, 9282; i) S. Yao, Y. Xiong, M. Brym, M. Driess, *J. Am. Chem. Soc.* **2007**, *129*, 7268.
- [6] S. Yao, M. Brym, C. V. Wüllen, M. Driess, *Angew. Chem. Int. Ed.* **2007**, *46*, 4159; *Angew. Chem.* **2007**, *119*, 4237.
- [7] R. S. Ghadwal, R. Azhakar, H. W. Roesky, K. Pröpper, B. Dittrich, C. Goedecke, G. Frenking, *Chem. Commun.* **2012**, *48*, 8186.

- [8] T. Fukuda, H. Hashimoto, S. Sakaki, H. Tobita, *Angew. Chem. Int. Ed.* **2016**, *55*, 188; *Angew. Chem.* **2016**, *128*, 196.
- [9] D. C. H. Do, A. V. Protchenko, M. Ángeles Fuentes, J. Hicks, E. L. Kolychev, P. Vasko, S. Aldridge, *Angew. Chem. Int. Ed.* **2018**, *57*, 13907; *Angew. Chem.* **2018**, *130*, 14103.
- [10] V. Nesterov, D. Reiter, P. Bag, P. Frisch, R. Holzner, A. Porzelt, S. Inoue, *Chem. Rev.* **2018**, *118*, 9678.
- [11] S. U. Ahmad, T. Szilvási, S. Inoue, *Chem. Commun.* **2014**, *50*, 12619.
- [12] S. Inoue, C. Eisenhut, *J. Am. Chem. Soc.* **2013**, *135*, 18315.
- [13] C. Eisenhut, N. C. Breit, T. Szilvási, E. Iran, S. Inoue, *Eur. J. Inorg. Chem.* **2016**, 2696.
- [14] D. Sarkar, D. Wendel, S. U. Ahmad, T. Szilvási, A. Pothig, S. Inoue, *Dalton Trans.* **2017**, *46*, 16014.
- [15] A. Porzelt, J. Schweizer, R. Baierl, P. Altmann, M. Holthausen, S. Inoue, *Inorganics* **2018**, *6*, 54.
- [16] R. C. Smith, L. B. Gleason, J. D. Protasiewicz, *J. Mater. Chem.* **2006**, *16*, 2445.
- [17] W. S. Sheldrick in *The Chemistry of Organic Silicon Compounds* (Eds.: S. Patai, Z. Rappoport), Wiley, Chichester, **1989**, pp. 227–303.
- [18] a) R. Withnall, L. Andrews, *J. Am. Chem. Soc.* **1986**, *108*, 8118; b) V. N. Khabashesku, Z. A. Kerzina, K. N. Kudin, O. M. Nefedov, *J. Organomet. Chem.* **1998**, *566*, 45.
- [19] M. R. Kaluderović, S. Gómez-Ruiz, B. Gallego, E. Hey-Hawkins, R. Paschke, G. N. Kaluderović, *Eur. J. Med. Chem.* **2010**, *45*, 519.
- [20] a) C. N. McMahon, S. J. Obrey, A. Keys, S. G. Bott, A. R. Barron, *Dalton Trans.* **2000**, 2151; b) N. R. Bunn, S. Aldridge, C. Jones, *Appl. Organomet. Chem.* **2004**, *18*, 425.
- [21] J. I. Bates, B. O. Patrick, D. P. Gates, *New J. Chem.* **2010**, *34*, 1660.
- [22] H. Schmidbaur, W. Findeiss, *Chem. Ber.* **1966**, *99*, 2187.
- [23] K. Hansen, T. Szilvási, B. Blom, M. Driess, *Angew. Chem. Int. Ed.* **2015**, *54*, 15060; *Angew. Chem.* **2015**, *127*, 15274.
- [24] V. Nesterov, N. C. Breit, S. Inoue, *Chem. Eur. J.* **2017**, *23*, 12014.

Manuscript received: November 8, 2018

Accepted manuscript online: November 16, 2018

Version of record online: December 20, 2018

## 8. N-heterocyclic carbene-stabilized germa-acylium ion: reactivity and utility in catalytic CO<sub>2</sub> functionalizations

**Title:** N-heterocyclic carbene-stabilized germa-acylium ion: reactivity and utility in catalytic CO<sub>2</sub> functionalizations

**Status** Article, published on August 10, 2020

**Journal** *J. Am. Chem. Soc.* 2020, 142, 36, 15403-15411

**Publisher** American Chemical Society

**Authors** Debotra Sarkar, Catherine Weetman, Sayan Dutta, Emeric Schubert, Christian Jandl, Debasis Koley, and Shigeyoshi Inoue

*Reprinted permission © 2020 American Chemical Society*

**Content** Catalytic conversion of CO<sub>2</sub> into value-added product (e.g. methanol) has been gaining considerable attention in the last decade owing to the high global energy demand and subsequent rising CO<sub>2</sub> emissions. Nevertheless, these transformations are highly challenging and often require high temperatures and pressures due to the strong C-O bond strength in CO<sub>2</sub> (552 kJ mol<sup>-1</sup>). Recently transition metal oxides have shown significant catalytic activity in this regard. DFT studies suggest that high charge density at the oxygen atom due to the zwitterionic nature of the metal-oxo bond, is plays a pivotal role in catalytic turnover. However, despite the extremely polarized E-O bond (E = Si-Ge), such application with group 14 molecular oxides are unknown.

In this study, we report the first example of heavier germanium analogue of an acylium ion, [ $\{m\text{-TerGe}(\text{O})(\text{NHC})_2\}\text{X}$ ] **3**, (X = Cl or BAr<sup>F</sup><sub>4</sub>, NHC = IMe<sub>4</sub>). Compound **3** was obtained through oxidation of germyliumylidene [ $\{m\text{-TerGe}(\text{NHC})_2\}\text{X}$ ] **2** with N<sub>2</sub>O. Treatment of **3** with Ph<sub>3</sub>SiOH led to the first solely donor-stabilized germanium ester [ $\{m\text{-TerGe}(\text{O})(\text{OSiPh}_3)\}(\text{NHC})$ ] **4**. Fascinating reactivity of **3** with Lawesson's [LR = (CH<sub>3</sub>OPhPS<sub>2</sub>)<sub>2</sub>] and Wollins reagents [WR = (PhPSe<sub>2</sub>)<sub>2</sub>], reagent gave rise to the corresponding heavier analogs [ $\{m\text{-TerGe}(\text{S})(\text{NHC})_2\}\text{X}$ ] **5** and [ $\{m\text{-TerGe}(\text{Se})(\text{NHC})_2\}\text{X}$ ] **6**. These reactivities demonstrate the carbonyl like behavior of compound **3**. Further, the polarized

## N-heterocyclic carbene-stabilized germa-acylium ion: reactivity and utility in catalytic CO<sub>2</sub> functionalizations

terminal [GeO] bond in the germa-acylium ion **3** was utilized to activate CO<sub>2</sub> and silane. Interestingly the reactivity of **3** with CO<sub>2</sub> was found to be reversible, thus mimicking the behavior of transition metal oxides. Additionally, its transition metal like nature is demonstrated as it was found to be an active catalyst in both CO<sub>2</sub> hydrosilylation and reductive *N*-functionalization of amines using CO<sub>2</sub> as the C<sub>1</sub> source. Mechanistic studies were performed both experimentally and computationally, which revealed the reaction proceeds *via* a NHC-siloxygermylene [{RGe(OSiHPh<sub>2</sub>)}(NHC)] **8**.

### Author Contributions

- Debotra Sarkar planned and executed all experiments (in parts together with, Emeric Schubert during his internship). Debotra Sarkar and Dr. Catherine Weetman co-wrote the manuscript. Sayan Dutta and Prof. Debasis Koley designed and performed the theoretical investigations. Dr. Christian Jandl conducted all SC-XRD measurements and processed the resulting data. All the work was performed under the supervision of Prof. Shigeyoshi Inoue.

## N-Heterocyclic Carbene-Stabilized Germa-acylium Ion: Reactivity and Utility in Catalytic CO<sub>2</sub> Functionalizations

Debotra Sarkar, Catherine Weetman, Sayan Dutta, Emeric Schubert, Christian Jandl, Debasis Koley,\* and Shigeyoshi Inoue\*

Cite This: *J. Am. Chem. Soc.* 2020, 142, 15403–15411

Read Online

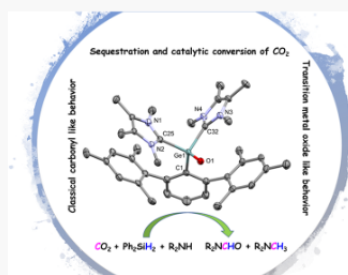
ACCESS |

Metrics & More

Article Recommendations

Supporting Information

**ABSTRACT:** The first acceptor-free heavier germanium analogue of an acylium ion, [RGe(O)(NHC)<sub>2</sub>]X (R = <sup>Me</sup>Ter = 2,6-(2,4,6-Me<sub>3</sub>C<sub>6</sub>H<sub>2</sub>)<sub>2</sub>C<sub>6</sub>H<sub>3</sub>; NHC = IMe<sub>4</sub> = 1,3,4,5-tetramethylimidazol-2-ylidene; X = (Cl or BArF = {(3,5-(CF<sub>3</sub>)<sub>2</sub>C<sub>6</sub>H<sub>3</sub>)<sub>4</sub>B}), was isolated by reacting [RGe(NHC)<sub>2</sub>]X with N<sub>2</sub>O. Conversion of the germa-acylium ion to the first solely donor-stabilized germanium ester [(NHC)RGe(O)(OSiPh<sub>3</sub>)] and corresponding heavier analogues ([RGe(S)(NHC)<sub>2</sub>]X and [RGe(Se)(NHC)<sub>2</sub>]X) demonstrated its classical acylium-like behavior. The polarized terminal GeO bond in the germa-acylium ion was utilized to activate CO<sub>2</sub> and silane, with the former found to be an example of reversible activation of CO<sub>2</sub>, thus mimicking the behavior of transition metal oxides. Furthermore, its transition-metal-like nature is demonstrated as it was found to be an active catalyst in both CO<sub>2</sub> hydrosilylation and reductive N-functionalization of amines using CO<sub>2</sub> as the C<sub>1</sub> source. Mechanistic studies were undertaken both experimentally and computationally, which revealed that the reaction proceeds via an N-heterocyclic carbene (NHC) siloxygermylene [(NHC)RGe(OSiHPh<sub>2</sub>)].



### INTRODUCTION

The catalytic conversion of CO<sub>2</sub> into useful commodity chemicals has drawn considerable attention in the last decades, due to the increasing global energy demands and concomitant rising CO<sub>2</sub> emissions.<sup>1–5</sup> CO<sub>2</sub> is chemically abundant and finds use as a C<sub>1</sub> building block. Albeit, these transformations are challenging due to the high C–O bond strength in CO<sub>2</sub> (532 kJ mol<sup>-1</sup>).<sup>3,4,6</sup> Pertinent to this work, the catalytic hydrosilylation of CO<sub>2</sub> to the corresponding silyl formate, acetals, silyl ether, and methane presents an attractive route for CO<sub>2</sub> utilization. The inherent stability of the Si–O bond and the propensity behind Si–H bond scission to form metal hydrides result in the exergonic nature of hydrosilylation vs hydrogenation. Furthermore, the high natural abundance of silicon makes it an ideal candidate for transformation of CO<sub>2</sub> into commodity chemicals.<sup>3,6,7</sup> As an extension to the hydrosilylation of CO<sub>2</sub>, the “diagonal approach” provides an alternative method for CO<sub>2</sub> utilization, as the combination of CO<sub>2</sub> and silane provides the C<sub>1</sub> source for N-formylation or N-methylation of amines.<sup>8</sup> Recently, transition metal oxides (TMOs) in high oxidation states have shown potential application in reductive CO<sub>2</sub> derivatization.<sup>9–14</sup> For example, high valent rhenium and tungsten oxo-anions are active catalysts in the hydrosilylation of CO<sub>2</sub>.<sup>13,14</sup> In this context, theoretical studies revealed the formation of a hypercoordinate silicate to be key in enabling turnover, as reduction of CO<sub>2</sub> occurs at the activated Si–H bond (Figure 1a).<sup>13</sup> In contrast, catalysis by cationic rhenium-oxide

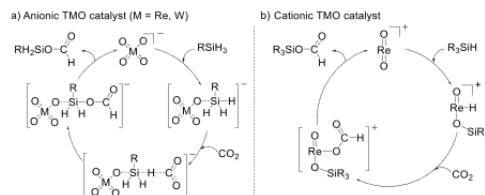


**Figure 1.** Activation of CO<sub>2</sub> with both anionic (a) and cationic (b) transition metal oxides.

catalysts proceeds via rhenium hydrides, as silane adds across the Re=O double bond, forming Re–H intermediates which are responsible for the resulting CO<sub>2</sub> reduction to silyl formate (Figure 1b).<sup>15</sup>

Recent years have seen a growing interest in the main group element’s ability to mimic transition metals, due to main group elements being more advantageous from both an economic and environmental point of view.<sup>16–19</sup> In this regard, heavier group-

Received: June 13, 2020

Published: August 10, 2020



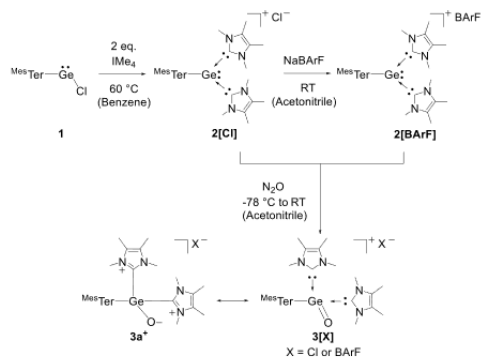
14 terminal oxides, [E=O] (E = Si, Ge, Sn), could provide an alternative to high oxidation state TMOs.<sup>20</sup> Similar to TMOs,<sup>10</sup> germanone (R<sub>2</sub>GeO)<sup>21</sup> and silanone (R<sub>2</sub>SiO)<sup>22–25</sup> readily undergo [2+2]-cycloaddition with CO<sub>2</sub> to form metal carbonates, as a result of the polarized E=O bond.<sup>20</sup> Interestingly, Si=O bond-mediated reversible cycloaddition of CO<sub>2</sub> has recently been demonstrated by Kato and co-workers.<sup>26</sup> It is also of note that group 13 molecular oxides have been found to activate CO<sub>2</sub>, also due to the highly polarized Al–O bond. This has been shown by both terminal aluminum oxide ions [R<sub>2</sub>AlO]<sup>–27,28</sup> and a dimeric [R<sub>2</sub>AlO]<sub>2</sub> complex.<sup>29</sup> However, to the best of our knowledge, the only example of further functionalization of either a group 13 or 14 carbonate to value-added products was reported by our group,<sup>29</sup> where an aluminum double bond was found to selectively catalyze the reduction of CO<sub>2</sub> to a formic acid equivalent, with a dialuminum carbonate being pivotal to the calculated mechanism. Beyond the sequestration of CO<sub>2</sub>, an elegant study by Driess and co-workers illustrated the activation of ammonia (NH<sub>3</sub>) with the polar Si=O bond, which strongly resembles transition metal reactivity.<sup>30</sup> Moreover, activation of E'–H bonds (E' = O, Si, C) has also been achieved by R<sub>2</sub>EO complexes (E = Si, Ge).<sup>21–23,31</sup> Despite these successes, the catalytic application of these oxides has not yet been explored. One of the potential difficulties in employing heavier group 14 oxides is the inherent thermodynamic instability of these complexes. The tendency to oligomerize is attributed to the highly zwitterionic nature of the E–O bond; therefore, rational steric and electronic stabilization is required to address such a challenge.<sup>20</sup> Additionally, hydrosilylation reactions also pose their own challenges due to their propensity to form stable metal–oxosilyl complexes. These compounds have a formal oxidation state of +4 and are highly stable species. This makes traditional redox-based catalysis very challenging due to the difficulties associated with reductive elimination and, therefore, release of the functionalized substrate.<sup>21–23,31</sup>

One potential method to overcome this difficulty is to use a metal center which is stable in both high and low oxidation states; thus, germanium presents itself as an ideal candidate. In recent years, the transition metal like ability of germanium has been shown to provide the first examples of low-valent main group dihydrogen activation and multiple bond catalysis,<sup>32–40</sup> with the latter example possible due to the ability of germanium to switch between its +2 and +4 oxidation states. With these incentives in mind, we targeted the synthesis of a Lewis base stabilized germanium oxide ion, to examine its application in CO<sub>2</sub> functionalization. In order to access such a species, we envisaged that N-heterocyclic carbene (NHC)-stabilized germyliumylidene<sup>41,42</sup> would provide the necessary steric and electronic requirements to provide access to the germa-acylium ion. Notably, [R–GeO]<sup>+</sup> are transient species, having only been detected by using high-pressure and Fourier transformation mass spectrometry (FTMS).<sup>43</sup>

## RESULTS AND DISCUSSION

The NHC-stabilized germyliumylidene (2[Cl], MesTerGe(IME<sub>4</sub>)<sub>2</sub>Cl, MesTer = 2,6-(2,4,6-Me<sub>3</sub>C<sub>6</sub>H<sub>2</sub>)<sub>2</sub>C<sub>6</sub>H<sub>3</sub>) was isolated by treating chlorogermylene (1, MesTerGeCl) with 2 equiv of IME<sub>4</sub> (IME<sub>4</sub> = 1,3,4,5-tetramethylimidazol-2-ylidene) in benzene at 60 °C (Scheme 1). This led to the immediate precipitation of compound 2[Cl], as colorless needles, which could be isolated in 84% yield. Compound 2[Cl] is soluble in

**Scheme 1. Synthesis of NHC-Stabilized Germyliumylidene Ion 2[Cl], Germa-acylium Ion 3[X], and Possible Resonance Structure of 3[X] (X = Cl, BArF)**



polar solvents such as acetonitrile and fluorobenzene but poorly soluble in nonpolar organic solvents. The solubility was improved by anion exchange. Treatment of compound 2[Cl] with Na[BArF] (BArF = 3,5-(CF<sub>3</sub>)<sub>2</sub>C<sub>6</sub>H<sub>3</sub>)<sub>4</sub>B) afforded 2-[BArF] (yield = 97%). Compounds 2[Cl] and 2[BArF] were both characterized by multinuclear NMR spectroscopy. In the <sup>1</sup>H and <sup>13</sup>C{<sup>1</sup>H} NMR spectrum of 2[BArF], a characteristic signal for [BArF] was observed at δ 7.40 ppm and δ 162.2 ppm (B–C, q, <sup>1</sup>J<sub>BC</sub> = 50.0 Hz), respectively. This indicates successful counteranion exchange. For both compounds, the carbene carbon resonance was found at δ 164.0 ppm in the <sup>13</sup>C{<sup>1</sup>H} NMR, which is in the range of NHC-stabilized germyliumylidene.<sup>44–47</sup>

Single-crystal X-ray diffraction (SC-XRD) analysis revealed that the central germanium is tricoordinate, with two NHCs and one *m*-terphenyl group coordinated (Figure 2). The Ge···Cl

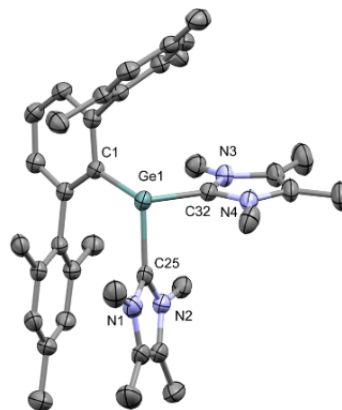


**Figure 2. Molecular structures of compound 2[Cl] in the solid state. Ellipsoids are set at the 50% probability level; hydrogen atoms and counterion are omitted for clarity. Selected bond lengths [Å] and bond angles [°]: Ge1–C1 2.044(3), Ge1–C32 2.063(3), Ge1–C25 2.093(3), C1–Ge1–C25 109.02(12), C1–Ge1–C32 102.17(13), and C32–Ge1–C25 91.36(12).**



distance in 2[Cl] is above 6 Å, indicating the absence of significant interactions between the germanium and chlorine atoms. The Ge–C<sup>NHC</sup> bond distances in 2[Cl] for the coordinated NHCs are almost identical, 2.093(3) Å and 2.063(3) Å, and are similar to the other NHC-stabilized germyliumylidenes.<sup>44–48</sup> The optimized geometry of 2<sup>+</sup> calculated at the R-BP86/def2-SVP level is in good agreement with the experimental data. Inspection of the frontier molecular orbitals reveals that the HOMO in 2<sup>+</sup> represents the  $\sigma$ -symmetric lone pair orbital located on the germanium center, whereas the LUMO possesses the  $\pi$ -symmetric vacant molecular orbital concentrated on the carbene carbons (Figure S50). Natural bond orbital (NBO) analysis suggests that the Ge–C<sup>NHC</sup> bonds are significantly polarized toward the carbene carbon atoms (C25: 75.9%, C32: 76.4%). Furthermore, calculated Wiberg bond indices (WBIs) of 0.735 and 0.723 support the single bond character of these bonds.

Since the electron-rich germanium(II) center can easily undergo oxidative addition in the presence of an oxidizing agent,<sup>44,49–51</sup> this prompted us to treat compound 2 with an oxygen transfer reagent, e.g., N<sub>2</sub>O, to target the isolation of a germa-acylium ion. Indeed, treatment of compound 2 with N<sub>2</sub>O (1 bar) led to the desired product (3, <sup>Mes</sup>TerGe(O)(IME<sub>4</sub>)<sub>2</sub>]<sup>+</sup>X<sup>−</sup>, X = Cl or BARf) in near quantitative yields (3[Cl] = 89% and 3[BARf] = 94%, Scheme 1). The <sup>1</sup>H NMR spectrum of compound 3 displays two distinct broad signals ( $\delta$  3.21 and  $\delta$  4.20 ppm) which are assigned as the *N*-methyl groups of the NHCs, while in the <sup>13</sup>C{<sup>1</sup>H} NMR spectrum the carbene carbon resonance has shifted upfield from compound 2 ( $\delta$ 164.0 ppm to  $\delta$ 149.9 ppm), indicating strong interaction between Ge and the carbene carbon.

The molecular structure of complex 3[BARf] was unambiguously confirmed by SC-XRD analysis (Figure 3a), which revealed a distorted tetrahedral geometry at the germanium center. The Ge–O bond in complex 3[BARf] is 1.697(3) Å, which is shorter than a tetracoordinate Ge–O single bond (1.76–1.82 Å) and falls within the range of donor/acceptor stabilized germanones (1.673–1.718 Å).<sup>49–53</sup> This bond is relatively elongated compared to three coordinate germanone 1.646(5) Å.<sup>21</sup> In the solid-state IR spectrum, compound 3 displays a strong absorption at 807 cm<sup>−1</sup> which is assigned as Ge=O. This is blue-shifted compared to the reported Ge=O stretching in Eind<sub>2</sub>Ge=O (917 cm<sup>−1</sup>) and red-shifted in comparison to the Ge–O single bond stretching frequency (769 cm<sup>−1</sup>).<sup>54</sup> Thus, structural and IR data suggest a strong dominance of a zwitterionic resonance form (3a<sup>+</sup>, Scheme 1) in the ground state. The calculated structure of 3<sup>+</sup> is in good agreement with the experimental structure (calculated IR 800.8 cm<sup>−1</sup>). Examination of the Ge–O bond by NBO and WBI analysis revealed a strong polarization toward the oxygen center (O1: 78.9%) and a WBI value of 0.896, indicating single bond character. Additionally, the NPA charges (Ge: +1.679 e and O: −1.230 e) in 3<sup>+</sup> further support the dominance of the zwitterionic resonance form 3a<sup>+</sup>. Inspection of the frontier orbitals show the HOMO−1 and HOMO in 3<sup>+</sup> comprised of the lone pair orbitals on the O atom, whereas the LUMO consists of the vacant  $p_x$  orbital on the carbene carbons (Figure 3b).

In order to examine a relationship to classical acyl transfer, we treated compound 3 with Ph<sub>3</sub>SiOH, and this resulted in the first example of an acceptor-free stable germanium ester, compound 4 [(<sup>Mes</sup>TerGe(O))(OSiPh<sub>3</sub>)(IME<sub>4</sub>)], with the concomitant formation of imidazolium salt (Scheme 2). Compound 4 was characterized by standard spectroscopic and analytic methods.

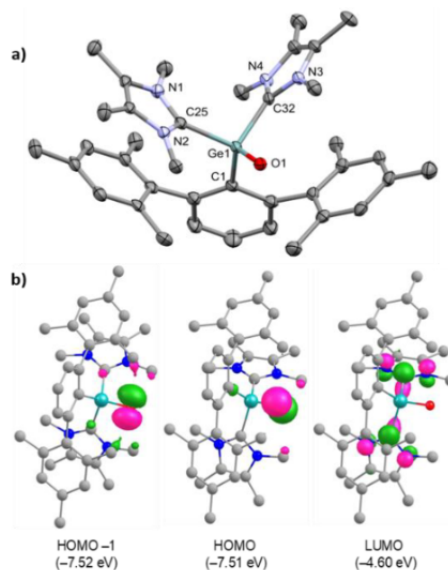
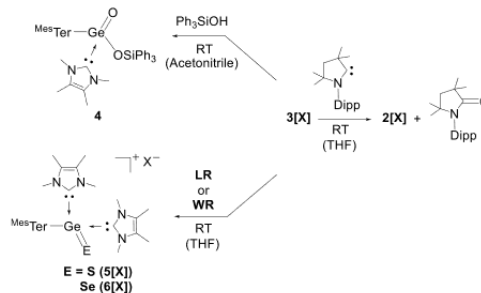


**Figure 3.** (a) Molecular structures of compound 3[BARf] in the solid state. Ellipsoids are set at the 50% probability level; hydrogen atoms, counterion and cocrystallized solvent molecules are omitted for clarity. Selected bond lengths [Å] and bond angles [°]: Ge1–O1 1.697(3), Ge1–C1 1.986(4), Ge1–C32 2.034(4), Ge1–C25 2.036(4), C1–Ge1–C32 104.88(15), C1–Ge1–C25 116.90(14), C32–Ge1–C25 104.30(15), O1–Ge1–C25 103.30(13), O1–Ge1–C32 109.26(13), O1–Ge1–C1 117.40(14). (b) Selected KS-MOs of 3<sup>+</sup> (isosurface = 0.07 au). The orbital energies are shown in parentheses. Hydrogen atoms are omitted for clarity.

**Scheme 2. Reactivity of Germa-acylium Ion 3[X] (X = Cl, BARf, LR = Lawesson's Reagent (CH<sub>3</sub>O)PhPS<sub>2</sub>), WR = Wollin's Reagent (PhPSe<sub>2</sub>), Dipp = 2,6-iPr<sub>2</sub>C<sub>6</sub>H<sub>3</sub>)**



In the <sup>13</sup>C{<sup>1</sup>H} NMR, the carbene carbon resonance was found at  $\delta$  153.2 ppm, and a distinct silicon resonance at  $\delta$  −19.3 ppm was observed in the <sup>29</sup>Si{<sup>1</sup>H} NMR spectrum. SC-XRD analysis further confirmed the coordination of one NHC to the germanium center (Figure 4). In 4, the Ge1–O1 bond length is 1.6825(16) Å, which is shorter than 3[BARf] (1.697(3) Å) as well as the donor–acceptor stable germa-ester complex 1.719(2) Å, reported recently by Nagendran, and marginally

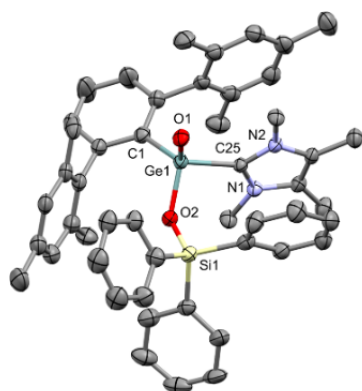


**Figure 4.** Molecular structures of compound **4** in the solid state (one out of two independent molecules in the asymmetric unit). Ellipsoids are set at the 50% probability level; hydrogen atoms and cocrystallized solvent molecules are omitted for clarity. Selected bond lengths [Å] and bond angles [°]: Ge1–O1 1.6825(16), Ge1–O2 1.8024(18), Ge1–C1 1.979(3), Ge1–C25 2.007(2), C1–Ge1–C25 109.45(10), C1–Ge1–O2 108.84(9), O1–Ge1–C1 115.64(10), O1–Ge1–O2 113.25(8), O1–Ge1–C25 110.45(9), O1–Ge1–C1 115.64(10), and O2–Ge1–C25 97.72(9).

longer than the NHC-stabilized germanone (1.670–1.672 Å) reported by Driess.<sup>49,52</sup> Expectedly, the Ge1–O2 bond length (1.8024(18) Å) is longer than the Ge1–O1 bond and is more in line with typical Ge–O single bond values.<sup>52,53</sup> Theoretical studies suggest the formation of **4** proceeds via a stable intermediate which contains a strong hydrogen bond from the hydroxyl proton in Ph<sub>3</sub>SiOH to the O1 center in 3M<sup>+</sup>. Proton transfer to O1 then occurs, followed by decoordination of IMe<sub>4</sub>, which then allows for proton abstraction from O1 to deliver the desired germanium ester (Figure S52).

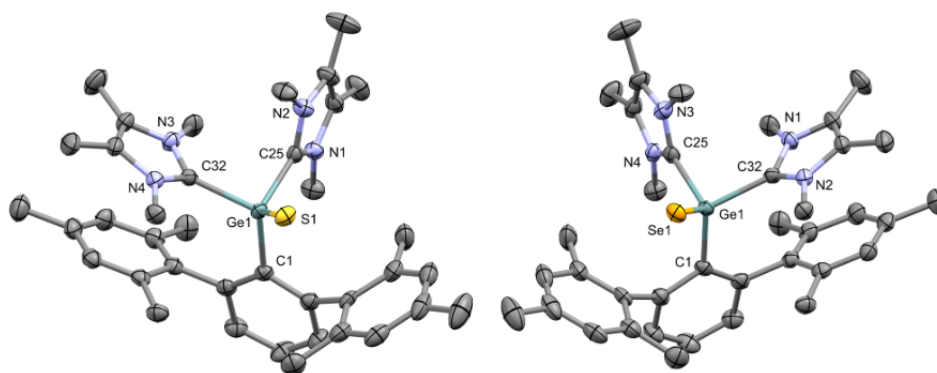


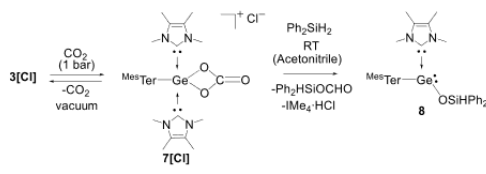
**Figure 5.** Molecular structures of compounds **5[BarF]** (left) and **6[BarF]** (right) in the solid state. Ellipsoids are set at the 50% probability level; hydrogen atoms, counterions, and cocrystallized solvent molecules are omitted for clarity. Selected bond lengths [Å] and bond angles [°]: **5[BarF]** Ge1–S1 2.104(7), Ge1–C1 1.990(2), Ge1–C32 2.043(3), Ge1–C25 2.038(3), C1–Ge1–C32 114.60(12), C1–Ge1–C25 106.74(11), C32–Ge1–C25 96.02(11), S1–Ge1–C25 111.23(8), S1–Ge1–C32 108.70(8), S1–Ge1–C1 117.45(8). **6[BarF]** Ge1–Se1 2.2372(5), Ge1–C1 1.993(3), Ge1–C32 2.039(4), Ge1–C25 2.039(4), C1–Ge1–C32 114.20(15), C1–Ge1–C25 106.92(14), C32–Ge1–C25 96.17(14), Se1–Ge1–C25 110.27(10), Se1–Ge1–C32 109.14(10), and Se1–Ge1–C1 117.90(9).

Recently, we have demonstrated the silyl–Wittig reaction with silanone, for a range of substrates,<sup>55</sup> in which one of the driving forces of this reaction was the formation of stable P=O bonds. To access heavier germa-acylium analogues we envisaged the use of Lawesson's [LR = (CH<sub>3</sub>OPhPS<sub>2</sub>)<sub>2</sub>] and Wollins reagents [WR = (PhPSe<sub>2</sub>)<sub>2</sub>], which are mild and convenient thionating and selenating reagents for ketones, esters, and amides, which enable the preparation of thio and seleno carbonyls, respectively.<sup>56,57</sup> Again, the driving force of these reactions is the formation of a stable P=O bond in a cycloreversion step that resembles the mechanism of Wittig reactions.<sup>58</sup> As such, we investigated the use of LR and WR with compound **3** (Scheme 2). Under ambient conditions, reaction of **3** with LR and WR afforded compounds [M<sup>cat</sup>TerGe(S)(IMe<sub>4</sub>)<sub>2</sub>]X (**5**) and [M<sup>cat</sup>TerGe(Se)(IMe<sub>4</sub>)<sub>2</sub>]X (**6**) (in **5**[Cl] = 39%, **5**[BarF] = 35% and **6**[Cl] = 30%, **6**[BarF] = 29% yields, respectively). The Ge–S bond length in **5**[BarF] (2.104(7) Å) is close to those of donor-stabilized Ge=S bonds (ranging from 2.053 to 2.095 Å) and shorter than the typical Ge–S single bond length (2.239 Å) (Figure 5).<sup>46,59–64</sup> Similarly, the Ge–Se bond length in **6**[BarF] (2.2372(5) Å) is sufficiently shorter than a Ge–Se single bond (2.461 Å) and falls within the range of tetracoordinated donor-stabilized Ge=Se bonds (Figure 5).<sup>60,61</sup> The Ge–S and Ge–Se bonds in compounds **5** and **6** are longer than the kinetically stabilized tricoordinate Ge=S and Ge=Se bonds, respectively.<sup>65</sup> Notably, compound **6**[BarF] represents the first example of a cationic germaselenium complex. NBO analyses on compounds **5**<sup>+</sup> and **6**<sup>+</sup> suggest that the Ge–Ch (Ch = O, S, Se) bond becomes less polarized in nature on descending the group (O: 78.9%, S: 60.5%, Se: 55.3%). Moreover, unlike the Ge–O bond in 3<sup>+</sup>, Ge–S and Ge–Se bonds show partial double bond character, as supported by the calculated WBI values of 1.279 and 1.302, respectively. We have theoretically explored the reaction mechanism for the formation of **5**. Our calculations suggest that the dissociation of the dimeric LR followed by the nucleophilic attack of O1 in 3M<sup>+</sup> at the electron-deficient phosphorus in the monomeric unit (LR<sup>M</sup>) initiates the reaction (Figure S53).

After examination of the acylium-like nature of compound 3, we turned our attention toward comparisons to TMO properties. The oxide (O<sup>2-</sup>) transfer from a terminal TMO to Lewis base was reported.<sup>66,67</sup> Inspired by this we treated compound 3 with a series of Lewis bases, such as PMe<sub>3</sub>, PPh<sub>3</sub>, IMe<sub>4</sub>, and IDipp. However, no reactivity was observed. Treatment of compound 3 with Me<sub>3</sub>cAAC [1-(2,6-diisopropylphenyl)-3,3,5,5-tetramethylpyrrolidine-2-ylidene], a strong π-acceptor as well as σ-donor, readily afforded compound 2 (yield 2[Cl] = 92%, 2[BArF] = 95%) with the concomitant formation of Me<sub>3</sub>cAAC=O (Scheme 2). DFT calculations on this oxide transfer are also in agreement with the observed experimental findings (Figure S54).

On treating an acetonitrile solution of compound 3 with CO<sub>2</sub> (1 bar), the resulting <sup>13</sup>C{<sup>1</sup>H} NMR spectrum revealed a new signal at δ 155.2 ppm, similar to the reported germanium carbonate (δ 154.7 ppm).<sup>21</sup> Additionally, in the <sup>1</sup>H NMR spectrum, a distinct downfield shift was observed for the coordinated NHC methyl protons (from δ 3.02, δ 3.03, to δ 3.73 ppm). This points to the formation of a symmetric compound. Surprisingly, these characteristic signals for the carbonate species disappear on degassing the solution (Scheme 3). Here,

**Scheme 3. Reversible Activation of CO<sub>2</sub> by 3[Cl] and Subsequent Hydrosilylation**



reformation of compound 3 can be observed through comparison of NMR signals (see SI, Figure S23). Such reversibility strongly resembles that of TMOs.<sup>10</sup> However, this reversible binding of CO<sub>2</sub> with a Ge–O bond is unprecedented compared to the previously known reactivity of heavier group 14 carbonyls with CO<sub>2</sub>.<sup>21–25</sup>

Unfortunately, due to the high instability of 7, we were unable to confirm its molecular structure by SC-XRD. Addition of 1 equiv of diphenylsilane (Ph<sub>2</sub>SiH<sub>2</sub>) was carried out under an atmosphere of CO<sub>2</sub>, which resulted in the formation of the siloxygermylene, compound 8 [Me<sub>3</sub>cTerGe(OSiHPh<sub>2</sub>)(IMe<sub>4</sub>)] (Scheme 3). Additionally, a trace amount of silyl formate and IMe<sub>4</sub>·HCl were observed during this reaction. For compound 8, the carbene carbon was found at δ 157.9 ppm, in the <sup>13</sup>C{<sup>1</sup>H} NMR spectrum, while in the <sup>29</sup>Si{<sup>1</sup>H} NMR spectrum the siloxy silicon was observed at δ –22.4 ppm. Furthermore, SC-XRD confirmed the identity of compound 8 (Figure 6), which revealed a tricoordinate germanium center bonded with one IMe<sub>4</sub>, a siloxy group, and Me<sub>3</sub>cTer ligand. Expectedly, the Ge1–O1 bond length in 8 (1.889(3) Å) is similar to the Ge–O bond length in the NHC-stabilized *tert*-butoxido germylene (1.883(10) Å)<sup>68</sup> but elongated compared to the Ge–O bond length in 3[BArF] (1.697(3) Å).

Due to the reversible nature of compound 7 and the formation of compound 8, our interest turned to the catalytic transformation of CO<sub>2</sub>, as this indicates the potential for a Ge(II)/ (IV) redox-based catalytic cycle. We found that compound 3 can transform CO<sub>2</sub> to the corresponding hydrosilylated products in both a stoichiometric and catalytic manner in the presence of

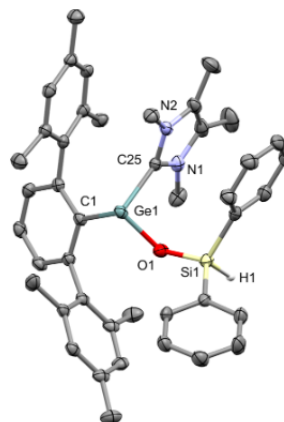


**Figure 6.** Molecular structures of compound 8 in the solid state. Ellipsoids are set at the 50% probability level; hydrogen atoms (except H1) are omitted for clarity. Selected bond lengths [Å] and bond angles [°]: Ge1–O1 1.889(3), Ge1–C1 2.047(3), Ge1–C25 2.095(3), C1–Ge1–O1 97.06(9), C1–Ge1–C25 97.07(9), and O1–Ge1–C25 89.59(9).

Ph<sub>2</sub>SiH<sub>2</sub>. After optimization, we found that use of 2.5 mol % of 3[Cl] at 50 °C provides suitable reaction conditions. Complete consumption of Ph<sub>2</sub>SiH<sub>2</sub> is observed within 5 h, by <sup>1</sup>H NMR, with the formation of silylformate, bis(silyl)acetal, and silylated methanol (Figure S27). Solvent screening found that the reaction best proceeds in polar solvents (e.g., acetonitrile) in comparison to nonpolar solvents (e.g., benzene). This is attributed to the low solubility of the catalyst in the nonpolar solvent. Additionally, to understand the role of the counteranion we have performed this reaction under the same conditions with 3[BArF]. However, no effective change in turnover was observed, concluding that the counteranion does not play an important role in this catalytic cycle. Furthermore, control experiments performed with IMe<sub>4</sub> under the optimized reaction conditions, found negligible turnover. Notably, for group 14 metal complexes, there are only a handful examples of catalytic reduction of CO<sub>2</sub>.<sup>69–71</sup> One example of heavier group 14 metal complexes was reported by Kato and Baccaredo, which showed hydrosilylation of CO<sub>2</sub> using a N,P-heterocyclic germylene and boron FLP-type system (FLP = frustrated Lewis pair),<sup>69</sup> while catalytic hydroboration of CO<sub>2</sub> has been successfully demonstrated with a N/Si<sup>+</sup>-based FLP system, low valent Ge(II) and Sn(II) hydrides, and very recently the parent silyliumylidene ion.<sup>70–72</sup>

The formation of silylformate during hydrosilylation reactions prompted us to investigate the use of compound 3 in the functionalization of amines, as they have been implicated as key intermediates in the N-formylation or N-methylation of amines.<sup>8</sup> Accordingly, we have examined the scope of the reductive functionalization of CO<sub>2</sub> with various amines, using Ph<sub>2</sub>SiH<sub>2</sub> as reductant and 3[Cl] as catalyst (Table 1). The study revealed that aliphatic amines proceed smoothly compared to aromatic amines. This is possibly attributed to the low nucleophilicity of the aromatic amine arising from the delocalization of the nitrogen lone pair with the phenyl ring.<sup>73</sup> In general, room-temperature catalysis favors formamide

# N-heterocyclic carbene-stabilized germa-acylium ion: reactivity and utility in catalytic CO<sub>2</sub> functionalizations

**Table 1.** N-Methylation of Amines Using 1 bar of CO<sub>2</sub> and 3 equiv of Ph<sub>2</sub>SiH<sub>2</sub>, in CD<sub>3</sub>CN and 2.5 mol % of 3[Cl]

amine	temp (°C)	time (h)	NMR yield <sup>a</sup>		
			a	b	c
diethylamine	20	6	28	-	70
	50	2	15	-	82
piperidine	20	12	27	-	72
	50	2	18	-	80
morpholine	20	10	22	32	35
	50	3	21	-	75
dicyclohexylamine	20	5	57	-	42
	50	3	16	-	78
N-methylaniline	20	24	41	10	38
	50	15	16	5	85

<sup>a</sup>For all amines, 99% conversion was observed. NMR yields were calculated according to the NMR standard (trimethoxybenzene).

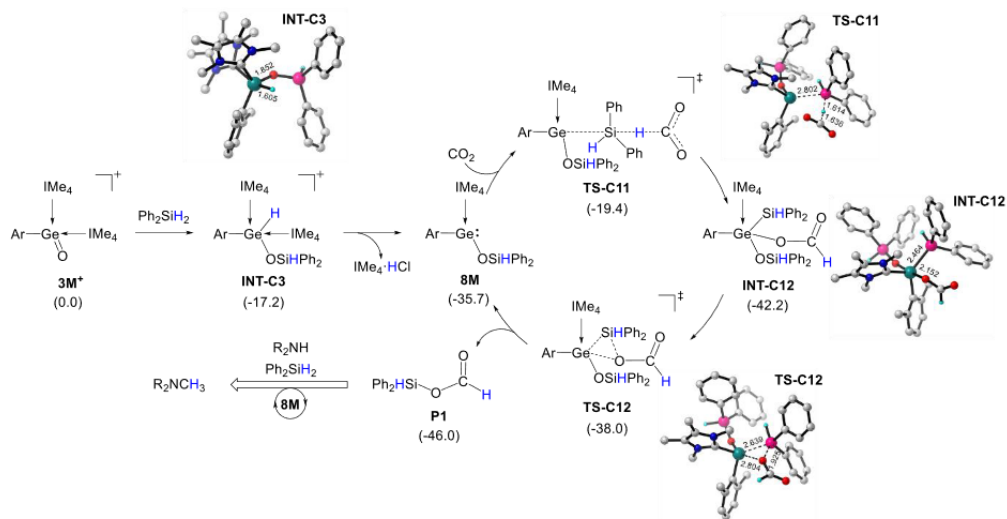
formation, whereas at elevated temperatures N-methylation is the major product along with reduced reaction times, which is in line with a recent study reported by Nguyen and co-workers.<sup>74</sup> In the cases of morpholine and N-methylaniline, the subsequent formation of formamide, aminal, and methylated amine is observed as a mixture, which are the 2e-, 4e-, and 6e-reduced products of CO<sub>2</sub> (Table 1). Again, control reactions with IMe<sub>4</sub> and IMe<sub>4</sub>·HCl under the standard reaction conditions revealed negligible turnover, suggesting either initial coordination of CO<sub>2</sub> or silane to compound 3. Interestingly, a stoichiometric reaction of 3 with Ph<sub>2</sub>SiH<sub>2</sub>, in the absence of CO<sub>2</sub> afforded the siloxygermylene 8 quantitatively (yield = 80%), with the concomitant formation of imidazolium chloride. Furthermore,

we found that compound 8 is able to transform CO<sub>2</sub> to the corresponding N-functionalized products in both a stoichiometric and catalytic manner. Use of 2.5 mol % of 8 in the reductive functionalization of morpholine, under the standard reactions conditions, led to similar results to that observed with compound 3 at both temperatures (see SI, Figures S48 and 49). This suggests that 8 may in fact be the resting state of the active cycle. However, stoichiometric reactions of 8 with the individual components resulted in no reaction, therefore suggesting a cooperative effect between the reaction components is required for turnover to be achieved.

A series of stoichiometric reactions were undertaken to probe the mechanism. Compound 3 was found to be inert toward amine, while it reacts with CO<sub>2</sub> (*vide supra*) and Ph<sub>2</sub>SiH<sub>2</sub>.

Based on experimental data, there are two potential pathways for entry into the active catalytic cycle: (i) coordination of CO<sub>2</sub> to form carbonate (akin to compound 7) and subsequent reduction by silane or (ii) initial silane reduction then CO<sub>2</sub> activation. We, therefore, have performed DFT calculations to unveil the mechanistic underpinnings of the germanium-mediated catalytic reactions. These were performed using truncated models, with the <sup>Me</sup>Ter ligand replaced with 2,6-dimethylphenyl (Ar). First, pathway (i) was examined, and we found that the binding of CO<sub>2</sub> to the Ge–O<sup>1</sup> bond in 3M<sup>+</sup> leads to the formation of a slightly stable germanium carbonate (INT-C1), by overcoming a very low energy barrier of only 1.0 kcal mol<sup>-1</sup> (Figure S55). However, the reduction of INT-C1 by silane to produce formoxysilane (P1) demands an extremely high energy barrier of 35.7 kcal mol<sup>-1</sup>. Hence, theoretical calculations suggest that pathway (i) is unfavorable.

Alternative pathway (ii), where 3M<sup>+</sup> is initially reduced by Ph<sub>2</sub>SiH<sub>2</sub>, requires an energy barrier of 2.1 kcal mol<sup>-1</sup> to afford the significantly more stable Ge(IV) hydride species (INT-C3). From here, dissociation of IMe<sub>4</sub> followed by CO<sub>2</sub> coordination/

**Scheme 4.** Proposed Mechanism for the Germanium-Catalyzed N-Functionalization of Amine with CO<sub>2</sub><sup>4f</sup>


<sup>a</sup>ΔG<sub>T</sub><sup>‡</sup> (kcal mol<sup>-1</sup>) values are given in brackets.

insertion into the Ge(IV) hydride was found to be unfavorable with a high energy barrier of 45.4 kcal mol<sup>-1</sup> (Figure S56). On the other hand, keeping IMe<sub>4</sub> within the vicinity of Ge(IV) enables the Lewis base to abstract the proton from the Ge center with a very low activation barrier of 0.4 kcal mol<sup>-1</sup>. The resulting intermediate finally delivers the siloxygermylene (**8M**), and IMe<sub>4</sub>-HCl is also formed with the assistance of the chloride counter anion (Scheme 4).

The role of **8M** in the formation of formoxysilane was explored (Scheme 4). This is proposed to occur in a concerted process via TS-C11, in which the free CO<sub>2</sub> acts as a hydride acceptor from the hypercoordinate silane (Figure S58). The resulting intermediate INT-C12 finally delivers formoxysilane accompanying an energy barrier of 4.2 kcal mol<sup>-1</sup>. Alternate pathways, where the CO<sub>2</sub> first coordinates to **8M** followed by reduction or via oxidative addition of Si-H across the Ge(II) center, were also explored, demanding the energy barriers of 20.5 and 16.7 kcal mol<sup>-1</sup>, respectively (Figure S59). Therefore, the second alternate route exhibiting slightly higher energy barrier compared to that for the concerted process depicted in Scheme 4 may be operative independently under the reaction conditions. To further validate the proposed mechanism, selected transition states were calculated using the bulkier *m*-terphenyl ligand rather than the truncated model system. These show comparable energy barriers (Table S1) and thus support the proposed mechanism as highlighted in Scheme 4.

The Ge(II) siloxygermylene species (**8**) is therefore proposed as the active catalyst in the generation of formoxysilane, which is key for further functionalization with amines. Compound **8** is accessible from the reaction of the germa-acylium ion precatalyst (**3**) and silane. Notably, this is different from other reported heavier carbonyl hydrosilylation reactions. Here we have shown the retention of the low valent Ge(II) center, whereas previous hydrosilylation of E=O (E = Si, Ge) bonds results in the formation of the higher oxidation state oxo-silyl species.<sup>21–23,31</sup>

## CONCLUSION

In summary, we have shown the successful isolation of a donor-stabilized germa-acylium ion (**3**). Analogous to classical acylium ions, this provides access to novel germanium analogues of carbonyl and heavier chalcogen derivatives, exemplified by the first example of an NHC-supported germanium ester. Moreover, its transition metal oxide like behavior was investigated, where the regeneration of germyliumylidene (**2**) was achieved via oxide transfer to Me<sub>3</sub>CAC, representing diverse electronic features of this heavier acylium analogue. This TMO behavior was further exploited in CO<sub>2</sub> functionalization reactions, where reversible CO<sub>2</sub> coordination was observed, as well as the ability of **3** to act as a precatalyst in CO<sub>2</sub> hydrosilylation and N-methylation of amines. A combined theoretical and experimental approach revealed a Ge(II) siloxygermylene species (**8**) to be the active species. This report further demonstrates the ability of main group metals to mimic their transition metal counterparts while also showing similar reactivity to that of the lightest group 14 congener.

## ASSOCIATED CONTENT

### Supporting Information

The Supporting Information is available free of charge at <https://pubs.acs.org/doi/10.1021/jacs.0c06287>.

Experimental procedures, full spectroscopic analysis, and DFT calculations (PDF)

Crystallographic data (CCDC 2006663–2006668) (CIF)

## AUTHOR INFORMATION

### Corresponding Authors

Shigeyoshi Inoue – Department of Chemistry, WACKER-Institute of Silicon Chemistry and Catalysis Research Center, Technische Universität München, 85748 Garching, Germany; [orcid.org/0000-0001-6685-6352](https://orcid.org/0000-0001-6685-6352); Email: [s.inoue@tum.de](mailto:s.inoue@tum.de)

Debasis Koley – Department of Chemical Sciences, Indian Institute of Science Education and Research (IISER) Kolkata, Mohanpur 741 246, India; [orcid.org/0000-0002-7912-3972](https://orcid.org/0000-0002-7912-3972); Email: [koley@iiserkol.ac.in](mailto:koley@iiserkol.ac.in)

### Authors

Debotra Sarkar – Department of Chemistry, WACKER-Institute of Silicon Chemistry and Catalysis Research Center, Technische Universität München, 85748 Garching, Germany; [orcid.org/0000-0001-5938-0691](https://orcid.org/0000-0001-5938-0691)

Catherine Weetman – Department of Chemistry, WACKER-Institute of Silicon Chemistry and Catalysis Research Center, Technische Universität München, 85748 Garching, Germany; [orcid.org/0000-0001-5643-9256](https://orcid.org/0000-0001-5643-9256)

Sayan Dutta – Department of Chemical Sciences, Indian Institute of Science Education and Research (IISER) Kolkata, Mohanpur 741 246, India; [orcid.org/0000-0002-8232-5989](https://orcid.org/0000-0002-8232-5989)

Emeric Schubert – Department of Chemistry, WACKER-Institute of Silicon Chemistry and Catalysis Research Center, Technische Universität München, 85748 Garching, Germany

Christian Jandl – Department of Chemistry, WACKER-Institute of Silicon Chemistry and Catalysis Research Center, Technische Universität München, 85748 Garching, Germany

Complete contact information is available at:

<https://pubs.acs.org/doi/10.1021/jacs.0c06287>

### Notes

The authors declare no competing financial interest.

## ACKNOWLEDGMENTS

We gratefully acknowledge financial support from WACKER Chemie AG, the European Research Council (SILION 637394), and the DAAD (fellowship D.S.). This project has received funding from the European Union's Horizon 2020 research and innovation program under the Marie Skłodowska-Curie grant agreement No. 754462 (fellowship C.W.). S.D. acknowledges the CSIR, India, for the Senior Research Fellowship (SRF) and IISER Kolkata for the computational facility. D.K. acknowledges the funding from the bilateral DST-DFG (INT/FRG/DFG/P-05/2017) scheme.

## REFERENCES

- (1) Liu, Q.; Wu, L.; Jackstell, R.; Beller, M. Using carbon dioxide as a building block in organic synthesis. *Nat. Commun.* **2015**, *6* (1), 5933–5948.
- (2) Maeda, C.; Miyazaki, Y.; Ema, T. Recent progress in catalytic conversions of carbon dioxide. *Catal. Sci. Technol.* **2014**, *4* (6), 1482–1497.
- (3) Fernández-Alvarez, F. J.; Oro, L. A. Homogeneous Catalytic Reduction of CO<sub>2</sub> with Silicon-Hydrides, State of the Art. *ChemCatChem* **2018**, *10* (21), 4783–4796.
- (4) Chen, J.; McGraw, M.; Chen, E. Y.-X. Diverse Catalytic Systems and Mechanistic Pathways for Hydrosilylative Reduction of CO<sub>2</sub>. *ChemSusChem* **2019**, *12* (20), 4543–4569.

- (5) Wang, X.; Xia, C.; Wu, L. Homogeneous carbon dioxide reduction with p-block element-containing reductants. *Green Chem.* **2018**, *20* (24), 5415–5426.
- (6) Zhang, Y.; Zhang, T.; Das, S. Catalytic transformation of CO<sub>2</sub> into C1 chemicals using hydrosilanes as a reducing agent. *Green Chem.* **2020**, *22*, 1800–1820.
- (7) Fernández-Alvarez, F. J.; Aitani, A. M.; Oro, L. A. Homogeneous catalytic reduction of CO<sub>2</sub> with hydrosilanes. *Catal. Sci. Technol.* **2014**, *4* (3), 611–624.
- (8) Das Neves Gomes, C.; Jacquet, O.; Villiers, C.; Thuéry, P.; Ephritikhine, M.; Cantat, T. A Diagonal Approach to Chemical Recycling of Carbon Dioxide: Organocatalytic Transformation for the Reductive Functionalization of CO<sub>2</sub>. *Angew. Chem., Int. Ed.* **2012**, *51* (1), 187–190.
- (9) Silvia, J. S.; Cummins, C. C. Binding, release, and functionalization of CO<sub>2</sub> at a nucleophilic oxo anion complex of titanium. *Chem. Sci.* **2011**, *2* (8), 1474–1479.
- (10) Knopf, I.; Ono, T.; Temprado, M.; Tofan, D.; Cummins, C. C. Uptake of one and two molecules of CO<sub>2</sub> by the molybdate dianion: a soluble, molecular oxide model system for carbon dioxide fixation. *Chem. Sci.* **2014**, *5* (5), 1772–1776.
- (11) Paparo, A.; Silvia, J. S.; Spaniol, T. P.; Okuda, J.; Cummins, C. C. Counteraction Effect on CO<sub>2</sub> Binding to Oxo Titanate with Bulky Anilide Ligands. *Chem. - Eur. J.* **2018**, *24* (64), 17072–17079.
- (12) Kamata, K.; Sugahara, K. Base Catalysis by Mono- and Polyoxyometalates. *Catalysts* **2017**, *7* (11), 345–369.
- (13) Morris, D. S.; Weetman, C.; Wennmacher, J. T. C.; Cokoja, M.; Drees, M.; Kühn, F. E.; Love, J. B. Reduction of carbon dioxide and organic carbonyls by hydrosilanes catalysed by the perchlorate anion. *Catal. Sci. Technol.* **2017**, *7* (13), 2838–2845.
- (14) Wang, M.-Y.; Wang, N.; Liu, X.-F.; Qiao, C.; He, L.-N. Tungstate catalysis: pressure-switched 2- and 6-electron reductive functionalization of CO<sub>2</sub> with amines and phenylsilane. *Green Chem.* **2018**, *20* (7), 1564–1570.
- (15) Mazzotta, M. G.; Xiong, M.; Abu-Omar, M. M. Carbon Dioxide Reduction to Silyl-Protected Methanol Catalyzed by an Oxorhenium Pincer PNN Complex. *Organometallics* **2017**, *36* (9), 1688–1691.
- (16) Power, P. P. Main-group elements as transition metals. *Nature* **2010**, *463* (7278), 171–177.
- (17) Weetman, C.; Inoue, S. The Road Travelled: After Main-Group Elements as Transition Metals. *ChemCatChem* **2018**, *10* (19), 4213–4228.
- (18) Hadlington, T. J.; Driess, M.; Jones, C. Low-valent group 14 element hydride chemistry: towards catalysis. *Chem. Soc. Rev.* **2018**, *47* (11), 4176–4197.
- (19) Stephan, D. W. Frustrated Lewis Pairs. *J. Am. Chem. Soc.* **2015**, *137* (32), 10018–10032.
- (20) Xiong, Y.; Yao, S.; Driess, M. Chemical Tricks To Stabilize Silanones and Their Heavier Homologues with E = O Bonds (E = Si-Pb): From Elusive Species to Isolable Building Blocks. *Angew. Chem., Int. Ed.* **2013**, *52* (16), 4302–4311.
- (21) Li, L.; Fukawa, T.; Matsuo, T.; Hashizume, D.; Fueno, H.; Tanaka, K.; Tamao, K. A stable germanone as the first isolated heavy ketone with a terminal oxygen atom. *Nat. Chem.* **2012**, *4*, 361–365.
- (22) Alvarado-Beltran, I.; Rosas-Sánchez, A.; Baceiredo, A.; Saffon-Merceron, N.; Branchadell, V.; Kato, T. A Fairly Stable Crystalline Silanone. *Angew. Chem., Int. Ed.* **2017**, *56* (35), 10481–10485.
- (23) Rosas-Sánchez, A.; Alvarado-Beltran, I.; Baceiredo, A.; Saffon-Merceron, N.; Massou, S.; Hashizume, D.; Branchadell, V.; Kato, T. Cyclic (Amino)(Phosphonium Bora-Ylide)Silanone: A Remarkable Room-Temperature-Persistent Silanone. *Angew. Chem., Int. Ed.* **2017**, *56* (50), 15916–15920.
- (24) Wendel, D.; Reiter, D.; Porzelt, A.; Altmann, P. J.; Inoue, S.; Rieger, B. Silicon and Oxygen's Bond of Affection: An Acyclic Three-Coordinate Silanone and Its Transformation to an Iminosiloxysilene. *J. Am. Chem. Soc.* **2017**, *139* (47), 17193–17198.
- (25) Burchert, A.; Yao, S.; Müller, R.; Schattner, C.; Xiong, Y.; Kaupp, M.; Driess, M. An Isolable Silicon Dicarboxylate Complex with Carbon Dioxide Activation with a Silylone. *Angew. Chem., Int. Ed.* **2017**, *56* (7), 1894–1897.
- (26) Rodríguez, R.; Alvarado-Beltran, I.; Saouli, J.; Saffon-Merceron, N.; Baceiredo, A.; Branchadell, V.; Kato, T. Reversible CO<sub>2</sub> Addition to a Si = O Bond and Synthesis of a Persistent SiO<sub>2</sub>-CO<sub>2</sub> Cycloadduct Stabilized by a Lewis Donor-Acceptor Ligand. *Angew. Chem., Int. Ed.* **2018**, *57* (10), 2635–2638.
- (27) Anker, M. D.; Coles, M. P. Aluminium-Mediated Carbon Dioxide Reduction by an Isolated Monoalumoxane Anion. *Angew. Chem., Int. Ed.* **2019**, *58* (50), 18261–18265.
- (28) Hicks, J.; Heilmann, A.; Vasko, P.; Goicoechea, J. M.; Aldridge, S. Trapping and Reactivity of a Molecular Aluminium Oxide Ion. *Angew. Chem., Int. Ed.* **2019**, *58* (48), 17265–17268.
- (29) Weetman, C.; Bag, P.; Szilvási, T.; Jandl, C.; Inoue, S. CO<sub>2</sub> Fixation and Catalytic Reduction by a Neutral Aluminum Double Bond. *Angew. Chem., Int. Ed.* **2019**, *58* (32), 10961–10965.
- (30) Xiong, Y.; Yao, S.; Müller, R.; Kaupp, M.; Driess, M. Activation of Ammonia by a Si=O Double Bond and Formation of a Unique Pair of Sila-Hemiaminal and Silanoic Amide Tautomers. *J. Am. Chem. Soc.* **2010**, *132* (20), 6912–6913.
- (31) Kobayashi, R.; Ishida, S.; Iwamoto, T. An Isolable Silicon Analogue of a Ketone that Contains an Unperturbed Si = O Double Bond. *Angew. Chem., Int. Ed.* **2019**, *58* (28), 9425–9428.
- (32) Spikes, G. H.; Peng, Y.; Fettinger, J. C.; Steiner, J.; Power, P. P. Different reactivity of the heavier group 14 element alkyne analogues Ar'MMAR' (M = Ge, Sn; Ar' = C<sub>6</sub>H<sub>3</sub>-2,6(C<sub>6</sub>H<sub>3</sub>-2,6-Pri<sub>2</sub>)<sub>2</sub>) with R<sub>2</sub>NO. *Chem. Commun.* **2005**, 6041–6043.
- (33) Wang, X.; Zhu, Z.; Peng, Y.; Lei, H.; Fettinger, J. C.; Power, P. P. Room-Temperature Reaction of Carbon Monoxide with a Stable Diarylgermylene. *J. Am. Chem. Soc.* **2009**, *131* (20), 6912–6913.
- (34) Del Rio, N.; Baceiredo, A.; Saffon-Merceron, N.; Hashizume, D.; Lutters, D.; Müller, T.; Kato, T. A Stable Heterocyclic Amino-(phosphanylidene-σ<sup>4</sup>-phosphorane) Germylene. *Angew. Chem., Int. Ed.* **2016**, *55* (15), 4753–4758.
- (35) Fukuda, T.; Hashimoto, H.; Sakaki, S.; Tobita, H. Stabilization of a Sialdehyde by its η<sup>2</sup> Coordination to Tungsten. *Angew. Chem., Int. Ed.* **2016**, *55* (1), 188–192.
- (36) Dube, J. W.; Graham, C. M. E.; Macdonald, C. L. B.; Brown, Z. D.; Power, P. P.; Ragogna, P. J. Reversible, Photoinduced Activation of P<sub>4</sub> by Low-Coordinate Main Group Compounds. *Chem. - Eur. J.* **2014**, *20* (22), 6739–6744.
- (37) Usher, M.; Protchenko, A. V.; Rit, A.; Campos, J.; Kolychev, E. L.; Tirfoin, R.; Aldridge, S. A Systematic Study of Structure and E-H Bond Activation Chemistry by Sterically Encumbered Germylene Complexes. *Chem. - Eur. J.* **2016**, *22* (33), 11685–11698.
- (38) Del Rio, N.; Lopez-Reyes, M.; Baceiredo, A.; Saffon-Merceron, N.; Lutters, D.; Müller, T.; Kato, T. N,P-Heterocyclic Germylene/B(C<sub>6</sub>F<sub>5</sub>)<sub>3</sub> Adducts: A Lewis Pair with Multi-reactive Sites. *Angew. Chem., Int. Ed.* **2017**, *56* (5), 1365–1370.
- (39) Schneider, J.; Sindlinger, C. P.; Freitag, S. M.; Schubert, H.; Wesemann, L. Diverse Activation Modes in the Hydroboration of Aldehydes and Ketones with Germanium, Tin, and Lead Lewis Pairs. *Angew. Chem., Int. Ed.* **2017**, *56* (1), 333–337.
- (40) Sugahara, T.; Guo, J.-D.; Sasamori, T.; Nagase, S.; Tokitoh, N. Regioselective Cyclotrimerization of Terminal Alkynes Using a Digermyne. *Angew. Chem., Int. Ed.* **2018**, *57* (13), 3499–3503.
- (41) Swamy, V. S. V. N.; Pal, S.; Khan, S.; Sen, S. S. Cations and dications of heavier group 14 elements in low oxidation states. *Dalton Trans.* **2015**, *44* (29), 12903–12923.
- (42) Engesser, T. A.; Lichtenthaler, M. R.; Schleep, M.; Krossing, I. Reactive p-block cations stabilized by weakly coordinating anions. *Chem. Soc. Rev.* **2016**, *45* (4), 789–899.
- (43) Benzi, P.; Operti, L.; Vagilo, A. G.; Splendore, M.; Volpe, P.; Speranca, M.; Gabrielli, R. Gas phase ion–molecule reactions of monogermene with oxygen and ammonia. *J. Organomet. Chem.* **1988**, *354* (1), 39–50.
- (44) Rit, A.; Tirfoin, R.; Aldridge, S. Exploiting Electrostatics To Generate Unsaturation: Oxidative Ge = E Bond Formation Using a

- Non  $\pi$ -Donor Stabilized [R(L)Ge:]<sup>+</sup> Cation. *Angew. Chem., Int. Ed.* **2016**, *55* (1), 378–382.
- (45) Xiong, Y.; Szilvási, T.; Yao, S.; Tan, G.; Driess, M. Synthesis and Unexpected Reactivity of Germyliumylidene Hydride [GeH]<sup>+</sup> Stabilized by a Bis(N-heterocyclic carbene)borate Ligand. *J. Am. Chem. Soc.* **2014**, *136* (32), 11300–11303.
- (46) Xiong, Y.; Yao, S.; Inoue, S.; Berkefeld, A.; Driess, M. Taming the germyliumylidene [ClGe:]<sup>+</sup> and germathionium [ClGe = S]<sup>+</sup> ions by donor-acceptor stabilization using 1,8-bis(tributylphosphazanyl)-naphthalene. *Chem. Commun.* **2012**, 48 (100), 12198–12200.
- (47) Roy, M. M. D.; Fujimori, S.; Ferguson, M. J.; McDonald, R.; Tokitoh, N.; Rivard, E. Neutral, Cationic and Hydride-substituted Siloxygermylenes. *Chem. - Eur. J.* **2018**, *24* (54), 14392–14399.
- (48) Xiong, Y.; Yao, S.; Tan, G.; Inoue, S.; Driess, M. A Cyclic Germadycarbene (“Germylone”) from Germyliumylidene. *J. Am. Chem. Soc.* **2013**, *135* (13), 5004–5007.
- (49) Yao, S.; Xiong, Y.; Driess, M. From NHC→germylenes to stable NHC→germanone complexes. *Chem. Commun.* **2009**, 6466–6468.
- (50) Yao, S.; Xiong, Y.; Wang, W.; Driess, M. Synthesis, Structure, and Reactivity of a Pyridine-Stabilized Germanone. *Chem. - Eur. J.* **2011**, *17* (17), 4890–4895.
- (51) Rupar, P. A.; Staroverov, V. N.; Baines, K. M. Reactivity Studies of N-Heterocyclic Carbene Complexes of Germanium(II). *Organometallics* **2010**, *29* (21), 4871–4881.
- (52) Sharma, M. K.; Sinhababu, S.; Mahawar, P.; Mukherjee, G.; Pandey, B.; Rajaraman, G.; Nagendran, S. Donor-acceptor-stabilized germanium analogues of acid chloride, ester, and acyl pyrrole compounds: synthesis and reactivity. *Chem. Sci.* **2019**, *10* (16), 4402–4411.
- (53) Sinhababu, S.; Yadav, D.; Karwasara, S.; Sharma, M. K.; Mukherjee, G.; Rajaraman, G.; Nagendran, S. The Preparation of Complexes of Germanone from a Germanium  $\mu$ -Oxo Dimer. *Angew. Chem., Int. Ed.* **2016**, *55* (27), 7742–7746.
- (54) Bakthavachalam, K.; Yuvaraj, K.; Mondal, B.; Prakash, R.; Ghosh, S. All-metallagermoxane with an adamantanoid cage structure: [(Cp<sup>\*</sup>Ru(CO)<sub>2</sub>Ge)<sub>4</sub>( $\mu$ -O)<sub>4</sub>] (Cp<sup>\*</sup> =  $\eta^5$ -C<sub>5</sub>Me<sub>5</sub>). *Dalton Trans.* **2015**, 44 (41), 17920–17923.
- (55) Reiter, D.; Frisch, P.; Szilvási, T.; Inoue, S. Heavier Carbonyl Olefination: The Sila-Wittig Reaction. *J. Am. Chem. Soc.* **2019**, *141* (42), 16991–16996.
- (56) Ozturk, T.; Ertas, E.; Mert, O. Use of Lawesson’s Reagent in Organic Syntheses. *Chem. Rev.* **2007**, *107* (11), 5210–5278.
- (57) Hua, G.; Woollins, J. D. Formation and Reactivity of Phosphorus-Selenium Rings. *Angew. Chem., Int. Ed.* **2009**, *48* (8), 1368–1377.
- (58) Byrne, P. A.; Gilheany, D. G. The modern interpretation of the Wittig reaction mechanism. *Chem. Soc. Rev.* **2013**, *42* (16), 6670–6696.
- (59) Veith, M.; Becker, S.; Huch, V. A Base-Stabilized Ge-S Double Bond. *Angew. Chem., Int. Ed. Engl.* **1989**, *28* (9), 1237–1238.
- (60) Siwatch, R. K.; Karwasara, S.; Sharma, M. K.; Mondal, S.; Mukherjee, G.; Rajaraman, G.; Nagendran, S. Reactivity of LGe-NR<sub>2</sub> and LGe(E)-NR<sub>2</sub> over LGe-Cl and LGe(E)-Cl toward Me<sub>3</sub>SiX (L = Aminotroponimate; NR<sub>2</sub> = N(SiMe<sub>3</sub>)<sub>2</sub>/NC<sub>4</sub>H<sub>9</sub>; E = S/Se; X = Br/CN). *Organometallics* **2016**, *35* (4), 429–438.
- (61) Harris, L. M.; Tam, E. C. Y.; Cummins, S. J. W.; Coles, M. P.; Fulton, J. R. The Reactivity of Germanium Phosphanides with Chalcogens. *Inorg. Chem.* **2017**, *56* (5), 3087–3094.
- (62) Pineda, L. W.; Jancik, V.; Roesky, H. W.; Herbst-Irmer, R. Germacarboxylic Acid: An Organic-Acid Analogue Based on a Heavier Group 14 Element. *Angew. Chem., Int. Ed.* **2004**, *43* (41), 5534–5536.
- (63) Ossig, G.; Meller, A.; Brönneke, C.; Müller, O.; Schäfer, M.; Herbst-Irmer, R. Bis[(2-pyridyl)bis(trimethylsilyl)methyl-C,N]-germanium(II): A Base-Stabilized Germylene and the Corresponding Germanethione, Germaneselenone, and Germanetellurone. *Organometallics* **1997**, *16* (10), 2116–2120.
- (64) Xiong, Y.; Yao, S.; Karni, M.; Kostenko, A.; Burchert, A.; Apeloig, Y.; Driess, M. Heavier congeners of CO and CO<sub>2</sub> as ligands: from zero-valent germanium (“germylone”) to isolable monomeric GeX and GeX<sub>2</sub> complexes (X = S, Se, Te). *Chem. Sci.* **2016**, *7* (8), 5462–5469.
- (65) Matsumoto, T.; Tokitoh, N.; Okazaki, R. The First Kinetically Stabilized Germanethiones and Germaneselenones: Syntheses, Structures, and Reactivities. *J. Am. Chem. Soc.* **1999**, *121* (38), 8811–8824.
- (66) Smeltz, J. L.; Lilly, C. P.; Boyle, P. D.; Ison, E. A. The Electronic Nature of Terminal Oxo Ligands in Transition-Metal Complexes: Ambiphilic Reactivity of Oxo-rhenium Species. *J. Am. Chem. Soc.* **2013**, *135* (25), 9433–9441.
- (67) Lohrey, T. D.; Bergman, R. G.; Arnold, J. Reductions of a Rhenium(III) Terminal Oxo Complex by Isocyanides and Carbon Monoxide. *Organometallics* **2018**, *37* (20), 3552–3557.
- (68) Paul, D.; Heins, F.; Krupski, S.; Hepp, A.; Daniluc, C. G.; Klahr, K.; Neugebauer, J.; Glorius, F.; Hahn, F. E. Synthesis and Reactivity of Intramolecularly NHC-Stabilized Germylenes and Stannylenes. *Organometallics* **2017**, *36* (5), 1001–1008.
- (69) Del Rio, N.; Lopez-Reyes, M.; Bacciredo, A.; Saffon-Merceron, N.; Lutters, D.; Müller, T.; Kato, T. N,P-Heterocyclic Germylene/B(C<sub>6</sub>F<sub>5</sub>)<sub>3</sub> Adducts: A Lewis Pair with Multi-reactive Sites. *Angew. Chem., Int. Ed.* **2017**, *56* (5), 1365–1370.
- (70) Hadlington, T. J.; Kefalidis, C. E.; Maron, L.; Jones, C. Efficient Reduction of Carbon Dioxide to Methanol Equivalents Catalyzed by Two-Coordinate Amido-Germanium(II) and -Tin(II) Hydride Complexes. *ACS Catal.* **2017**, *7* (3), 1853–1859.
- (71) Leong, B.-X.; Lee, J.; Li, Y.; Yang, M.-C.; Siu, C.-K.; Su, M.-D.; So, C.-W. A Versatile NHC-Parent Silyliumylidene Cation for Catalytic Chemo- and Regioselective Hydroboration. *J. Am. Chem. Soc.* **2019**, *141* (44), 17629–17636.
- (72) von Wolff, N.; Lefèvre, G.; Berthet, J. C.; Thuéry, P.; Cantat, T. Implications of CO<sub>2</sub> Activation by Frustrated Lewis Pairs in the Catalytic Hydroboration of CO<sub>2</sub>: A View Using N/Si<sup>+</sup> Frustrated Lewis Pairs. *ACS Catal.* **2016**, *6* (7), 4526–4535.
- (73) Henderson, W. A.; Schultz, C. J. The Nucleophilicity of Amines. *J. Org. Chem.* **1962**, *27* (12), 4643–4646.
- (74) Nicholls, R. L.; McManus, J. A.; Rayner, C. M.; Morales-Serna, J. A.; White, A. J. P.; Nguyen, B. N. Guanidine-Catalyzed Reductive Amination of Carbon Dioxide with Silanes: Switching between Pathways and Suppressing Catalyst Deactivation. *ACS Catal.* **2018**, *8* (4), 3678–3687.

## 9. Germylumylidene: a versatile low valent group 14 catalyst

**Title:** Germylumylidene: a versatile low valent group 14 catalyst

**Status** Article, (Draft)

**Authors** Debotra Sarkar, Catherine Weetman, Sayan Dutta, Emeric Schubert, Debasis Koley, and Shigeyoshi Inoue

**Content** Transition metal mimetic reactivity of low valent group 14 elements has attracted significant interest in recent decades. In particular, the development and application of main group-based catalysts as an alternative to the costly transition metals are the “Holy Grail” for modern main group chemistry. However, their catalytic application is limited due to challenges in reductive elimination from the resultant high-oxidation state complex. In this regard, low valent germanium compounds can provide new impetus to main group catalysis, as they are stable in both higher (+IV) and low oxidation states (+II). Few examples of neutral germylene mediated catalysis are known. However, their catalytic performance is low and unselective, thus limiting their catalytic use.

Bis NHC-stabilized germylumylidene [ $\{m\text{-TerGe}(\text{NHC})_2\}\text{X}$ ] **1**, (X = Cl or BArF), has a unique electronic nature. In comparison to traditional germylene or germylum ions, it is a stronger Lewis base and possesses weak  $\pi$ -accepting character due to the strong donation from NHCs. Inspired by this electronic feature, we have utilized germylumylidene **1** in the catalytic reduction of CO<sub>2</sub> with amines and silane, under mild conditions. Furthermore, the versatility of **1** is explored in the catalyzed hydroboration and cyanosilylation of carbonyls.

### Author Contributions

- Debotra Sarkar planned and executed all experiments (in parts together with, Emeric Schubert during his Internship). Debotra Sarkar and Dr. Catherine Weetman co-wrote the manuscript. Sayan Dutta and Prof. Debasis Koley designed and performed the theoretical analyses. All the work was performed under the supervision of Prof. Shigeyoshi Inoue.



## COMMUNICATION

## Germlyiumylidene: A versatile low valent group 14 catalyst

Debotra Sarkar,<sup>[a]</sup> Catherine Weetman,<sup>[a,b]</sup> Sayan Datta,<sup>[c]</sup> Emeric Schubert,<sup>[a]</sup> Debasis Koley,<sup>[c]</sup> Shigeyoshi Inoue\*<sup>[a]</sup>

[a] Debotra Sarkar, Dr. Catherine Weetman, Emeric Schubert, Prof. Dr. Shigeyoshi Inoue  
Department of Chemistry, WACKER-Institute of Silicon Chemistry and Catalysis Research Center  
Technische Universität München, Lichtenbergstraße 4, 85748 Garching, Germany  
E-mail: [s.inoue@tum.de](mailto:s.inoue@tum.de)

[b] Current address: Dr. Catherine Weetman, Department of Pure and Applied Chemistry, University of Strathclyde, Glasgow, G1 1XL

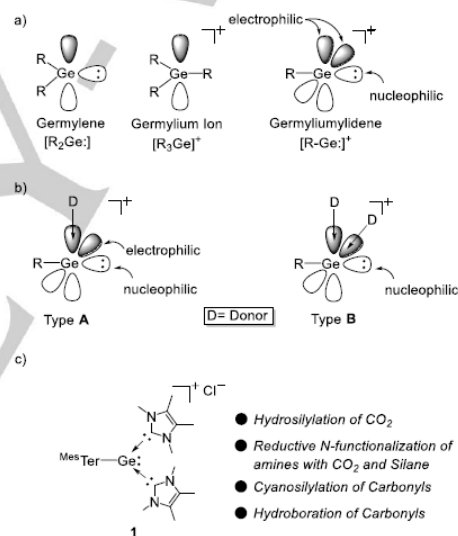
[c] Sayan Datta, Prof. Dr. Debasis Koley  
Department of Chemical Science  
IISER Kolkata  
Mohanpur-741246, India

Supporting information for this article is given via a link at the end of the document.

**Abstract:** Germlyiumylidene  $[R\text{-Ge}]^+$  can act as both Lewis acid (LA) and Lewis Base (LB), owing to its lone pair, positive charge and two vacant orbitals on the germanium atom. Utilizing this unique electronic feature, we report the first example of NHC-stabilized germlyiumylidene  $[\text{MesTerGe}(\text{NHC})_2]\text{Cl}$  (**1**), ( $\text{MesTer} = 2,6\text{-}(\text{2,4,6}\text{-}\text{Me}_3\text{C}_6\text{H}_2)_2\text{C}_6\text{H}_3$ ;  $\text{NHC} = \text{IME}_4 = 1,3,4,5\text{-tetramethylimidazol-2-ylidene}$ ) catalyzed reduction of  $\text{CO}_2$  with amines and silane, under mild conditions. Furthermore, the versatility of **1** is explored in the catalyzed hydroboration and cyanosilylation of carbonyls.

The ability of main group complexes' to mimic transition metals has gained tremendous attention in recent years, driven by the desire for new sustainable processes.<sup>[1]</sup> Activation of small molecules by low-oxidation state main group centers has been achieved and is the preliminary step towards transition metal-free catalysis.<sup>[1a, 1e]</sup> However, their catalytic application is still limited due to challenges in reductive elimination from the resultant high-oxidation state complex.<sup>[1d, 1e, 2]</sup> Recently, low valent germanium compounds have found themselves to be a diverse tool in enabling chemical transformations, attributed to the relative ease in which the +II and +IV oxidation states can be accessed.<sup>[2b-g, 3]</sup> This includes the first example of low-valent main group dihydrogen activation and the use of multiple bonds (digermynes) in catalysis.<sup>[2f, 3a]</sup> Among the low valent germanium compounds, germlyiumylidenes  $[R\text{-Ge}]^+$  possess a unique electronic feature,<sup>[4]</sup> due to the presences of a lone pair and two vacant p-orbitals at the germanium center. It, therefore, combines the characteristics of germlyium cations  $[R_3\text{Ge}]^+$  and germlylenes  $[R_2\text{Ge}]$  (Scheme 1a) and can simultaneously act as an electrophile and nucleophile.<sup>[4]</sup> This ambiphilicity has been utilized in the activation of various small molecules,<sup>[3e, 5]</sup> including the thermodynamically robust H-H bond.<sup>[3e]</sup>

The reactivity of germlyiumylidenes can be tuned depending on the number of donor ligands employed to stabilised the vacant p-orbitals of germanium (Scheme 1b). Based on this, germlyiumylidenes can be classified into two types, i) two-coordinate germlyiumylidenes, which have both electrophilic and nucleophilic centers (Scheme 1b, Type A), and ii) three-



**Scheme 1.** (a) Electronic features of germlyiumylidene, (b) Lewis based stabilized germlyiumylidenes, and (c) this work.

coordinate germlyiumylidenes where the nucleophilic character is more pronounced due to the occupancy of the two p-orbitals (Scheme 1b, Type B).<sup>[4]</sup> Despite these unique electronic features, the catalytic application of germlyiumylidenes is in its infancy, with only the recent examples from the groups of Rivard and Nagendran currently reported. These show the roles of germlyiumylidenes of types A and B, respectively, in the hydroboration of carbonyls.<sup>[6]</sup> Very recently, we have reported hydrosilylation of  $\text{CO}_2$  with a germaacylium ion  $[\text{MesTerGe}(\text{O})(\text{NHC})_2]\text{Cl}$ , which proceeds through the active germlyene species  $[\text{MesTerGe}(\text{OSiHPh}_2)(\text{NHC})]$ .<sup>[7]</sup> Importantly, in our case the Lewis basicity of Ge(II) facilitates the hydride transfer from silane to  $\text{CO}_2$  via the formation of a hypervalent silane intermediate. Moreover, it has been shown that the Lewis acidity and Lewis basicity are both important for the catalytic

## COMMUNICATION

transformation of CO<sub>2</sub>.<sup>[2d, 2e, 2h, 8]</sup> This encouraged us to examine the recently reported bis NHC stabilized germyliumylidene [MesTerGe(NHC)<sub>2</sub>]Cl (**1**) towards a range of catalytic reductive functionalization reactions, with a particular emphasis on C=O reduction i.e., CO<sub>2</sub> and carbonyls.

Following a similar protocol to the previous NHC-stabilized germylene catalysis, compound **1** was found to transform CO<sub>2</sub> into the corresponding hydrosilylated products in both a stoichiometric and catalytic manner presence of phenylsilane (PhSiH<sub>3</sub>). The <sup>1</sup>H NMR spectrum revealed the complete consumption of PhSiH<sub>3</sub> within 2.5 h, with the formation of silylformate, bis(silyl)acetal and silylated methanol observed (see SI, Figure S1). As expected, use of more sterically protected silanes required increased reaction times (PhSiH<sub>3</sub> 2.5 h vs Ph<sub>2</sub>SiH<sub>2</sub> 3.5 h), and in the case of Ph<sub>3</sub>SiH, higher temperatures and prolonged reaction times are required (28 h at 80 °C). Furthermore, solvent optimization studies found increased rates of reaction in polar solvents (e.g., CD<sub>3</sub>CN) compared to non-polar solvents (e.g., C<sub>6</sub>D<sub>6</sub>). This, however, can also be attributed to the low solubility of the catalyst in non-polar solvents. To consider the influence of the counter ion in catalysis, the reaction was performed using the anion-exchanged **1**[BARF] catalyst in CD<sub>3</sub>CN, no significant change in the rate of reaction was found. This points towards the dependence on the cationic germanium center during the catalysis. With the above points considered, use of 5 mol% of **1** with PhSiH<sub>3</sub> in CD<sub>3</sub>CN at 60 °C provides the optimal reaction conditions for this study.

Whilst the catalytic activity of **1** is lower in comparison to our previously reported germaacylium ion catalyst,<sup>[7]</sup> germyliumylidene **1** has the added advantage of being a more robust catalyst as well as requiring fewer synthetic steps. Using the optimized conditions mentioned above, the longevity of catalyst **1** was examined in which additional PhSiH<sub>3</sub> and 1 bar of CO<sub>2</sub> were added to the J-Youngs NMR tube at the end of the cycle. This process could be repeated four times before a small drop in turnover was observed (TOF: Run 1 = 8 h<sup>-1</sup> vs Run 4 = 6 h<sup>-1</sup>). In contrast, the previously reported germaacylium ion catalyst decomposed after the third cycle.

A series of stoichiometric reactions were undertaken to probe the mechanism. No reaction was observed with **1** and CO<sub>2</sub> in the absence of silane, even after prolonged heating at 60 °C. Additionally, no reaction was observed with varying equivalents of hydrosilane under the optimal catalytic conditions. This suggests a cooperative silane/CO<sub>2</sub> mechanism, and therefore, the mechanism was investigated computationally.

As an extension to hydrosilylation of CO<sub>2</sub>, the reductive N-functionalization of amines provides a diagonal approach for CO<sub>2</sub> utilization, as the combination of CO<sub>2</sub> and silanes provides the C1 source for N-formylation or N-methylation of amines.<sup>[9]</sup> Accordingly, we examined the scope of reductive functionalization of CO<sub>2</sub> with various amines as listed in Table 1. The study revealed that aliphatic secondary amines proceed smoothly compared to aromatic secondary amines. For example, the aliphatic amines (Table 1, Entry 1-4) are converted to corresponding 2e<sup>-</sup> (formamide), 4e<sup>-</sup> (aminal) and 6e<sup>-</sup> (methylamine) reduced products within 2 h, whereas N-Methylaniline (Table 1, Entry 5) requires 16 h. This is possibly attributed to the low nucleophilicity of the aromatic amine arising from the delocalization of nitrogen lone pair with the phenyl ring.<sup>[10]</sup>

**Scheme 2.** Plausible mechanism of **1** catalyzed N-functionalization of amines with CO<sub>2</sub> and PhSiH<sub>3</sub>

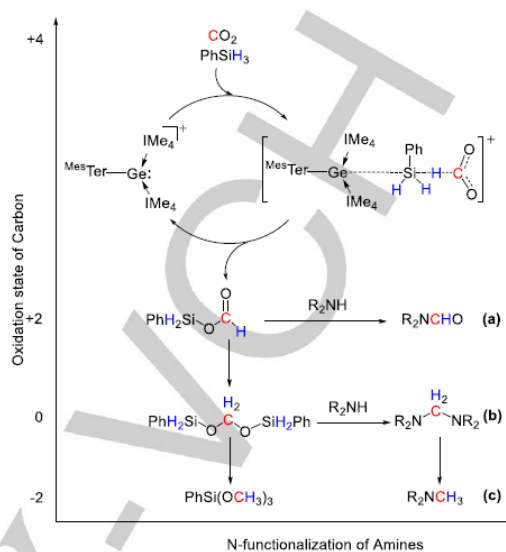
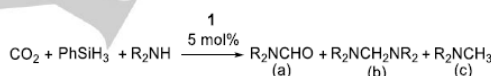


**Table 1.** N-methylation of amines using 1 bar CO<sub>2</sub>, 3 eq. PhSiH<sub>3</sub> in CD<sub>3</sub>CN and 5 mol% of **1** (All reactions carried out at 60 °C). TOF = (Conversion/catalyst loading)/time



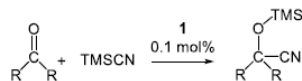
Entry	Amine	NMR Yield (%)			TOF (h <sup>-1</sup> )
		a	b	c	
1	Diethylamine	73	4	22	9.4
2	Piperidine	82	0	16	9.4
3	Morpholine	81	0	17	9.4
4	Dicyclohexylamine	47	0	47	19.8
5	N-Methylaniline	70	25	4	1.25

To examine the scope of germyliumylidene catalysis, we turned our attention towards the cyanosilylation of carbonyls. Cyanosilylation is one of the most fundamental carbon-carbon bond forming reactions in organic chemistry, where the resulting cyanohydrin silyl ether [R<sub>2</sub>C(OTMS)CN] serves as a synthon for numerous biologically relevant molecules such as α-hydroxyacids, α-amino acids, and β-amino alcohols.<sup>[11]</sup> Catalysts for cyanosilylation of carbonyls typically utilizes transition metals,<sup>[11]</sup> whilst in contrast, only a handful of heavier main group compounds have been exploited as a single site cyanosilylation catalyst.<sup>[2c, 2g, 12]</sup> In this context, recently, Khan and co-workers demonstrated the role of a neutral NHC-stabilized germylene in the catalyzed cyanosilylation of aldehydes. Here, the Lewis acidity of germanium facilitated the cyanide transfer to the carbonyl moiety via formation of a donor-accepter complex

## COMMUNICATION

[TMSCN → Ge(II)].<sup>[29]</sup> We, therefore, envisaged enhanced activity of germyliumylidenes over germlylenes, due to the cationic germanium center. Accordingly, cyanosilylation was performed with various carbonyls, as listed in Table 2.

**Table 2.** Cyanosilylation: carbonyl (1.00 mmol), TMSCN (1.02 mmol), solvent (0.4 mL CD<sub>3</sub>CN), room temperature and 0.1 mol% of **1**. TOF = (Conversion/catalyst loading)/time

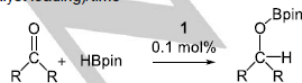


Entry	Carbonyl	NMR Yield (%)	Time (h)	TOF (h <sup>-1</sup> )
1	Propanal	>99	0.5	1800
2	Pivaldehyde	>99	0.5	1900
3	Cyclohexanecarboxaldehyde	>99	0.5	1800
4	4-Pyridinecarboxaldehyde	>99	0.5	1900
5	Benzaldehyde	>99	1.1	900
6	4-Cyanobenzaldehyde	>99	1.5	660
7	2-Naphthalenecarboxaldehyde	>99	1.5	660
8*	Benzophenone	>99	4	25
9*	Acetophenone	>99	14	7
10*	4-Fluoroacetophenone	>99	16	6
11*	4-Methoxyacetophenone	>99	15	6.6

\* For ketones 1.00 mol% of **1** and 50 °C temperature was required.

Catalytic cyanosilylation of aldehydes and ketones, mediated by **1**, proceed under mild conditions compared to the previously reported germlylenes.<sup>[29]</sup> Notably, in our case, low catalyst loadings (0.1 mol%) and reduced reaction times (≤90 min) are required for complete conversion of both aromatic and aliphatic aldehydes, yielding the corresponding cyanohydrin silyl ether (for aliphatic aldehydes TOF = ≥1800 h<sup>-1</sup> and aromatic aldehyde TOF = 900 h<sup>-1</sup>). For benzophenone, increased catalyst loadings (1 mol%) and higher temperatures (50 °C) are required, likely due to the increased steric protection around the carbonyl moiety.

**Table 3.** Hydroboration: carbonyl (1.00 mmol), HBpin(1.02 mmol), solvent (0.4 mL CD<sub>3</sub>CN), room temperature and 0.1 mol% of catalyst. TOF = (Conversion/catalyst loading)/time



Entry	Carbonyl	NMR Yield (%)	Time (h)	TOF (h <sup>-1</sup> )
1	Propanal	>99	0.1	>5900

2	Pivaldehyde	>92	24	38
3	Cyclohexanecarboxaldehyde	>99	4	250
4	4-Pyridinecarboxaldehyde	>99	3.5	280
5	Benzaldehyde	>99	0.5	1700
6	4-Cyanobenzaldehyde	>99	0.6	1600
7	2-Naphthalenecarboxaldehyde	>99	0.6	1600

Hydroboration is an attractive method for mild and selective reduction of carbonyls. Neutral tetrelene (R<sub>2</sub>E, E = Si-Sn) catalyzed hydroboration of carbonyls is known,<sup>[2b, 13]</sup> and recently, germyliumylidene catalyzed hydroboration of carbonyls has also been reported.<sup>[6]</sup> Encouraged by these studies, we screened catalytic activity of **1** towards various carbonyls with pinacol borane (HBpin) as the hydroboration reagent. In line with previous studies, less bulky substituents (e.g., propanal, Table 3, entry 1) proceed rapidly with low catalyst loadings (0.1 mol%), whereas more sterically demanding substrates (e.g., *t*-BuCHO, Table 3, entry 2) require longer reaction times. Notably, this catalysis proceeds with much lower catalyst loadings than those previously reported for cationic germanium catalysts.<sup>[6b]</sup>

In conclusion, we have demonstrated for the first-time utilization of a well-defined low valent group 14 tetrelumylidene complex for diverse organic transformations, including the first example of germyliumylidene **1** catalyzed hydrosilylation of CO<sub>2</sub> and N-methylation of amines using CO<sub>2</sub> as a C1 source. Additionally, exploiting the electronic features of **1**, other organic transformations such as cyanosilylation and hydroboration of carbonyls has been achieved under mild conditions. With the observed high catalytic activity and versatile transformations, this robust NHC-stabilized germyliumylidene catalyst provides a viable alternative towards transition metal-free catalysis.

## Acknowledgements

We gratefully acknowledge financial support from WACKER Chemie AG, the European Research Council (SILION 637394) and the DAAD (fellowship for D.S.). This project has received funding from the European Union's Horizon 2020 research and innovation program under the Marie Skłodowska-Curie grant agreement No 754462 (Fellowship CW).

**Keywords:** NHC • Main Group • Germanium • Cation • CO<sub>2</sub> conversion

- [1] a) P. P. Power, *Nature* **2010**, *463*, 171-177; b) S. Yadav, S. Saha, S. S. Sen, *ChemCatChem* **2015**, *8*, 486-501; c) C. Weetman, S. Inoue, *ChemCatChem* **2018**, *10*, 4213-4228; d) T. J. Hadlington, M. Driess, C. Jones, *Chem. Soc. Rev.* **2018**, *47*, 4176-4197; e) T. Chu, G. I. Nikonov, *Chem. Rev.* **2018**, *118*, 3608-3680; f) M.-A. Légaré, C. Pranckevicius, H. Braunschweig, *Chem. Rev.* **2019**, *119*, 8231-8261.
- [2] a) H. F. T. Klare, M. Oestreich, *Dalton Trans.* **2010**, *39*, 9176-9184; b) T. J. Hadlington, M. Hermann, G. Frenking, C. Jones, *J. Am. Chem. Soc.* **2014**, *136*, 3028-3031; c) R. K. Sivatch, S. Nagendran, *Chem. Eur. J.* **2014**, *20*, 13551-13556; d) T. J. Hadlington, C. E. Kefalidis, L. Maron, C. Jones, *ACS Catal.* **2017**, *7*, 1853-1859; e) N. Del Rio, M.

## COMMUNICATION

- Lopez-Reyes, A. Baceiredo, N. Saffon-Merceron, D. Lutters, T. Müller, T. Kato, *Angew. Chem. Int. Ed.* **2017**, *56*, 1365-1370; f) T. Sugahara, J.-D. Guo, T. Sasamori, S. Nagase, N. Tokitoh, *Angew. Chem. Int. Ed.* **2018**, *57*, 3499-3503; g) R. Dasgupta, S. Das, S. Hiwase, S. K. Pati, S. Khan, *Organometallics* **2019**, *38*, 1429-1435; h) B.-X. Leong, J. Lee, Y. Li, M.-C. Yang, C.-K. Siu, M.-D. Su, C.-W. So, *J. Am. Chem. Soc.* **2019**, *141*, 17629-17636.
- [3] a) G. H. Spikes, J. C. Fettinger, P. P. Power, *J. Am. Chem. Soc.* **2005**, *127*, 12232-12233; b) X. Wang, Z. Zhu, Y. Peng, H. Lei, J. C. Fettinger, P. P. Power, *J. Am. Chem. Soc.* **2009**, *131*, 6912-6913; c) A. Jana, D. Ghoshal, H. W. Roesky, I. Objartel, G. Schwab, D. Stalke, *J. Am. Chem. Soc.* **2009**, *131*, 1288-1293; d) J. W. Dube, C. M. E. Graham, C. L. B. Macdonald, Z. D. Brown, P. P. Power, P. J. Ragogna, *Chem. Eur. J.* **2014**, *20*, 6739-6744; e) K. Inomata, T. Watanabe, Y. Miyazaki, H. Tobita, *J. Am. Chem. Soc.* **2015**, *137*, 11935-11937; f) T. Y. Lai, K. L. Gullett, C.-Y. Chen, J. C. Fettinger, P. P. Power, *Organometallics* **2019**, *38*, 1421-1424.
- [4] V. S. V. S. N. Swamy, S. Pal, S. Khan, S. S. Sen, *Dalton Trans.* **2015**, *44*, 12903-12923.
- [5] a) Y. Xiong, S. Yao, S. Inoue, A. Berkefeld, M. Driess, *Chem. Commun.* **2012**, *48*, 12198-12200; b) A. Rit, R. Tirfoin, S. Aldridge, *Angew. Chem. Int. Ed.* **2016**, *55*, 378-382; c) R. J. Mangan, A. Rit, C. P. Sindlinger, R. Tirfoin, J. Campos, J. Hicks, K. E. Christensen, H. Niu, S. Aldridge, *Chem. Eur. J.* **2020**, *26*, 306-315.
- [6] a) M. M. D. Roy, S. Fujimori, M. J. Ferguson, R. McDonald, N. Tokitoh, E. Rivard, *Chem. Eur. J.* **2018**, *24*, 14392-14399; b) S. Sinhababu, D. Singh, M. K. Sharma, R. K. Siwatch, P. Mahawar, S. Nagendran, *Dalton Trans.* **2019**, *48*, 4094-4100.
- [7] D. Sarkar, C. Weetman, S. Dutta, E. Schubert, C. Jandl, D. Koley, S. Inoue, *J. Am. Chem. Soc.* **2020**, *142*, 15403-15411.
- [8] a) D. Mukherjee, D. F. Sauer, A. Zanardi, J. Okuda, *Chem. Eur. J.* **2016**, *22*, 7730-7733; b) N. von Wolff, G. Lefèvre, J. C. Berthet, P. Thuéry, T. Cantat, *ACS Catal.* **2016**, *6*, 4526-4535.
- [9] a) C. Das Neves Gomes, O. Jacquet, C. Villiers, P. Thuéry, M. Ephritikhine, T. Cantat, *Angew. Chem. Int. Ed.* **2012**, *51*, 187-190; b) F. J. Fernández-Alvarez, L. A. Oro, *ChemCatChem* **2018**, *10*, 4783-4796; c) Y. Zhang, T. Zhang, S. Das, *Green Chem.* **2020**, *22*, 1800-1820.
- [10] W. A. Henderson, C. J. Schultz, *J. Org. Chem.* **1962**, *27*, 4643-4646.
- [11] M. North, D. L. Usanov, C. Young, *Chem. Review.* **2008**, *108*, 5146-5226.
- [12] a) Z. Yang, M. Zhong, X. Ma, S. De, C. Anusha, P. Parameswaran, H. W. Roesky, *Angew. Chem. Int. Ed.* **2015**, *54*, 10225-10229; b) Z. Yang, Y. Yi, M. Zhong, S. De, T. Mondal, D. Koley, X. Ma, D. Zhang, H. W. Roesky, *Chem. Eur. J.* **2016**, *22*, 6932-6938; c) M. K. Sharma, S. Sinhababu, G. Mukherjee, G. Rajaraman, S. Nagendran, *Dalton Trans.* **2017**, *46*, 7672-7676; d) V. S. V. S. N. Swamy, M. K. Bisai, T. Das, S. S. Sen, *Chem. Commun.* **2017**, *53*, 6910-6913; e) S. Yadav, R. Dixit, K. Vanka, S. S. Sen, *Chem. Eur. J.* **2018**, *24*, 1269-1273; f) M. K. Bisai, T. Das, K. Vanka, S. S. Sen, *Chem. Commun.* **2018**, *54*, 6843-6846; g) W. Wang, M. Luo, J. Li, S. A. Pullarkat, M. Ma, *Chem. Commun.* **2018**, *54*, 3042-3044.
- [13] a) Y. Wu, C. Shan, Y. Sun, P. Chen, J. Ying, J. Zhu, L. Liu, Y. Zhao, *Chem. Commun.* **2016**, *52*, 13799-13802; b) J. Schneider, C. P. Sindlinger, S. M. Freitag, H. Schubert, L. Wesemann, *Angew. Chem. Int. Ed.* **2017**, *56*, 333-337; c) V. Nesterov, R. Baierl, F. Hanusch, A. E. Ferao, S. Inoue, *J. Am. Chem. Soc.* **2019**, *141*, 14576-14580.

## 10. Summary and outlook

This Ph.D. dissertation started with the initial goal to explore the reactivity of the silyliumylidene  $[\{m\text{-TerSi}(\text{IME}_4)_2\}^+\text{Cl}^-]$  **1**, previously reported by our group. Besides the already reported reactivity of **1** towards  $\text{CO}_2$  and  $\text{PhCCH}$  our target was to systematically investigate the reactivity of the **1** towards other small molecules such as chalcogen and  $\text{H}_2\text{O}$ . Fortunately, the reactivity of the **1** towards elemental chalcogen gave rise to the elusive heavier silaacylium cation, while the reactivity of **1** with  $\text{H}_2\text{O}$  led to the long sought-after molecule silaaldehyde. Also, the isolation, reactivity, and catalytic application of germyliumylidene  $[\{m\text{-TerGe}(\text{IME}_4)_2\}^+\text{Cl}^-]$  **11** put insight into the low valent group 14 chemistry. Striking reactivity of germyliumylidene **11** towards  $\text{N}_2\text{O}$  led to the solely donor stabilized germaacylium ion, which shows fascinating reactivity towards catalytic utilization of  $\text{CO}_2$ . A detailed summary is given below.

### Heavier silaacylium ion

The reactivity of  $[\{m\text{-TerSi}(\text{IME}_4)_2\}^+\text{Cl}^-]$  with chalcogens led to the solely donor stabilized heavier silaacylium compounds  $[\{m\text{-Ter}(\text{SiE})(\text{IME}_4)_2\}^+\text{Cl}^-]$  (E= S **2**, Se **3** and Te **4**) (Figure 45). Compounds **2-4** are isolated in good yields (compound **2** = 85%, **3** = 56%, **4** = 87%). Further, DFT calculations revealed the zwitterionic nature of the Si-E bond.

Thus, heavier silaacylium can be demonstrated by two resonance canonical forms **A** and **B** (Figure 45), where canonical form **B** is dominant due to the strong donation from the NHCs. Further fascinating reactivity of **2-4** with  $\text{AuI}$  led to the regeneration of the tetryliumylidene **1**. Notably, this represents the first example of chalcogen transfer *via* low valent Si(II) compound to the coinage metal compound ( $\text{AuI}$ ). Interestingly, sila-chalcogen scrambling was demonstrated, which was in line with the energy of silicon-chalcogen bond  $\{\mathbf{4} (90.8 \text{ kcal mol}^{-1}) \rightarrow \mathbf{3} (62.7 \text{ kcal mol}^{-1}) \rightarrow \mathbf{2} (47.5 \text{ kcal mol}^{-1})\}$  (Figure 46).

## Summary and outlook

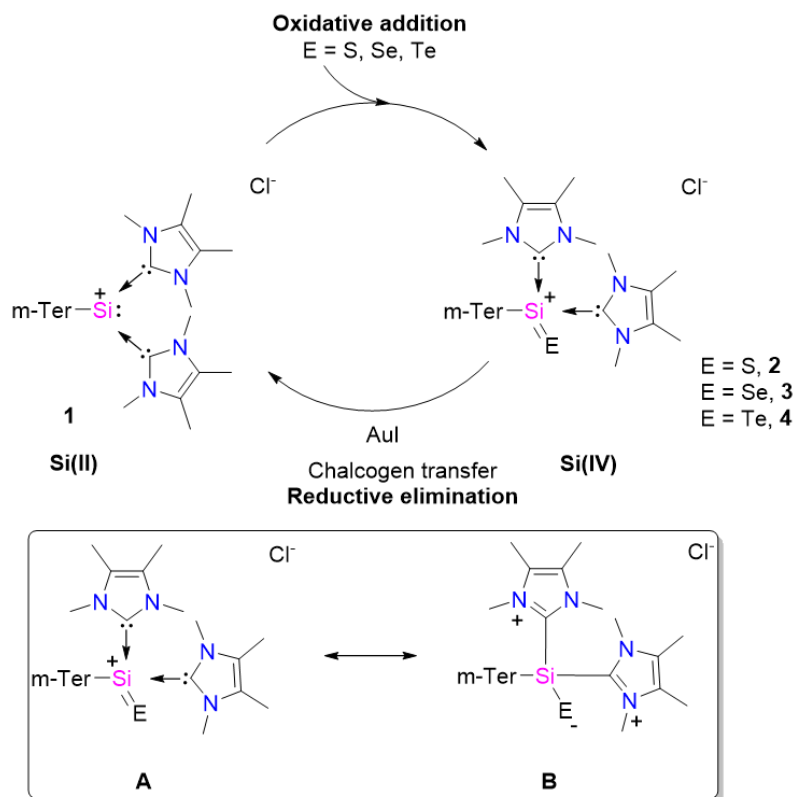


**Figure 45:** Isolation and reactivity of heavier silaacylium ions.

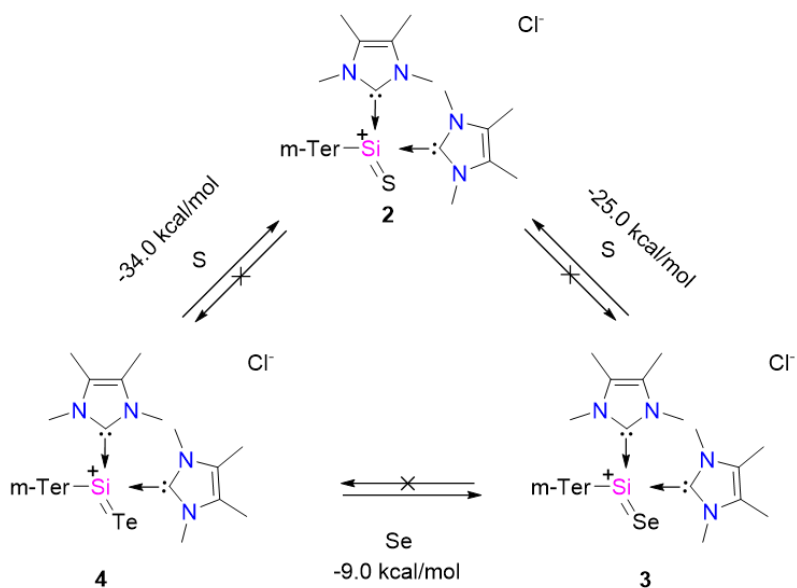


**Figure 46:** Chalcogen-scrambling reaction of heavier silaacylium ions.

The reactivities, as mentioned above, encouraged us to use silyliumylidene **1** as a potential chalcogen transfer catalyst. It is to be noted that catalytic chalcogen transfer from elemental chalcogen to an organic substrate is rare.<sup>166</sup> For example, there is only a handful of transition metal-mediated catalytic chalcogen transfers to unsaturated C-C bonds known.<sup>167</sup> Unfortunately, no catalytic or stoichiometric chalcogen transfer from **2-4** towards alkenes or alkynes was observed. Whilst the potential for this chemistry is clear, small modifications to the ligand design maybe enable catalytic activity and is something to consider in the future.

## Silaaldehyde

Compounds containing Si-O double bonds are long-sought-after species within the class of organosilicon compounds.<sup>5</sup> A number of kinetically and thermodynamically stabilized silanones ( $R_2Si=O$ ) have been reported. However, due to the lack of steric protection isolation of silaaldehydes  $\{R-Si(O)H\}$  in the condensed phase is challenging. Inspired by the reactivity of the **1** towards small molecules (e.g.,  $PhCCH$ ,  $CO_2$ ,  $H_2S$ , and chalcogens),<sup>95, 107, 108, 168</sup>, we treated compound **1** with  $H_2O$  in an attempt to isolate a silaaldehyde  $\{[m-Ter(H)SiO]\{IME_4\}$ .

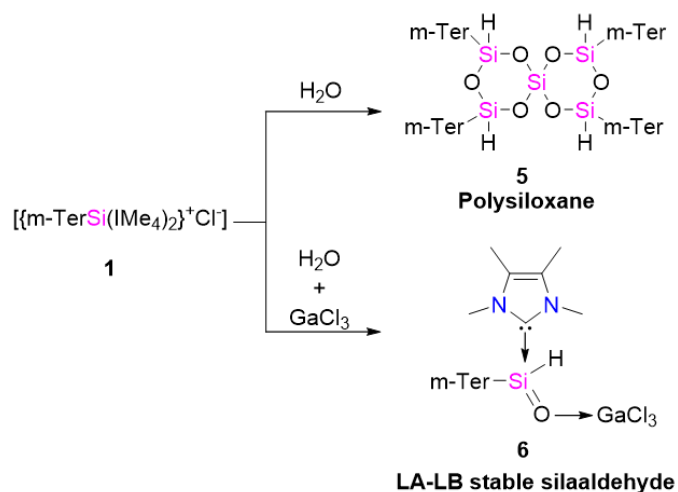


**Figure 47:** Isolation of silaaldehyde.

However, in the absence of a Lewis acid reaction of **1** with  $H_2O$  yielded the polysiloxane complex **5**, which is a combination of four silaaldehyde  $\{m-Ter(H)SiO\}$  and one  $SiO_2$  moiety (Figure 47). Encouraged by this result, we utilized a Lewis Acid to prevent the oligomerization of the silaaldehyde. Indeed the reactivity of **1** with  $H_2O$  in the presence of  $GaCl_3$  leads to the desired

## Summary and outlook

silaaldehyde complex  $[[\{m\text{-Ter(H)SiO}\}\{\text{GaCl}_3\}](\text{IME}_4)]$  **6** (Figure 47). However, the use of other Lewis acids such as  $\text{B}(\text{C}_6\text{H}_5)_3$ ,  $\text{ZnCl}_2$  etc., did not provide the corresponding silaaldehyde complexes. Despite being masked by  $\text{GaCl}_3$ , compound **6** shows analogous reactivity to classical aldehyde compounds  $\text{R-CO(H)}$  (Figure 48). The reaction with the masked silaaldehyde **6** and  $\text{GaCl}_3$  leads to the silaacyl halide complex  $[[\{m\text{-Ter(Cl)SiO}\}\{\text{GaCl}_3\}](\text{IME}_4)]$  **7**. Further, hydrolysis of **6** with  $\text{IME}_4$  gives rise to the corresponding silanoic acid  $[[\{m\text{-Ter(OH)SiO}\}\{\text{GaCl}_3\}](\text{IME}_4)]$  **8** (unstable), which further dimerizes to the corresponding sila-carboxylate ester **9**. Intriguingly, Phospha-Peterson type reactivity of the silaaldehyde **6** and  $\text{P}(\text{TMS})_3$  enabled access to the phosphasilene compound  $[\{m\text{-Ter(H)Si(PTMS)}\}(\text{IME}_4)]$  **10**. Moreover, the functionalization of **6** gives rise to a novel platform to gain access to otherwise elusive compounds. Thus, showing the relationship to classical carbonyl chemistry.

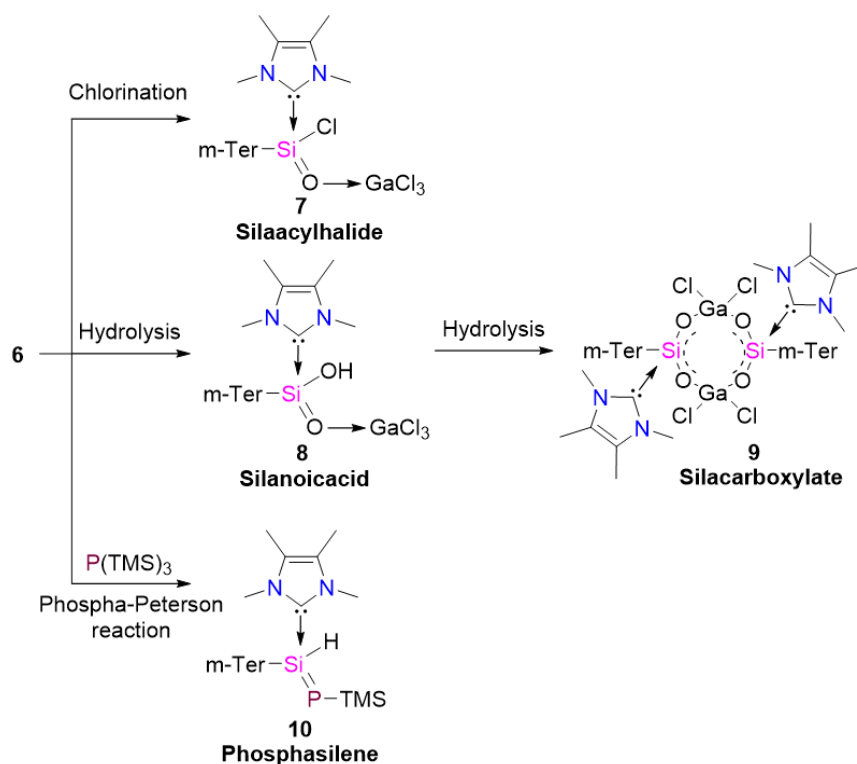


**Figure 48:** Diverse reactivity of silaaldehyde.

Analogous to the synthesis of  $[\{m\text{-Ter(H)Si(PTMS)}\}(\text{IME}_4)]$  **10**, the reactivity of **6** with heavier  $\text{E}'(\text{TMS})_3$  ( $\text{E}' = \text{As-Sb}$ ) reagents could provide access to the heavier analogs of **10** containing  $\text{Si}=\text{E}'$  bonds). Heavy  $\text{Si}=\text{E}$  bonds are rare and could be utilized as ligands to functionalize low valent group 14 complexes and activation of small molecules.



## Germyliumylidene and germaacylium ion

The germanium analog of the acylium ion, so-called germaacylium  $[R\text{-GeO}]^+$  ion are transient species.<sup>157</sup> We envisioned an NHC stabilized bulky aryl germyliumylidene  $[\{\text{Ar-Ge}(\text{NHC})_2\}^+\text{X}^-]$  might be a suitable precursor to isolate the corresponding germaacylium  $[\{\text{Ar-GeO}(\text{NHC})_2\}^+\text{X}^-]$ . Thus, we synthesized germyliumylidene  $[\{m\text{-TerGe}(\text{IME}_4)_2\}^+\text{Cl}^-]$  **11** by treatment of  $m\text{-TerGeCl}$  with two equivalents of  $\text{IME}_4$ . Germyliumylidene **11** possesses high nucleophilicity due to the coordination of two adjacent NHCs. Nucleophilic  $\text{Ge}(\text{II})$  complexes are prone to oxidative

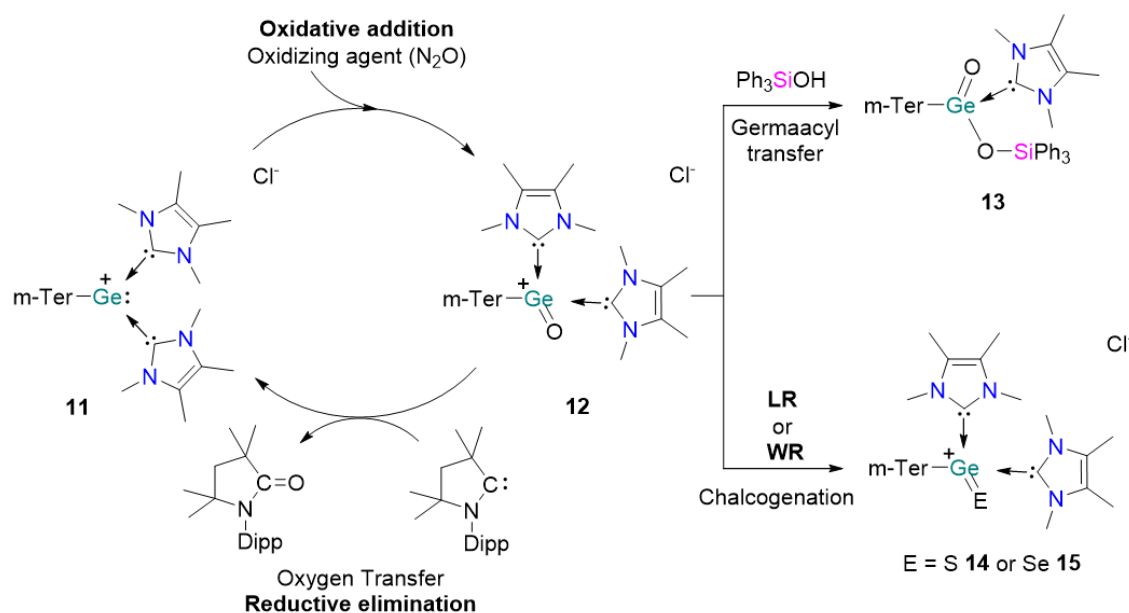


**Figure 49:** Isolation and reactivity of germaacylium ion.

addition. Indeed, the reactivity of germyliumylidene with  $\text{N}_2\text{O}$  led to the desired germaacylium ion, compound  $[\{m\text{-TerGeO}(\text{IME}_4)_2\}^+\text{Cl}^-]$  **12** (Figure 49). Intriguingly reaction of **12** with  $\text{Ph}_3\text{SiOH}$  gave rise to the solely donor stabilized germaester  $[\{m\text{-TerGeO}(\text{OSiPh}_3)\}(\text{IME}_4)]$  **13**. Treatment of **12** with Lawesson's reagent  $(\text{CH}_3\text{OPhPS}_2)_2$  and Wollin's reagents  $(\text{PhPSe}_2)_2$  provides the corresponding heavier silaacylium analogous  $[\{m\text{-TerGeE}(\text{IME}_4)_2\}^+\text{Cl}^-]$  (E = S **14** or Se **15**) (Figure 49). These reactivities indicated classical carbonyl type behavior of **12**. Further fascinating reactivity was observed as the regeneration of **11** was possible *via* the treatment of **12** with  $\text{Me}_c\text{AAC}$  (1-(2,6-diisopropylphenyl)-3,3,5,5-tetramethylpyrrolidine-2-ylidene). Facile oxide

## Summary and outlook

transfer from **12** to <sup>Me</sup>cAAC shows a similarity between **12** and transition metal oxides. Further, this transition metal oxide type behavior of **12** was explored towards CO<sub>2</sub> functionalization, where reversible complexation of CO<sub>2</sub> across Ge=O bond was observed. This encouraged us to utilize **12** as precatalyst in CO<sub>2</sub> hydrosilylation and in N-methylation of amines (Figure 50). A combined theoretical and experimental study revealed that an NHC-stabilized siloxy-germylene  $[\{m\text{-TerGe}(\text{OSiHPh}_2)\}(\text{IMe}_4)]$  **16** is the active species in this catalytic cycle. Moreover, our study demonstrated that transition metal-oxo mimetic reactivity of a heavier group 14 oxide, whilst also showing similar reactivity to that of the classical carbonyl.

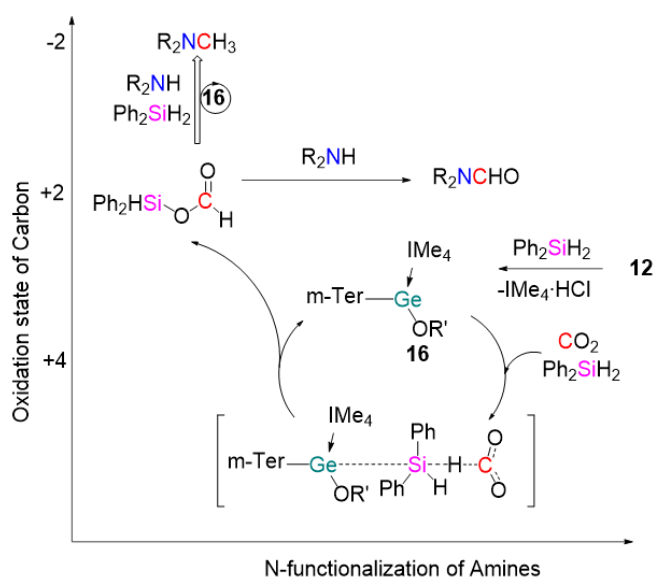


**Figure 50:** Schematic diagram of reductive functionalization of CO<sub>2</sub> with **16** (R' = Ph<sub>2</sub>SiH).

Further reactivity studies of **12** could also provide new insights by enabling access to new species. For example, similar to the synthesis of **13**, the reactivity of **12** with pyrrole (C<sub>4</sub>H<sub>4</sub>NH), Ph<sub>3</sub>SiSH or H<sub>2</sub>O may lead to elusive germaamide  $[\{m\text{-TerGe}(\text{O})(\text{NC}_4\text{H}_4)\}(\text{IMe}_4)]$ , germathioester  $[\{m\text{-TerGe}(\text{O})(\text{SSiPh}_3)\}(\text{IMe}_4)]$  or germanoic acid  $[\{m\text{-TerGe}(\text{O})(\text{OH})\}(\text{IMe}_4)]$  species, respectively. Additionally, the oxide transfer reactions of **12** could be employed in a catalytic regime. For example, catalytic synthesis of isocyanate (R-NC=O) from isonitrile (R-NC) could be possible in the presence of N<sub>2</sub>O and using **11** as a catalyst.

## Catalytic application of germyliumylidene

Low valent Ge(II) compounds have shown interesting catalytic activity in diverse catalytic applications (e.g., cyanosilylation or hydroboration of ketones and aldehydes).<sup>21-23, 27, 61, 62, 141, 142</sup> In those catalytic cycles, the electrophilicity of the germanium plays a prominent role. However, a nucleophilic Ge(II) center never has been utilized for such purposes. Inspired by the unique electronic feature of the germyliumylidene  $[\{m\text{-TerGe}(\text{IME}_4)_2\}^+\text{Cl}^-]$  **11**, we utilized **11** in diverse organic transformations, including the first example of a germyliumylidene catalyzed reductive functionalization of  $\text{CO}_2$  (hydrosilylation and N-methylation of amines using  $\text{CO}_2$  as C1 source). Intriguingly, other organic transformations such as catalytic cyanosilylation and hydroboration of ketones and aldehydes was also achieved under ambient conditions. Notably, with the catalytic efficiencies, **11** is the most active germanium catalyst presently available for such organic transformations.

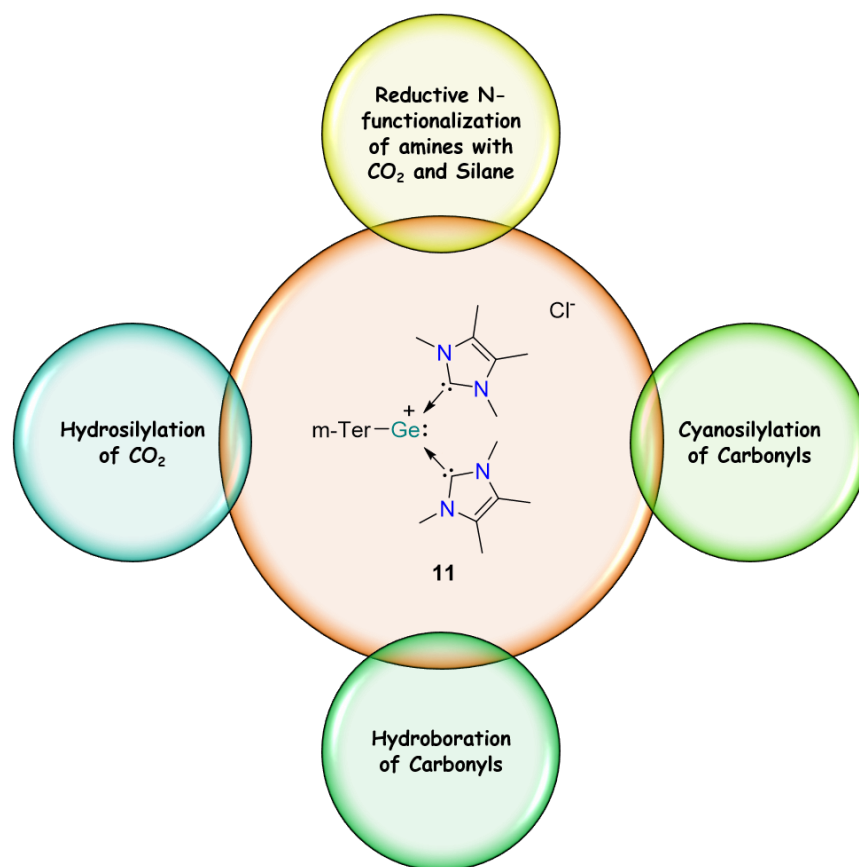


**Figure 51:** Catalytic application of germyliumylidene  $[\{m\text{-TerGe}(\text{IME}_4)_2\}^+\text{Cl}^-]$  **11**.

## Summary and outlook

Whilst the versatile catalytic ability of germyliumylidene **11** was shown further reductive functionalization of CO<sub>2</sub> could also be envisaged, with RS-CH<sub>3</sub> or R<sub>2</sub>P-CH<sub>3</sub> likely possible if carried out in the presence of silane and RSH or R<sub>2</sub>PH. Additionally, as reported with the lighter silyliumylidenes, the stereo chemically active lone pair of germanium in **11** could also be utilized for the coordination chemistry of transition metal complexes. The strong  $\sigma$ -donation ability of compound **11** could enhance the electron density to the transition metal center and enhance the reactivity at each metal center.

In conclusion, this thesis succeeded in the isolation, reactivity, and catalytic application of NHC-stabilized novel tetryliumylidene ions. The intriguing reactivity of silyliumylidene [ $\{m\text{-TerSi}(\text{IMe}_4)_2\}^+\text{Cl}^-$ ] **1** towards small molecules (chalcogen, CS<sub>2</sub>, and H<sub>2</sub>O) led to the various unprecedented main group compounds such as heavier silaacylium cations **2-4** or donor-acceptor stable silaaldehyde complex **6**. Interestingly, the latter has served a precursor for several stable silacarbonyl complexes (**7-9**), and phosphasilene **10**, demonstrated the similarities with its lighter congeners. Further, the facile access of the NHC-stabilized aryl germyliumylidene [ $\{m\text{-TerGe}(\text{IMe}_4)_2\}^+\text{Cl}^-$ ] **11** has been achieved. Exploiting the Lewis basicity of [ $\{m\text{-TerGe}(\text{IMe}_4)_2\}^+\text{Cl}^-$ ], we have utilized **11** as a catalyst in various numerous organic transformations, including the catalytic functionalization of CO<sub>2</sub>.

Interestingly the fascinating reactivity of **11** with N<sub>2</sub>O gave rise to a solely donor stabilized germaacylium ion **12**. Both classical carbonyl as well as transition metal oxide behavior of the germaacylium has been demonstrated. Most impressively, the reversible activation of CO<sub>2</sub> by **12** and its application in reductive functionalization of the CO<sub>2</sub> put new impetus in the field to the catalytic utilization of group 14 molecular oxides. Moreover, tetryliumylidenes have shown themselves to be a promising alternative to transition metals due to their unique electronic feature and versatile application towards the activation of small molecules and catalysis. Nevertheless, lots more to discover, this thesis has provided an excellent base to explore this chemistry further.

## 11. Bibliographic details for complete references

The published results are ordered according to the topics heavier silacylium, silaldehyde, germaacylium ion and further chronological based on online publication in the corresponding journal. The supporting information of (**chapter 6-8**), are not included in this thesis. Data are available free of charge on the websites of the journals. Only supporting information of (**chapter 9**) is included.

Supporting Information  
©Wiley-VCH 2019  
69451 Weinheim, Germany

## Germlyiumylidene: A versatile low valent group 14 catalyst

Debotra Sarkar,<sup>[a]</sup> Catherine Weetman,<sup>[a,b]</sup> Sayan Datta,<sup>[c]</sup> Emeric Schubert,<sup>[a]</sup> Debasis Koley,<sup>[c]</sup>  
Shigeyoshi Inoue\*<sup>[a]</sup>

**Abstract:** Germlyiumylidene [R-Ge:]<sup>+</sup> can act as both Lewis acid (LA) and Lewis Base (LB), owing to its lone pair, positive charge and two vacant orbitals on the germanium atom. Utilizing this unique electronic feature, we report the first example of NHC-stabilized germlyiumylidene [M<sup>ter</sup>TerGe(NHC)<sub>2</sub>]Cl (1), (M<sup>ter</sup>Ter= 2,6-(2,4,6-Me<sub>3</sub>C<sub>6</sub>H<sub>2</sub>)<sub>2</sub>C<sub>6</sub>H<sub>3</sub>; NHC= IMe<sub>4</sub> = 1,3,4,5-tetramethylimidazol-2-ylidene) catalyzed reduction of CO<sub>2</sub> with amines and silane, under mild conditions. Furthermore, the versatility of 1 is explored in the catalyzed hydroboration and cyanosilylation of carbonyls.

DOI: 10.1002/anie.2016XXXXX

## SUPPORTING INFORMATION

## Table of Contents

<b>1. Experimental details</b> .....	<b>2</b>
<b>1.1. General information</b> .....	<b>2</b>
1.1.1 General procedure for catalytic hydrosilylation of CO <sub>2</sub> .....	2
1.1.2. General procedure for catalytic N-functionalization amines with CO <sub>2</sub> .....	4
1.1.3. General procedure for catalytic cyanosilylation of carbonyls.....	9
1.1.4. General procedure for catalytic hydroboration of carbonyls .....	20
<b>2. References</b> .....	<b>27</b>

## 1. Experimental details

## 1.1. General information

All experiments and manipulations were carried out under dry oxygen-free argon atmosphere using standard Schlenk techniques or in a glovebox. The <sup>1</sup>H, <sup>13</sup>C{<sup>1</sup>H} NMR spectra of the compounds were measured on Bruker 400 MHz and 500 MHz spectrometer. Chemical shifts are referenced to (residual) solvent signals (<sup>1</sup>H and <sup>13</sup>C{<sup>1</sup>H} NMR). Deuterated solvent CD<sub>3</sub>CN was obtained from Deutero Deutschland GmbH and dried over 4 Å molecular sieves. Carbon dioxide (5.0) was purchased from Westfalen AG and used as received. Unless otherwise stated, all reagents were purchased from commercial sources and used as received. Gernylumylidene [(<sup>m</sup>TerGe(IMEt)<sub>2</sub>Cl] **1** was synthesized according to the literature procedure.<sup>11</sup>

1.1.1 General procedure for catalytic hydrosilylation of CO<sub>2</sub>

Compound **1** (5.0 mol %) in 0.5 mL CD<sub>3</sub>CN, silane (10 mg, .03 mmol) were added to a J-Young NMR tube. The solution was freeze-pump thaw and degassed two times before being refilled with 1 bar of CO<sub>2</sub>. The <sup>1</sup>H NMR spectrum was recorded. Then the tube was placed in a preheated oil bath (60 °C). Notably, for Ph<sub>3</sub>SiH hydrosilylation of CO<sub>2</sub> was performed at 80 °C temperature, so the heating bath was adjusted accordingly. The reactions were monitored by <sup>1</sup>H NMR spectroscopy at regular intervals until the silane was consumed.

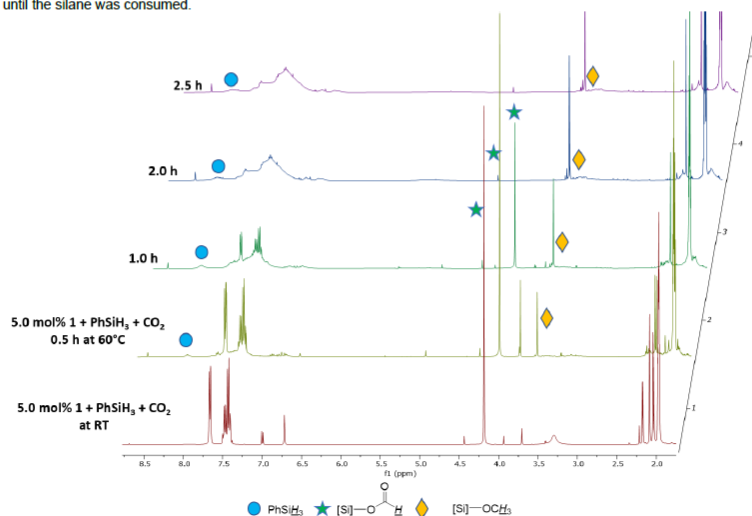


**Figure S1.** Stacked <sup>1</sup>H NMR spectra, compound **1** (5.0 mol%) in CD<sub>3</sub>CN, with PhSiH<sub>3</sub> (10.0 mg) and CO<sub>2</sub> (1 bar).

## SUPPORTING INFORMATION

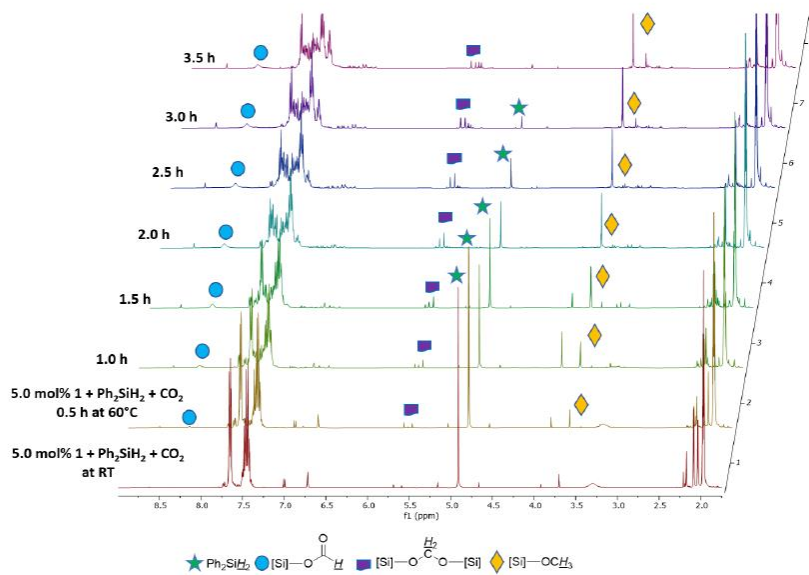


Figure S2. Stacked <sup>1</sup>H NMR spectra, compound 1 (5.0 mol%) in CD<sub>3</sub>CN, with Ph<sub>2</sub>SiH<sub>2</sub> (10.0 mg) and CO<sub>2</sub> (1 bar).

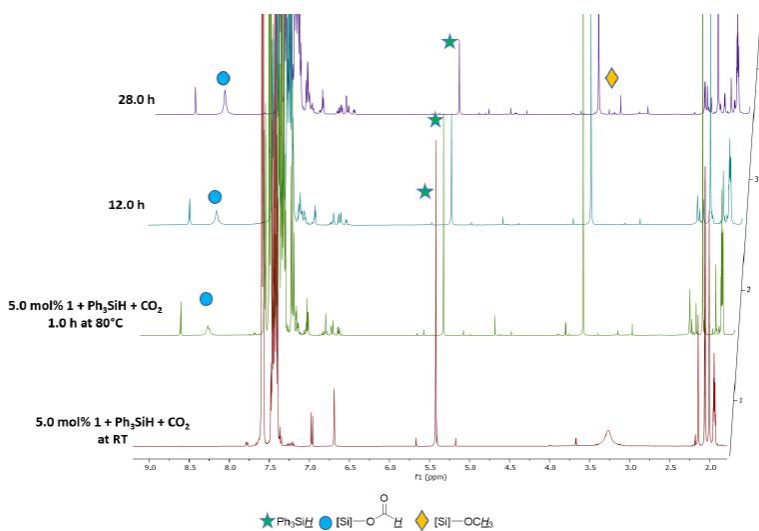


Figure S3. Stacked <sup>1</sup>H NMR spectra, compound 1 (5.0 mol%) in CD<sub>3</sub>CN, with Ph<sub>3</sub>SiH (10.0 mg) and CO<sub>2</sub> (1 bar), full conversion reaction time was not measured.



## SUPPORTING INFORMATION

1.1.2. General procedure for catalytic N-functionalization amines with CO<sub>2</sub>

We have performed the N-functionalization of amine with CO<sub>2</sub> at 60 °C. Therefore, all samples were prepared the following way. Compound 1 (5 mol %) in 0.5 mL CD<sub>3</sub>CN, amine (10 mg, 1 eq), silane (3 eq) were added to the J-Young NMR tube. The solution was freeze-pump-thaw degassed two times before being refilled with 1 bar of CO<sub>2</sub>. The reactions were monitored by <sup>1</sup>H NMR spectroscopy. For the elevated temperature measurement, the tube was placed in a preheated oil bath (60 °C) and monitored regularly.

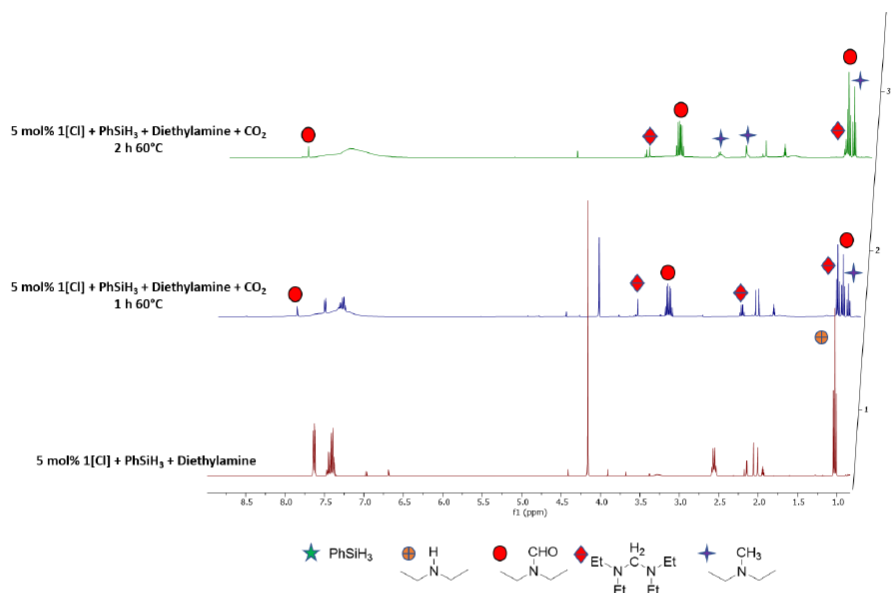


Figure S4. Stacked <sup>1</sup>H NMR spectra of reductive functionalization of CO<sub>2</sub> with diethylamine and PhSiH<sub>3</sub> at 60 °C in CD<sub>3</sub>CN.

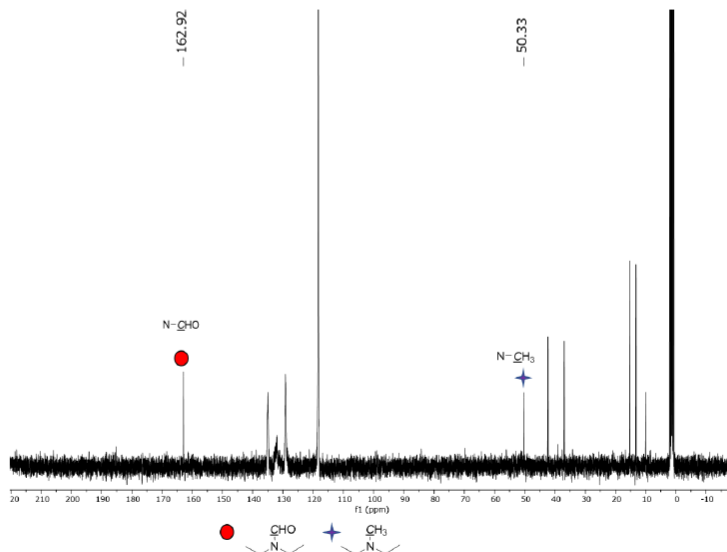


Figure S5. <sup>13</sup>C NMR spectra of reductive functionalization of CO<sub>2</sub> with diethylamine and PhSiH<sub>3</sub> at 60 °C in CD<sub>3</sub>CN.

## SUPPORTING INFORMATION

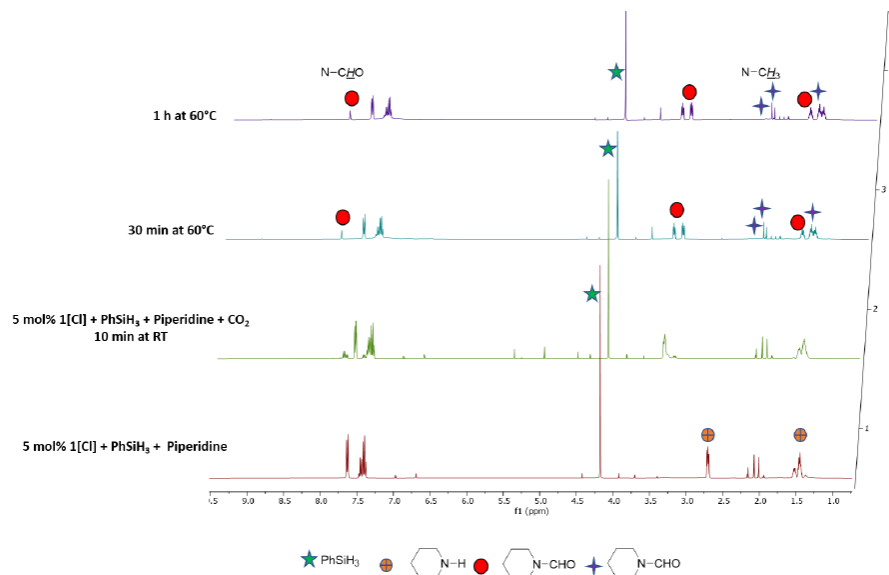


Figure S6. Stacked  $^1\text{H}$  NMR spectra of reductive functionalization of  $\text{CO}_2$  with piperidine and  $\text{PhSiH}_3$  at  $60^\circ\text{C}$  in  $\text{CD}_3\text{CN}$ .

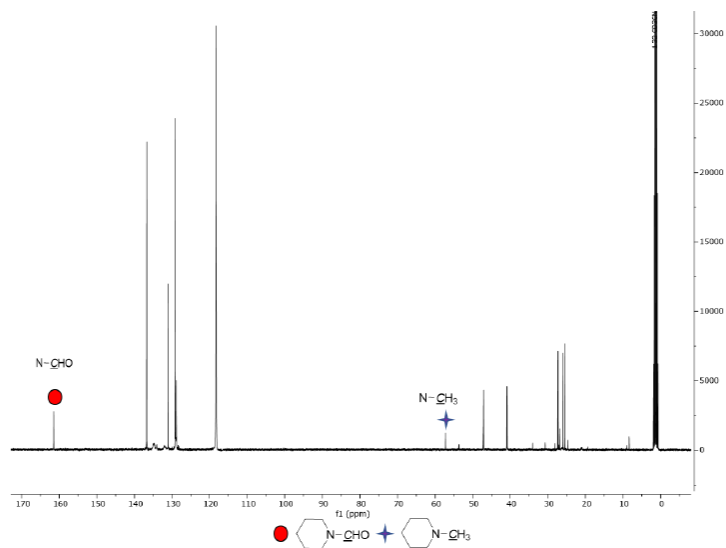


Figure S7.  $^{13}\text{C}$  NMR spectra of reductive functionalization of  $\text{CO}_2$  with piperidine and  $\text{PhSiH}_3$  at  $60^\circ\text{C}$  in  $\text{CD}_3\text{CN}$ .

## SUPPORTING INFORMATION

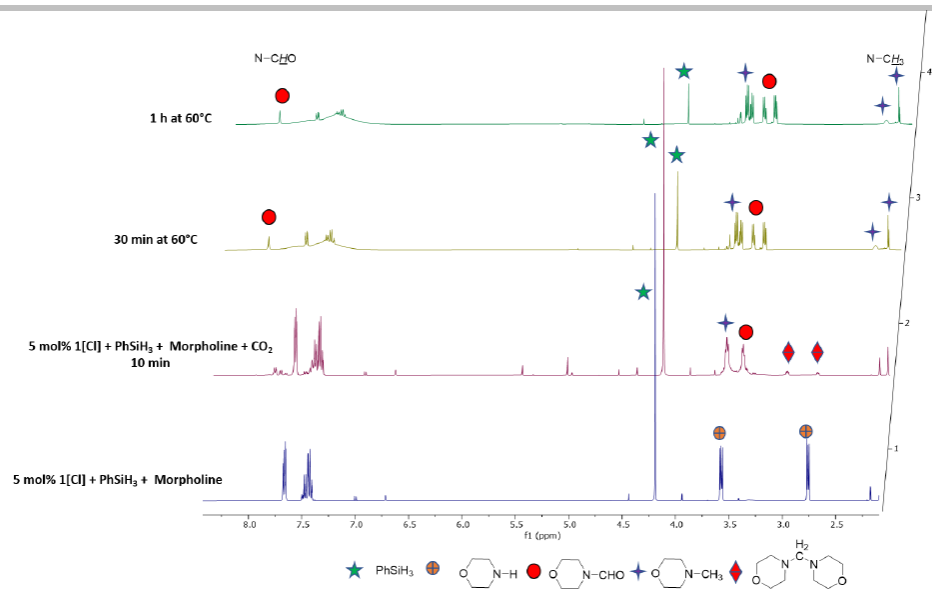


Figure S8. Stacked  $^1\text{H}$  NMR spectra of reductive functionalization of  $\text{CO}_2$  with morpholine and  $\text{PhSiH}_3$  at  $60^\circ\text{C}$  in  $\text{CD}_3\text{CN}$ .

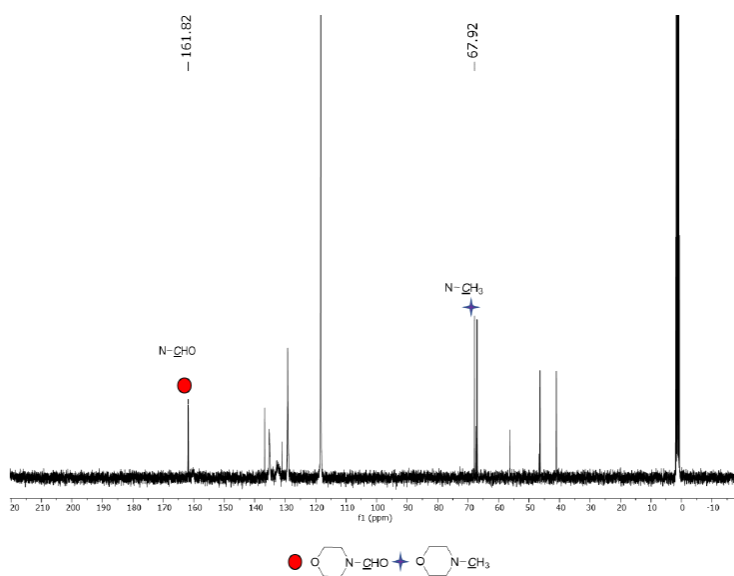


Figure S9.  $^{13}\text{C}$  NMR spectra of reductive functionalization of  $\text{CO}_2$  with morpholine and  $\text{PhSiH}_3$  at  $60^\circ\text{C}$  in  $\text{CD}_3\text{CN}$ .

## SUPPORTING INFORMATION

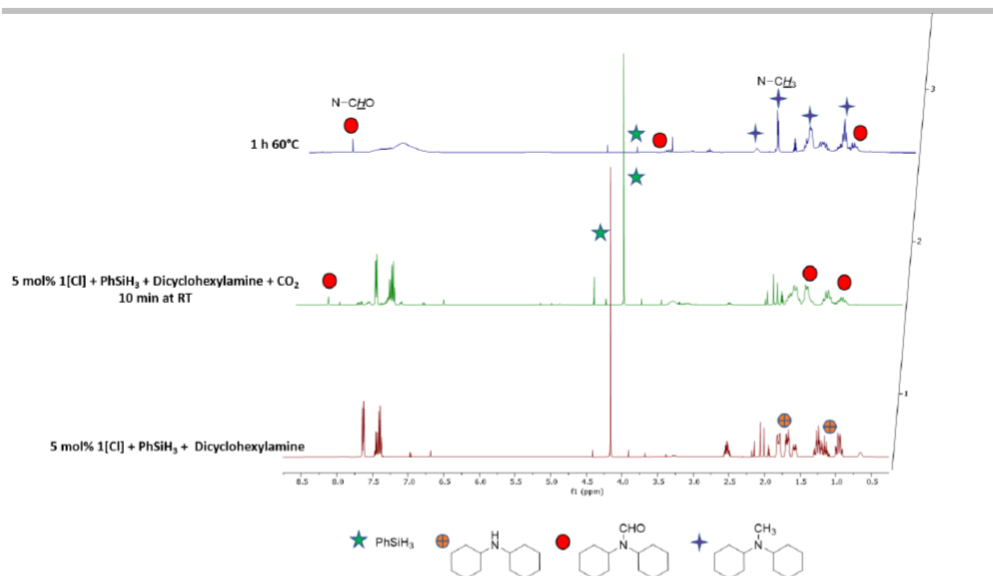


Figure S10. Stacked  $^1\text{H}$  NMR spectra of reductive functionalization of  $\text{CO}_2$  with dicyclohexylamine and  $\text{PhSiH}_3$  at  $60^\circ\text{C}$  in  $\text{CD}_3\text{CN}$ .

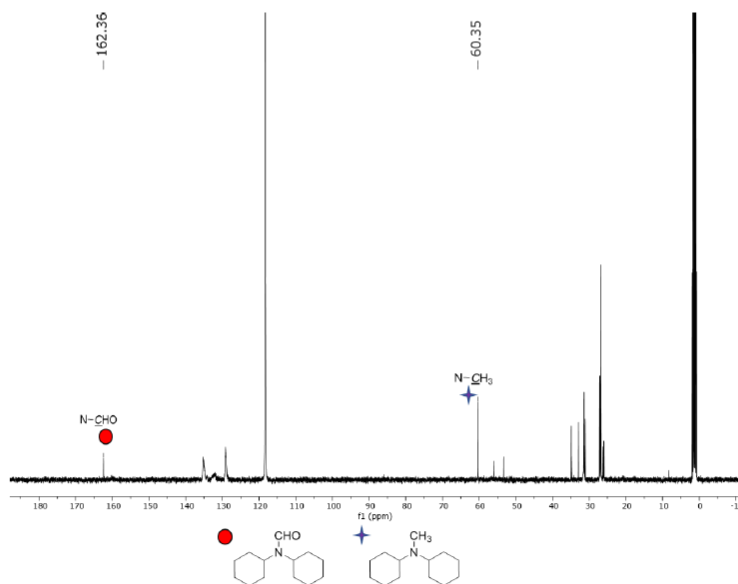


Figure S11. Stacked  $^1\text{H}$  NMR spectra of reductive functionalization of  $\text{CO}_2$  with dicyclohexylamine and  $\text{PhSiH}_3$  at  $60^\circ\text{C}$  in  $\text{CD}_3\text{CN}$ .

## SUPPORTING INFORMATION

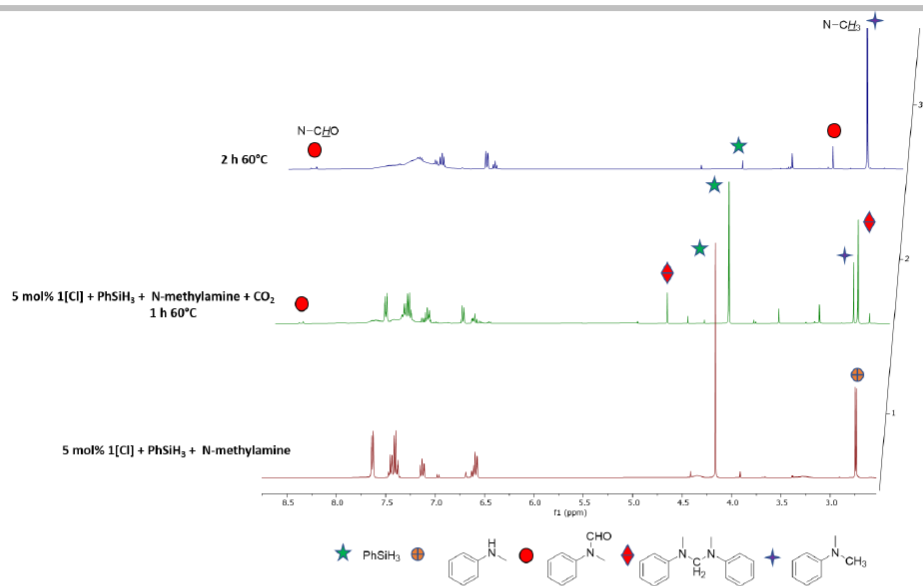


Figure S12. Stacked <sup>1</sup>H NMR spectra of reductive functionalization of CO<sub>2</sub> with N-methylamine and PhSiH<sub>3</sub> at 60 °C in CD<sub>3</sub>CN.

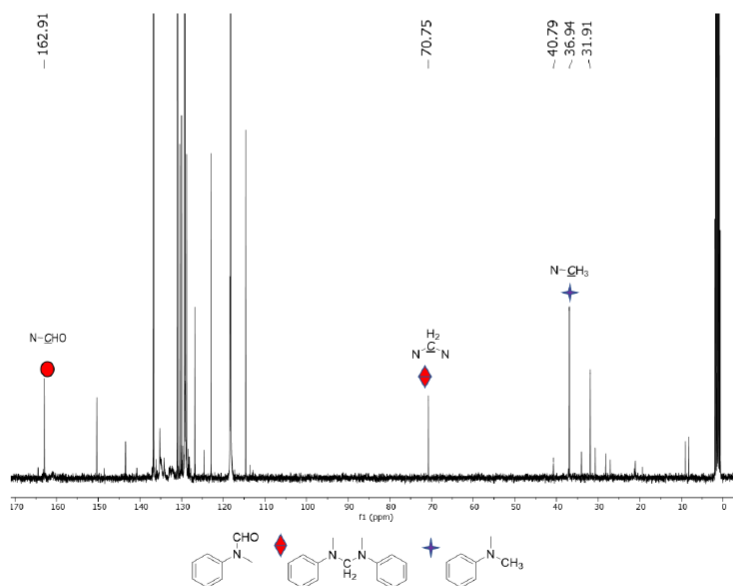


Figure S13. Stacked <sup>13</sup>C NMR spectra of reductive functionalization of CO<sub>2</sub> with N-methylamine and PhSiH<sub>3</sub> at 60 °C in CD<sub>3</sub>CN.

## SUPPORTING INFORMATION

## 1.1.3. General procedure for catalytic cyanosilylation of carbonyls

0.01 mol% of **1** in 0.5 ml of CD<sub>3</sub>CN, aldehyde (10 mg, 1 eq) and 1.01 equivalent of TMSCN were added to an NMR tube. The tube was sealed by wrapping parafilm around the cap. The reactions were monitored regularly using <sup>1</sup>H NMR spectroscopy. Notably for ketones 1.0 mol% of **1** and elevated temperatures (50 °C) were required.

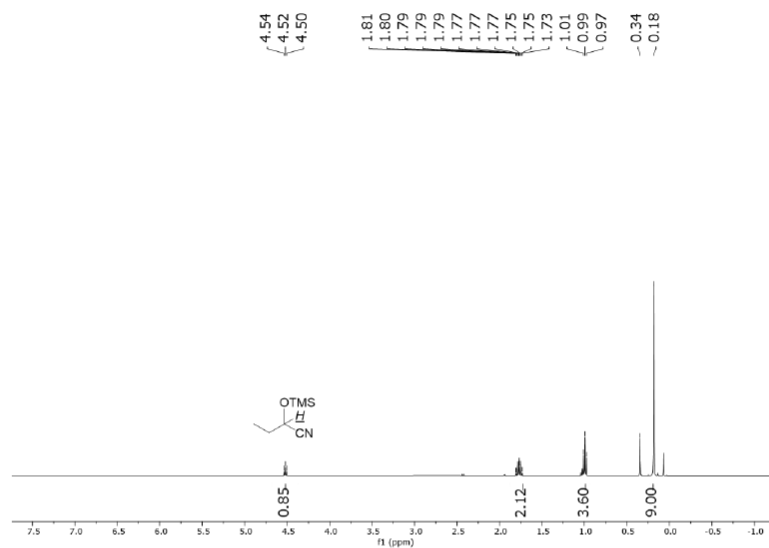


Figure S14. <sup>1</sup>H NMR spectra of CH<sub>3</sub>CH<sub>2</sub>CH(OTMS)CN in CD<sub>3</sub>CN.

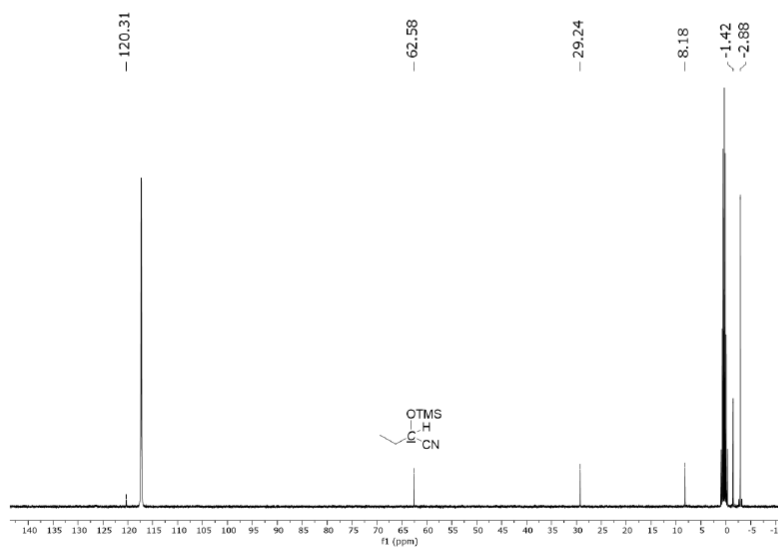


Figure S15. <sup>13</sup>C NMR spectra of CH<sub>3</sub>CH<sub>2</sub>CH(OTMS)CN in CD<sub>3</sub>CN.

## SUPPORTING INFORMATION

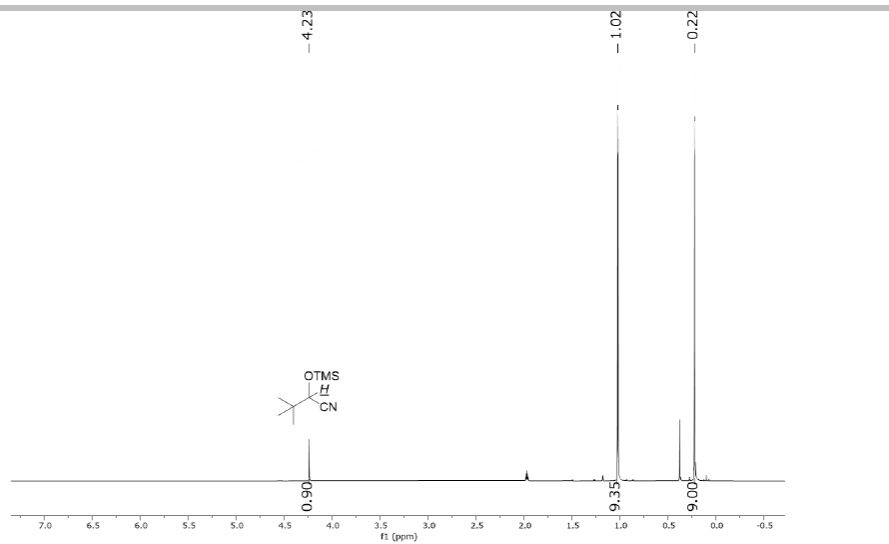


Figure S16.  $^1\text{H}$  NMR spectra of  $(\text{CH}_3)_3\text{CH}(\text{OTMS})\text{CN}$  in  $\text{CD}_3\text{CN}$ .

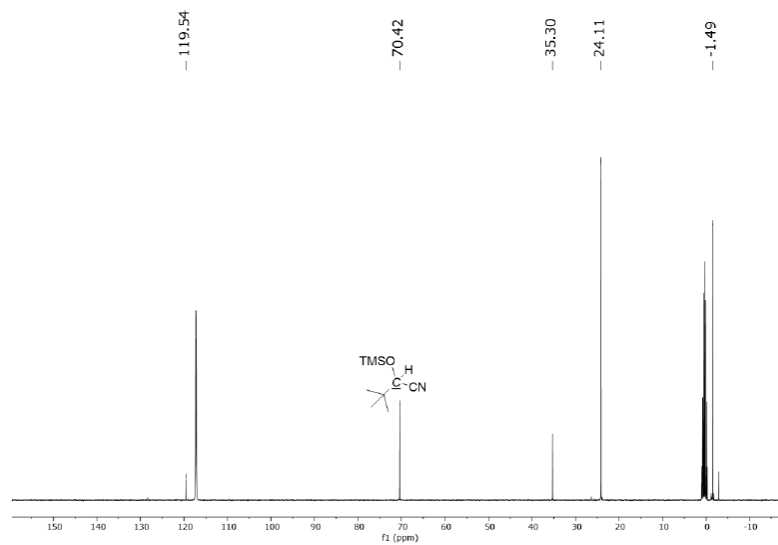


Figure S17.  $^{13}\text{C}$  NMR spectra of  $(\text{CH}_3)_3\text{CH}(\text{OTMS})\text{CN}$  in  $\text{CD}_3\text{CN}$ .

## SUPPORTING INFORMATION

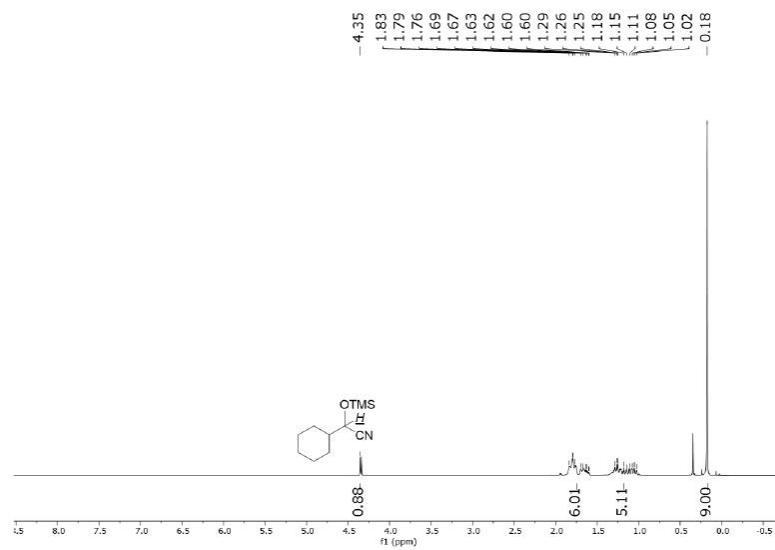


Figure S18.  $^1H$  NMR spectra of  $C_6H_{11}CH(OTMS)CN$  in  $CD_3CN$ .

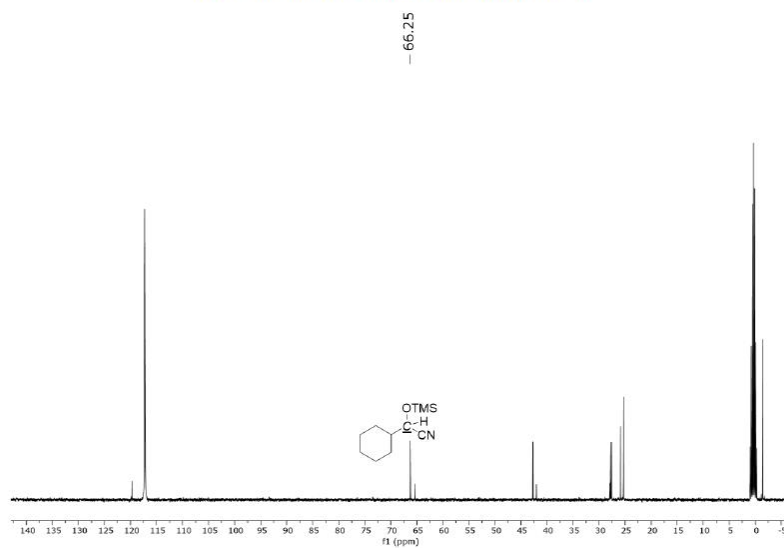
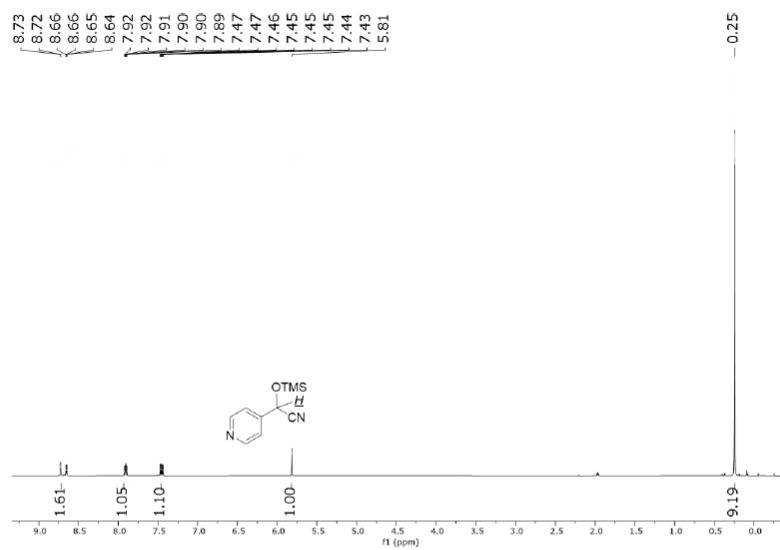
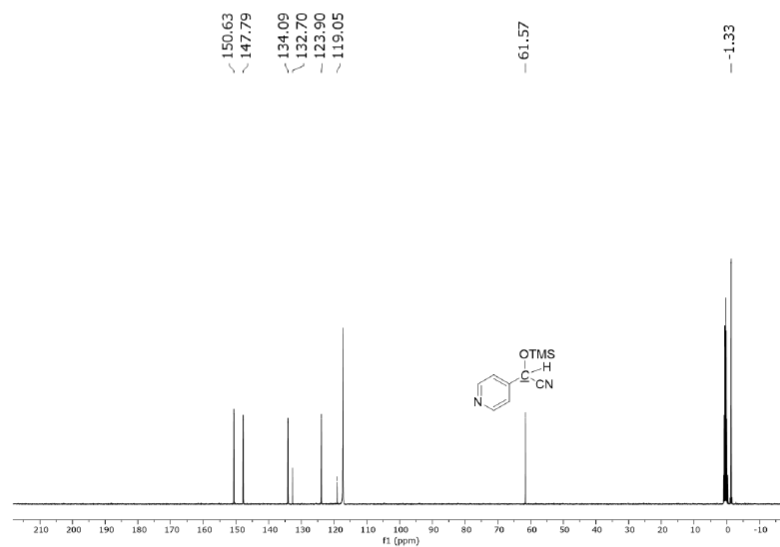


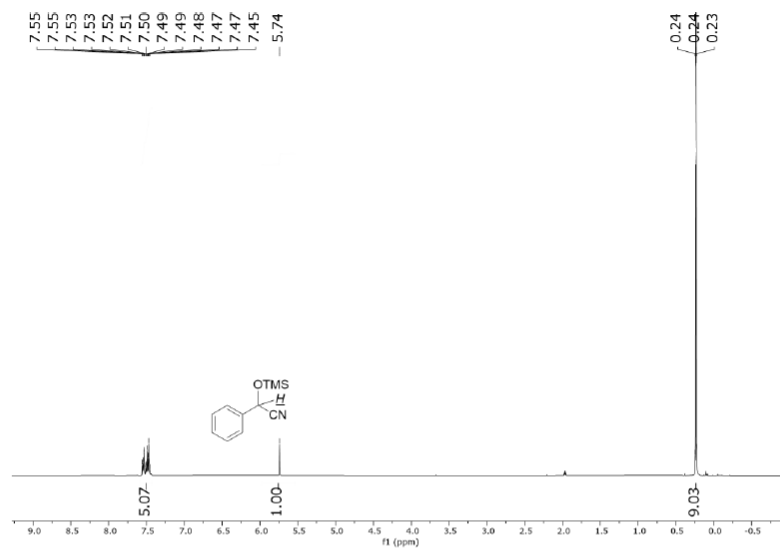
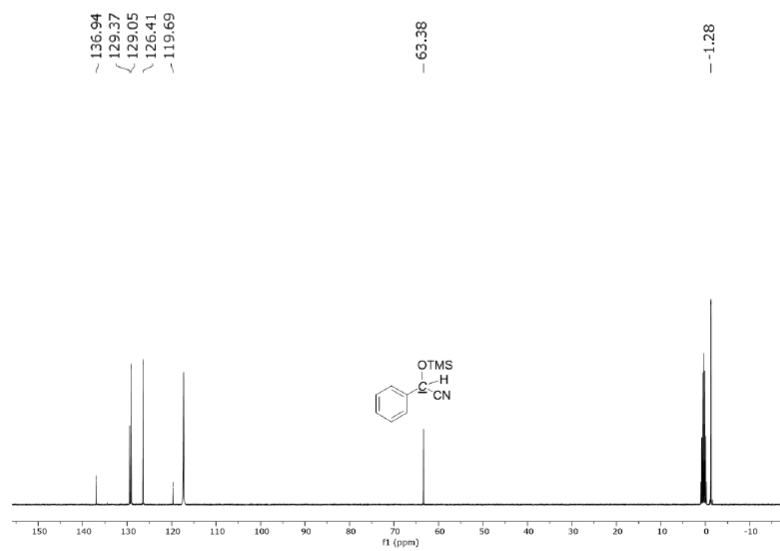
Figure S19.  $^{13}C$  NMR spectra of  $C_6H_{11}CH(OTMS)CN$  in  $CD_3CN$ .



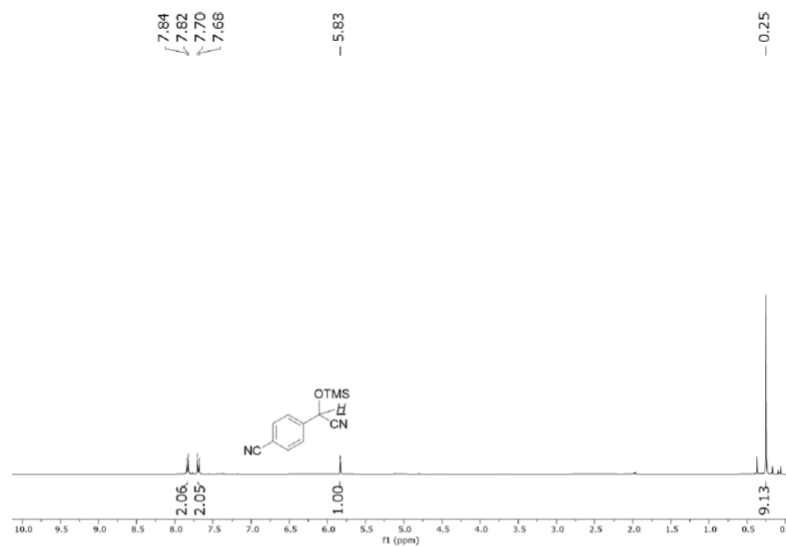
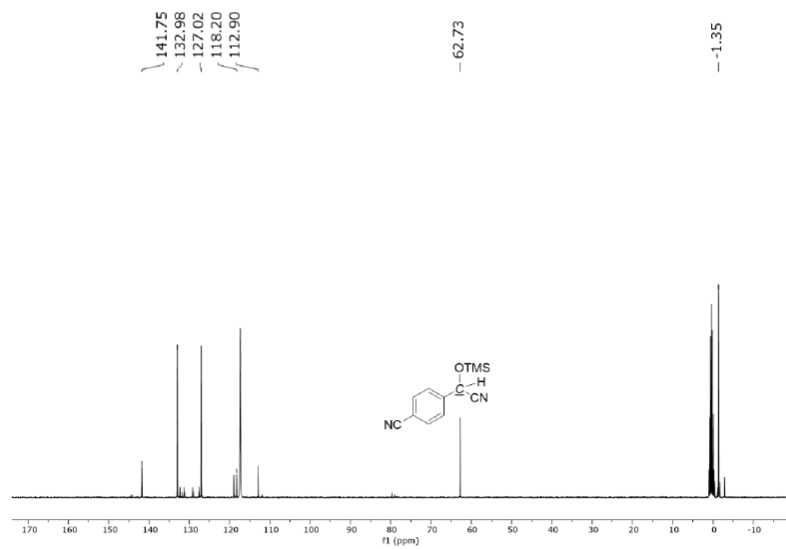
## SUPPORTING INFORMATION

Figure S20.  $^1\text{H}$  NMR spectra of  $(\text{NC}_5\text{H}_4)\text{CH}(\text{OTMS})\text{CN}$  in  $\text{CD}_3\text{CN}$ .Figure S21.  $^{13}\text{C}$  NMR spectra of  $(\text{NC}_5\text{H}_4)\text{CH}(\text{OTMS})\text{CN}$  in  $\text{CD}_3\text{CN}$ .

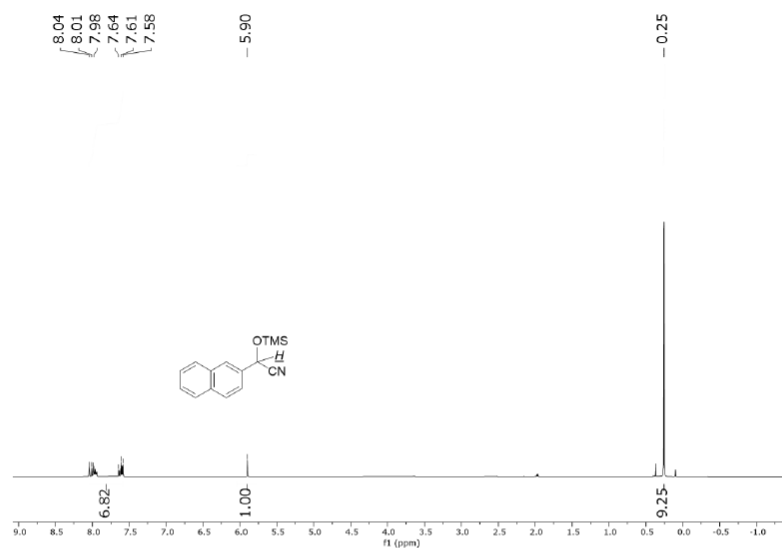
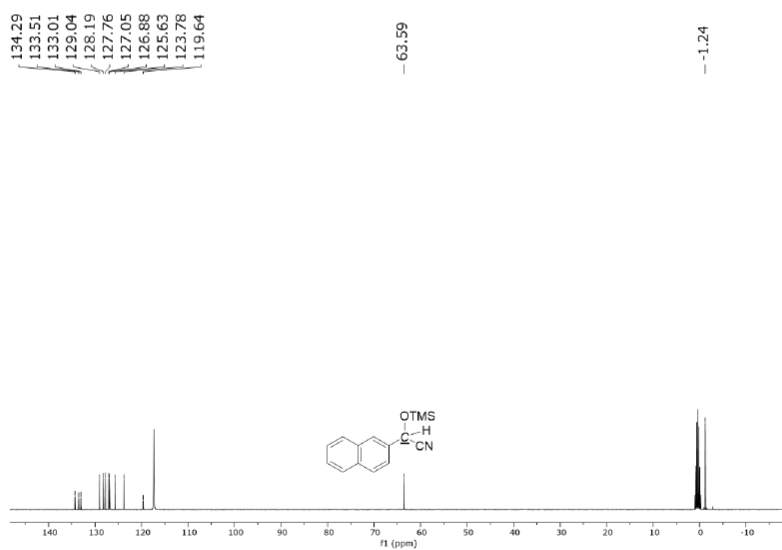
## SUPPORTING INFORMATION

Figure S22.  $^1\text{H}$  NMR spectra of PhCH(OTMS)CN in  $\text{CD}_3\text{CN}$ .Figure S23.  $^{13}\text{C}$  NMR spectra of PhCH(OTMS)CN in  $\text{CD}_3\text{CN}$ .

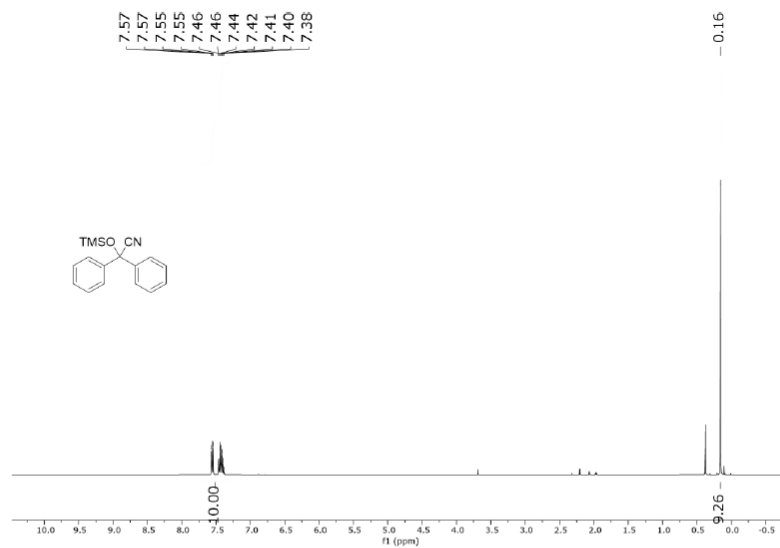
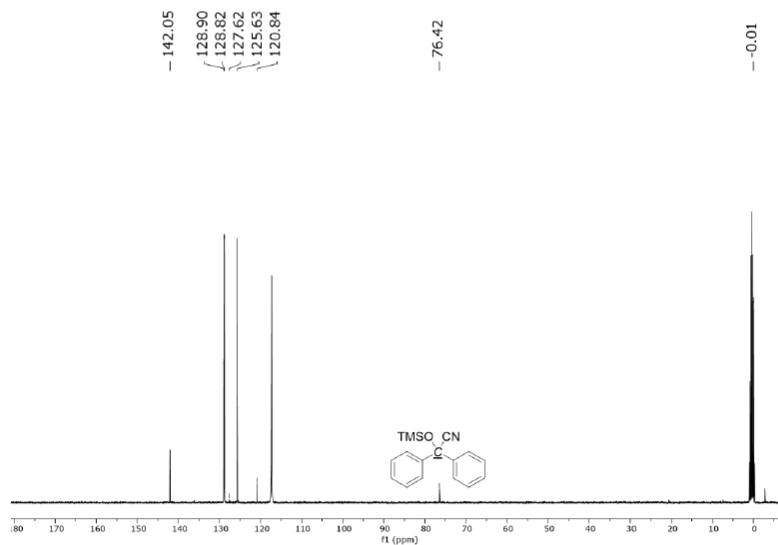
## SUPPORTING INFORMATION

Figure S24.  $^1\text{H}$  NMR spectra of  $(\text{CN})\text{PhCH}(\text{OTMS})\text{CN}$  in  $\text{CD}_3\text{CN}$ .Figure S25.  $^{13}\text{C}$  NMR spectra of  $(\text{CN})\text{PhCH}(\text{OTMS})\text{CN}$  in  $\text{CD}_3\text{CN}$ .

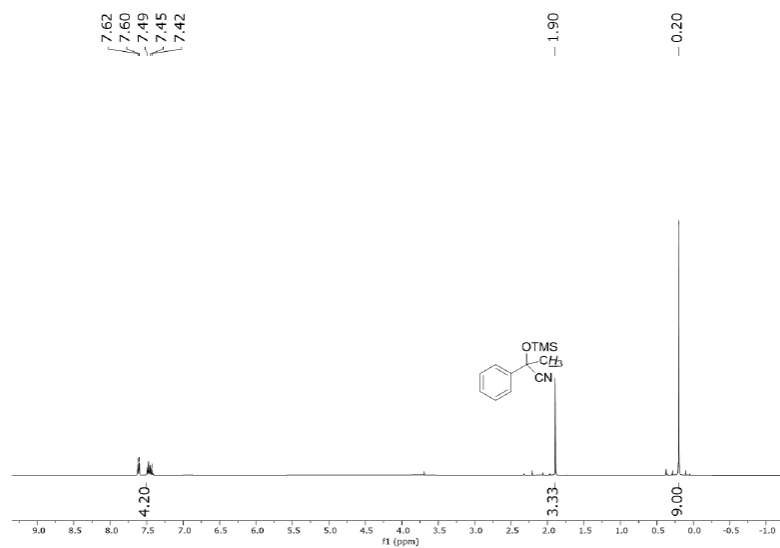
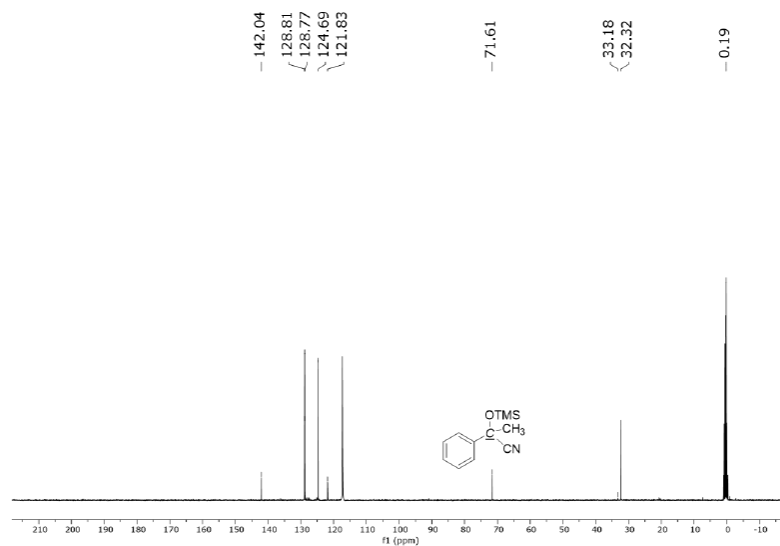
## SUPPORTING INFORMATION

Figure S26.  $^1\text{H}$  NMR spectra of  $(\text{C}_{10}\text{H}_7)\text{CH}(\text{OTMS})\text{CN}$  in  $\text{CD}_3\text{CN}$ .Figure S27.  $^{13}\text{C}$  NMR spectra of  $(\text{C}_{10}\text{H}_7)\text{CH}(\text{OTMS})\text{CN}$  in  $\text{CD}_3\text{CN}$ .

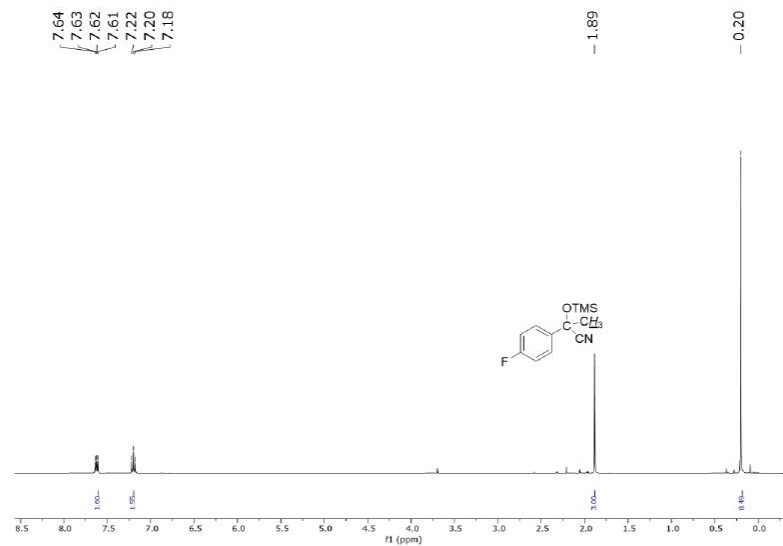
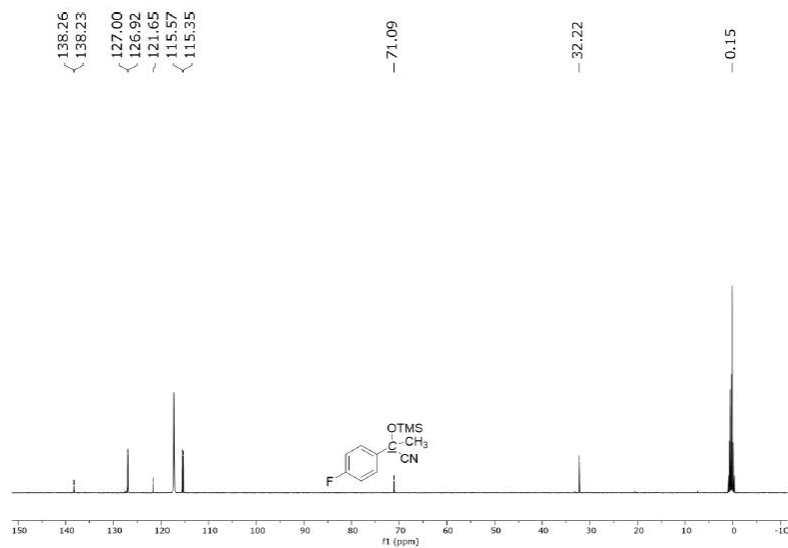
## SUPPORTING INFORMATION

Figure S28.  $^1\text{H}$  NMR spectra of  $\text{Ph}_2\text{C}(\text{OTMS})\text{CN}$  in  $\text{CD}_3\text{CN}$ .Figure S29.  $^{13}\text{C}$  NMR spectra of  $\text{Ph}_2\text{C}(\text{OTMS})\text{CN}$  in  $\text{CD}_3\text{CN}$ .

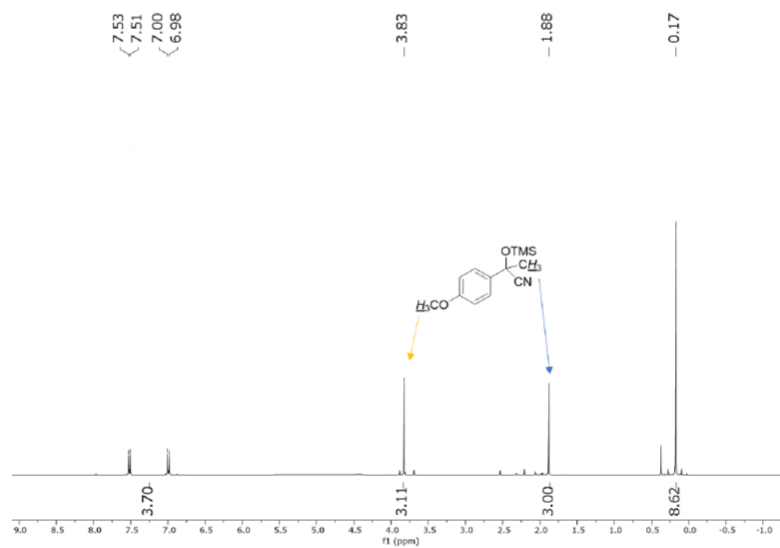
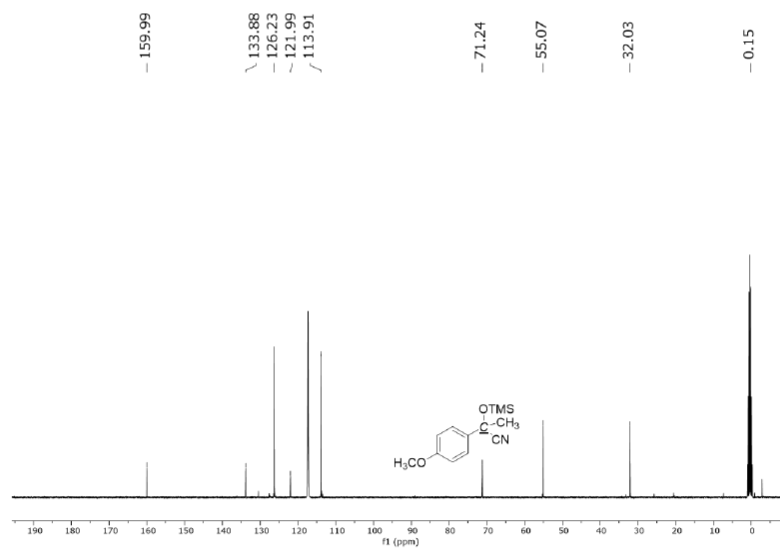
## SUPPORTING INFORMATION

Figure S30.  $^1\text{H}$  NMR spectra of  $\text{Ph}(\text{CH}_3)\text{C}(\text{OTMS})\text{CN}$  in  $\text{CD}_3\text{CN}$ .Figure S31.  $^{13}\text{C}$  NMR spectra of  $\text{Ph}(\text{CH}_3)\text{C}(\text{OTMS})\text{CN}$  in  $\text{CD}_3\text{CN}$ .

## SUPPORTING INFORMATION

Figure S32.  $^1\text{H}$  NMR spectra of (F)PhCH(OTMS)CN in  $\text{CD}_3\text{CN}$ .Figure S33.  $^{13}\text{C}$  NMR spectra of (F)PhCH(OTMS)CN in  $\text{CD}_3\text{CN}$ .

## SUPPORTING INFORMATION

Figure S34.  $^1\text{H}$  NMR spectra of  $\text{MeOPh}(\text{CH}_3)\text{C}(\text{OTMS})\text{CN}$  in  $\text{CD}_3\text{CN}$ .Figure S35.  $^{13}\text{C}$  NMR spectra of  $\text{MeOPh}(\text{CH}_3)\text{C}(\text{OTMS})\text{CN}$  in  $\text{CD}_3\text{CN}$ .



## SUPPORTING INFORMATION

## 1.1.4. General procedure for catalytic hydroboration of carbonyls

0.01 mol% **1** in 0.5 ml of CD<sub>3</sub>CN, aldehyde (10 mg, 1 eq) and 1.1 equivalent of HBpin were added to an NMR tube. The tube was sealed by wrapping parafilm around the cap. The reactions were monitored regularly using <sup>1</sup>H NMR spectroscopy.

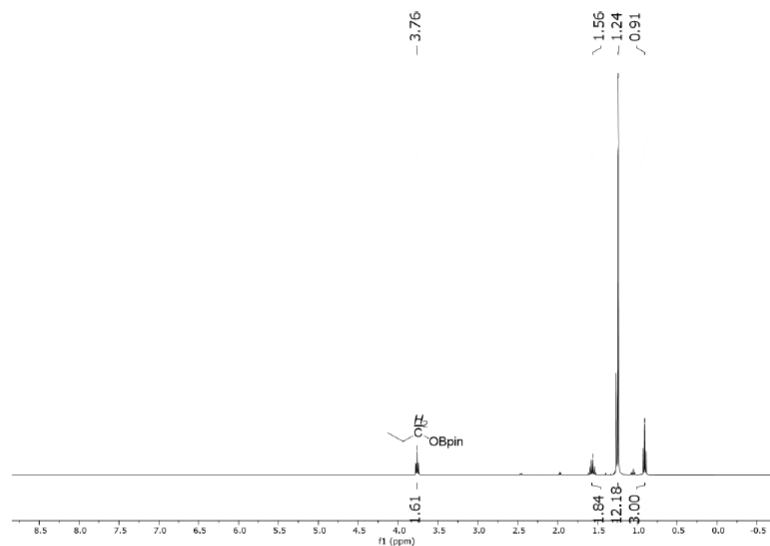


Figure S36. <sup>1</sup>H NMR spectra of Et(CH<sub>2</sub>)OBpin in CD<sub>3</sub>CN.

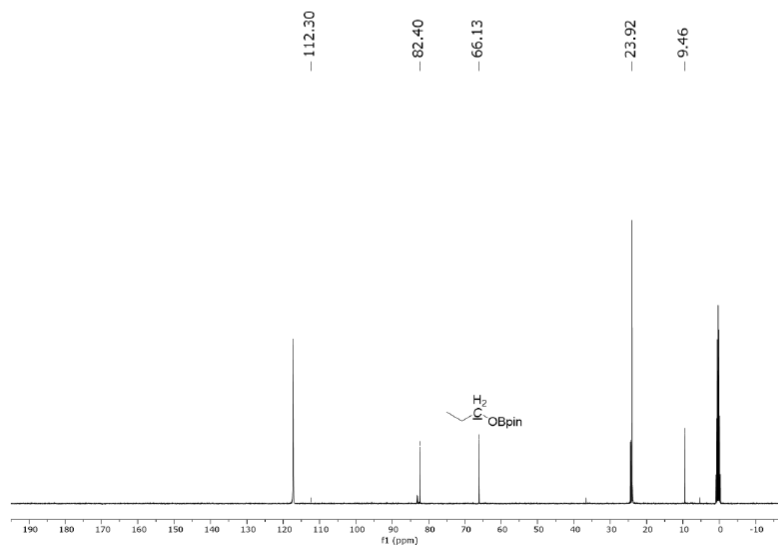
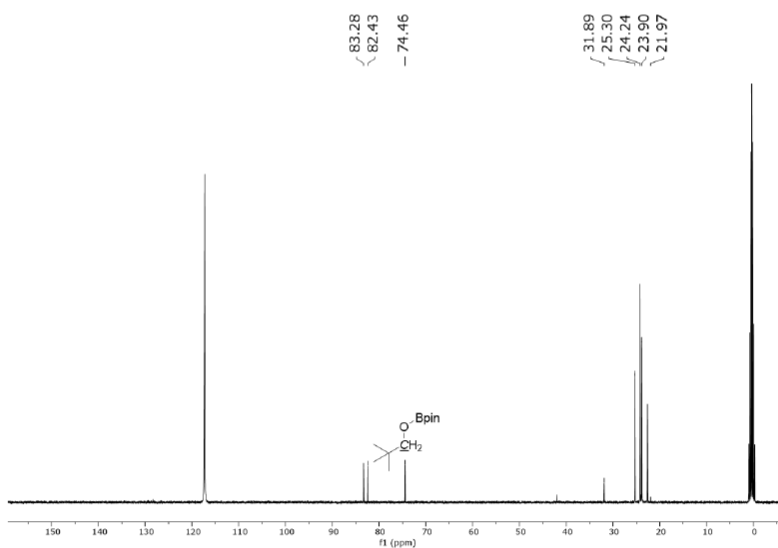
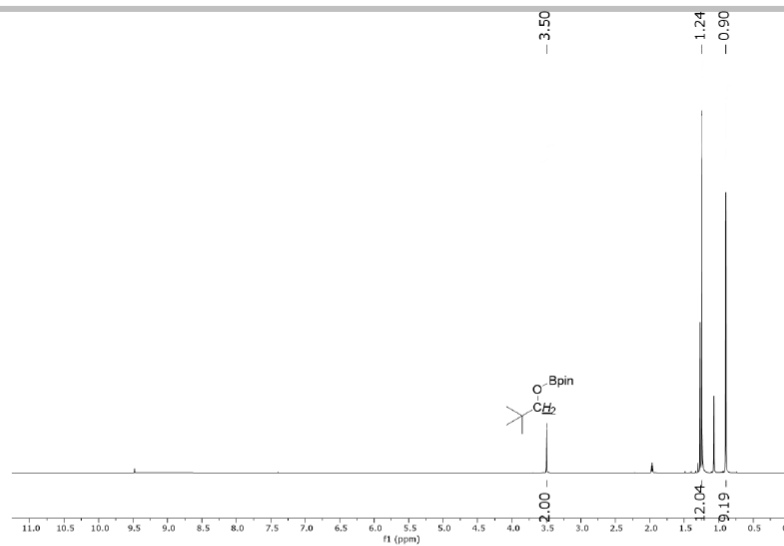
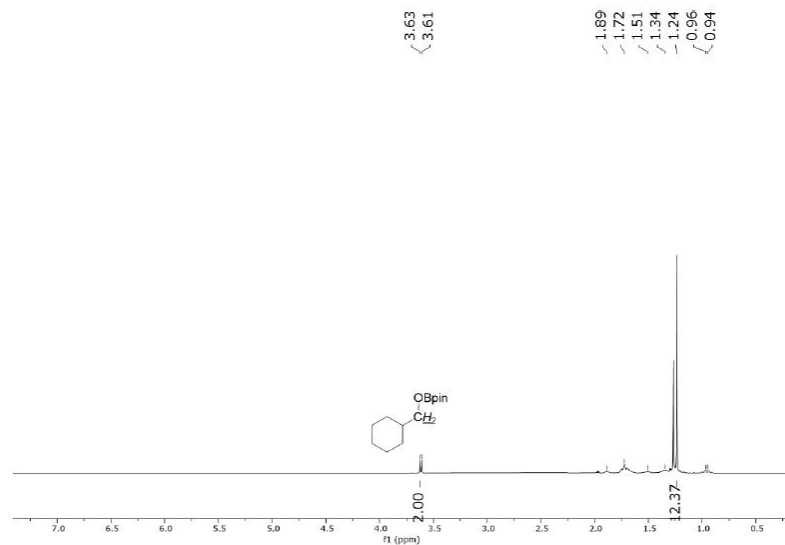
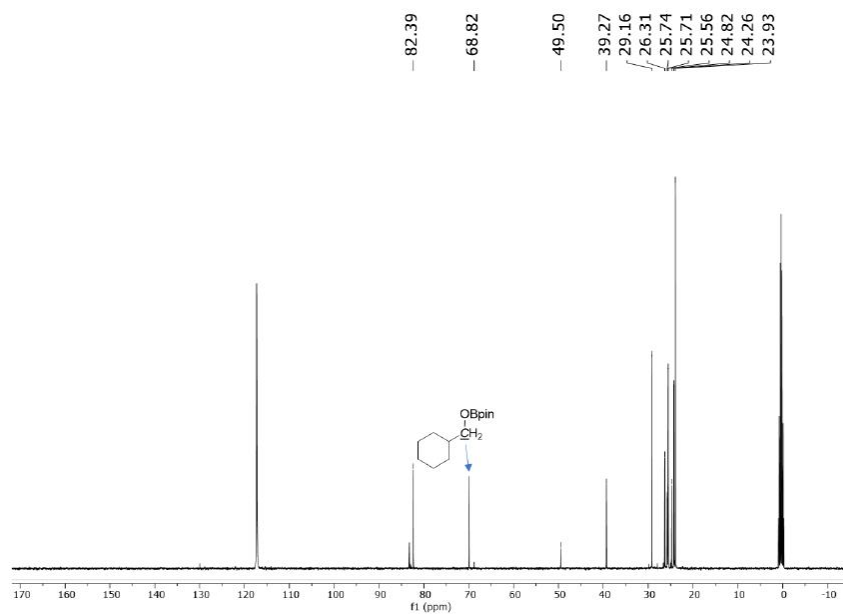


Figure S37. <sup>13</sup>C NMR spectra of Et(CH<sub>2</sub>)OBpin in CD<sub>3</sub>CN.

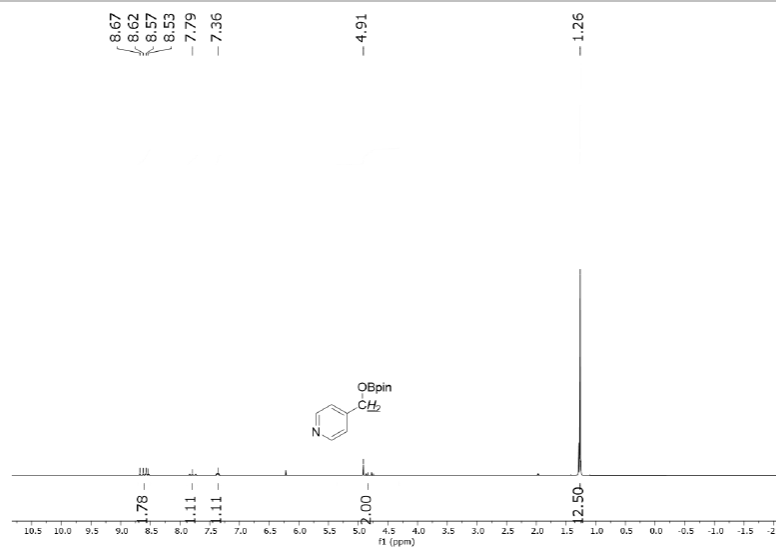
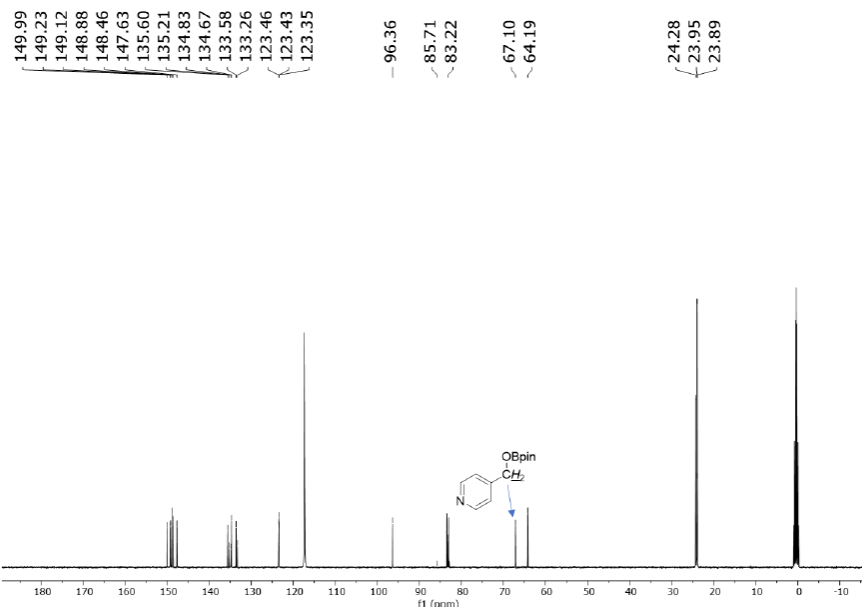
## SUPPORTING INFORMATION



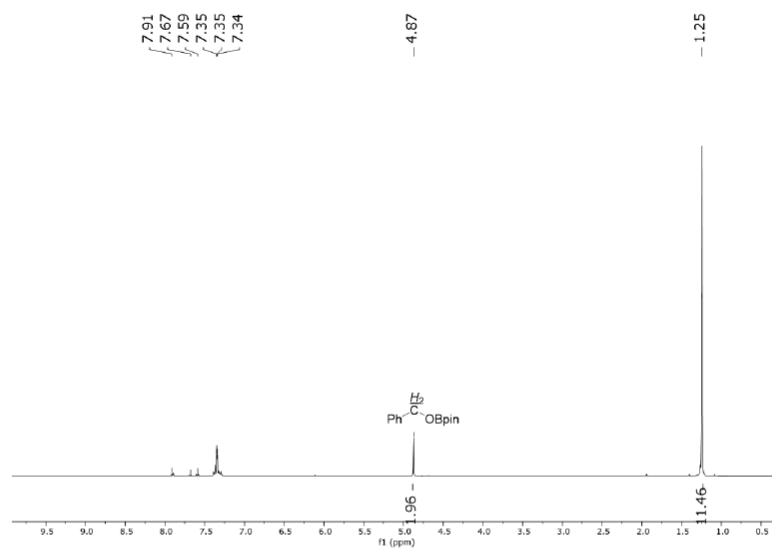
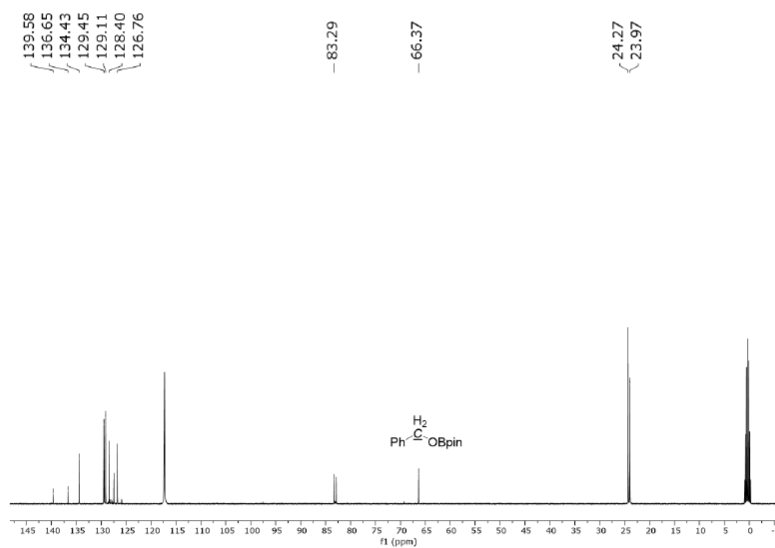
## SUPPORTING INFORMATION

Figure S40.  $^1\text{H}$  NMR spectra of  $(\text{C}_6\text{H}_{11})\text{CH}_2(\text{OBpin})$  in  $\text{CD}_3\text{CN}$ .Figure S41.  $^{13}\text{C}$  NMR spectra of  $(\text{C}_6\text{H}_{11})\text{CH}_2(\text{OBpin})$  in  $\text{CD}_3\text{CN}$ .

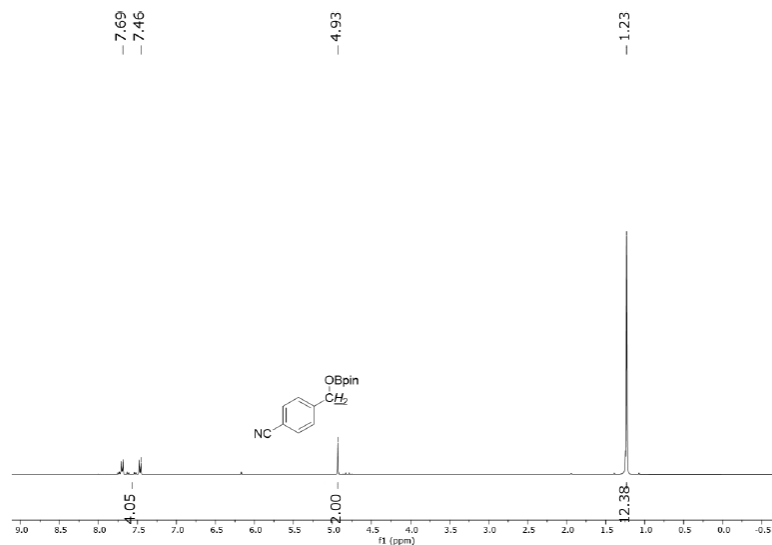
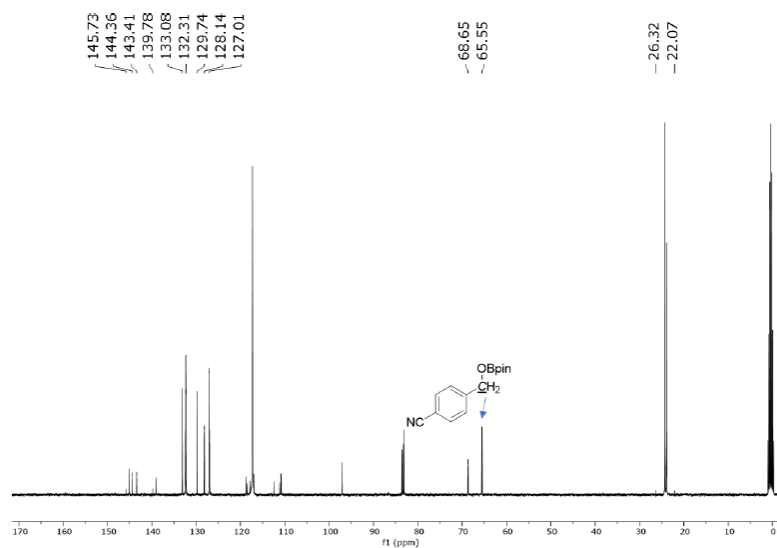
## SUPPORTING INFORMATION

Figure S42. <sup>1</sup>H NMR spectra of (NC<sub>5</sub>H<sub>4</sub>)CH<sub>2</sub>OBpin in CD<sub>3</sub>CN.Figure S43. <sup>13</sup>C NMR spectra of (NC<sub>5</sub>H<sub>4</sub>)CH<sub>2</sub>OBpin in CD<sub>3</sub>CN.

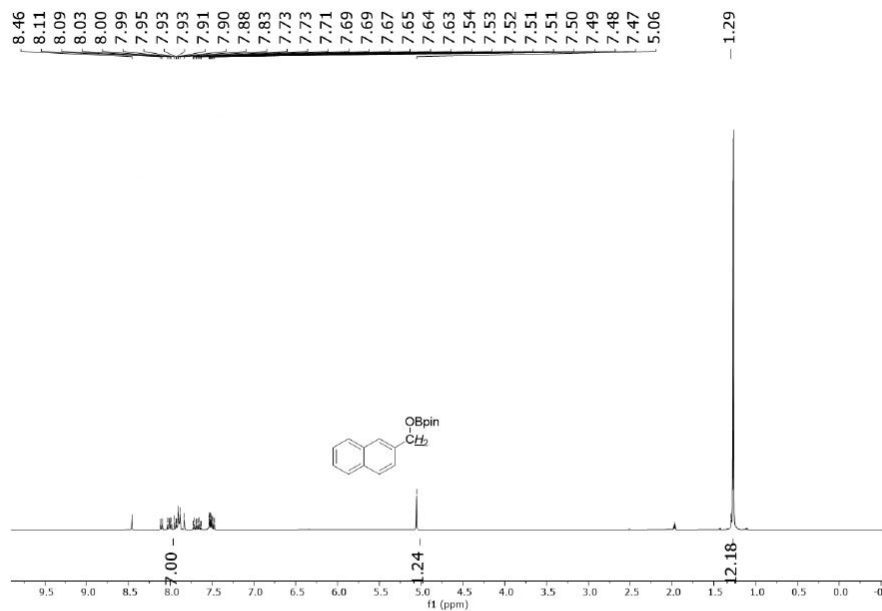
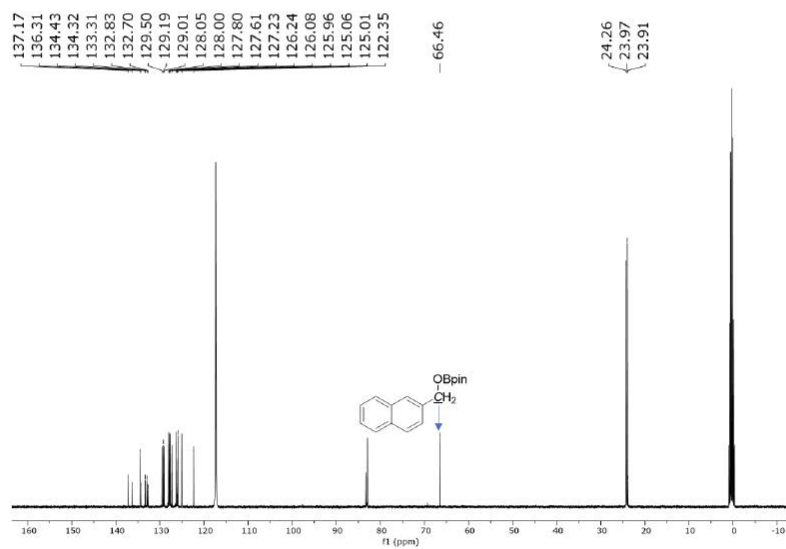
## SUPPORTING INFORMATION

Figure S44. <sup>1</sup>H NMR spectra of Ph(CH<sub>2</sub>)OBpin in CD<sub>3</sub>CN.Figure S45. <sup>13</sup>C NMR spectra of Ph(CH<sub>2</sub>)OBpin in CD<sub>3</sub>CN.

## SUPPORTING INFORMATION

Figure S46.  $^1\text{H}$  NMR spectra of  $\text{CNPh}(\text{CH}_2)\text{OBpin}$  in  $\text{CD}_3\text{CN}$ .Figure S47.  $^{13}\text{C}$  NMR spectra of  $\text{CNPh}(\text{CH}_2)\text{OBpin}$  in  $\text{CD}_3\text{CN}$ .

## SUPPORTING INFORMATION

Figure S48.  $^1\text{H}$  NMR spectra of  $(\text{C}_{10}\text{H}_7)(\text{CH}_2)\text{OBpin}$  in  $\text{CD}_3\text{CN}$ .Figure S49.  $^{13}\text{C}$  NMR spectra of  $(\text{C}_{10}\text{H}_7)(\text{CH}_2)\text{OBpin}$  in  $\text{CD}_3\text{CN}$ .

SUPPORTING INFORMATION

---

**2. References**

- [1] D. Sarkar, C. Weetman, S. Dutta, E. Schubert, C. Jandl, D. Koley, S. Inoue, *J. Am. Chem. Soc.* **2020**, *142*, 15403-15411.



**Title:** Chalcogen-atom transfer and exchange reactions of NHC-stabilized heavier silaacylium ions

**Status** Communication, published online October 27, 2017

**Journal** Dalton Trans., 2017, 46, 16014–16018

**Publisher** Royal Society of Chemistry

**DOI** 10.1039/c7dt03998k

**Authors** Deotra Sarkar, Daniel Wendel, Syed Usman Ahmad, Tibor Szilvási, Alexander Pöthig and, Shigeyoshi Inoue

*Reprinted with permission. © 2017 The Royal Society of Chemistry*

## Chalcogen-atom transfer and exchange reactions of NHC-stabilized heavier silaacylium ions

D. Sarkar, D. Wendel, S. U. Ahmad, T. Szilvási, A. Pöthig and S. Inoue, *Dalton Trans.*, 2017, **46**, 16014

**DOI:** 10.1039/C7DT03998K

If you are not the author of this article and you wish to reproduce material from it in a third party non-RSC publication you must [formally request permission](#) using Copyright Clearance Center. Go to our [Instructions for using Copyright Clearance Center page](#) for details.

Authors contributing to RSC publications (journal articles, books or book chapters) do not need to formally request permission to reproduce material contained in this article provided that the correct acknowledgement is given with the reproduced material.

## Bibliography- licenses for copyrighted content

**Title:** The Quest for Stable Silaaldehydes: Synthesis and Reactivity of a Masked Silacarbonyl

**Status** Communication, published November 16, 2018

**Journal** Chem. Eur.J.2019, 25,1198 –1202

**Publisher** WILEY-VCH Verlag GmbH & Co. KGaA, Weinheim

**DOI** 10.1002/chem.201805604

**Authors** Debotra Sarkar, Vitaly Nesterov, Tibor Szilvási, Philipp J. Altmann, Shigeyoshi Inoue

*Reprinted with permission. © 2019 Wiley-VCH Verlag GmbH & Co. KGaA, Weinheim*

### Thank you for your order!

Dear Mr. DEBOTRA SARKAR,

Thank you for placing your order through Copyright Clearance Center's RightsLink® service.

#### Order Summary

Licensee: TU MUNICH  
Order Date: Jul 11, 2020  
Order Number:4865940261137  
Publication: Chemistry - A European Journal  
Title: The Quest for Stable Silaaldehydes: Synthesis and Reactivity of a Masked Silacarbonyl  
Type of Use: Dissertation/Thesis  
Order Total: 0.00 EUR

View or print complete [details](#) of your order and the publisher's terms and conditions.

Sincerely,

Copyright Clearance Center

Tel: +1-855-239-3415 / +1-978-646-2777  
[customercare@copyright.com](mailto:customercare@copyright.com)  
<https://myaccount.copyright.com>

## Bibliography- licenses for copyrighted content

**Title:** N-Heterocyclic Carbene-Stabilized Germa-acylium ion: Reactivity and Utility in catalytic CO<sub>2</sub> Functionalizations

**Status** Article, published on August 10, 2020

**Journal** J. Am. Chem. Soc. 2020, 142, 36, 15403–15411

**Publisher** American Chemical Society

**DOI** 10.1021/jacs.0c06287

**Authors** Debotra Sarkar, Catherine Weetman, Sayan Dutta, Emeric Schubert, Christian Jandl, Debasis Koley, and Shigeyoshi Inoue



N-Heterocyclic Carbene-Stabilized Germa-acylium Ion: Reactivity and Utility in Catalytic CO<sub>2</sub> Functionalizations  
Author: Debotra Sarkar, Catherine Weetman, Sayan Dutta, et al  
Publication: Journal of the American Chemical Society  
Publisher: American Chemical Society  
Date: Aug 1, 2020  
*Copyright © 2020, American Chemical Society*

### PERMISSION/LICENSE IS GRANTED FOR YOUR ORDER AT NO CHARGE

This type of permission/license, instead of the standard Terms & Conditions, is sent to you because no fee is being charged for your order. Please note the following:

- Permission is granted for your request in both print and electronic formats, and translations.
- If figures and/or tables were requested, they may be adapted or used in part.
- Please print this page for your records and send a copy of it to your publisher/graduate school.
- Appropriate credit for the requested material should be given as follows: "Reprinted (adapted) with permission from (COMPLETE REFERENCE CITATION). Copyright (YEAR) American Chemical Society." Insert appropriate information in place of the capitalized words.
- One-time permission is granted only for the use specified in your request. No additional uses are granted (such as derivative works or other editions). For any other uses, please submit a new request.

BACK

CLOSE WINDOW

## 11.1. References

1. W. Kutzelnigg, *Angew. Chem. Int. Ed.*, 1984, **23**, 272-295.
2. Y. Mizuhata, T. Sasamori and N. Tokitoh, *Chem. Rev.*, 2009, **109**, 3479-3511.
3. R. C. Fischer and P. P. Power, *Chem. Rev.*, 2010, **110**, 3877-3923.
4. H. F. T. Klare and M. Oestreich, *Dalton Trans.*, 2010, **39**, 9176-9184.
5. Y. Xiong, S. Yao and M. Driess, *Angew. Chem. Int. Ed.*, 2013, **52**, 4302-4311.
6. E. Rivard, *Chem. Soc. Rev.*, 2016, **45**, 989-1003.
7. V. S. V. S. N. Swamy, S. Pal, S. Khan and S. S. Sen, *Dalton Trans.*, 2015, **44**, 12903-12923.
8. J. C. L. Walker, H. F. T. Klare and M. Oestreich, *Nat. Rev. Chem.*, 2020, **4**, 54-62.
9. S. Yadav, S. Saha and S. S. Sen, *ChemCatChem*, 2015, **8**, 486-501.
10. X. Wang and L. Andrews, *J. Am. Chem. Soc.*, 2003, **125**, 6581-6587.
11. P. P. Power, *Nature*, 2010, **463**, 171-177.
12. C. Weetman and S. Inoue, *ChemCatChem*, 2018, **10**, 4213-4228.
13. R. L. Melen, *Science*, 2019, **363**, 479-484.
14. G. H. Spikes, J. C. Fettinger and P. P. Power, *J. Am. Chem. Soc.*, 2005, **127**, 12232-12233.
15. S. Yadav, S. Saha and S. S. Sen, *ChemCatChem*, 2016, **8**, 486-501.
16. C. Shan, S. Yao and M. Driess, *Chem. Soc. Rev.*, 2020, DOI: 10.1039/D0CS00815J.
17. C. Gunanathan and D. Milstein, *Acc. Chem. Res.*, 2011, **44**, 588-602.
18. D. V. Gutsulyak, W. E. Piers, J. Borau-Garcia and M. Parvez, *J. Am. Chem. Soc.*, 2013, **135**, 11776-11779.
19. M. G. Scheibel, J. Abbenseth, M. Kinauer, F. W. Heinemann, C. Würtele, B. de Bruin and S. Schneider, *Inorg. Chem.*, 2015, **54**, 9290-9302.
20. T. Chu and G. I. Nikonov, *Chem. Rev.*, 2018, **118**, 3608-3680.
21. T. J. Hadlington, M. Hermann, G. Frenking and C. Jones, *J. Am. Chem. Soc.*, 2014, **136**, 3028-3031.
22. R. K. Siwatch and S. Nagendran, *Chem. Eur. J.*, 2014, **20**, 13551-13556.
23. T. J. Hadlington, C. E. Kefalidis, L. Maron and C. Jones, *ACS Catal.*, 2017, **7**, 1853-1859.
24. N. Del Rio, M. Lopez-Reyes, A. Baceiredo, N. Saffon-Merceron, D. Lutters, T. Müller and T. Kato, *Angew. Chem. Int. Ed.*, 2017, **56**, 1365-1370.
25. T. J. Hadlington, M. Driess and C. Jones, *Chem. Soc. Rev.*, 2018, **47**, 4176-4197.
26. T. Sugahara, J.-D. Guo, T. Sasamori, S. Nagase and N. Tokitoh, *Angew. Chem. Int. Ed.*, 2018, **57**, 3499-3503.
27. R. Dasgupta, S. Das, S. Hiwase, S. K. Pati and S. Khan, *Organometallics*, 2019, **38**, 1429-1435.
28. B.-X. Leong, J. Lee, Y. Li, M.-C. Yang, C.-K. Siu, M.-D. Su and C.-W. So, *J. Am. Chem. Soc.*, 2019, **141**, 17629-17636.
29. D. Bourissou, O. Guerret, F. P. Gabbaï and G. Bertrand, *Chem. Rev.*, 2000, **100**, 39-92.
30. D. Martin, M. Soleilhavoup and G. Bertrand, *Chem. Sci.*, 2011, **2**, 389-399.
31. M. Asay, C. Jones and M. Driess, *Chem. Rev.*, 2011, **111**, 354-396.
32. G. Trinquier, *J. Am. Chem. Soc.*, 1990, **112**, 2130-2137.
33. Y. Apeloig, R. Pauncz, M. Karni, R. West, W. Steiner and D. Chapman, *Organometallics*, 2003, **22**, 3250-3256.
34. R. S. Ghadwal, H. W. Roesky, S. Merkel, J. Henn and D. Stalke, *Angew. Chem. Int. Ed.*, 2009, **48**, 5683-5686.

## References

35. A. C. Filippou, Y. N. Lebedev, O. Chernov, M. Straßmann and G. Schnakenburg, *Angew. Chem. Int. Ed.*, 2013, **52**, 6974-6978.
36. V. Nesterov, D. Reiter, P. Bag, P. Frisch, R. Holzner, A. Porzelt and S. Inoue, *Chem. Rev.*, 2018, **118**, 9678-9842.
37. S. Fujimori and S. Inoue, *Eur. J. Inorg. Chem.*, 2020, **2020**, 3131-3142.
38. Y.-P. Zhou and M. Driess, *Angew. Chem. Int. Ed.*, 2019, **58**, 3715-3728.
39. N. V. Sidgwick, *The Electronic Theory Of Valency* Oxford At The Clarendon Press, 1927.
40. P. P. Gaspar, M. Xiao, D. H. Pae, D. J. Berger, T. Haile, T. Chen, D. Lei, W. R. Winchester and P. Jiang, *J. Organomet. Chem.*, 2002, **646**, 68-79.
41. M. Driess, *Nat. Chem.*, 2012, **4**, 525-526.
42. C. M. Weinstein, G. P. Junor, D. R. Tolentino, R. Jazzar, M. Melaimi and G. Bertrand, *J. Am. Chem. Soc.*, 2018, **140**, 9255-9260.
43. Y. Wang and J. Ma, *J. Organomet. Chem.*, 2009, **694**, 2567-2575.
44. Y. Peng, B. D. Ellis, X. Wang and P. P. Power, *J. Am. Chem. Soc.*, 2008, **130**, 12268-12269.
45. X. Wang, Z. Zhu, Y. Peng, H. Lei, J. C. Fettinger and P. P. Power, *J. Am. Chem. Soc.*, 2009, **131**, 6912-6913.
46. Y. Peng, J.-D. Guo, B. D. Ellis, Z. Zhu, J. C. Fettinger, S. Nagase and P. P. Power, *J. Am. Chem. Soc.*, 2009, **131**, 16272-16282.
47. L. Li, T. Fukawa, T. Matsuo, D. Hashizume, H. Fueno, K. Tanaka and K. Tamao, *Nat. Chem.*, 2012, **4**, 361.
48. A. Meltzer, S. Inoue, C. Präsang and M. Driess, *J. Am. Chem. Soc.*, 2010, **132**, 3038-3046.
49. A. Jana, I. Objartel, H. W. Roesky and D. Stalke, *Inorg. Chem.*, 2009, **48**, 798-800.
50. M. Usher, A. V. Protchenko, A. Rit, J. Campos, E. L. Kolychev, R. Tirfoin and S. Aldridge, *Chem. Eur. J.*, 2016, **22**, 11685-11698.
51. A. V. Protchenko, K. H. Birj Kumar, D. Dange, A. D. Schwarz, D. Vidovic, C. Jones, N. Kaltsoyannis, P. Mountford and S. Aldridge, *J. Am. Chem. Soc.*, 2012, **134**, 6500-6503.
52. D. Wendel, A. Porzelt, F. A. D. Herz, D. Sarkar, C. Jandl, S. Inoue and B. Rieger, *J. Am. Chem. Soc.*, 2017, **139**, 8134-8137.
53. T. Ochiai, D. Franz and S. Inoue, *Chem. Soc. Rev.*, 2016, **45**, 6327-6344.
54. D. Wendel, D. Reiter, A. Porzelt, P. J. Altmann, S. Inoue and B. Rieger, *J. Am. Chem. Soc.*, 2017, **139**, 17193-17198.
55. A. V. Zabula, T. Pape, A. Hepp, F. M. Schappacher, U. C. Rodewald, R. Pöttgen and F. E. Hahn, *J. Am. Chem. Soc.*, 2008, **130**, 5648-5649.
56. R. Rodriguez, D. Gau, T. Kato, N. Saffon-Merceron, A. De Cózar, F. P. Cossío and A. Baceiredo, *Angew. Chem. Int. Ed.*, 2011, **50**, 10414-10416.
57. F. Lips, J. C. Fettinger, A. Mansikkamäki, H. M. Tuononen and P. P. Power, *J. Am. Chem. Soc.*, 2014, **136**, 634-637.
58. T. J. Hadlington, M. Hermann, G. Frenking and C. Jones, *Chem. Sci.*, 2015, **6**, 7249-7257.
59. J. W. Dube, C. M. E. Graham, C. L. B. Macdonald, Z. D. Brown, P. P. Power and P. J. Ragona, *Chem. Eur. J.*, 2014, **20**, 6739-6744.
60. R. Rodriguez, Y. Contie, R. Nougúé, A. Baceiredo, N. Saffon-Merceron, J.-M. Sotiropoulos and T. Kato, *Angew. Chem. Int. Ed.*, 2016, **55**, 14355-14358.
61. J. Schneider, C. P. Sindlinger, S. M. Freitag, H. Schubert and L. Wesemann, *Angew. Chem. Int. Ed.*, 2017, **56**, 333-337.
62. V. Nesterov, R. Baierl, F. Hanusch, A. E. Ferao and S. Inoue, *J. Am. Chem. Soc.*, 2019, **141**, 14576-14580.
63. G. A. Olah, *J. Org. Chem.*, 2001, **66**, 5943-5957.

## References

64. G. A. Olah, *J. Am. Chem. Soc.*, 1972, **94**, 808-820.
65. K.-C. Kim, C. A. Reed, D. W. Elliott, L. J. Mueller, F. Tham, L. Lin and J. B. Lambert, *Science*, 2002, **297**, 825-827.
66. A. Sekiguchi, T. Fukawa, V. Y. Lee, M. Nakamoto and M. Ichinohe, *Angew. Chem. Int. Ed.*, 2003, **42**, 1143-1145.
67. J. B. Lambert, L. Lin, S. Keinan and T. Müller, *J. Am. Chem. Soc.*, 2003, **125**, 6022-6023.
68. T. A. Engesser, M. R. Lichtenthaler, M. Schleep and I. Krossing, *Chem. Soc. Rev.*, 2016, **45**, 789-899.
69. M. Kira, T. Hino and H. Sakurai, *J. Am. Chem. Soc.*, 1992, **114**, 6697-6700.
70. I. Masaaki, F. Hiroshi and S. Akira, *Chem. Lett.*, 2000, **29**, 600-601.
71. C. A. Reed, Z. Xie, R. Bau and A. Benesi, *Science*, 1993, **262**, 402-404.
72. R. Panisch, M. Bolte and T. Müller, *J. Am. Chem. Soc.*, 2006, **128**, 9676-9682.
73. T. Müller, C. Bauch, M. Bolte and N. Auner, *Chem. Eur. J.*, 2003, **9**, 1746-1749.
74. H. F. T. Klare, K. Bergander and M. Oestreich, *Angew. Chem. Int. Ed.*, 2009, **48**, 9077-9079.
75. A. Schäfer, M. Reißmann, S. Jung, A. Schäfer, W. Saak, E. Brendler and T. Müller, *Organometallics*, 2013, **32**, 4713-4722.
76. Q. Wu, E. Irran, R. Müller, M. Kaupp, H. F. T. Klare and M. Oestreich, *Science*, 2019, **365**, 168-172.
77. O. Allemann, S. Duttwyler, P. Romanato, K. K. Baldridge and J. S. Siegel, *Science*, 2011, **332**, 574-577.
78. V. J. Scott, R. Çelenligil-Çetin and O. V. Ozerov, *J. Am. Chem. Soc.*, 2005, **127**, 2852-2853.
79. B. Shao, A. L. Bagdasarian, S. Popov and H. M. Nelson, *Science*, 2017, **355**, 1403-1407.
80. M. Talavera, G. Meißner, S. G. Rachor and T. Braun, *Chem. Commun.*, 2020, **56**, 4452-4455.
81. D. J. Scott, N. A. Phillips, J. S. Sapsford, A. C. Deacy, M. J. Fuchter and A. E. Ashley, *Angew. Chem. Int. Ed.*, 2016, **55**, 14738-14742.
82. A. E. Douglas and B. L. Lutz, *Canad. J. Phys.*, 1970, **48**, 247-253.
83. N. Grevesse and A. J. Sauval, *Astron. Astrophys.*, 1970, **9**, 232.
84. C. Gerdes, W. Saak, D. Haase and T. Müller, *J. Am. Chem. Soc.*, 2013, **135**, 10353-10361.
85. P. Jutzi, A. Mix, B. Rummel, W. W. Schoeller, B. Neumann and H.-G. Stammler, *Science*, 2004, **305**, 849-851.
86. M. Driess, S. Yao, M. Brym and C. van Wüllen, *Angew. Chem. Int. Ed.*, 2006, **45**, 6730-6733.
87. Y. Xiong, S. Yao, S. Inoue, E. Irran and M. Driess, *Angew. Chem. Int. Ed.*, 2012, **51**, 10074-10077.
88. Y. Xiong, S. Yao, S. Inoue, J. D. Epping and M. Driess, *Angew. Chem. Int. Ed.*, 2013, **52**, 7147-7150.
89. A. C. Filippou, B. Baars, O. Chernov, Y. N. Lebedev and G. Schnakenburg, *Angew. Chem. Int. Ed.*, 2014, **53**, 565-570.
90. H.-X. Yeong, H.-W. Xi, Y. Li, K. H. Lim and C.-W. So, *Chem. Eur. J.*, 2013, **19**, 11786-11790.
91. N. C. Breit, T. Szilvási, T. Suzuki, D. Gallego and S. Inoue, *J. Am. Chem. Soc.*, 2013, **135**, 17958-17968.
92. A. Hinz, *Angew. Chem. Int. Ed.*, **n/a**.
93. P. P. Power, *Chem. Rev.*, 1999, **99**, 3463-3504.
94. T. Agou, N. Hayakawa, T. Sasamori, T. Matsuo, D. Hashizume and N. Tokitoh, *Chem. Eu. J.*, 2014, **20**, 9246-9249.
95. S. U. Ahmad, T. Szilvasi and S. Inoue, *Chem. Commun.*, 2014, **50**, 12619-12622.
96. P. Frisch and S. Inoue, *Dalton Trans.*, 2019, **48**, 10403-10406.
97. Y. Li, Y.-C. Chan, B.-X. Leong, Y. Li, E. Richards, I. Purushothaman, S. De, P. Parameswaran and C.-W. So, *Angew. Chem. Int. Ed.*, 2017, **56**, 7573-7578.
98. P. Jutzi, *Chem. Eu. J.*, 2014, **20**, 9192-9207.
99. P. Jutzi, A. Mix, B. Neumann, B. Rummel, W. W. Schoeller, H.-G. Stammler and A. B. Rozhenko, *J. Am. Chem. Soc.*, 2009, **131**, 12137-12143.

## References

100. P. Jutzi, K. Leszczyńska, B. Neumann, W. W. Schoeller and H.-G. Stammler, *Angew. Chem. Int. Ed.*, 2009, **48**, 2596-2599.
101. S. Inoue and K. Leszczyńska, *Angew. Chem. Int. Ed.*, 2012, **51**, 8589-8593.
102. P. Jutzi, K. Leszczyńska, A. Mix, B. Neumann, W. W. Schoeller and H.-G. Stammler, *Organometallics*, 2009, **28**, 1985-1987.
103. K. Leszczyńska, K. Abersfelder, A. Mix, B. Neumann, H.-G. Stammler, M. J. Cowley, P. Jutzi and D. Scheschkewitz, *Angew. Chem. Int. Ed.*, 2012, **51**, 6785-6788.
104. K. Leszczyńska, K. Abersfelder, M. Majumdar, B. Neumann, H.-G. Stammler, H. S. Rzepa, P. Jutzi and D. Scheschkewitz, *Chem. Commun.*, 2012, **48**, 7820-7822.
105. P. Jutzi, K. Leszczyńska, A. Mix, B. Neumann, B. Rummel, W. Schoeller and H.-G. Stammler, *Organometallics*, 2010, **29**, 4759-4761.
106. S. L. Powley and S. Inoue, *Chem. Rec.*, 2019, **19**, 2179-2188.
107. S. U. Ahmad, T. Szilvási, E. Irran and S. Inoue, *J. Am. Chem. Soc.*, 2015, **137**, 5828-5836.
108. A. Porzelt, J. Schweizer, R. Baierl, P. Altmann, M. Holthausen and S. Inoue, *Inorganics*, 2018, **6**, 54.
109. K. Leszczyńska, A. Mix, R. J. F. Berger, B. Rummel, B. Neumann, H.-G. Stammler and P. Jutzi, *Angew. Chem. Int. Ed.*, 2011, **50**, 6843-6846.
110. E. Fritz-Langhals, *Org. Process Res. Dev.*, 2019, **23**, 2369-2377.
111. P. Jutzi, F. Kohl, P. Hofmann, C. Krüger and Y.-H. Tsay, *Chem. Ber.*, 1980, **113**, 757-769.
112. T. Probst, O. Steigelmann, J. Riede and H. Schmiclbaur, *Angew. Chem. Int. Ed.*, 1990, **29**, 1397-1398.
113. D. L. Reger and P. S. Coan, *Inorg. Chem.*, 1996, **35**, 258-260.
114. H. V. R. Dias and Z. Wang, *J. Am. Chem. Soc.*, 1997, **119**, 4650-4655.
115. H. V. R. Dias and W. Jin, *J. Am. Chem. Soc.*, 1996, **118**, 9123-9126.
116. Y. Ding, H. W. Roesky, M. Noltemeyer, H.-G. Schmidt and P. P. Power, *Organometallics*, 2001, **20**, 1190-1194.
117. M. Stender, A. D. Phillips and P. P. Power, *Inorg. Chem.*, 2001, **40**, 5314-5315.
118. M. Driess, S. Yao, M. Brym and C. van Wüllen, *Angew. Chem. Int. Ed.*, 2006, **45**, 4349-4352.
119. M. J. Taylor, A. J. Saunders, M. P. Coles and J. R. Fulton, *Organometallics*, 2011, **30**, 1334-1339.
120. H. Aii, F. Nakadate, K. Mochida and T. Kawashima, *Organometallics*, 2011, **30**, 4471-4474.
121. A. Schäfer, W. Saak, D. Haase and T. Müller, *Chem. Eur. J.*, 2009, **15**, 3945-3950.
122. D. C. H. Do, A. V. Protchenko, M. Á. Fuentes, J. Hicks, P. Vasko and S. Aldridge, *Chem. Commun.*, 2020, **56**, 4684-4687.
123. J. Li, C. Schenk, F. Winter, H. Scherer, N. Trapp, A. Higelin, S. Keller, R. Pöttgen, I. Krossing and C. Jones, *Angew. Chem. Int. Ed.*, 2012, **51**, 9557-9561.
124. A. Hinz, *Chem. Eur. J.*, 2019, **25**, 3267-3271.
125. P. A. Rugar, R. Bandyopadhyay, B. F. T. Cooper, M. R. Stinchcombe, P. J. Ragona, C. L. B. Macdonald and K. M. Baines, *Angew. Chem. Int. Ed.*, 2009, **48**, 5155-5158.
126. C. L. B. Macdonald, R. Bandyopadhyay, B. F. T. Cooper, W. W. Friedl, A. J. Rossini, R. W. Schurko, S. H. Eichhorn and R. H. Herber, *J. Am. Chem. Soc.*, 2012, **134**, 4332-4345.
127. P. A. Rugar, V. N. Staroverov and K. M. Baines, *Science*, 2008, **322**, 1360-1363.
128. J. C. Avery, M. A. Hanson, R. H. Herber, K. J. Bladek, P. A. Rugar, I. Nowik, Y. Huang and K. M. Baines, *Inorg. Chem.*, 2012, **51**, 7306-7316.
129. Y. Xiong, S. Yao, S. Inoue, A. Berkefeld and M. Driess, *Chem. Commun.*, 2012, **48**, 12198-12200.
130. Y. Xiong, S. Yao, G. Tan, S. Inoue and M. Driess, *J. Am. Chem. Soc.*, 2013, **135**, 5004-5007.
131. Y. Xiong, T. Szilvási, S. Yao, G. Tan and M. Driess, *J. Am. Chem. Soc.*, 2014, **136**, 11300-11303.
132. A. P. Singh, H. W. Roesky, E. Carl, D. Stalke, J.-P. Demers and A. Lange, *J. Am. Chem. Soc.*, 2012, **134**, 4998-5003.

## References

133. M. Bouška, L. Dostál, A. Růžička and R. Jambor, *Organometallics*, 2013, **32**, 1995-1999.
134. S. Khan, G. Gopakumar, W. Thiel and M. Alcarazo, *Angew. Chem. Int. Ed.*, 2013, **52**, 5644-5647.
135. H. Braunschweig, M. A. Celik, R. D. Dewhurst, M. Heid, F. Hupp and S. S. Sen, *Chem. Sci.*, 2015, **6**, 425-435.
136. K. Inomata, T. Watanabe, Y. Miyazaki and H. Tobita, *J. Am. Chem. Soc.*, 2015, **137**, 11935-11937.
137. C. P. Sindlinger, F. S. W. Aicher and L. Wesemann, *Inorg. Chem.*, 2017, **56**, 548-560.
138. F. Diab, F. S. W. Aicher, C. P. Sindlinger, K. Eichele, H. Schubert and L. Wesemann, *Chem. Eur. J.*, 2019, **25**, 4426-4434.
139. A. Rit, R. Tirfoin and S. Aldridge, *Angew. Chem. Int. Ed.*, 2016, **55**, 378-382.
140. X. Zhou, P. Vasko, J. Hicks, M. Á. Fuentes, A. Heilmann, E. L. Kolychev and S. Aldridge, *Dalton Trans.*, 2020, **49**, 9495-9504.
141. M. M. D. Roy, S. Fujimori, M. J. Ferguson, R. McDonald, N. Tokitoh and E. Rivard, *Chem. Eur. J.*, 2018, **24**, 14392-14399.
142. S. Sinhababu, D. Singh, M. K. Sharma, R. K. Siwatch, P. Mahawar and S. Nagendran, *Dalton Trans.*, 2019, **48**, 4094-4100.
143. B. Rhodes, J. C. W. Chien and M. D. Rausch, *Organometallics*, 1998, **17**, 1931-1933.
144. P. Jutzi, R. Dickbreder and H. Nöth, *Chem. Ber.*, 1989, **122**, 865-870.
145. S. Hino, M. Brynda, A. D. Phillips and P. P. Power, *Angew. Chem. Int. Ed.*, 2004, **43**, 2655-2658.
146. M.-A. Légaré, C. Pranckevicius and H. Braunschweig, *Chem. Rev.*, 2019, **119**, 8231-8261.
147. D. L. Nelson, M. M. Cox and A. L. Lehninger, *Lehninger principles of biochemistry (7th edition)*, 2017, 75-106.
148. D. Scheschkewitz, *Functional Molecular Silicon Compounds I*, Springer International Publishing, 1 edn., 2014.
149. D. Scheschkewitz, *Functional Molecular Silicon Compounds II*, Springer International Publishing, 1 edn., 2014.
150. A. Nowek and J. Leszczyński, *J. Phys. Chem.*, 1996, **100**, 7361-7366.
151. R. S. Ghadwal, R. Azhakar, H. W. Roesky, K. Propper, B. Dittrich, C. Goedecke and G. Frenking, *Chem. Commun.*, 2012, **48**, 8186-8188.
152. S. Yao, M. Brym, C. van Wüllen and M. Driess, *Angew. Chem. Int. Ed.*, 2007, **46**, 4159-4162.
153. M. K. Sharma, S. Sinhababu, P. Mahawar, G. Mukherjee, B. Pandey, G. Rajaraman and S. Nagendran, *Chem. Sci.*, 2019, **10**, 4402-4411.
154. S. Yao, Y. Xiong and M. Driess, *Chem. Commun.*, 2009, DOI: 10.1039/B914060C, 6466-6468.
155. S. Sinhababu, D. Yadav, S. Karwasara, M. K. Sharma, G. Mukherjee, G. Rajaraman and S. Nagendran, *Angew. Chem. Int. Ed.*, 2016, **55**, 7742-7746.
156. S. Yao, Y. Xiong, W. Wang and M. Driess, *Chem. Eur. J.*, 2011, **17**, 4890-4895.
157. P. Benzi, L. Operti, G. A. Vaglio, P. Volpe, M. Speranca and R. Gabrielli, *J. Organomet. Chem.*, 1988, **354**, 39-50.
158. T. Ozturk, E. Ertas and O. Mert, *Chem. Rev.*, 2007, **107**, 5210-5278.
159. G. Hua and J. D. Woollins, *Angew. Chem. Int. Ed.*, 2009, **48**, 1368-1377.
160. J. L. Smeltz, C. P. Lilly, P. D. Boyle and E. A. Ison, *J. Am. Chem. Soc.*, 2013, **135**, 9433-9441.
161. T. D. Lohrey, R. G. Bergman and J. Arnold, *Organometallics*, 2018, **37**, 3552-3557.
162. J. S. Silvia and C. C. Cummins, *Chem. Sci.*, 2011, **2**, 1474-1479.
163. I. Knopf, T. Ono, M. Temprado, D. Tofan and C. C. Cummins, *Chem. Sci.*, 2014, **5**, 1772-1776.
164. D. S. Morris, C. Weetman, J. T. C. Wennmacher, M. Cokoja, M. Drees, F. E. Kühn and J. B. Love, *Catal. Sci. Technol.*, 2017, **7**, 2838-2845.
165. M.-Y. Wang, N. Wang, X.-F. Liu, C. Qiao and L.-N. He, *Green Chem.*, 2018, **20**, 1564-1570.
166. W. Adam and R. M. Bargon, *Chem. Rev.*, 2004, **104**, 251-262.



## References

167. M. Arisawa, T. Ichikawa and M. Yamaguchi, *Chem. Commun.*, 2015, **51**, 8821-8824.
168. D. Sarkar, D. Wendel, S. U. Ahmad, T. Szilvasi, A. Pothig and S. Inoue, *Dalton Trans.* , 2017, **46**, 16014-16018.